



THE HONG KONG  
POLYTECHNIC UNIVERSITY

香港理工大學

Pao Yue-kong Library  
包玉剛圖書館

---

## Copyright Undertaking

This thesis is protected by copyright, with all rights reserved.

**By reading and using the thesis, the reader understands and agrees to the following terms:**

1. The reader will abide by the rules and legal ordinances governing copyright regarding the use of the thesis.
2. The reader will use the thesis for the purpose of research or private study only and not for distribution or further reproduction or any other purpose.
3. The reader agrees to indemnify and hold the University harmless from and against any loss, damage, cost, liability or expenses arising from copyright infringement or unauthorized usage.

If you have reasons to believe that any materials in this thesis are deemed not suitable to be distributed in this form, or a copyright owner having difficulty with the material being included in our database, please contact [lbsys@polyu.edu.hk](mailto:lbsys@polyu.edu.hk) providing details. The Library will look into your claim and consider taking remedial action upon receipt of the written requests.

The Hong Kong Polytechnic University  
Department of Applied Biology & Chemical Technology

---

**NEUROPROTECTIVE EFFECT BY  
Z-LIGUSTILIDE EXTRACTED FROM *RADIX  
ANGELICA SINENSIS* FOR THE TREATMENT OF  
CEREBRAL ISCHEMIA**

---

**JUNRONG DU**

A THESIS SUBMITTED IN PARTIAL FULFILMENT OF  
THE REQUIREMENTS FOR THE DEGREE OF DOCTOR OF  
PHILOSOPHY

**January 2006**

## **CERTIFICATE OF ORIGINALITY**

I hereby declare that this thesis is my own work and that, to the best of my knowledge and belief, it reproduces no material previously published or written nor material which has been accepted for the award of any other degree or diploma, except where due acknowledgement has been made in the text.

..... (Signed)

JUNRONG DU

.....(Name of Student))

**ABSTRACT OF THESIS ENTITLED ‘NEUROPROTECTIVE EFFECT BY  
Z-LIGUSTILIDE EXTRACTED FROM *RADIX ANGELICA SINENSIS* FOR  
THE TREATMENT OF CEREBRAL ISCHEMIA ’**

Submitted by

**JUNRONG DU**

For the degree of Doctor of Philosophy

At the Hong Kong Polytechnic University in January 2006

**ABSTRACT**

Stroke resulting from cerebral ischemia is one of the leading causes of death and disability. To date, there is not yet any neuroprotective agent for the treatment of stroke. Involvement of oxidative stress in ischemic brain damage is established (Cassarino and Bennett, 1999; Simonian and Coyle, 1996). The overproduction of reactive oxygen species (ROS) such as superoxide anion, hydroxyl radical, and nitric oxide can directly react with and damage biomacromolecules by virtue of their reactivity that leads to neuronal cell death through necrosis, or, if in less intense cases, may mediate neuronal apoptosis through a cascade of biochemical process following cerebral ischemia (Li, et al., 1995; Ratan et al., 1994; Whitemore et al., 1995). Therefore, lipophilic antioxidants are of neuroprotective potential in the development of ischemic brain damage. Z-ligustilide (3-butylidene-4, 5-dihydro-phthalide, LIG) is a highly lipophilic compound extracted from *Radix Angelica sinensis* (Oliv.) Diels (Umbelliferae), known as Danggui in Chinese. Previous studies have shown that LIG has various bioactivities. Studies in this thesis evaluated, for the first time, the neuroprotective effect and the associated mechanisms of LIG in cerebral ischemia. In order to design the dosage regimen of LIG *in vivo*, its cellular permeability and transport pathways were first determined in Caco-2 monolayers. Our results show that

oral application is the preferred route for the systemic administration of LIG. The free radical scavenging efficacy and the antioxidant activities of LIG were then evaluated in different *in vitro* ROS reactive systems, hydrogen peroxide-damaged C6 glioma cells and forebrain ischemic mice, respectively. We ascertain that LIG is a novel antioxidant and has significant protective effects against oxidative injury. The neuroprotective effects of LIG have been proven in transient forebrain ischemic mice and focal ischemic rats by measuring the histological, physiological, neurological or biochemical improvements after cerebral ischemia. The results suggest that postischemic treatment with LIG significantly ameliorates infarction volume by inhibiting both the apoptotic and necrotic cell death, and improving neurological deficits after transient cerebral ischemia. In addition, the multiple mechanisms, including the antioxidant, anti-apoptotic, and anti-inflammation properties, contribute to the neuroprotection of LIG. This thesis consists of 7 chapters, beginning with a general introduction, and then followed by the methodology section. There are then four chapters on results, and at the end, there is a general discussion.

# LIST OF PUBLICATIONS

## SCI Papers

1. Chang Y, Ke Y, **DU JR**, Ho K, Zhu L, Gu XS, Xu Y, Wang Q, Li L, Wang C, Halpern GM, Qian ZM (2005) Increased DMT1 expression might be associated with the neurotoxicity of L-DOPA. Mol Pharmacol. Nov 29; [Epub ahead of print]
2. Chen Y, Qian ZM, **Du JR**, Duan X, Chang Y, Wang Q, Wang C, Ma YM, Xu Y, Li L, Ke Y (2005) Iron loading inhibits ferroportin1 expression in PC12 cells. Neurochem Int. 47(7):507-513.
3. **Du JR**, Li X, Zhang R, Qian ZM (2005) Tanshinone inhibits intimal hyperplasia in the ligated carotid artery in mice. J Ethnopharmacol. 98(3):319-322.
4. Chang YZ, Qian ZM, Wang K, Zhu L, Yang XD, **Du JR**, Jiang L, Ho KP, Wang Q, Ke Y (2005) Effects of development and iron status on ceruloplasmin expression in rat brain. J Cell Physiol. 204(2): 623-631.

5. Ke Y, Chang YZ, Duan XL, **Du JR**, Zhu L, Wang K, Yang XD, Ho KP, Qian ZM (2005) Age-dependent and iron-independent expression of two mRNA isoforms of divalent metal transporter 1 in rat brain. *Neurobiol Aging*. 26(5):739-48.
6. Ke Y, Ho KP, **Du JR**, Zhu L, Xu YJ, Wang Q, Wang CY, Li LZ, Ge XH, Chang YZ, Qian ZM (2005) Role of soluble ceruloplasmin on iron uptake by midbrain and hippocampus neurons. *Journal of Cellular Biochemistry* (In press)
7. Chang YZ, Qian ZM, Leung G, **Du JR**, Zhu L, Wang Q, Xu YJ, Wang CY, Ho KP, Ke Y (2005) Expression of ferroportin1, hephaestin and ceruloplasmin in rat heart. *American Journal of Physiology Heart and Circulatory Physiology* ('Revision Invitation' - Revised)
8. Chang YZ, Ke Y, **Du JR**, Zhu L, Xu YJ, Li LZ, Ge XH, Wang Q, Wang CY, Duan XL, Ho KP, Qian ZM (2005) Ceruloplasmin expression and its role in iron transport in C6 glioma cells. *Neuromolecular Medicine* ('Revision Invitation' - Revised)

9. **Du JR**, Bai B, Kuang X, Yu Y, Wang CY, Ke Y, Xu YJ, Qian ZM (2005)  
Ligustilide inhibits spontaneous and agonists- or K<sup>+</sup> depolarization-induced contraction of rat uterus. *Journal of Ethnopharmacology* (Submitted)
10. **Du JR**, Bai B, Kuang X, Yu Y, Wang CY, Ke Y, Xu YJ, Qian ZM (2005)  
Ligustilide attenuates pain behavior-induced by acetic acid and formalin.  
*Journal of Cellular Biochemistry* (Submitted)
11. Kuang X, Yao Y, **Du JR**, Liu YX, Wang CY, Qian ZM (2005)  
Neuro-protective role of Z-ligustilide in forebrain ischemic brain injury.  
*Journal of Cerebral Blood Flow and Metabolism* (Submitted)

#### **National Journal Papers**

1. **Du JR**, Bai B, Yuan Y, Wang CY, Qian ZM (2005) New progress of the study on volatile oil of the angelica. *Chinese Journal of Chinese Materia Medica* 中国中药杂志 30(18): 1400-1406
2. **Du JR**, Yao Yao, Yu Y, Wang CY, Qian ZM (2005) Biological activities and applications of Lycopene. *Chinese Pharmaceutical Journal* 中国药学杂志 *In press*

3. **Du JR**, Ruan JL, Alexander Tzang, Qian ZM (2005) Treatment of dysmenorrhea with traditional Chinese medicine: current knowledge. Chinese Journal of Integrated Traditional and Western Medicine 中国中西医结合杂志  
*In press*
4. Ran YW, **Du JR**, Bao B, Zhang R, Qian ZM (2004) High cholesterol level upregulate the expression of Caveolin-1. Journal of Biomedical Engineering 生物医学工程学杂志21(2): 276-279
5. Ruan JL, **Du JR**, Alexander Tzang, Qian ZM (2003) Study on components, pharmacological role and clinical application of *Leonurus Japonicu*: an update. Chinese Traditional and Herbal Drugs 中草药 34(11): 15-19
6. Ruan JL, **Du JR**, Zhao ZX, Alexander Tzang, Qian ZM (2003) Recent advances in study on components and pharmacological role of *Radix Paeoniae rubra*. Chinese Pharmacological Bulletin 中国药理学通报 19(9): 965-970
7. Alexander Tzang, Yuan QP, **DU JR**, Ruan JL, Qian ZM (2002) New development of modern traditional Chinese medicine. Journal of Chinese Pharmaceutical University 中国药科大学学报 33: s322-324

## Conference Abstracts or Papers

1. Ke Y, **Du JR**, Duan XL, Wang Q, Xu YJ, Li LZ, Wng CY, Ho KP, Jiang L, Ma YM, Niu LJ, Wang L, Zhang JQ, Qian ZM (2005) Effects of ceruloplasmin on iron transport in midbrain and hippocampus neurons. The 9<sup>th</sup> National Conference on Neuroendocrinology of Chinese Association of Physiological Sciences, Jiaozou, PRC Spet 20-23, 2005. CAPS News Communication 24(Suppl. III): 18-19
2. Duan XL, Chang YZ, Ke Y, **Du JR**, Wang Q, Xu YJ, Li LZ, Wng CY, Ho KP, Jiang L, Ma YM, Zhang JQ, Niu LJ, Wang L, Qian ZM (2005) Increased DMT1(-IRE) expression might be associated with the neurotoxicity of L-DOPA. The 9<sup>th</sup> National Conference on Neuroendocrinology of Chinese Association of Physiological Sciences, Jiaozou, PRC Spet 20-23, 2005. CAPS News Communication 24(Suppl. III): 19-20
3. Chang YZ, Ke Y, **Du JR**, Duan XL, Wang Q, Xu YJ, Li LZ, Wng CY, Ho KP, Jiang L, Ma YM, Zhang JQ, Niu LJ, Wang L, Qian ZM (2005) Ferroportin1/hephaestin system and iron export from cells in the heart. The 9<sup>th</sup> National Conference on Neuroendocrinology of Chinese Association of Physiological Sciences, Jiaozou, PRC Spet 20-23, 2005. CAPS News Communication 24(Suppl. III): 20

4. Ke Y, **Du JR**, Wang Q, Wang CY, Zhou B, Ho KP, Qian ZM (2004) Iron-independent Expression of Two mRNA Isoforms of Divalent Metal Transporter 1 (DMT 1/NRAMP2/DCT1) in Rat Brain. (APS - Am. Physiological Soc., Topic:105-APS Endocrinology & Metabolism) Experimental Biology 2004 April 17 – 21, Washington, DC Abs#9192
  
5. Cheng YZ, Ke Y, Daniel KL Lee, Ho KP, Agnete Svendsen, Xie JX, Wang J, Yuan QP, Zhou B, Loh CN, Wang Q, Li J, Wen ZM, **Du JR**, Li FY, Qian ZM (2003) Effect of iron on expression of ceruloplasmin homologue hephaestin in cultured rat astrocytes. The 3<sup>rd</sup> National Congress of Neurosciences, Qiandao, PRC, Sept 20-23, pp114-115
  
6. Cheng YZ, Ke Y, Daniel KL Lee, Ho KP, Agnete Svendsen, Yuan QP, Zhou B, Loh CN, Wang Q, Li J, **Du JR**, Xie JX, Li FY, Qian ZM (2003) Expression of ceruloplasmin homologue Hephaestin in developing rat brain. The 3<sup>rd</sup> National Congress of Neurosciences, Qiandao, PRC, Sept 20-23, pp98-99
  
7. Ke Y, Ho KP, Cheng YZ, Xie JX, Daniel KL Lee, **Du JR**, Agnete Svendsen, Yuan QP, Zhou B, Loh CN, Wang Q, Li J, Wang J, Wen ZM, Li FY, Qian ZM (2003) Iron-independent and Age-dependent Expression of DMT 1(Nramp2/DCT1) in Different Brain Regions of Rats. The 3<sup>rd</sup> National Congress of Neurosciences, Qiandao, PRC, Sept 20-23, pp133

8. Qian ZM, Cheng YZ, Ke Y, Agnete Svendsen, Daniel KL Lee, Yuan QP, Zhou B, Wang Q, **Du JR**, Ho KP (2003). Iron-dependent transcriptional Expression of the Ceruloplasmin Homologue Hephaestin in Rat Brain. The 3<sup>rd</sup> National Congress of Neurosciences, Qiandao, PRC, Sept 20-23, pp 134
9. Ho KP, Agnete Svendsen, Cheng YZ, Ke Y, Xie JX, Daniel KL Lee, Yuan QP, Zhou B, Loh CN, Wang J, Li J, **Du JR**, Wang Q, Wen ZM, Li FY, Qian ZM (2003) Expression and Distribution of the Ceruloplasmin Homologue Hephaestin in the Brain: A Immunohisto-chemistry Study. The 3<sup>rd</sup> National Congress of Neurosciences, Qiandao, PRC, Sept 20-23, pp274
10. Ho KP, Ke Y, Cheng YZ, Xie JX, Daniel KL Lee, **Du JR**, Agnete Svendsen, Yuan QP, Zhou B, Loh CN, Wang Q, Li J, Wang J, Wen ZM, Li FY, Qian ZM (2003) Effects of Dietary Iron on Expression of Ceruloplasmin in Rat Brain. The 3<sup>rd</sup> National Congress of Neurosciences, Qiandao, PRC, Sept 20-23, pp274-275
11. Chen YM, Duan XL, Cheng YZ, Ke Y, **Du JR**, Daniel KL Lee, Agnete Svendsen, Xie JX, Yuan QP, Zhou B, Ho KP, Loh CN, Wang Q, Li J, Wang J, Wen ZM, Li FY, Qian ZM (2003) Effects of intracellular iron and NO on Expression of Ferroportin 1 in PC 12 cells. The 3<sup>rd</sup> National Congress of Neurosciences, Qiandao, PRC, Sept20-23, pp135

12. Agnete Svendsen, Cheng YZ, Ke Y, Xie JX, Daniel KL Lee, Ho KP, Wang Q, **Du JR**, Yuan QP, Zhou B, Loh CN, Li J, Wang J, Wen ZM, Li FY, Qian ZM (2003) Effects of Iron on Expression of Ferroportin1 and Hephaestin in Rat Heart. The 3<sup>rd</sup> National Congress of Neurosciences, Qiandao, PRC, Sept 20-23, pp136-137

### **Patents**

1. Qian ZM, **Du JR**, Wang CY. Application of ligustilide in the preparation of drugs for the prevention and treatment of dysmenorrheal. Patent application number: CN 200510021300.9. Patent application date: July 15, 2005
2. Qian ZM, **Du JR**, Wang CY. Application of ligustilide in the preparation of drugs for the prevention and treatment of cerebral ischemia disease. Patent application number: CN 200510021301.3. Patent application date: July 15, 2005
3. Qian ZM, Wang CY, **Du JR**. The fast preparation method of high-purity ligustilide. Patent application number: CN 200510021261.2. Patent application date: July 8, 2005
4. Qian ZM, Wang CY, **Du JR**. A kind of the soft capsule of (z)-ligustilide. Patent

application number: CN 200510021302.8 Patent application date: July 15,  
2005

5. Qian ZM, Wang CY, **Du JR**. The preparation method and pharmaceutical preparations of cyclodextrin or cyclodextrin ramification inclusion of ligustilide. Patent application number: CN 200510021303.2. Patent application date: July 15, 2005

## ACKNOWLEDGEMENTS

I am especially indebted to my Chief Supervisor, Dr. Zhong Ming Qian, for his outstanding guidance, sincere encouragement, and helpful advice throughout the course of this work. It would have been impossible for me to complete this thesis without his help. I am also grateful to my co-supervisor, Mr Alexander Tzang, for his valuable suggestions and strong support.

I am much indebted to the Department Research Committee of ABCT Department and the Research Committee of the Hong Kong Polytechnic University for giving me this chance to finish my study at this university.

I would like to thank Mr. CH Cheung, Ms. Seral Yang and all other technicians in the Applied Biology Section of the Department of ABCT for their valuable technical assistance. I would also like to thank Mr. C.Y. Wang, Ms. Q. Wang, Dr. Y. Ke and all colleagues in our research group for their kind help and strong support. Moreover, I would like to thank Prof. Z.R. Zhang for his kind encouragement and support.

Finally I thank my family members for their support and sacrifices without which this work would not have been possible. My family has offered me much wisdom and encouragement throughout my educational career and is always there to support me in so many ways.

# TABLE OF CONTENTS

<b>Certification of originality.....</b>	<b>1</b>
<b>ABSTRACT .....</b>	<b>2</b>
<b>LIST OF PUBLICATION.....</b>	<b>4</b>
<b>ACKNOWLEDGEMENTS.....</b>	<b>13</b>
<b>TABLE OF CONTENTS.....</b>	<b>14</b>
<b>LIST OF FIGURES.....</b>	<b>23</b>
<b>LIST OF TABLES.....</b>	<b>39</b>
<b>LIST OF ABBREVIATIONS.....</b>	<b>40</b>
<b>CHAPTER 1</b>	
<b>INTRODUCTION.....</b>	<b>44</b>
1.1 INTRODUCTION STATEMENT .....	44
1.2 PATHOPHYSIOLOGY OF CEREBRAL ISCHEMIA.....	45
1.2.1 Background.....	45
1.2.2 Excitotoxicity.....	47
1.2.2.1 Excitatory Neurotransmitter: Glutamate.....	47
1.2.2.2 Receptor-mediated Excitotoxicity .....	47
1.2.2.3 Nonreceptor-mediated Excitotoxicity.....	49
1.2.3 Inflammation.....	49
1.2.4 Oxidative Stress.....	51
1.2.5 Apoptosis.....	52
1.3 STRATEGIES FOR THE TREATMENT OF CEREBRAL ISCHEMIA .....	54
1.3.1 Thrombolytic Therapy.....	55
1.3.1.1 Intravenous Thrombolysis.....	55
1.3.1.2 Intraarterial Thrombolysis.....	56

1.3.2	Anticoagulant Therapy.....	58
1.3.2.1	Heparin.....	59
1.3.2.2	Aspirin .....	60
1.3.2.3	Ancrod.....	61
1.3.3	Neuroprotective Therapy.....	62
1.3.3.1	Anti-Excitotoxicity.....	62
1.3.3.2	Antioxidant Therapy.....	64
1.3.3.3	Anti-inflammatory Therapy.....	65
1.3.3.4	Antiapoptotic Therapy.....	67
1.3.3.5	Hypothermia Therapy.....	68
1.3.4	Summary.....	69
1.4	ANIMAL MODELS OF ACUTE CEREBRAL ISCHEMIA .....	71
1.4.1	Global Models.....	71
1.4.1.1	Two Vessel Occlusion.....	71
1.4.1.2	Three Vessel Occlusion.....	72
1.4.1.3	Four Vessel Occlusion.....	72
1.4.2	Thromboembolytic Model.....	73
1.4.3	Focal Models.....	73
1.4.4	Attentions to the Evaluation of Neuroprotective Agents in Animal Models....	75
1.4.4.1	Appropriate Animal Model.....	75
1.4.4.2	Therapeutic Windows of Opportunity.....	76
1.4.4.3	Hypothermia.....	77
1.4.4.4	Drug Dose Design .....	77
1.4.4.5	Ways of Giving Drugs.....	78
1.4.5	Summary.....	78
1.5	NATURAL 3-ALKYLPHTHALIDE DERIVATIVES.....	79
1.5.1	Distribution and Categories of derivatives of 3-alkylphthalide in Plants.....	79
1.5.2	Pharmacological Profiles of 3-alkylphthalides.....	82
1.5.2.1	Protection on Cerebral Ischemic Injury.....	82
1.5.2.2	Effect on Central Nervous System .....	83

1.5.2.3 Relaxing Effect on Muscle.....	84
1.5.2.4 Regulation on Microcirculation .....	86
1.5.2.5 Antiproliferative Effects on Smooth Muscle Cells.....	87
1.5.2.6 Essence for Food Additive.....	87
1.5.2.7 Insecticidal Effect .....	88
1.5.3 Clinical Application of Derivatives of 3-Alkylphthalide.....	88
1.5.3.1 Treatment of Essential Oil of <i>Radix Angelica sinensis</i> for Irregular Menstruation and Amenorrhoea.....	88
1.5.3.2 Treatment of Butylphthalide for Acute Ischemic Stroke.....	89
1.6 PRIMARY PROPERTIES OF LIGUSTILIDE.....	90
1.7 OBJECTIVES.....	91
1.7.1 Part 1.....	91
1.7.2 Part 2.....	91
1.7.3 Part 3.....	92
1.7.4 Part 4.....	92
<b>CHAPTER 2</b>	
<b>MATERIALS, APPARATUS AND METHODS.....</b>	<b>107</b>
2.1 MATERIALS.....	107
2.1.1 Reagents and Analysis Kits.....	107
2.1.2 Apparatus.....	111
2.1.3 Animals.....	112
2.2 GENERAL METHODS.....	112
2.2.1 Cell Culture.....	112
2.2.1.1 Cell Culture Medium, Solutions and Reagents.....	113
2.2.1.2 Trypan Blue Staining of Cell.....	113
2.2.1.3 Cryopreservation of Cells.....	114
2.2.1.4 Thawing of Cryopreserved Cells.....	114
2.2.1.5 Caco-2 Cell Culture.....	115
2.2.1.6 C6 Glioma Cell Culture.....	116

2.2.2	Methods of Molecular Biology.....	116
2.2.2.1	DNA Preparation.....	116
2.2.2.2	Detection of Fragmented DNA by Agarose Gel Electrophoresis.....	118
2.2.2.3	Protein Preparation and Determination.....	119
2.2.2.4	Western Blot.....	121
2.2.3	Methods of Biochemistry and Chemistry.....	123
2.2.3.1	MTT Assay.....	123
2.2.3.2	DPPH Free Radical Scavenging Assay.....	124
2.2.3.3	Ferric Thiocyanate Assay .....	125
2.2.3.4	Thiobarbituric Acid Reactive Substances Assay .....	127
2.2.3.5	HPLC Measurement of Z-ligustilide.....	129
2.2.3.6	Measurement of MDA content and Activities of SOD and GSHPx .....	131
2.2.3.7	Measurement of NO content and iNOS activity.....	132
2.2.3.8	Measurement of Caspase-like Activities.....	133
2.2.4	Histochemical Methods.....	134
2.2.4.1	Microscopic Analysis of Nuclear Fragmentation .....	134
2.2.4.2	TTC Staining of Infarct Brain Tissue.....	135
2.2.4.3	Hematoxylin and Eosin Staining.....	136
2.2.4.4	Immunohistochemical Method.....	137
2.2.4.5	TUNEL Staining.....	139

### **CHAPTER 3**

#### **TRANSEPITHELIAL TRANSPORT OF Z-LIGUSTILIDE ACROSS CACO-2 MONOLAYERS.....143**

3.1	ABSTRACT.....	143
3.2	INTRODUCTION.....	144
3.3	MATERIALS AND METHODS.....	145
3.3.1	Materials .....	145
3.3.1.1	Materials.....	145

3.3.1.2	LIG Preparation .....	146
3.3.2	Methods.....	146
3.3.2.1	HPLC Assay of LIG .....	146
3.3.2.2	Stability Studies of LIG in Assay Buffer .....	148
3.3.2.3	Preparation of Caco-2 Monolayers.....	148
3.3.2.4	Transport Studies of LIG Across Caco-2 Monolayers.....	150
3.3.2.5	Statistic Analysis.....	152
3.4	RESULTS.....	152
3.4.1	HPLC Assay of LIG.....	152
3.4.1.1	Calibration Curves.....	153
3.4.1.2	Intra and Inter-day Variability.....	153
3.4.2	Assessment of Caco-2 Monolayers Integrity.....	153
3.4.3	Stability Studies of LIG under Transport Condition .....	154
3.4.4	Transport of LIG Across Caco-2 Monolayers.....	154
3.4.4.1	Temperature Dependency of LIG Transport in Bidirections of Caco-2 Monolayers.....	154
3.4.4.2	Effects of Additives on LIG Transport Across Caco-2 Monolayers.....	155
3.5	DISCUSSION.....	155

## **CHAPTER 4**

	<b>ANTIOXIDANT PROPERTIES AND PROTECTIVE EFFECTS of Z-LIGUSTILIDE ON HYDROGEN PEROXIDE-INDUCED OXIDATIVE DAMAGE IN C6 CELLS.....</b>	<b>165</b>
4.1	ABSTRACT.....	165
4.2	INTRODUCTION.....	166
4.3	MATERIALS AND METHODS.....	168
4.3.1	Materials.....	168
4.3.1.1	Materials.....	168

4.3.1.2	LIG Preparation.....	169
4.3.2	METHODS.....	169
4.3.2.1	DPPH Radical Scavenging Assay.....	169
4.3.2.2	Measurement of Autooxidation of Linoleic Acid .....	170
4.3.2.3	Assay for Lipid Peroxidation of Rat Cerebral Cortex Mitochondria.....	171
4.3.2.4	C6 Cell Culture .....	172
4.3.2.5	Assessment of Cell Viability.....	172
4.3.2.6	Microscopic Analysis of Nuclear Fragmentation.....	173
4.3.3	Statistical Analysis.....	174
4.4	RESULTS.....	174
4.4.1	DPPH Radical Scavenging Activity .....	174
4.4.2	Inhibition on Autooxidation of Linoleic Acid.....	175
4.4.3	Inhibition on Lipid Peroxidation of Rat Cerebral Cortex Mitochondria .....	175
4.4.4	Protection on C6 Cells Against Hydrogen Peroxide-induced Cytotoxicity...176	
4.4.5	Prevention of Hydrogen Peroxide-induced Apoptosis in C6 Cells .....	177
4.5	DISCUSSION.....	177

## **CHAPTER 5**

	<b>NEUROPROTECTION OF Z-LIGUSTILIDE AGAINST FOREBRAIN ISCHEMIA IN MICE MEDIATED BY ANTIOXIDATION AND ANTIAPOPTOSIS.....</b>	<b>190</b>
5.1	ABSTRACT .....	190
5.2	INTRODUCTION.....	191
5.3	MATERIALS AND METHODS.....	194
5.3.1	Materials.....	194
5.3.1.1	Chemicals .....	194
5.3.1.2	Animal Preparation.....	195
5.3.1.3	Drug Preparation.....	195
5.3.2	Methods.....	195

5.3.2.1	Murine Forebrain Ischemic Model.....	196
5.3.2.2	LIG Treatment Schedule.....	196
5.3.2.3	Brain Tissue Preparation.....	197
5.3.2.4	Estimation of Neuronal Loss .....	198
5.3.2.5	Measurement of Antioxidant Enzyme Activities.....	198
5.3.2.6	Measurement of Lipid Peroxidation.....	199
5.3.2.7	Western Blot Analyses .....	200
5.3.2.8	Caspase-3 Activity Assay.....	202
5.3.2.9	TUNEL Staining.....	203
5.3.2.10	DNA Fragmentation Assay.....	204
5.3.2.11	Statistical Analysis.....	205
5.4	RESULTS.....	205
5.4.1	Neuronal Protection .....	206
5.4.2	Antioxidant Potential.....	206
5.4.3	Expression of Bcl-2 and Bax .....	207
5.4.4	Cytochrome C Release .....	207
5.4.5	Activation of Caspase 3.....	208
5.4.6	Formation of Apoptotic-positive Cells.....	208
5.4.7	Formation of DNA Fragmentation.....	209
5.5	DISCUSSION.....	210

## **CHAPTER 6**

	<b>Z-LIGUSTILIDE THERAPY PROTECTS BRAIN AGAINST BOTH APOPTOSIS AND NECROSIS IN FOCAL CEREBRAL ISCHEMIA IN RATS.....</b>	<b>228</b>
6.1	ABSTRACT .....	228
6.2	INTRODUCTION.....	231
6.3	MATERIALS AND METHODS.....	233
6.3.1	Materials.....	234

6.3.1.1	Chemicals.....	234
6.3.1.2	Animal Preparation.....	234
6.3.1.3	Drug Preparation.....	235
6.3.2	Methods.....	235
6.3.2.1	Focal Cerebral Ischemia Model.....	235
6.3.2.2	Neurological Deficit Scores.....	236
6.3.2.3	Experimental Treatment Schedule.....	238
6.3.2.4	Measurement of Body Temperature.....	238
6.3.2.5	Estimation of Ischemic Infarction Size .....	239
6.3.2.6	Brain Tissue Preparation.....	240
6.3.2.7	Western Blot Analyses .....	241
6.3.2.8	Caspase-like Activity Assay .....	243
6.3.2.9	Immunohistochemical Examination .....	244
6.3.2.10	NO Content Measurement .....	245
6.3.2.11	Determination of iNOS Activity .....	246
6.3.2.12	TUNEL Staining.....	246
6.3.2.13	Statistical Analysis.....	247
6.4	RESULTS.....	248
6.4.1	Infarction Size in Ischemic Rats.....	248
6.4.2	Body Temperature Changes following Transient MCAO.....	248
6.4.3	Neurological Deficit Scores.....	249
6.4.4	Cytosolic Release of Cytochrome C .....	250
6.4.5	Activation of Caspase-3 and Caspase-8 .....	250
6.4.6	Induction of iNOS Activity .....	251
6.4.7	Activation of Microglia .....	252
6.4.8	Formation of TUNEL-positive Cells.....	253
6.5	DISCUSSION.....	254
 <b>CHAPTER 7</b>		
<b>GENERAL DISCUSSION.....</b>		<b>279</b>

**REFERENCES.....288**

## LIST OF FIGURES

**Figure 1-1.** The structures of 3-alkylphthalides and their derivatives. (1). 3-alkylphthalides (structure number 1-12); (2). Mono- or bi-hydroxy derivatives of 3-alkylphthalide (structure number 13-35); (3). Demeric derivatives of 3-alkylphthalide (structure number 36-51).

**Figure 1-2.** The configuration structures of ligustilide. Molecular Weight: 190.24.

**Figure 2-2.** Reaction between TBA and MDA to yield the TBA-MDA adduct.

**Figure 2-1.** Reaction of DPPH<sup>•</sup> with a hydrogen donor.

**Figure 3-1.** A typical HPLC profile of LIG recorded at 280 nm. (Analytical column: Alltima C<sub>18</sub>, 5μm, 150mm×4.6 mm; guard column: C<sub>18</sub>, 5μm, 7.5mm×4.6 mm; mobile phase: methanol-5% isopropyl alcohol (60:40); flow rate: 1.0 ml/min; temperature: ambient.) The retention time of LIG is 9.02 min under the condition described above.

**Figure 3-2.** LIG standard curve. A calibration curve fitted by plotting the mean of the three peak areas (y) against the quantity of LIG (x) gave the following regression equation:  $y=1861.6x + 40.174$  with determination coefficient  $r = 0.9995$ .

**Figure 3-3.** The TEER values of Caco-2 cells during differentiation. The data represent means  $\pm$  SD ( $n = 24$ ).

**Figure 3-4.** The percent change of TEER values of Caco-2 monolayers before (Control) or after addition of the LIG solution (1.5 mM LIG). The data represent mean  $\pm$  SD ( $n = 3$ ).

**Figure 3-5.** The stability of LIG in pH 7.4 HBBS buffer, measured as the chromatographic peak areas. The data represent the mean  $\pm$  SD ( $n = 3$ ).

**Figure 3-6.** The transport profile of LIG in bidirections across the Caco-2 monolayers at 37 °C or 4 °C. The data represent the mean  $\pm$  SD ( $n = 3$ ).

**Figure 3-7.** The effect of temperature on the permeability of LIG in AP-BL (■) or BL-AP (□) direction across the Caco-2 monolayers. The data represent the mean  $\pm$  SD ( $n = 3$ ).

**Figure 3-8.** The transport profile of AP-BL of LIG across the Caco-2 monolayers in the assay buffer (■), 10  $\mu$ M Cyclosporin A (▲), or calcium-free assay buffer (○) in the apical medium. The data represent the mean  $\pm$  SD ( $n = 3$ ).

**Figure 3-9.** The permeability of AP-BL flux of LIG in the Caco-2 monolayers in the

presence or absence of additives in the apical medium. The data represent the mean  $\pm$  SD (n = 3).

**Figure 4-1.** The scavenging effect of LIG on DPPH radical. The free radical scavenging activity was measured by the degree of decoloration of a DPPH solution. The indicated concentration of LIG was added to a 100 $\mu$ M ethanolic solution of DPPH. Decoloration percentage was measured at the indicated incubation time at 25 °C. Each value represents the average obtained in three different experiments in each of which four measurements were made. The data points without error bar indicate that standard deviation is too small to be seen. Key: ( $\Delta$ ) 5 mM LIG; ( $\bullet$ ) 20 mM LIG; ( $\blacktriangle$ ) 80 mM LIG.

**Figure 4-2.** The percentage reduction of the DPPH radical by LIG. The free radical scavenging activity was measured after 180 min incubation at 25 °C. Each value represents the average obtained in three different experiments in each of which four measurements were made.

**Figure 4-3.** The antioxidant activity of LIG on the oxidation of linoleic acid emulsion. The activity was determined by the thiocyanate method. The indicated concentration of LIG or volume-matched vehicle was added to the linoleic acid emulsion. The amount of peroxides was measured in the linoleic acid emulsion at the indicated incubation time at 37 °C. Each value represents the average obtained in three different

experiments performed in triplicate. Key: (◆) control; (□) 5 mM LIG; (◇) 20 mM LIG; (▲) 80 mM LIG.

**Figure 4-4.** The percentage inhibition of the lipid peroxidation of LIG in the linoleic acid emulsion. The free radical scavenging activity was measured after a 96 h incubation at 37 °C. Values represent mean  $\pm$  SD (n = 4). Each value represents the average obtained in three different experiments.

**Figure 4-5.** The inhibition effect of LIG on Fe<sup>2+</sup>/ascorbate-induced lipid peroxidation in rat cerebral cortex mitochondria. Brain mitochondria (3 mg of protein /ml) were incubated with the Fe<sup>2+</sup>/ascorbate acid generating system, in the presence of 10  $\mu$ l of the indicated concentrations of LIG or just the control solvent for 30 min at 37 °C. TBARS was measured as described in materials and methods. Values represent mean  $\pm$  SD (n = 4). Each value represents the average obtained in three different experiments performed.

**Figure 4-6.** The inhibition effect of LIG on the NADPH-dependent lipid peroxidation in rat cerebral cortex mitochondria. Brain mitochondria (3 mg of protein/ml) were incubated with the NADPH generating system, in the presence of 10  $\mu$ l of the indicated concentrations of LIG or just the control solvent for 30 min at 37 °C. TBARS was measured as described in materials and methods. Values represent mean  $\pm$  SD (n = 4).

**Figure 4-7.** Representative photomicrographs showing the protective effect of LIG on H<sub>2</sub>O<sub>2</sub>-induced C6 cell injury. The C6 cells were incubated in the presence of the various indicated concentrations of LIG for 24 h and then 500 μM H<sub>2</sub>O<sub>2</sub> for another 24 h. A: normal cells, B: H<sub>2</sub>O<sub>2</sub> -treated cells which showed a significant decrease in cell number and most of them demonstrated the round shape, C-F: LIG (final concentration of 0.5, 5, 25 and 50 μM, respectively) prevented H<sub>2</sub>O<sub>2</sub>-induced cell injury in a concentration-dependent manner. 100-fold magnification.

**Figure 4-8.** The protective effect of LIG on H<sub>2</sub>O<sub>2</sub>-induced cytotoxicity in C6 cells with the MTT assay. The C6 cells were incubated in the presence of the various indicated concentrations of LIG for 24 h and then 500 μM H<sub>2</sub>O<sub>2</sub> for another 24 h. H<sub>2</sub>O<sub>2</sub>-treated cells showed greatly reduction in cell viability. LIG prevented H<sub>2</sub>O<sub>2</sub>-induced cytotoxicity in a dose-dependent manner. Each value is the mean ± SD (n = 6) expressed as a percentage of control cultures. \**P* < 0.05, \*\**P* < 0.01 vs the group of H<sub>2</sub>O<sub>2</sub> treatment.

**Figure 4-9.** The effect of LIG on H<sub>2</sub>O<sub>2</sub>-induced apoptotic cell death in the C6 cells with Hoechst 33342 staining. The C6 cells were incubated in the presence of the various indicated concentrations of the tested samples for 24 h and then 500 μM H<sub>2</sub>O<sub>2</sub> for another 24 h. A: normal cells, B: the H<sub>2</sub>O<sub>2</sub>-treated cells which showed chromatin condensation and/or nuclear fragmentation, C-F: LIG (final concentration of 0.5, 5, 25 and 50 μM, respectively) prevented H<sub>2</sub>O<sub>2</sub>-induced apoptotic cell death in a

dose-dependent manner. Original magnification:  $\times 400$ .

**Figure 5-1.** The effect of LIG to salvage on the cerebral neurons in the forebrain ischemia/reperfusion mice. HE staining was performed as described in Materials and Methods. Animals received the treatment of an orally administrated LIG, or a volume-matched vehicle at the start of reperfusion and again daily in the subsequent 5 days. A-C: the total hippocampal CA1 and the cortex of the sham-operated control, D-F: the total hippocampal CA1 and the cortex of the vehicle-treated control, G-I: the total hippocampal CA1 and the cortex of 20 mg/kg LIG, H-J: the total hippocampal CA1 and the cortex of 80 mg/kg LIG. Lower panel (K) represents the analyses of normal neurons in a neuronal cell density per 0.5 mm linear length of the CA1 subfield ( $\times 400$  magnification). Results represent the means  $\pm$  SD of six animals of each group.  $**P < 0.01$  versus the vehicle-treated control group.

**Figure 5-2.** The antioxidative effects of LIG in the ischemic brain tissue of mice subjected to 30 min of BCCAO/ 5 d reperfusion. The data represent the mean  $\pm$  SD (n = 6). Animals received the treatment of the orally administrated LIG, or volume-matched vehicle at the start of reperfusion and again daily in the subsequent 5 days. A. The effect of LIG on the level of SOD of the ischemic brain tissue. B. The effect of LIG on the activity of GSHPx of the ischemic brain tissue. C. The effect of LIG on the MDA content of the ischemic brain tissues.  $*P < 0.05$ ,  $**P < 0.01$  versus the vehicle-treated control group.

**Figure 5-3.** Effect of LIG on Bcl-2 expression in the ischemic brain tissues of mice subjected to 30min of BCCAO/5 d reperfusion. Animals received LIG (20 or 80 mg/kg, orally administrated) or a volume-matched vehicle (con) at the start of reperfusion and again daily in subsequent 5 days. Western blot analysis was performed as described in Materials and Methods. A: The expected molecular weight of Bcl-2 ~26 kDa and  $\beta$ -actin ~43 kDa bands appearing on each gel. B: Quantification of the effect of LIG on the expression of Bcl-2 in the ischemia-reperfusion brain. Expression values were normalized for  $\beta$ -actin and expressed as a percentage of sham group. Results are expressed as mean  $\pm$  SD of 3 separate experiments.  $**P < 0.01$  versus the control group.

**Figure 5-4.** The effect of LIG on Bax expression in the ischemic brain tissues of mice subjected to 30min of BCCAO/5 d reperfusion. Animals received LIG (20 or 80 mg/kg, orally administrated) or a volume-matched vehicle (control) at the start of reperfusion and again daily in the subsequent 5 days. Western blot analysis was performed as describes in Materials and Methods. A: The expected molecular weight of Bax ~20 kDa and  $\beta$ -actin ~43 kDa bands appearing on each gel. B: Quantification of the effect of LIG on the expression of Bax in the ischemia-reperfusion brain. Expression values were normalized for  $\beta$ -actin and expressed as a percentage of the sham group. Results are expressed as the mean  $\pm$  SD of 3 separate experiments.  $*P < 0.05$ ,  $**P < 0.01$  versus the control group.

**Figure 5-5.** The effect of LIG on the cytosolic cytochrome c expression in the ischemic brain tissue subjected to 30min of BCCAO /5 d of reperfusion. Animals received LIG (20 or 80 mg/kg, orally administrated) or volume-matched vehicle (control) at the start of reperfusion and again daily in the subsequent 5 days. Western blot analysis was performed as describes in Materials and Methods. A: The expected molecular weight of the cytochrome c ~11 kDa and  $\beta$ -actin ~43 kDa bands appearing on each gel. B: Quantification of the effect of LIG on the expression of cytosolic cytochrome c in the ischemia-reperfusion brain. The expression values were normalized for  $\beta$ -actin and expressed as a percentage of the sham group. Results are expressed as the mean  $\pm$  SD of 3 separate experiments. \* $P < 0.05$  versus the control group.

**Figure 5-6.** The effect of LIG on the expression of cleaved caspase-3 in the ischemic brain tissue of mice subjected to 30min of BCCAO /5 d of reperfusion. Animals received LIG (20 or 80 mg/kg, orally administrated) or the volume-matched vehicle (con) at the start of reperfusion and again daily in the subsequent 5 days. Western blot analysis was performed as described in Materials and Methods. A: The expected molecular weight of cleaved caspase-3 ~19 kDa and  $\beta$ -actin ~43 kDa bands appearing on each gel. B: Quantification of the effect of LIG on the expression of cleaved caspase-3 in ischemia-reperfusion brain. Expression values were normalized for  $\beta$ -actin and expressed as a percentage of the sham group. Results are expressed as the mean  $\pm$  SD of 3 separate experiments. \* $P < 0.05$ , \*\* $P < 0.01$  versus the control group.

**Figure 5-7.** The inhibition of caspase-3 activity in the ischemic brain tissue by the treatment of LIG on mice subjected to 30 min of BCCAO/5 days reperfusion. Animals received LIG (20 or 80 mg/kg, orally administrated) or volume-matched vehicle (control) at the start of reperfusion and again daily in subsequent 5 days. The activity of caspase 3 was measured as described in Materials and Methods. Caspase activity was expressed as the optical density unit percent of the sham-operated control group at 405 nm. Data shown are the mean  $\pm$  SD (n = 6). \* $P$  < 0.05, \*\* $P$  < 0.01 versus the vehicle-treated control group.

**Figure 5-8.** The effect of LIG on the development of the apoptotic cells in the ischemic cortex of mice subjected to 30 min of BCCAO /5 days of reperfusion. (A-D) Representative photographs of TUNEL staining in the cerebral cortex. TUNEL-positive apoptotic cells exhibit condensation and fragmentation of nuclei and apoptotic bodies around the nuclear membrane without cytoplasmic staining (arrow). A: sham-operated control, B: vehicle-treated control, C and D: 80 or 20 mg/kg LIG orally administrated at the start of reperfusion and the subsequent 5 days. The magnification was 400  $\times$ . (E) Quantification of the apoptotic cells in the ischemic cortex. Results represent the mean  $\pm$  SD of four animals of each group. \* $P$  < 0.05, \*\* $P$  < 0.01 versus the vehicle-treated control group.

**Figure 5-9.** The effect of LIG on the formation of DNA laddering in the ischemic brain of mice subjected to 30 min of BCCAO/ 5 d reperfusion. The internucleosomal

DNA-fragmentation was analysed electrophoretically as described in Methods. Animals were divided into the sham-operated control (sham), and the vehicle-treated control (con), LIG-treated groups at doses of 20 or 80 mg/kg LIG, orally administered at the start of reperfusion and again daily in subsequent 5 days. M represents the 100-bp DNA ladder marker. A: representative findings of the agarose gel electrophoresis showing DNA laddering. B: The results of densitometric analysis representing mean  $\pm$  SD of four animals. \* $P < 0.05$ , \*\* $P < 0.01$  versus the control group.

**Figure 6-1.** The location of cerebral infarcts and regions sampled for histological analyses in the focal cerebral ischemic rat. Panels show coronal sections at bregma -1.3 to -3.3 mm from representative (A) the vehicle-treated and (B) the LIG-treated animals, respectively. The infarct tissues are shown in gray. In the ipsilateral (ischemic) hemisphere: a= the region of the dorsolateral cortex at the borders of infarcts in the vehicle-treated animals. This region was typically spared in the LIG-treated animals and can be considered part of the ischemic penumbra. b = the region of the lateral cortex in the ischemic core of infarcts in both the vehicle- and LIG-treated animals.

**Figure 6-2.** Illustrative coronal sections showing the infarct area in the ipsilateral hemisphere of the MCAO rats. The infarct area was stained as a distinct pale-stained area in the rats subjected to 2 h of ischemia/24 h of reperfusion (left) and attenuation of the infarct area by treatment with orally administered 20 or 80 mg/kg LIG at the start

and again at 4 h of reperfusion.

**Figure 6-3.** The dose-dependent inhibitory effect of LIG on the infarct volume of the ischemic hemisphere in rats subjected to 2 h MCAO/24 h reperfusion. Animals received LIG (20 or 80 mg/kg, orally administrated) or the volume-matched vehicle (control) at the start and again at 4 h of reperfusion. The infarct volume was significantly decreased by treatment with 20 or 80 mg/kg LIG. Results are expressed as the mean  $\pm$  SD of 4~5 animals. **\*\* $P < 0.01$**  versus the vehicle-treated control group.

**Figure 6-4.** The effect of LIG on the core body temperature of rats during 24 h of reperfusion following 30 min of MCAO. Rats were treated with either LIG (20, 80 mg/kg) or vehicle immediately following MCAO and again at 4 h postischemia. All data are represented as the mean  $\pm$  SD (n = 14~16).

**Figure 6-5.** The dose-dependent inhibitory effect of LIG on the neurological scores of the rats subjected to 2 h MCAO/24 h reperfusion. Animals received LIG (20 or 80 mg/kg, orally administrated) or the volume-matched vehicle (control) at the start and again at 4 h of reperfusion. The neurological deficit scores were significantly decreased by the treatment with 20 or 80 mg/kg LIG. Results are expressed as the mean  $\pm$  SD of 14 ~16 animals. **\*\* $P < 0.01$**  versus the vehicle-treated control group.

**Figure 6-6.** The effect of LIG on the cytosolic cytochrome c expression in the

ischemic brain tissues of rats subjected to 2 h MCAO/24 h reperfusion. Animals received LIG (20 or 80 mg/kg, orally administrated) or the volume-matched vehicle (control) at the start and again at 4 h of reperfusion. Western blot analysis was performed as described in Materials and Methods. A: The expected molecular weight of cytochrome c ~11 kDa and  $\beta$ -actin ~43 kDa bands appearing on each gel. B: Quantification of the effect of LIG on the expression of cytosolic cytochrome c in the ipsilateral hemisphere. Expression values were normalized for  $\beta$ -actin and expressed as a percentage of the sham group value. Results are expressed as the mean  $\pm$  SD of 3 separate experiments. \* $P < 0.05$  versus the vehicle-treated control group.

**Figure 6-7.** The effect of LIG on the cleaved caspase-3 expression in the ischemic brain tissues of rats subjected to 2 h MCAO/24 h reperfusion. Animals received LIG (20 or 80 mg/kg, orally administrated) or the volume-matched vehicle (control) at the start and again at 4 h of reperfusion. Western blot analysis was performed as described in Materials and Methods. A: The expected molecular weight of cleaved caspase-3 ~19 kDa and  $\beta$ -actin ~43 kDa bands appearing on each gel. B: Quantification of the effect of LIG on the expression of the cleaved caspase-3 in the ipsilateral hemisphere. Expression values were normalized for  $\beta$ -actin and expressed as a percentage of sham group. Results are expressed as the mean  $\pm$  SD of 3 separate experiments. \* $P < 0.05$ , \*\* $P < 0.01$  versus the vehicle-treated control group.

**Figure 6-8.** The effect of LIG on the cleaved caspase-8 expression in the ischemic

brain tissues of rats subjected to 2 h MCAO/24 h reperfusion. Animals received LIG (20 or 80 mg/kg, orally administrated) or the volume-matched vehicle (control) at the start and again at 4 h of reperfusion. Western blot analysis was performed as described in Materials and Methods. A: The expected molecular weight of cleaved caspase-8 ~20 kDa and  $\beta$ -actin ~43 kDa bands appearing on each gel. B: Quantification of the effect of LIG on the expression of the cleaved caspase-3 in the ipsilateral hemisphere. Expression values were normalized for  $\beta$ -actin and expressed as a percentage of sham group. Results are expressed as the mean  $\pm$  SD of 3 separate experiments. \* $P < 0.05$ , \*\* $P < 0.01$  versus the vehicle-treated control group.

**Figure 6-9.** The inhibition of the caspase-like activities by the treatment of LIG in the ischemic brain tissues rats subjected to 2 h MCAO/24 h reperfusion. Animals received LIG (20 or 80 mg/kg, orally administrated) or the volume-matched vehicle (control) at the start and 4 h of reperfusion. The activity of the caspase 8 (solid column) or caspase 3 (open column) was measured as described in Materials and Methods. Caspase activity was expressed as the optical density unit percent of the sham-operated control group at 405 nm. Data shown are the mean  $\pm$  SD (n = 4). \*\* $P < 0.01$  versus the vehicle-treated control group.

**Figure 6-10.** The effect of LIG on iNOS positive cells within the infarct penumbra of the focal ischemic rats subjected to 2 h MCAO/24 h of reperfusion. The iNOS positive staining was mainly detected in the microglia (arrows). A: the sham-operated control,

B: the vehicle-treated control, C and D: 20 or 80 mg/kg LIG orally administered at the start and again at 4 h of reperfusion. The magnification was 400 ×. Lower panel (E) represents the analyses of iNOS positive cells per high power field. Results represent the mean ± SD of four animals of each group. \**P* < 0.05, \*\**P* < 0.01 versus the vehicle-treated control group.

**Figure 6-11.** The effect of LIG on iNOS activity in the ischemic brain tissues of rats after 2 h of MCAO /24 h of reperfusion. Animals received oral administration of LIG (20 or 80 mg/kg) or the volume-matched vehicle at the start and again at 4 h of reperfusion. Results represent the mean ± SD (n = 6). \**P* < 0.05, \*\**P* < 0.01, versus the vehicle-treated group.

**Figure 6-12.** The effect of LIG on the NO content in the ischemic brain tissues of rats subjected to 2 h of MCAO/24 h of reperfusion. Animals received oral administration of LIG (20 or 80 mg/kg) or the volume-matched vehicle at the start and again at 4 h of reperfusion. The level of NO was analyzed by the Griess reaction described as Methods. Results represent the mean ± SD (n = 6). \**P* < 0.05, versus the vehicle-treated group.

**Figure 6-13.** The effect of LIG on the development of OX42 positive microglial cells within the infarct penumbra of focal ischemic rats subjected to 2 h of ischemia/24 of reperfusion. The cell specific positive staining of OX42 was detected in the activated

microglia (arrows). A: the sham-operated control, B: the vehicle-treated control, C and D: 20 or 80 mg/kg LIG orally administrated at the start and again at 4 h of reperfusion. The magnification was 400 ×. Lower panel (E) represents the analyses of activated microglia. Results represent the mean ± SD of four animals of each group. \*\* $P < 0.01$  versus the vehicle-treated control group.

**Figure 6-14.** The effect of LIG on the development of TUNEL-positive cells in the ischemic cortical penumbra of the focal ischemic rats subjected to 2 h of ischemia/24 h of reperfusion. (A) Representative photographs of TUNEL staining in the ischemic cortical penumbra. TUNEL-positive apoptotic cells exhibit a condensation and fragmentation of nuclei and apoptotic bodies around the nuclear membrane without cytoplasmic staining (arrow). TUNEL-positive necrotic cells exhibit a diffused labeling compared to the apoptotic cells, without the fragmentation of nuclei or apoptotic bodies (arrowhead). a: the sham-operated control, b: the vehicle-treated control, c and d: 80 or 20 mg/kg LIG orally administrated at the start and again at 4 h of reperfusion. The magnification was 400 ×. (B) Quantification of apoptotic and necrotic cells in the ischemic penumbra. Results represent the mean ± SD of four animals of each group. \* $P < 0.05$ , \*\* $P < 0.01$  versus the vehicle-treated control group.

**Figure 6-15.** The effect of LIG on the development of TUNEL-positive cells in the ischemic cortical core of the focal ischemic rats subjected to 2 h of ischemia/24 h of reperfusion. (A) Representative photographs of TUNEL staining in the ischemic

cortical core. TUNEL-positive apoptotic cells exhibit a condensation and fragmentation of nuclei and the apoptotic bodies around the nuclear membrane without cytoplasmic staining (arrow). TUNEL-positive necrotic cells exhibit a diffused labeling compared to the apoptotic cells, without a fragmentation of nuclei or apoptotic bodies (arrowhead). a: the sham-operated control, b: the vehicle-treated control, c and d: 80 or 20 mg/kg LIG orally administrated at the start and again at 4 h of reperfusion. The magnification was 400 ×. (B) Quantification of apoptotic and necrotic cells in the ischemic core. Results represent the mean ± SD of four animals of each group. \* $P < 0.05$ , \*\* $P < 0.01$  versus the vehicle-treated control group.

## **LIST OF TABLES**

**Table 3-1.** Intra-Assay variability in the HPLC analysis of LIG.

**Table 3-2.** Inter-Assay variability in the HPLC analysis of LIG.

## LIST OF ABBREVIATIONS

AMPA	$\alpha$ -amino-3-hydroxy-5-methyl-4-isoxazole propionic acid
APES	Aminopropyltriethoxysilane
ATCC	American Type Culture Collection
ATP	Adenosine triphosphate
BBB	Blood brain barrier
BCCAO	Occlusion of bilateral common carotid arteries
BSA	Bovine serum albumin
Caco-2	Human colon adenocarcinoma cells
CCA	Common carotid artery
CNS	Central nervous system
COX-2	Cyclooxygenase 2
DAB	3,3'-diaminobenzidine
DEVD- <i>p</i> NA	Asp-Glu-Val-Asp- <i>p</i> -nitroanilide
DMEM	Dulbecco's modified Eagle's medium
DMSO	Dimethyl sulphoxide
DPPH	2,2-diphenyl-1-picrylhydrazyl
EDTA	Ethylenediamine tetraacetic acid
FBS	Fetal bovine serum
FDA	Food and Drug Administration
GABA	Gamma-aminobutyric acid

GSH	Glutathione
GSHPx	Glutathione peroxidase
h	Hour (s)
HBSS	Hank's balanced salt solution
HEPES	N-(2-hydroxyethyl) piperazine-N'-(2-ethanesulfonic acid)
ICAM-1	Intercellular adhesion molecule 1
IETD- <i>p</i> NA	Ile-Glu-Thr-Asp - <i>p</i> -nitroanilide
IHC	Immunohistochemistry
iNOS	Inducible nitric oxide synthase
LIG	Z-ligustilide
LMWHs	Low-molecular-weight heparins
MCA	Middle cerebral artery
MCAO	Occlusion of middle cerebral artery
MDA	Malondialdehyde
min	Minute(s)
MTT	3-(4,5-dimethyl-2-thiazoloyl)-2,5-diphenyl-2H-tetrazolium bromide
NADPH	Reduced nicotinamide adenine dinucleotide phosphate
NBP	3-n-butylphthalide
NMDA	N-methyl-D-aspartate
NO	Nitric oxide
NOS	Nitric-oxide synthase
NRGE	Nonreceptor-mediated glutamate excitotoxicity

Papp	Apparent permeability coefficients
PBS	Phosphate-buffered saline
P- gp	P-glycoprotein
PMSF	Phenylmethyl sulfonyl fluoride
PVDF	Polyvinylidene difluoride
rCBF	Regional cerebral blood flow
RT	Room temperature
SDS	Sodium dodecyl sulfate
SDS-PAGE	Sodium dodecyl sulfate- polyacrylamide gel electrophoresis
sec	Second(s)
SMC	Smooth muscle cell
SOD	Superoxide dismutase
TBA	2-thiobarbituric acid
TBE	Tris-boric acid EDTA solution
TBARS	Thiobaritric acid reactive substances
TBS	Tris buffered solution
TBS-T	TBS containing 0.1% Tween-20
TE	Tris-EDTA solution
TEER	Transepithelial electrical resistance
TNF	Tumor necrosis factor
tPA	Tissue plasminogen activator
TUNEL	Terminal deoxynucleotidyl transferase (TdT)-mediated dUTP

nick-end-labeling

UFH

Unfractionated heparin

# CHAPTER 1

## INTRODUCTION

### 1.1 Introduction Statement

The aim of this chapter is to provide a general introduction to this thesis.

Ischemic cerebrovascular disease is the third leading cause of death, and the first cause of disability and morbidity in industrialized countries. Stroke is also the second most common cause of dementia (Bonita, 1992). Approximately 20% of stroke patients do not survive the first month and less than 30% of those who survive the first six months would become dependent on others (Warlow, 1998). In correlation with the socio-economic importance of ischemic stroke, an impressive number of neuroprotective compounds have been developed for clinical trial in the last few decades. The only effective therapy currently available is tissue plasminogen activator (tPA) approved by the Food and Drug Administration (FDA), USA (Albers, 1999; Traynelis and Lipton, 2001). However, the risk of cerebral hemorrhage associated with tPA use means that only a small percentage (approximately 7%) of the ischemic stroke patients qualifies for this therapy. Neuroprotective agents with different modes of action and an extended application time window are therefore urgently required.

3-alkylphthalide derivatives, which exist widely in natural Umbelliferaceae plants, have been shown to possess various bioactive effects. Recent studies have shown that 3-n-butylphthalide, a component isolated from the seeds of *Apium graveolens* Linn, has many significant protective effects on brain ischemic damage, including reducing the neuronal apoptosis and the infarct volume in transient focal cerebral ischemia in rats, lengthening the life span and improving the neurological deficit in stroke-prone

and spontaneously hypertensive rats (Chang and Wang, 2003; Liu and Feng, 1995; Zhang and Feng, 1996). This agent has been proven effective in clinical trials and approved for the treatment of acute ischemic stroke by the State Food and Drug Administration of China (Cui et al., 2005; Wang and Huang, 2003).

3-n-butylidene-4,5-dihydrophthalide (ligustilide) is a characteristic phthalide component of Umbelliferae plants and has been considered as the main biologically active component of many important medical plants, such as the roots of *Angelica sinensis* (Lin et al., 1979), *Ligusticum wallichii* (Wang et al., 1984), *Ligusticum chuangxiong* (Naito et al., 1996), and *Cnidium officinale* (Bohrmann et al., 1967). It was reported that about 50% of the essential oil from the roots of *Angelicae sinensis* comprise of ligustilide (Fang et al., 1979; Li et al., 2001), and Z-ligustilide (LIG) is the main configuration since its content is 10 times as much as the E-form (Li et al., 2001). LIG has a chemical structure similar to 3-butylphthalide except the different active dihydrobenzene and 3-double bond, which is related to the antioxidant activity. Since the involvement of oxidative stress in neuronal loss following ischemia has been well established (Li, et al., 1995; Ratan et al., 1994; Whittemore et al., 1995), the structural features of LIG suggest that it may be of neuroprotective potential in cerebral ischemia. However, there is not yet any related study reported.

## **1.2 Pathophysiology of Cerebral Ischemia**

### **1.2.1 Background**

Stroke compromises blood flow to the brain and can result from a number of conditions. Hemorrhagic stroke refers to the bleeding in the brain or on its surface whereas ischemic stroke (cerebral ischemic damage) occurs when blood flow to the brain is reduced. In clinic, most strokes (~85%) are ischemic and may be classified as focal or global. Focal ischemia results from the occlusion of a cerebral artery by a

thrombus or an embolism, which leads to the loss of blood flow in a specific region, whereas global ischemia is caused by a decrease or cessation of blood flow in the entire brain. Neuronal function and survival require an appropriate supply of blood to the nervous system. The reduction of blood flow to the brain can result in a decrease of perfusion pressure (pH), and blood oxygen content and an increase in carbon dioxide content. All of these factors contribute to vasodilation. If vasodilation cannot compensate for the decreased blood pressure, the blood flow would decrease and the oxygen extraction fraction increase. If the neurons are still deprived of oxygen, adenosine triphosphate (ATP) levels are maintained by increasing glycolysis (Frizzell et al., 1991). When blood pressure is sufficiently compromised, all of these compensatory mechanisms put together would be unable to maintain the neuronal function and survival, then cell death begins to appear. In general, the types of neuronal cell death may be classified as necrosis or apoptosis based on the morphological features. Necrotic neuronal cell is characterized by cell swelling, rupture of the protoplasmic and nuclear membranes, and the membranes of organelles (Trump et al., 1984). The necrotic process is correlated with a strong inflammatory reaction due to the spilling of cell content into the extracellular space. Apoptotic cells are characterized by a cytoplasmic and nuclear condensation with preserved membranes and phagocytosed by microglia (Wyllie et al., 1984). Which kind of the death outcome occurs mainly depends on the severity of insults (Leist and Nicotera, 1998; Onteniente et al., 2003). Previous studies have shown that when the regional cerebral blood flow (rCBF) drops below 10% of the control values, such as in the core of the lesion in a stroke, cells die through the energy-independent pathway that mainly include a necrotic process within a few minutes or hours, and probably a “death-receptor” apoptosis as well (Benchoua et al., 2002). In the remaining arterial territory, or penumbra, rCBF levels are kept at up to 40% of control values due to retrograde perfusion by anastomosis from the adjacent arteries. In this area, the ATP levels remain high enough to allow apoptosis, an energy dependent mechanism, and cell death is delayed by hours or even days. Therefore, neuroprotective therapies, which focus on the delayed neurodegenerative progress, will provide promising

approaches to promote neuronal survival and function in cerebral ischemia.

In the past 20 years numerous efforts have been made to understand the neuropathological mechanisms involved in cerebral ischemia. The increased knowledge shows that the ischemic delayed damage results from a complex sequence of neurotoxic events. The major pathophysiologic mechanisms of this cascade include excitotoxicity, inflammation, oxidative stress and apoptosis.

## **1.2.2 Excitotoxicity**

### **1.2.2.1 Excitatory Neurotransmitter: Glutamate**

Glutamate serves as a neurotransmitter for both fast excitatory synaptic transmissions and slow long-term excitatory changes (Michaelis, 1998).

The physiological action of glutamate is mediated through the activation of glutamate receptors found throughout the CNS. Glutamate receptors can be broadly divided into two classes: ionotropic and metabotropic (Greenamyre and Porter 1994; Michaelis 1998; Ozawa et al., 1998). Ionotropic glutamate receptors can be further subdivided into three categories: NMDA (N-methyl-D-aspartate), AMPA ( $\alpha$ -amino-3-hydroxy-5-methyl-4-isoxazolepropionic acid) and kainite receptors. Ionotropic glutamate receptors directly mediate glutamate excitotoxicity whereas metabotropic glutamate receptors are G-protein-linked receptors that are important in activating various second messengers (Ozawa et al., 1998).

### **1.2.2.2 Receptor-mediated Excitotoxicity**

While glutamate mediating excitatory transmission is indispensable for normal information processing and neuronal plasticity, an excess and sustained activation of ionotropic glutamate receptors would result in fulminant neuronal death (Michaelis,

1998).

Brain tissue has a relatively high consumption of oxygen and glucose, and depends almost exclusively on oxidative phosphorylation for energy production. Cerebral ischemic impairment restricts the delivery of substrates, particularly oxygen and glucose, and impairs the energy required to maintain ionic gradients (Martin et al., 1994). With energy depletion, membrane potential is lost and neurons and glia depolarize (Katsura et al., 1994). Consequently, somatodendritic as well as presynaptic voltage-dependent  $\text{Ca}^{2+}$  channels become activated and excitatory amino acids are released into the extracellular space. At the same time, the energy-dependent processes, such as the presynaptic reuptake of excitatory amino acids, are impeded, which further increases the accumulation of glutamate in the extracellular space. As a result of the glutamate-mediated overactivation of NMDA and AMPA receptors,  $\text{Na}^+$  and  $\text{Cl}^-$  enter the neurons via channels for monovalent ions. Water follows passively, as the influx of  $\text{Na}^+$  and  $\text{Cl}^-$  is much larger than the efflux of  $\text{K}^+$ . The ensuing edema can affect the perfusion of regions surrounding the ischemic core negatively, and also have remote effects that are produced via increased intracranial pressure, vascular compression and herniation.

It is well known that  $\text{Ca}^{2+}$  is involved in the activation of numerous enzymes and is therefore the key to initiating a multitude of biochemical pathways. For this reason, intracellular  $\text{Ca}^{2+}$  levels are tightly controlled in normal condition. The activation of NMDA receptors and metabotropic glutamate receptors contribute to a  $\text{Ca}^{2+}$  overload (Park et al., 1989). This, combined with the inability of ATP-dependent extrusion and sequestration of intracellular  $\text{Ca}^{2+}$  ions, allows the  $\text{Ca}^{2+}$  to reach toxic level in the ischemic neurons (Choi and Rotham, 1990). The cytotoxic increase in  $\text{Ca}^{2+}$  observed in ischemic neurons results in the inappropriate activation of  $\text{Ca}^{2+}$ -dependent processes, which contribute to cell death via apoptosis or necrosis.  $\text{Ca}^{2+}$  activates proteolytic enzymes, such as calpains (Minger et al., 1998). They can catalyze the breakdown of cytoskeletal proteins, including actin and spectrin (Furukawa et al.,

1997), as well as extracellular matrix proteins, such as laminin (Chen and Strickland, 1997). Lipolytic enzymes like  $\text{Ca}^{2+}$ -dependent phospholipase A2 are also activated by the high intracellular  $\text{Ca}^{2+}$  levels in the ischemic neurons (Sapirstein and Bonventre, 2000). These enzymes degrade the phospholipids cell membrane and increase the free fatty acid (e.g., arachidonic acid) concentration. Degradation of membrane phospholipids as well as membrane instability due to rising fatty acid levels produce membrane damage. In addition, nitric oxide (NO) synthesized by the  $\text{Ca}^{2+}$ -dependent enzyme, neuronal nitric-oxide synthase (NOS) reacts with a superoxide anion to form the highly reactive species, peroxynitrite, that can directly damage lipids, proteins, and DNA and lead to neuronal cell death (Chan, 2001; Iadecola, 1997). Moreover, excessive  $\text{Ca}^{2+}$ -induced mitochondrial damage causes increased mitochondrial membrane permeability, which can result in a mitochondrial release of cytotoxic substances such as cytochrome c and thus provide a trigger for the apoptosis of neurons (Fujimura et al., 1998).

### **1.2.2.3 Nonreceptor-mediated Excitotoxicity**

Nonreceptor-mediated glutamate excitotoxicity (NRGE) occurs in a large variety of neural cells that lack ionotropic glutamate receptors. Cysteine is the rate-limiting amino acid substrate for intracellular glutathione (GSH) synthesis and shares the common transporter with the glutamate (Bannai and Tateishi, 1986). The elevated glutamate inhibits the cysteine transport and then leads to a rapid depletion of GSH, a major cellular antioxidant, which results in an increased vulnerability of cells to oxidative stress and ultimately cell death (Murphy et al., 1989).

### **1.2.3 Inflammation**

Cerebral ischemia induces a marked response of resident microglia and hematopoietic cells, including monocytes and macrophages, and elicits a strong intrinsic inflammatory response involving the activation of microglia, recruitment of

granulocytes, and infiltration of macrophages in the ischemic area (Clark et al., 1994; Del Zoppo et al., 2000; Komine-Kobayashi et al., 2004). Therefore, the inflammatory response in the central nervous system is considered important in the pathological process after the onset of cerebral ischemia.

The  $\text{Ca}^{2+}$ -related activation of intracellular second-messenger systems, the increase in oxygen free radicals, as well as the hypoxia itself, trigger the expression of a number of proinflammatory genes by inducing the synthesis of transcription factors, including nuclear factor- $\kappa\text{B}$  (O'Neill and Kaltschmidt, 1997), hypoxia inducible factor 1 (Ruscher et al., 1998), interferon regulatory factor 1 (Iadecola et al., 1999) and STAT3 (Planas et al., 1996). Thus, mediators of inflammation, such as platelet-activating factor, tumor necrosis factor ( $\text{TNF}\alpha$ ) and interleukin $1\beta$  ( $\text{IL-1}\beta$ ), are produced by the injured brain cells (Gong et al., 1998; Rothwell and Hopkins, 1995; Zhang et al., 1998). Consequently, the expression of adhesion molecules on the endothelial cell surface is induced, including intercellular adhesion molecule 1 (ICAM-1), P-selectins and E-selectins (Haring et al., 1996; Lindsberg et al., 1996; Zhang et al., 1998). Adhesion molecules interact with complementary surface receptors on neutrophils. The neutrophils, in turn, adhere to the endothelium, cross the vascular wall and enter the brain parenchyma. Macrophages and monocytes follow neutrophils, migrating into the ischemic brain and becoming the predominant cells five to seven days after ischemia. Chemokines, for example interleukin 8 and monocyte chemoattractant protein 1, are produced in the injured brain and guide the migration of blood borne inflammatory cells towards their target (Ivacko et al., 1997; Yamasaki et al., 1995). Resident brain cells are also involved in the inflammatory response. Four to six hours after ischemia, astrocytes become hypertrophic, while microglial cells retract their processes and assume an ameboid morphology that is typical of the activated microglia (Komine-Kobayashi et al., 2004).

There is increasing evidence that post-ischemic inflammation contributes to ischemic damage by many mechanisms. Whereas microvascular obstruction by neutrophils can

worsen the degree of ischemia, the production of toxic mediators by the activated inflammatory cells and injured neurons also has important consequences. Inducible NOS (iNOS), which is not normally present in healthy tissues, is induced by cytokines in infiltrating neutrophils, activated brain glial and vascular cells following ischemic stress (Samdani et al., 1997). Once expressed, iNOS is continuously active and leads to a long-lasting (from several hours to days) NO generation, compared to cNOS-dependent NO synthesis which lasts a few minutes only. Furthermore, the iNOS enzyme produces much greater amounts of NO (in micromolar range) than either nNOS or eNOS (picomolar levels) (Ogden and Moore, 1995). Therefore, the toxic amounts of NO produced by iNOS greatly contribute to a secondary late phase damage of cerebral ischemia (Samdani et al., 1997). The pathogenic potential of NO produced by iNOS is underscored by the observations that pharmacological inhibition of iNOS reduces ischemic brain injury and that iNOS null mice have a reduction in ischemic damage (Iadecola, 1997; Iadecola et al., 1997; Zhao et al., 2003). The delaying nature of the protection exerted by iNOS inhibition or gene deletion is consistent with the hypothesis that ischemic injury evolves over several days (Baird et al., 1997; Dereski et al., 1993). In addition, ischemic neurons express another inflammatory-related enzyme, cyclooxygenase 2 (COX-2), that mediates ischemic injury by producing superoxide and toxic prostanoids (Nogawa et al., 1997). And NO produced by iNOS can enhance the COX-2 activity in an ischemic brain (Nogawa et al., 1998). It is reported that the inflammatory reaction might also be linked to apoptosis because antibodies against adhesion molecules attenuate post-ischemic inflammation and reduce apoptotic cell death in the ischemic brain (Chopp et al., 1996).

#### **1.2.4 Oxidative Stress**

Oxidative stress is due to the action of highly reactive free radicals such as the ROSs superoxide anion and hydroxyl radical, and the RNS peroxynitrite (Cassarino and Bennett, 1999; Fukuyama et al., 1998; Simonian and Coyle, 1996).

ROS and RNS are generated under normal cellular functioning, mainly during mitochondrial respiration. These constantly produced free radicals are scavenged by endogenous superoxide dismutase (SOD), glutathione peroxidase (GSHPx) and catalase. Other small molecular antioxidants, including GSH, ascorbic acid, and  $\alpha$ -tocopherol, are also involved in the detoxification of free radicals (Fulbert and Cals, 1992). Brain consumes about as much as 20% of  $O_2$  in the body and derives nearly all energy from mitochondrial oxidative phosphorylation, which generates ATP at the same time as it reduces molecular oxygen into water. And neurons contain high content of polyunsaturated fatty acids (target molecules of lipid peroxidation) in the plasma membrane, low levels of catalase (an antioxidant enzyme that catalyzes decomposition of  $H_2O_2$  to  $O_2$ ) and are thus prone to oxidative stress.

During cerebral ischemia, energy failure induces the depolarization of the plasma membrane that results in the activation of voltage-dependent  $Ca^{2+}$  channels and  $Ca^{2+}$ -permeable glutamate receptors. Entry and accumulation of  $Ca^{2+}$  in neurons can produce free radicals through the activation of prooxidant pathways including phospholipases (Sapirstein and Bonventre, 2000), NOS (Chan, 2001; Iadecola, 1997), xanthine oxidase (Atlante et al., 2000), and the loss of mitochondrial potential (Radi et al., 1994). In addition to  $Ca^{2+}$ , transition metals such as  $Fe^{2+}$ , and  $Zn^{2+}$  may contribute to the generation of free radicals under ischemia (Koh et al., 1996; Kondo et al., 1995). The accumulated ROS and RNS are likely to perturb the endogenous antioxidative defenses of the brain and disturb the prooxidants-antioxidants balance. These oxidants can directly react with and damage the cellular DNA, lipid, and proteins by virtue of their reactivity that leads to neuronal cell death through necrosis, or, in less intense cases, may mediate neuronal apoptosis through a cascade of well-orchestrated molecular events (Li, et al., 1995; Ratan et al., 1994; Whittemore et al., 1995).

### **1.2.5 Apoptosis**

Apoptosis is an active program of cell 'suicide' whereby the cell activates (or is forced to activate due to an injurious stimulus) a self-destructive mechanism which causes cell body shrinkage, condensation of nuclear chromatin, nuclear fragmentation and is ultimately phagocytosed. It has been recognized as another pattern of ischemic neuronal death. Studies suggest that many different signaling pathways are involved in apoptosis, but in all cases the final pathway resulting in cell death is the activation of a family of proteases (caspases) (Raff, 1998).

Caspases are aspartate-specific cysteine proteases and exist as zymogens in cells. They can be divided into two functional groups based on their perceived role in apoptosis: initiator and effector (Bratton and Cohen, 2001). There are two main initiator pathways to the activation of the effector caspases: the death receptor Fas pathway and the mitochondrial pathway. The death receptor Fas pathway involves the stimulation of members of the tumor necrosis factor-receptor (TNF-R) super family, and the main initiator caspase is the energy-independent caspase 8. The mitochondrial pathway can be called into action in two principle ways: by DNA damage or by the withdrawal of the action of cell survival factors (cytokines, hormones, cell-to-cell contact factors). In the presence of DNA damage, p53 protein activates pro-apoptotic proteins (e.g. Bax) and promotes a release of cytochrome c from the mitochondria. This complexes with a protein apoptotic protease-activating factor-1 (Apaf-1) and together they activate the initiator caspase 9, the main initiator caspase of the mitochondrial pathway. In normal cells, survival factors continuously activate anti-apoptotic mechanisms, and the withdrawal of cell survival factors will disturb the balance between anti-apoptotic and pro-apoptotic proteins, leading to a loss of the stimulation of anti-apoptotic Bcl-2 protein action with resultant unopposed action of Bax. Downstream of these initiators are the executor caspases (e.g., caspase-3), which are responsible for the destruction and inactivation of cell constituents such as the DNA repair enzymes, protein kinase C, cytoskeletal components, etc. A DNAase is activated and cuts genomic DNA between the nucleosomes, and generates DNA fragments of approximately 180 base pairs (Kroemer and Reed, 2000; Nakagawa et al., 2000; Weber and Vincenz, 2001). After

disposition by the effector caspases, the cells are reduced to a cluster of membrane-bound bodies. The dying cell displays several “eat-me” signals such as a surface exposure of phosphatidylserine and changes in cell surface sugars, which can be detected and phagocytosed by the activated microglia and infiltrating macrophages following cerebral ischemia.

Studies demonstrate that both the initiator and executor caspases are activated during the neurodegenerative process following cerebral ischemia (Benchoua et al., 2001). Moreover, the apoptotic neurons in the core of focal ischemia are related to the activation of energy-independent pathways, such as the “death-receptors” pathway, whereas the energy-consuming mitochondrial pathway is not involved at this stage. In contrast, pathways activated during the secondary expansion of the lesion into the penumbral area include the mitochondrial pathway (Benchoua et al., 2001), in agreement with the energy requirements of the apoptosome (Benchoua et al., 2002; Cecconi, 2001). Taken together, apoptosis is involved in an acute phase and delayed process of the ischemic neuronal damage.

### **1.3 Strategies for the Treatment of Cerebral Ischemia**

As post-mitotic cells, neurons are incapable of division and regeneration. This inability magnifies the impact of brain injury and thus the importance of treatment approaches as well. As reviewed in chapter 1.2, cerebral ischemic damage is mediated by multiple mechanisms that act at different times after the induction of ischemia. Accordingly, the rational treatment of ischemic brain injury has to be multifaceted in order to target the different pathogenic factors (Furuichi et al., 2004). Thus, therapeutic interventions can aim at re-establishing the flow or protecting the brain from factors which initiate ischemic brain damage. In recent years, three major strategies have been developed for the treatment of acute cerebral ischemia.

### **1.3.1 Thrombolytic Therapy**

Thrombolytic therapies aim to disintegrate the emboli responsible for cerebral artery occlusion, thus restoring blood flow to the ischemic brain regions. Intravenous and intraarterial thrombolytic therapies have been applied in recent years.

#### **1.3.1.1 Intravenous Thrombolysis**

Presently, recombinant tissue-plasminogen activator (t-PA) is the only approved thrombolytic therapy for stroke. This protein converts the inactive enzyme plasminogen to plasmin. Plasmin disintegrates fibrin, the principal component of embolus. Administration of t-PA therefore results in the destruction of emboli and the resumption of blood flow through the occluded arteries. The FDA approved this treatment on the basis of the results of the National Institute of Neurological Disorders and Stroke Recombinant Tissue Plasminogen Activator Stroke Study (The NINDS, 1995), in which 624 patients with ischemic stroke were intravenously administered with t-PA (0.9 mg per kilogram of body weight, with a maximum of 90 mg) within 3 hours after the onset of symptoms, about half of which were treated within the first 90 minutes. The study was carried out in two parts. In part 1, the primary end point was a neurologic improvement in 24 hours indicated by an improvement of 4 or more points in the score on the 42-point National Institutes of Health Stroke Scale (Lyden et al., 1994) or a complete neurologic recovery. In part 2, the pivotal efficacy trial, the primary end point was the global odds ratio for a favorable outcome, with the use of four measures of complete or near-complete neurologic recovery. Of the patients treated with t-PA, 31 to 50 percent had a complete or near-complete recovery in three months, as compared with 20 to 38 percent of the patients given placebo (The NINDS, 1995), and the benefit was similar in one year (Kwiatkowski et al., 1999).

The chief hazard of t-PA therapy was the dose-dependent risk of symptomatic brain hemorrhage, which occurred in 6.4 percent of the patients given t-PA, as compared

with 0.6 percent of those given placebo (The NINDS, 1995; The NINDS, 1997). This risk eliminates any benefit if t-PA is administered more than three hours after the onset of the stroke (Hacke et al., 1995). For a patient to benefit from the t-PA treatment, therefore, administration of t-PA must be given in less than three hours after the stroke onset and there must be no evidence of intracranial bleeding. There are numerous other exclusion criteria, including age, history of bleeding, history of anticoagulant consumption, and the blood levels of platelets of the patients (Adams et al., 1996). Due to the stringent screening criteria, only a fraction of the stroke patients qualify for the t-PA treatment. Moreover, the mortality rates in the two treatment groups were similar in three months [17 percent in the t-PA group and 20 percent in the placebo group (The NINDS, 1995)] and in one year [24 percent and 28 percent respectively (Kwiatkowski et al., 1999)]. A greater severity of the initial neurologic deficit and evidence of edema or a mass effect on the baseline CT scan were associated with a higher risk of symptomatic intracerebral hemorrhage (The NINDS, 1997). These restrictions diminish the practicality and effectiveness of the use of t-PA.

Streptokinase, another thrombolytic, is a protein extracted from the cultures of streptococci (Lizano and Johnston, 1995; Tewodros et al., 1996). It activates plasminogen (Kim et al., 2000; Ringdahl and Sjöbring, 2000). Three trials of streptokinase were initiated (Donnan, et al., 1996; The MAST-ESG, 1996; The MAST-IG, 1995). The dosage tested was 1.5 million units, the same as that given to patients with acute myocardial infarction, and treatment was initiated within four to six hours after the onset of symptoms. However, all of them were halted because of an excess rate of poor outcomes or an excess mortality among the streptokinase-treated acute ischemic patients.

### **1.3.1.2 Intraarterial Thrombolysis**

To attenuate the hemorrhage drawback of the intravenous thrombolytics treatment, local intraarterial thrombolysis performed with a microcatheter that is placed into,

beyond, and proximal to an arterial occlusion is in use worldwide on the basis of the results of two randomized trials (Del Zoppo et al., 1998; Furlan et al., 1999) and numerous case series. In the past, the agents most commonly studied were intraarterial urokinase (Ezura and Kagawa, 1992; Barnwell et al., 1994; Mori et al., 1988), t-PA (Sasaki et al., 1995; Zeumer et al., 1993), and prourokinase (Del Zoppo et al., 1998; Furlan et al., 1999). Approximately 40 percent of the patients who underwent this treatment had complete arterial recanalization, and approximately 35 percent had partial recanalization. These rates of recanalization were higher than those reported for patients who underwent intravenous thrombolytic therapy (Mori et al., 1992; Wolpert et al., 1993; Yamaguchi et al., 1993). Recently, intraarterial reteplase, a modified recombinant t-PA, was studied. Reteplase maintains the serine protease domain (responsible for thrombolytic effect) while it lacks the Kringle 1 domain, the epidermal growth factor domain, the finger domain and the oligosaccharide side chains. It has a longer half-life than t-PA, allowing for bolus administration and making for simplicity of administration, whereas t-PA must be infused (Martin et al., 1991). Other studies showed that reteplase was a more powerful thrombolytic, and with a safety profile comparable to that of rt-PA (Martin et al., 1993; Smalling et al., 1995).

In two small clinical trials (Qureshi et al., 2001; Qureshi et al., 2002), patients with ischemic stroke, who were poor candidates for intravenously administered therapy because of the severity of neurological deficits, an interval of three hours or more from the onset of symptoms, or a recent major surgery, were administered to a maximum total dose of 8 U of reteplase intra-arterially in 1-U increments via superselective catheterization. Complete or near-complete perfusion was achieved in the arteries in 14 patients (88%), and partial recanalization and a minimal response in the arteries were achieved in one patient each. Neurological improvement (defined as a decrease of four or more points in National Institutes of Health Stroke Scale score) was observed in 7 (44%) of the 16 patients in 24 hours. Symptomatic intracerebral hemorrhage occurred in one patient. Three other patients experienced intracerebral

hemorrhages that did not result in a neurological worsening. In addition, a high rate of recanalization and clinical improvement were observed in patients with ischemic stroke using low-dose reteplase (4 U of reteplase intra-arterially in 1-U increments) with adjunctive mechanical disruption of the clot. Moreover, this strategy may reduce the risk of intracerebral hemorrhage observed with thrombolytics. These results suggested that intra-arterially administered reteplase resulted in a high rate of recanalization. Therefore, this strategy should be considered in treating patients who are considered poor candidates for intravenous thrombolysis.

Up to date, intraarterial thrombolysis has not been compared with intravenous thrombolysis by randomized trials, so the relative merits of these two routes of therapy in patients with acute ischemic stroke are unknown. In patients with a possible middle-cerebral-artery occlusion, intravenous thrombolysis with t-PA treatment is recommended within three hours after the onset of symptoms; while intraarterial thrombolysis may be justified in these patients if treatment is to begin three to six hours after the onset of symptoms.

No randomized trials of thrombolytic treatment for vertebrobasilar stroke has been completed. A recent small case series suggested a possible benefit of intravenous t-PA if treatment is initiated within three hours after the appearance of symptoms (Grond et al., 1998). Because of the very poor outcome among patients with basilar-artery occlusion and the reported good recovery after intraarterial therapy initiated more than six hours after the onset of symptoms, cerebral arteriography performed on an emergency basis, followed by intraarterial thrombolysis during the three-to-six-hour period, can be recommended in patients with basilar-artery occlusion who are judged to have a poor prognosis (Brandt et al., 1996; Cross et al., 1997).

### **1.3.2 Anticoagulant Therapy**

Anticoagulant therapies aim to prevent the formation of emboli clot in the cerebral

arteries, thus preserving blood flow in the potential ischemic brain regions.

### **1.3.2.1 Heparin**

Heparin is a family of sulfated glycosaminoglycans. It inhibits coagulation both *in vivo* and *in vitro*, by activating antithrombin III. Patients with ischemic stroke caused by embolism are often treated with intravenous anticoagulant heparin. In the International Stroke Trial, 19,435 patients with ischemic stroke were randomly assigned to receive subcutaneous heparin at a dose of 5000 or 12,500 IU twice daily or no heparin at all, with or without 300 mg of aspirin per day, within 48 hours after the onset of symptoms (The IST, 1997). There was no difference among the treatment groups in the primary outcome (death within 14 days or death or dependency in 6 months). Among the patients who received heparin, there was a significant 0.9 percent reduction in the absolute risk of recurrent ischemic stroke during the first 14 days, an effect that was counterbalanced by a significant 0.8 percent increase in the absolute risk of hemorrhagic stroke. Hemorrhagic complications, including the need for transfusion, fatal extracranial bleeding, and hemorrhagic stroke, were associated with the high-dose regimen of heparin, but the activated partial-thromboplastin time was not monitored, and one third of the patients were treated before a CT scan of the head was obtained to rule out the possibility of brain hemorrhage. The results of the low-dose regimen of heparin were more encouraging, with a significant 1.2 percent decrease in the absolute risk of death or nonfatal recurrent stroke in 14 days and a rate of hemorrhagic complications in the same range as that of taking the aspirin alone.

Low-molecular-weight heparins (LMWHs) increase the action of antithrombin III on factor Xa but not thrombin, since the molecules are too small to bind to both the enzymes and the inhibitor (Salzman, 1992). Thus LMWHs may be associated with a lower risk of hemorrhage and more powerful antithrombotic effects than standard unfractionated heparin (UFH). Three trials of low-molecular-weight heparin in patients with acute ischemic stroke were completed. In one of them, administration of

nadroparin calcium or placebo was started within two days after the onset of stroke in 312 patients; more patients in the nadroparin group recovered (Kay et al, 1995). These results were not confirmed in a larger trial, which involved 750 patients (Hommel, 1998). In a placebo-controlled trial of another low-molecular-weight heparin, danaparoid, in which 1281 patients were treated within 24 hours after the onset of stroke, there was no difference in the rate of recurrence or progression of stroke between those who received the drug and those who received placebo (The Publications Committee for TOAST Investigators, 1998). Subgroup analysis did suggest a potential benefit of danaparoid in patients with occlusion or severe stenosis of the internal carotid artery (Adams et al., 1999). A meta-analysis of data from trials of early treatment with anticoagulant drugs for patients with acute ischemic stroke suggests no clinical benefit with such treatment (Sandercock, 1999). Treatment with LMWH after an acute ischemic stroke appears to decrease the occurrence of deep vein thrombosis compared with standard UFH, but there were too few events to provide reliable information on their effects on other important outcomes, including death, pulmonary embolism, or intracranial hemorrhage (Hankey, et al., 2005). Therefore, further very-large-scale trials may be worthwhile for the evaluation of the efficacy of LMWH.

### **1.3.2.2 Aspirin**

Antiplatelet agents prevent the aggregation of platelets (essential for clot formation) and are widely used in the secondary prevention of ischemic stroke. There is a number of antiplatelet drugs involving in the various mechanisms of platelet activation, and aspirin is the most commonly used for treating ischemic stroke in clinic. Early treatment with aspirin was evaluated in three trials in which more than 40,000 patients were treated within 48 hours after the onset of symptoms. In the International Stroke Trial, there was no difference among patients treated with aspirin, heparin, and neither of these drugs in the rate of death within 14 days or death or dependency in 6 months (The IST, 1997). Secondary analyses revealed a significant decrease in the rate of

recurrence of ischemic stroke in two weeks among patients treated with aspirin (2.8 percent vs. 3.9 percent among those not treated with aspirin). However, there was no difference among the groups in the combined end point of severe disability and death.

In the Chinese Acute Stroke Trial, where 160 mg of aspirin or placebo was given daily for four weeks to 21,106 patients with acute ischemic stroke, the mortality rate in one month in the aspirin group was slightly but significantly lower than that of the placebo group (3.3 percent vs. 3.9 percent), but there was no difference between the groups in the overall rate of death or severe disability (Chinese Acute Stroke Trial Collaborative Group, 1997). As in the International Stroke Trial, the rate of recurrent ischemic stroke in the aspirin group was lower than that of the placebo group in one month (1.6 percent vs. 2.1 percent), and so was the rate of death or nonfatal recurrent stroke (5.3 percent vs. 5.9 percent). A combined analysis of the results of the International Stroke Trial and the Chinese Acute Stroke Trial suggested that early death, recurrent stroke, or late death can be prevented by administering aspirin in one out of 100 acute stroke patients (Pathansali and Bath, 1998).

### **1.3.2.3 Ancrod**

Ancrod, a new defibrinogenating compound, converts fibrinogen into soluble fibrin products, with a subsequent decrease in plasma concentrations of fibrinogen and a depletion of the substrate needed for thrombus formation (Atkinson, 1998). In a trial of 500 patients randomly assigned to receive ancrod or placebo within three hours after the onset of symptoms, total or near-total recovery in three months was achieved in 42 percent of the patients given ancrod, as compared with 34 percent of those given placebo ( $P = 0.04$ ) (Sherman et al., 2000).

Taken together, although anticoagulants are expected to prevent the formation of emboli clot in the cerebral arteries and thus preserve blood flow in the potential ischemic brain regions, no data from clinical trials are available to validate this

treatment for ischemic stroke, despite its theoretical appeal. In addition, the associated risk of hemorrhage in the ischemic area is still associated with the anticoagulant therapies, and thus there is no consensus on the best time to start anticoagulant therapy.

### **1.3.3 Neuroprotective Therapy**

There has been much interest in the neuroprotective agents that may protect neurons from the effects of ischemia. Neuroprotective therapies aim to halt or reverse the detrimental biochemical processes that are activated in neurons by ischemia. As there are many processes that are stimulated by ischemia, there is also a whole host of neuroprotective agents. Available data derived from experimental models suggest that neuroprotective agents can reduce neuronal death and improve neurological function following hypoxic-ischemic insults. Many neuroprotective agents are currently undergoing clinical trials. In addition, novel neuroprotective compounds are being studied *in vitro* and *in vivo*. The *in vitro* models show that these agents target the different pathways involved in cerebral ischemia and are then subdivided into specific categories on this basis.

#### **1.3.3.1 Anti-Excitotoxicity**

The activation of ionotropic glutamate receptors, through the attendant failure of ion homeostasis and the increase in intracellular  $\text{Ca}^{2+}$  concentration, is a major factor involved in initiating ischemic cell death. A straightforward therapeutic approach, therefore, is to block the receptors that are activated by glutamate (Prass and Dirnagl, 1998). The NMDA receptor controls an ion channel that is permeable to  $\text{Ca}^{2+}$ ,  $\text{Na}^+$  and  $\text{K}^+$ . Antagonists at this receptor demonstrate robust neuroprotection when given before or at the time of occlusion of the middle cerebral artery (MCA) in models of permanent or temporary ischemia. There is a general agreement that the therapeutic time window of an effective NMDA-receptor antagonists in these models is narrow, closing at around one or two hours after the occlusion of the artery. The AMPA

receptor gates  $\text{Na}^+$  and  $\text{K}^+$  conductance, and  $\text{Na}^+$  influx via the AMPA or kainite receptor induces  $\text{Ca}^{2+}$  influx indirectly by depolarizing the resting membrane potential and subsequently alleviating the  $\text{Mg}^{2+}$  block of the NMDA receptor. AMPA receptor-antagonist treatment affords robust neuroprotection in several rodent models of focal cerebral ischemia, which potentially exceeds the time window during which NMDA-receptor antagonists are effective (Turski et al., 1998). However, it should be remembered that glutamate has an important physiological role as a neurotransmitter in the brain. Although blocking glutamate receptors protects against excitotoxicity, it can also have serious unwanted effects, such as psychotomimesis, respiratory depression or cardiovascular dysregulation.

The use of several NMDA-receptor antagonists was discontinued in Phase I and Phase II studies because of some unacceptable adverse effects. The major problems with these compounds are psychomimetic effects (agitation, hallucinations, paranoia and delirium), sedation, catatonia and concerns about potential neurotoxicity (Lees, 1997). Only selfotel, a competitive antagonist at the NMDA binding site of the NMDA receptor, and aptiganel, a non-competitive NMDA-receptor antagonist that acts as an open-channel blocker, have been studied in Phase III trials. However, the trials were terminated prematurely because of an unfavorable risk–benefit ratio (Davis et al., 1997; Ikonomidou and Turski, 2002). Clomethiazole is an anti-epileptic drug that causes neuronal hyperpolarization by enhancing the activity of GABA at  $\text{GABA}_A$ -receptors. The rationale behind its use is that it could inhibit ischemia-induced neuronal depolarizations and counteract the actions of glutamate. The drug protected against ischemic cell damage in animal models of permanent and transient focal brain ischemia (Sydserff et al., 1995a; Sydserff et al., 1995b). A large Phase III trial, involving 1350 patients, produced negative results (Wahlgren et al., 1999).

Excitotoxicity is well established as an important trigger and executioner of tissue damage in focal cerebral ischemia. Excitotoxic mechanisms can cause acute cell death

(necrosis) but can also initiate molecular events that lead to a delayed type of cell death, apoptosis. In addition, the intracellular signaling pathways activated during excitotoxicity trigger the expression of genes that initiate post-ischemic inflammation, another pathogenic process that contributes to ischemic injury. Thus, excitotoxicity is a prime target for stroke therapy. The therapeutic efficacy of strategies that inhibit excitotoxicity *in vivo* and *in vitro*, which focus on the inhibition of specific glutamate receptors, provides evidence for the pathophysiological role of excitotoxicity, while raising the hope that clinically relevant strategies can be developed that counteract to key pathophysiological entity.

### **1.3.3.2 Antioxidant Therapy**

It is well known that free radicals can directly react with and damage the cellular DNA, lipid, and proteins by virtue of the reactivity that lead to neuronal cell death through necrosis, or, if less intense, may mediate neuronal apoptosis through a cascade of well-orchestrated molecular events. Therefore, oxidative stress plays a central role in producing neuronal damage following acute cerebral ischemia. Antioxidants are expected to relieve oxidative stress by enhancing the intracellular radical scavenging potential. Especially, lipid-soluble antioxidants are likely to appear more efficacious because of their ability to cross the blood-brain barrier.

Several cerebral enzymes, including SOD, GSHPx, glutathione reductase, and catalase, are endogenous antioxidants that can process specific free radical scavenging properties. CuZn-SOD, a cytosolic dimeric enzyme, has been cloned and used to reduce superoxide radical-associated ischemic brain damage. Unfortunately, investigators obtained varying degrees of success or failure when free, nonmodified SOD was used to ameliorate ischemic brain injury (Chan et al., 1993). The extremely short half-life of CuZn-SOD (6 min) in circulating blood and its failure to pass the blood-brain barrier (BBB) make it difficult to employ enzyme therapy in cerebral ischemia. Although modified enzyme (e.g. polyethylene glycol-conjugated SOD or

liposome-entrapped SOD) has an increased half-life, BBB permeability, and cellular uptake, it showed conflicting results in ischemic brain injuries (Imaizumi et al., 1990; Chan et al., 1993). The fact that the results are mixed makes it imperative to employ other experimental strategies so that the role of SOD can be fully established in cerebral ischemia.

Tirilazad is a non-glucocorticoid 21-aminosteroid lipid-peroxidation inhibitor that acts as a free-radical scavenger (Francel et al., 1993). In animals with focal ischemia, this drug improved their neurological function and reduced the infarct volume (Schmid-Elsaesser et al., 1998). However, it did not improve the overall functional outcome in two large Phase III studies (A RANTTAS, 1996; Peters et al., 1996). Because it was suggested that the lack of efficacy might be caused by the use of a dose that was too low (6 mg/kg/day for 3 days), higher doses were tested. These trials were stopped prematurely because of safety problems and further clinical study of tirilazad in ischemic stroke were suspended (Haley, 1998).

The seleno-organic compound, ebselen, which has an antioxidant activity through a glutathione-peroxidase like action, was studied in Japan. This drug appeared to improve outcome in one month, but not in three months after the start of the treatment (Yamaguchi et al., 1998). Further efficacy studies with this compound might be justified.

### **1.3.3.3 Anti-inflammatory Therapy**

There is increasing evidence that post-ischemic inflammation contributes to ischemic brain injury. Cerebral ischemic damage could be reduced: (1) when the infiltration of neutrophils is prevented by the induction of systemic neutropenia; (2) when adhesion molecules or their receptors are blocked by neutralizing antibodies and in mice with the deletion of *Icam-1* (Connolly et al., 1996); (3) when the action of crucial inflammatory mediators, such as IL-1, is blocked (Loddick and Rothwell, 1996); and

(4) in mice with a deletion of the gene encoding interferon regulatory factor 1, a transcription factor that coordinates the expression of inflammation-related genes (Iadecola et al., 1999). Post-ischemic inflammation is, therefore, a promising target for therapeutic intervention in ischemic stroke. Treatments aiming at down regulating the neutrophilic infiltration, as well as drugs inhibiting enzymes that produce toxic mediators, such as iNOS and COX-2, could be viable strategies for targeting the late stages of injury. Furthermore, the potential beneficial effects of inflammation in tissue repair and remodeling need to be considered when developing treatment strategies.

The neuroprotective effects of lubeluzole can be explained, at least partially, by a down regulation of the NOS pathway, which reduces NO-related neurotoxicity (Lesage et al., 1996). In a small Phase II trial, a dose of 7.5 mg lubeluzole given within 6 h of the showing of the first symptoms, followed by an administration of 10 mg per day for five days, was associated with reduced mortality. A double-dose regimen, which yielded a plasma concentration equivalent to the levels associated with neuroprotection in rats, was associated with increased mortality (Diener et al., 1996). Although this was probably caused by an imbalance of randomization that was unrelated to the drug, three large Phase III trials of a 7.5 mg dose of lubeluzole, involving 3177 patients, were conducted. All three failed to demonstrate a beneficial effect of lubeluzole on the primary outcome parameters (Diener, 1998; Diener, 1999; Grotta, 1997), and further clinical development was abandoned.

In addition, it was reported that anti-ICAM-1 antibodies could reduce the infarct volume in transient focal ischemia (Zhang et al., 1994). Enlimomab, a murine monoclonal antibody against ICAM-1, was also been studied in a Phase III trial. Yet again, the results in the clinical situation did not fulfill the expectations generated in the laboratory (Enlimomab Acute Stroke Trial Investigators, 1997). There was even a trend of an early neurological deterioration in patients receiving active treatment. A probable explanation was that the murine antigens present in the enlimomab preparation themselves provoked an inflammatory response that cancelled out any

beneficial effects by raising the body temperature. Irrespective of the outcome of this ICAM-1 trial, however, there is a strong rationale for using the anti-inflammatory therapy in ischemic stroke.

#### **1.3.3.4 Antiapoptotic Therapy**

Apoptosis is the last stage in the sequence of cell death. Interfering this stage would no doubt be an efficient way of curing ischemic stroke, in which caspases are the most important. Caspase activity is blocked *in vivo* and *in vitro* by administering small peptides that bind covalently and irreversibly to the catalytic pocket after alkylating the cysteine residue (Nicholson and Thornberry, 1997). Caspase inhibitors not only attenuate the volume of dead tissue in focal ischemia but also decrease neurological deficit (Endres et al., 1998; Hara et al., 1997; Himi T, 1998), which thereby reflects a possible functional preservation of the ischemic neuronal tissue. In milder ischemia, the inhibitors are particularly effective as they reduce tissue injury synergistically when injected with MK801, an NMDA-receptor antagonist, or with growth factors, such as fibroblast growth factor. Moreover, unlike NMDA-receptor antagonists, caspase inhibitors reduce injury even when injected many hours after brief ischemia (Fink et al., 1998). A single intracerebroventricular injection of zDEVD-fmk, a relatively selective caspase-3 inhibitor, is effective if given at 9 h after 30 min reversible ischemia (Fink et al., 1998) and when administered after 3 h in a neonatal hypoxic–ischemic model (Cheng et al., 1998).

However, the effectiveness of blocking caspase activity is still open to dispute (Loetscher et al., 2001). Firstly, it is still undetermined whether caspase inhibitors truly rescue cells, i.e. restore cell viability and function, instead of simply blocking the apoptotic molecular cascade. Some researchers reported that caspase inhibition by synthetic peptides in rodent models of global ischemia reduced neuronal loss but was not sufficient to maintain the functional integrity of the rescued neurons (Gillardon et al., 1999; Von Coelln et al., 2001). Secondly, broad-range inhibitors may interact with

cital cysteine proteases, which may only result in the deregulation of apoptosis. Recent studies have shown that caspase inhibition might promote cell death by switching the outcome from apoptosis to necrosis (Hartmann et al., 2001; Lemaire et al., 1998; Nicotera et al., 2000). This switch appears to occur in states of intracellular energy depletion, common in many acute and chronic neurodegenerative diseases, and particularly crucial in cerebral ischemia. Thus, the use of caspase inhibitors in acute cerebral ischemia should be cautiously evaluated before being used for any therapeutic purpose.

#### **1.3.3.5 Hypothermia Therapy**

The deleterious effect of hyperthermia on the outcome of stroke has long been recognized in both rodent and human (Thornhill and Corbett, 2001). By contrast, its beneficial effect has been established in experimental models of stroke (Ginsberg et al., 1992; Schwab et al., 2001). In 1991, Sterz et al showed that inducing mild hypothermia (33–34 °C) either during or immediately following cardiac arrest significantly improved the neurobehavioral outcome in dogs (Sterz et al., 1991). Immediate postischemic moderate hypothermia (30–32 °C) was shown to be effective in preventing CA1hippocampal ischemic neuronal injury in the setting of global ischemia, as measured histologically (Busto et al., 1989). In Pabello's group (Pabello et al., 2004), brief periods of deep hypothermia (28 °C) were examined in a neonatal model by employing transient focal ischemia in a 7-day-old rat pup. The pups underwent permanent MCA occlusion coupled with a temporary (1 h) occlusion of the ipsilateral common carotid artery (CCA). After various times (3 days-6 weeks), the lesion was assessed by using 2,3,5-triphenyltetrazolium chloride (TTC) or hematoxylin and eosin (H&E) stains. Their results showed that intra-ischemic hypothermia resulted in significant protection in terms of survival, lesion size, and histology. Post-ischemic hypothermia was not effective in reducing the lesion size early after ischemia, but significantly reduced the eventual long-term damage (2-6 weeks). Late-onset post-ischemic hypothermia did not reduce the infarct volume.

Therefore, both intra-ischemic and post-ischemic hypothermia provided neuroprotection in the neonatal rat, but with different effects on the degenerative time course. The animal study suggests that the sooner hypothermia is initiated after the onset of ischemia, the more cerebral tissue is preserved (Carroll and Beck, 1992; Minamisawa et al., 1990).

Numerous studies suggest that hypothermia protects brain tissue from the effects of ischemia in a multiple mechanism. For example, it could reduce the metabolic rate (Kawamura, et al., 2000), and lessen the ischemic overdose of excitatory neurotransmitters (Li et al., 1999). These attenuate the influx of intracellular calcium, the herald of subsequent neuronal death. Additionally, hypothermia suppresses the synthesis of oxygen free radicals involved in the ischemic neurons (Zhao et al., 1996). It also improves the integrity of the blood brain barrier, thus diminishing cerebral edema and lowering the risk of hemorrhagic transformation (Kawai et al., 2000).

It was reported that low body temperature (approx 32 °C) in stroke patients in admission led to a more favorable outcome (Kammersgaard et al., 2002; Krieger et al., 2001; Wang et al., 2000), thus indicating the probable value of hypothermia in patients with acute stroke. Neuroprotection conferred by mild to moderate hypothermia is likely to undergo phase III clinical trials in various clinical settings. Preliminary studies suggest that mild to moderate hypothermia is a useful adjunct to thrombolytic therapy for ischemic stroke. Thus, timing, degree, and duration rules are being developed and methods of cooling further perfected to optimize the safety and efficacy of this promising approach (Hammer and Krieger, 2003).

#### **1.3.4 Summary**

With regard to the treatment of ischaemic stroke, two major approaches have been developed. One approach is to preserve the blood perfusion to the compromised region by dissolving the clot using thrombolytic drugs, or preventing the formation of clot by

anticoagulants. At present, t-PA is the most used thrombolytic drug for the treatment of acute ischaemic stroke. However, the use of t-PA is restricted to administration within 3 h of the stroke, which is a challenging admission target. Furthermore, its use increases the risk of hemorrhagic transformation (Wardlaw et al., 1997), which limits its acceptability. Clinical studies have also been performed by using local intra-arterial thrombolysis with prourokinase (Furlan et al., 1999), and intravenous administration of ancrod, a defibrinogenating compound (Sherman et al., 2000). These have produced encouraging clinical data but neither is currently registered for general use in the treatment of stroke.

The second approach is to develop compounds, the so-called neuroprotective agents, that interfere with the biochemical cascade of events involved in cerebral ischemia leading to cell death. The general assumption is that the core area of damage (infarction) will not be salvaged but that the area surrounding the core (the penumbra), despite being compromised with a low blood flow, can be saved by some appropriate conditions (either a blood reflow or an administration of a neuroprotectant). Evidence indicates that if left untreated, the penumbral region will become part of the core region (Ginsberg, 2003). In past decades, accumulating substantial knowledge have indicated that the ischemic injury cascade is highly complex, thus offering multiple targets for investigation and pharmacologic intervention. As described above, a variety of different pharmacologic classes of compounds is currently being investigated for their ability to protect neurons from the effects of cerebral ischemia. These neuroprotective agents act at different points on the complex cascade of events believed to underlie ischemic brain damage. However, although many neuroprotective agents have been shown to be beneficial in preclinical trials, their therapeutic potential in clinical setting remains to be determined (Kidwell et al., 2001). Further clinical trials are still necessary to ascertain the safety and efficacy of these agents to the stroke population and provide data that will be the basis for the approval of prescribing information for these agents when they are marketed.

## **1.4 Animal Models of Acute Cerebral Ischemia**

Ischemic stroke is one of the leading causes of death and also a major cause of long-lasting disability in major industrialized countries (Bonita, 1992). Presently, thrombolytic therapy with tPA is the only approved thrombolytic therapy for ischemic stroke in clinic (The NINDS, 1995). But the use of it is restricted to the administration within 3h of the stroke. Furthermore, its use increases the risk of hemorrhagic transformation (Wardlaw et al., 1997), which limits its acceptability. Therefore, to develop the potential efficacy of any drug in ischemic stroke patients, animal models of cerebral ischemia must be established and rightly used. Over the past decade, many animal models of cerebral ischemia have been developed by reducing blood supply to the brain tissues. These models can be classified as global, thromboembolytic and focal.

### **1.4.1 Global Models**

Global models involve blocking (occluding) the major blood vessels that supply the forebrain and result in ischemia over a large portion of the brain. There are three main types of global models.

#### **1.4.1.1 Two Vessel Occlusion**

Levine and Sohn first reported the model of two vessel occlusion by occluding the bilateral common carotid artery in rats (Levine and Sohn, 1969). Later, the murine model of two vessel occlusion was also used to study the delayed neuronal death due to the ischemic insult (Matsunaga et al., 2003). This model operates easily and the cost is low, but it is generally believed only to result in mild ischemia because the basilar artery can still supply blood to the ischemic region by the Willis circle.

An improved model of the two vessel occlusion plus hypotension was founded by Smith (Smith et al., 1984). In this model, it is necessary to keep the blood pressure of the rat between 45-50 mmHg to result in a low blood supply in the brain. This model only needs an one-stage surgery, and physiological parameters can be measured, but it needs to induce hypotension and sometimes post-ischemic seizures can be observed.

The two vessel occlusion model in gerbil, an animal without the Willis circle, was founded by Kirino (Kirino, 1982). This model can results in more severe damage in gerbil than normal animals, and only simple surgery is needed. Thus, it is rapid for screening purposes, and can get delayed and selective neurodegeneration and reliable measurement of damage (Kirino et al., 1986). But it has some drawbacks, including the limited source of the animals and the difficulties in undertaking physiological measurements and the variable outcome due to variations in cerebral circulation.

#### **1.4.1.2 Three Vessel Occlusion**

As its name implied, the three vessel occlusion model occludes three vessels: the bilateral common carotid artery and the basilar artery. This model was founded by Kameyama in 1985 (Kameyama, 1985). This model not only blocks the main vessels, but also the collateral vessels, and thus making a severe ischemia. But the surgery of the three vessel occlusion is very complicated, and is likely to induce hemorrhage when electrocoagulating the basilar artery.

#### **1.4.1.3 Four Vessel Occlusion**

Because of the abundant collateral circulation and the bilateral blood supply, it is hard to induce an ideal global ischemia model by merely blocking the bilateral common carotid artery and the basilar artery. So the four vessel occlusion model came into being in 1979 (Pulsinelli and Brierley, 1979). This model can induce severe ischemic damage when the rats are conscious, and there are definite criteria to fulfill for the

ischemia to become successful. This model involves a complicated surgery technique through a two-stage operative procedure, which largely confines its application. In addition, this model can result in variable outcome within animals of both one strain and different strains.

#### **1.4.2 Thromboembolytic Model**

Photochemical technique is often used in the induction of thromboembolytic models. It involves an intravenous administration of the photosensitive dye, rose Bengal, and an irradiation of specific areas of the brain with a focused light beam at a specific wavelength (Watson et al., 1985). The dye reacts with the light to produce oxygen radicals which peroxidize the endothelial lipids (i.e. damage them and stimulate the clotting reactions in those areas), resulting in platelet aggregation and thrombosis. No craniectomy but a mere a retraction of the skin over the skull is required. The resultant lesion develops rapidly outward from the core, together with an edema formation (Dietrich et al., 1987; Green and Cross, 1994). The size of the initial core area in this model appears to be determined by the diameter of the light beam. When performed correctly, this method produces consistent infarcts (Nakase et al., 1997). However, unlike other occlusion models, there is not a penumbral region of the type as seen in focal stroke, and the time course of blood-brain barrier disruption is very different in human cerebral ischemia (Forsting et al., 1994). Therefore, this model has limited validity in focal ischemia research.

Another method to induce thromboembolytic models involves the injection of blood clot fragment (about 100-300  $\mu\text{m}$  after crushing) into the internal carotid artery (Papadopoulos et al., 1987) or the base of the MCA (Wang, et al., 2001). Although these result in an acute emboli that block the cerebral arteries, the location or size of the infarct varies with these models.

#### **1.4.3 Focal Models**

The focal models are often said to be of greater relevance to acute ischemic stroke which produces brain infarction (Mhairi Macrae, 1992). The focal models occlude a specific vessel, usually the MCA because the majority of human ischemic strokes result from the occlusion in the region of the MCA. The MCA occlusion (MCAO) models can be permanent or transient (removal of the blockade to allow reperfusion). Since spontaneous recanalization frequently occurs in the ischemic stroke patients in clinic (Saito et al., 1987), it is proposed that MCAO incorporated with reperfusion mimics the clinical situation more closely and has been used extensively (Mhairi Macrae, 1992).

A model of reversible MCAO, i.e. reperfusion following ischemia, can be prepared by the application of endothelin-1 (a very potent vasoconstrictor) to the exposed MCA in rats (Robinson et al., 1990). Endothelin-1 causes vasoconstriction of the MCA for a period of time, followed by a relaxation allowing for reperfusion. The amount of endothelin-1 applied affects the strength and duration of the MCA vasoconstriction, and thereby the severity of the infarction. Other methods to induce ischemia-reperfusion involve the temporary occlusion of the arteries using surgical clips, hooks or ligature snares (Shigeno et al., 1985).

The most popular MCAO technique in use today is the intraluminal filament model (Longa et al., 1989). In this model, a nylon filament (coated with poly-L-lysine) is put in the internal carotid artery all the way up to a few millimeters beyond the MCA in rats or mice. Ischemia with a subsequent reperfusion can be achieved by removing the intraluminal filament. In this technique, the infarction size can be controlled by the length of time in which the nylon thread is being left inside. No craniectomy is required, and surgical intervention is relatively simple compared to that of the global ischemic model. When performed correctly under controlled experiments, the location and size of the infarcts are very consistent in experimental rats or mice.

#### **1.4.4 Attentions to the Evaluation of Neuroprotective Agents in Animal Models**

Many data show that the changing of several physiological parameters had effects on the outcome of ischemic stroke in both human and animal models. This concordance should provide confidence in the value of animal models. However, although >37 potential neuroprotective agents have been studied in >114 clinical trials (Kidwell et al., 2001), none is clinically efficacious and in use in the Western World. One possible answer to the question why the neuroprotective agents efficacious in animal model were not effective in clinical trials is that the compounds had not been administered in clinical trials in the same way that was efficacious in animals. Moreover, the animal model may not be appropriately applied. Therefore, the following attentions should be considered in the evaluation of neuroprotective agents in animal models.

##### **1.4.4.1 Appropriate Animal Model**

Any suggestion about which is the 'best' rodent model to test putative neuroprotective agents is likely to prove contentious. Most investigators have personal considerations about the major published models (Green and Cross, 1994; Traystman, 2003) and often claim that their model has particular relevance, even though the predictive value cannot be demonstrated in the absence of a clinically efficacious drug. Nevertheless, the MCAO model is now widely accepted as the primary model. In general, efficacy in the reperfusion MCAO models might be acceptable since the drug might be combined with a thrombolytic for the treatment of acute cerebral ischemia or the late onset of spontaneous reperfusion which occurs in 50% of the stroke patients (Ringelstein et al., 1992; Saito et al., 1987).

Many animal species, such as mice, gerbils, rats, cats, dogs or primates, have been used to study brain ischemia and evaluate the effect of different neuroprotective agents. Rats are mostly used due to their similar cranial circulation to that of the human

(Mhairi Macrae, 1992; Yamori et al., 1976), the low cost and ease of experimentation. Also, cheap mice are often used for the screening study. Although the behavioral profile of rats or mice is somewhat limited, it is extensively documented. Moreover, it is reasonable to suggest that several species be studied, if possible, because of the evidence that neuroprotective drugs can have very different effects in different species. Besides, as we know, stroke is primarily a problem of mid or late life. Therefore, the animals used in experiments should not be almost invariably young but rather aged.

#### **1.4.4.2 Therapeutic Windows of Opportunity**

One of the most important and obvious factors to bear in mind when considering the acute treatment of ischemic stroke is that patients are treated after they have had stroke. The “therapeutic window of opportunity” is the time from the initial blood vessel occlusion in animal models or the onset of symptoms in patients to drug administration. Potential therapeutic agents must, therefore, be shown to be efficacious when given after the insult. This would rule out a significant number of experimental studies where claims for the possible value of a drug in stroke have been made solely on the basis of results demonstrating efficacy when the drug has been given before (or both before and during) the ischemic insult.

Although there is some evidence that it might take many hours for damage to develop in the human brain (Baron, 1999), the biomedical changes that follow an ischemic insult in animal brains have been reported to be a time-course process (Dirnagl et al., 1999). For example, glutamate release occurs in minutes and neuro-inflammation occurs after several hours. It seems reasonable to assume that neuroprotective agents that work on a specific biochemical mechanism must be given at the time when the mechanism is active. For example, NMDA receptor antagonists only protect in stroke models for up to 60-90 min post-occlusion (Massieu et al., 1993) since glutamate release occurs early in the ischemic biochemical cascade (Dirnagl et al., 1999). And t-PA is effective when given within 3h clinically (The NINDS, 1995) as well as in

animal models (Brinker et al., 1999). Therefore, compounds, acting on mechanisms that occur later in the ischemic biochemical cascade have a reasonably large window of opportunity in cerebral ischemia, and are thus more effective neuroprotection in clinic.

#### **1.4.4.3 Hypothermia**

The deleterious effect of hyperthermia on the outcome of stroke in both rodent and human have long been recognized (Schwab et al., 1998; Thornhill and Corbett, 2001). Higher concentrations of glutamate and glycine are present in the cerebrospinal fluid of patients with hyperthermia, indicating that excitotoxic effects might contribute to the adverse impact of hyperthermia (Castillo et al., 1999). By contrast, the beneficial effect of hypothermia is well established in experimental models of stroke (Schwab et al., 2001). In addition, low body temperature in stroke patients in admission leads to a more favorable outcome (Kammersgaard et al., 2002; Wang et al., 2000), which indicates the probable value of hypothermia. Therefore, the body temperature should be controlled in the animal experiments.

#### **1.4.4.4 Drug Dose Design**

A major problem with some compounds is that important adverse events limit the possibility of achieving dose levels that have maximal neuroprotective effects in animals (Muir and Lees, 1995). Many compounds examined in clinical trials had even produced marked adverse events (such as sedation and ataxia) in rats when they were given at doses that were neuroprotective (Dawson et al., 2001). Therefore, a relatively high selectivity of neuroprotective effect should be the key feature of potential agents for the treatment of acute cerebral ischemia in clinic. Recent studies indicate that a much higher drug exposure might be required to provide neuroprotection in the model of permanent ischemia than that of transient ischemia (Sydserff et al., 2002). This observation might be clinically important. The ability to attain the exposure necessary

to provide protection in permanent ischemia in animals might have the potential significance clinically.

#### **1.4.4.5 Ways of Giving Drugs**

The blood brain barrier (BBB) provides an exquisite regulation of the internal chemical environment of the central nervous system (CNS) by regulating the internal environment with a mechanism of low passive permeability combined with a highly selective transport system between the blood and the brain (Bartus, 1999). While this system may protect the brain by maintaining a controlled environment, it also creates a barrier for the transport of drugs from the blood to the brain parenchyma (Bartus et al., 1996). In fact, only a fraction of all bioactive drugs possesses the ability to penetrate the BBB, which greatly limits the outcome of the treatment of CNS diseases.

The intracranial administration of drugs in animal studies allows very high local concentrations of the particular agents. However, this is usually not possible in humans. Dantrolene (Nakayama et al., 2002), propofol (Yano et al., 2000), and lisuride (Caldwell et al., 1997) are given in that manner. Thus, it remains unclear whether the beneficial effects of these agents could still be replicated with a route of application that is more common in the clinical environment. In addition, allopurinol (Mink, et al., 1991), polyunsaturated fatty acids (Blondeau et al., 2002), progesterone (Cervantes et al., 2002), cyclosporin A and FK506 (Uchino et al., 2002), and, in most studies, estrogen as well (Horsburgh et al., 2002; Watanabe et al., 2001) have to be applied chronically and the effect of an acute systemic application remains doubtful. In this regard, the potential preconditioning effect of a chronically applied drug and its acute neuroprotective effect when administered immediately before the ischemic injury must be distinguished.

#### **1.4.5 Summary**

Acute ischemic strokes result from the occlusion of a major cerebral artery by a thrombus or an embolism, which leads to a loss of blood flow in a specific region. A key feature in the development of neuroprotective agents is the use of animal models of stroke. In past decades, accumulated knowledge has greatly elucidated the mechanisms that follow an ischemic stroke, and many compounds, interfering with these mechanisms, have been proved to be beneficial for cerebral ischemia in animal models. However, none of these potential neuroprotective agents is clinically efficacious and in use in the Western world. Theoretically, animal models of stroke are generally regarded to have clinical relevance and it is reasonable to propose that a drug that attenuates ischaemia-induced damage in the appropriate models will also prove effective in humans when given in an equivalent manner. The observed lack of efficacy of these drugs may be due to delays in the initiation of treatment, inadequate doses, inadequate drug penetration, adverse effects, or insufficient matching of a drug's mode of action to the mechanism of brain injury (Fisher and Bogousslavsky, 1998; Lee et al., 1999). For example, thrombotic, embolic, and small-vessel strokes may all involve the deep white matter, where no synapses are found. Thus, it is unlikely that a neuroprotective drug that acts at the synaptic level, such as the NMDA receptor antagonist (Massieu et al., 1993), would be effective in protecting the ischemic white matter. Perhaps even more important, arterial occlusion and inadequate circulation in collateral vessels may preclude the adequate delivery of the drug to a substantial portion of the ischemic tissue. In future, therefore, it is strongly recommended that animal models should be modified to reflect more accurately the complexity of human stroke and compounds be administered to patients using exactly the same conditions (such as exposure and time window) that produce functional and histological protection in animals.

## **1.5 Natural 3-alkylphthalide Derivatives**

### **1.5.1 Distribution and Categories of Derivatives of 3-alkylphthalide in Plants**

3-alkylphthalides, widely present in Umbelliferae plants, are important derivations of phthalide. The chemical studies of these constituents have started in the late nineteenth century. Since then, numerous studies have been done to isolate 3-alkylphthalides from plants and identify their structures (Fig 1.1). Butylphthalide 1, Butylidephthalide 2 and 3, and Neocnidilide 4 were first isolated from *Apium graveolens* in the late nineteenth century. Barton et al. discovered Butylphthalide 1 and Sedanolide 5 in the seeds of *A. graveolens* (Barton et al., 1963). Naves et al. isolated 1, 2, 4 from *Levisteum officinale* and suggested that these compounds also existed in other plants that had a relationship with *L. officinale* (Naves, 1943). Mituhashi et al. systematically studied the components of plants belonging to the genus Umbelliferae and pointed out that 3-hydroxyphthalide was the typical compound of Umbelliferae plants (Mituhashi et al., 1960). In addition, they isolated Ligustilide 6 from *Ligusticum acutilobum* in the next year and corrected some mistakes made by previous scientists because the compounds they isolated were not pure enough. Two groups of Yamaishi and Bjeldanes simultaneously isolated 3-n-Butyl-4, 5-dihydrophthalide 7 from Senkyu and the seeds of *A. graveolens* respectively (Bjeldanes and Kim, 1977; Yamagishi and Kanesshima, 1977). Butylphthalide 1 and Ligustilide 6 were also isolated from *Angelica sinensis*, known as Danggui in Chinese (Lin et al., 1979; Wang et al., 1985). Mitsuhashi et al. isolated Cnidilide 11 from *Cnidium officinale* (Mitsuhashi and Muramatsu, 1964). Fehr isolated 3a, 4-dihydroisobutylidenephthalide 12 from *A. graveolens* (Fehr, 1979).

With the development and the wide use of instrumental analysis, mono-hydroxy, bi-hydroxy and dimeride derivations of 3-alkylphthalide were further discovered, among which a series of 3-hydroxyphthalides including mono-, bi-hydroxy such as 13, 14, 15, 16, 17, 18, 19, 20, 21 were isolated (Kobayashi et al., 1987; Kobayashi and Mitsuhashi, 1987). Wang et al. isolated 18, 20, 24 from Senkyu (Wang et al., 1984). Kobayashi et al. found Butylidenephthalide 2 and Senkyunolide (Senkyunolide A) 9 from the rhizomes of *Cnidium officinale* Makino (Kobayashi et al., 1984). Kaouadji et al. isolated 25, 41, 48 from *Ligusticum wallichii* rhizoma (Kaouadji et al., 1986).

Kobayashi et al. isolated Senkyunolide J 34 from the commercial *C. officinale* rhizoma (Kobayashi et al., 1987). Kobayashi et al. isolated Senkyunolide M 33 and Senkyunolide L 35 from *L. wallichii* (Kobayashi and Mitsuhashi, 1987). Compound 17, 21, 22 were also isolated from senkyu (Naito et al., 1992). Two new phthalides, Senkyunolide R 26 and S 27 were isolated from *Ligusticum chuanxiong* rhizoma (Naito et al., 1996). Banerjee et al. isolated Angeodide 36 and Angelicolide 37, two dimerides of phthalide, from *Angelica glauca* Edgew and identified their structures (Banerjee et al., 1982; Banerjee et al., 1984). Angelicide 49 was isolated from *A. sinensis* (Chen and Zhang, 1984). Cichy et al. obtained Angeolide 36 from *L. officinale* and discovered Levistolide A 39, Levistolide B 40 (Cichy et al., 1984). Kaouadji et al. isolated 6, 9, 29 from *L. wallichii* (Kaouadji et al., 1983). Wang et al. reported that they obtained a new dimeride named Wallichilide 42 from *L. wallichii* (Wang et al., 1984). Delgado et al. isolated 6, 38, 46 from a Mexican plant *Ligusticum porteri* (Delgado et al., 1988). Hon et al. isolated a new dimeride 43 from *A. sinensis* (Hon et al., 1990). Naito et al. isolated Senkyunolide P 50 and Tokinolide B 51 from the rhizome of *L. chuanxiong* (Naito et al., 1991). Li et al. extracted E-Ligustilide 10 from *A. sinensis* (Li et al., 2001). Lin et al. first reported the existence of 16 compounds in Danggui including Sendanenolide 8, Senkyunolide B 13, Senkyunolide C 14, Senkyunolide D 15, Senkyunolide E 16, Senkyunolide F 17, Senkyunolide G 18, Senkyunolide H 23, 3-butylidene-7-hydroxyphthalide 24, Z-6,7-epoxyligustilide 25, E-6,7-dihydroxy-di-hydroxydigustilide 28, Senkyunolide I 29, Z-6-hydroxy-7-methoxy-dihydroxydigustilide 30, Coniferyl ferulate 31, 2-(1-Oxopentyl) -benzoic acid methyl ester 32 and Z,Z'-3,3',8,8'-diligustilide 44 (Lin et al., 1998). Recently, a new dimeric derivative and a pair of epimer were isolated from the rhizome of *A. sinensis* (Su et al., 2005) and their structures were identified as Z-3',8,3'a,7'a-tetrahydro-6,3',7,7'a-diligustilide-8'-one 45, Z,Z'-6,6',7, 3'a-diligustilide 46 and the 8-epimer 47 of 46.

Chemical studies on the natural 3-alkylphthalides have been carried out for more than a hundred years. According to the structure characteristics, the natural 3-alkylphthalides and their derivatives can be classified into three groups: (1)

compounds of 3-alkylphthalides (structure number 1-12, Fig 1.1); (2) mono- or bi-hydroxy derivatives of 3-alkylphthalide (structure number 13-35, Fig 1.1); (3) demeric derivatives of 3-alkylphthalide (structure number 36-51, Fig 1.1).

## **1.5.2 Pharmacological Profiles of 3-alkylphthalides**

As described in chapter 1.5.1, numerous studies have indicated that 3-alkylphthalides are the characteristic components of important medical plants, especial Umbelliferae plants. In the past over hundred years, more than fifty 3-alkylphthalides were isolated, and most of them have been shown to possess various bioactive effects.

### **1.5.2.1 Protection on Cerebral Ischemic Injury**

Butylphthalide, one of the most stable 3-alkylphthalides, was first isolated from *Apium graveolens* in the nineteenth century in Europe. Studies have showed that synthetic butylphthalide has marked effect for the treatment of ischemic cerebrovascular diseases, which may result from the improvement of the cerebral microcirculation dysfunction, antioxidant effect, anti-apoptosis, and inhibition on iNOS expression and NO production (Chang and Wang, 2003; Chong and Feng, 1999; Hu and Li, 2004; Xu and Feng, 1999). The synthetic dl- and l-butylphthalide have been proved to induce dilation of the pial arterioles and the increase in blood flow velocity in focal brain ischemia rats induced by MCAO (Xu and Feng, 1999). According to the study by Chong and Feng, dl-butylphthalide (20 mg/kg, i.p.) significantly decreased the content of malondialdehyde in the cerebral cortex of rats subjected to 1 h of reperfusion following 6 h of MCAO (Chong and Feng, 1999). A study by Chang and Wang (2003) showed that butylphthalide, especially its *s*-(-)-enantiomer almost completely inhibited the cerebral neuronal apoptosis induced by ischemia-reperfusion. *s*-(-)-butylphthalide at doses of 5 and 10 mg/kg (i.p.) could significantly reduce the

release of cytochrome c, decrease the activation of caspase-3, and inhibit DNA fragmentation in focal cerebral ischemia rats subjected to 24 h of reperfusion following 2 h of MCAO. Moreover, the neuroprotective effect of 3-*n*-butylphthalide was proved to be, in part, due to the inhibition of the production of NO and the expression of iNOS in chronic episodic hypoxia (Hu and Li, 2004).

#### **1.5.2.2 Effect on Central Nervous System**

It was reported that *Radix Angelica sinensis* had some inhibitory effect on the central nervous system (Schmidt et al., 1924). Xie and Tao found that ligustilide exhibited mild inhibitory effect in the nervous system, which suggested that ligustilide was probably one of the active components of the central nervous inhibition of *Radix Angelica sinensis* (Xie and Tao, 1985). Their results showed that ligustilide (98 mg/kg, i.p.) significantly decreased the spontaneous movement of mice; 98 or 196 mg/kg (i.p.) of ligustilide antagonized the central excitation reaction induced by ketamine in mice, shortening the latency of mice sleep and the lasting time induced by the pentobarbital and decreased body temperature of mice from  $37.9 \pm 0.2$  °C and  $38.1 \pm 0.2$  °C to  $36.8 \pm 0.4$  °C and  $35.9 \pm 0.2$  °C, respectively; 294 mg/kg ligustilide (i.p.) inhibited the electric-induced irritating reaction of the mice. In addition, Matsumoto et al. found that intraperitoneal injection of ligustilide (5-20 mg/kg) or butylidenephthalide (10-30 mg/kg) could reverse the pentobarbital sleep decrease in isolated mice, and both components (20 mg/kg, i.p.) attenuated the suppressive effects of yohimbine, methoxamine and a benzodiazepine inverse agonist, FG7142, on the pentobarbital sleep in some group-housed mice. These results suggested that the central noradrenergic and/or GABA<sub>A</sub> systems were implicated in the effects of these components (Matsumoto et al., 1998).

Juice squeezed from fresh celery leaves has long been used in China for the treatment of epilepsy. Two anticonvulsive compounds, butylphthalide and ligustilide, were isolated from the seeds of the plant *Apium graveolens* (Yu and You, 1984). Yu and

You reported that both the natural compounds and synthetic dl-butylphthalide produced very similar protection action against maximal electroshock seizure test, minimal electroshock threshold test, metrazol seizure threshold test and maximal audiogenic seizure in mice and rats. The ip ED<sub>50</sub> of dl-butylphthalide was found to be 75.0 ± 8.9 mg/kg in mice and 76.0 ± 3.8 mg/kg in rats. In the essential oil of *Ligusticum sinense* (Oliv) cv. Chaxiong, 5 phthalides with anticonvulsive activities were also isolated and identified as butylidenephthalide, ligustilide, butylphthalide, neocnidilide, and senkyunolide on the basis of spectral data (Luo et al., 1996). The preventive effect of butylphthalide was detected in rats with chronic epilepsy. The rat chronic epilepsy was produced by coriaria lactone (0.9-1.5 mg/kg, i.m.) twice a week for 3 months. The effects of coriaria lactone, butylphthalide (700 mg/kg, i.g.) and diazepam (1.5-5.0 mg/kg, i.p.) on learning and memory were studied a by step-down test and parallel experiments were performed to study the behavior and morphological changes of the hippocampus (Yu et al., 1988). It was found that coriaria lactone elicited amnesia and disrupted the acquisition process in the step-down test. Both butylphthalide and diazepam antagonized the learning and memory deficits with butylphthalide being much stronger than diazepam. Examination of the hippocampus of the butylphthalide group revealed no sign of abnormality as compared with the control group.

### **1.5.2.3 Relaxing Effect on Muscle**

#### **A. Effect on Smooth Muscle**

The effects of butylidenephthalide, ligustilide, and butylphthalide purified from the neutral oil of *Ligusticum wallichii* were studied on isolated smooth muscle (Ko, 1980). Among these 3 compounds, butylidenephthalide was the most active in inhibiting rat uterine contractions induced by prostaglandin F<sub>2α</sub>, oxytocin, and acetylcholine. Butylidenephthalide inhibited contractile responses of the ileum to agonists, including acetylcholine, K<sup>+</sup>, and Ba<sup>2+</sup>, in normal Tyrode solution and to exogenous Ca<sup>2+</sup> in high

$K^+$  (80 mM),  $Ca^{2+}$ -free Tyrode solution, and also vas deferens responses to norepinephrine. Butylidenephthalide is a nonspecific antispasmodic and was weaker in potency than papaverine. However, as the inhibitory effects of butylidenephthalide on phasic contraction and tonic contraction of preparations, including depolarized and nondepolarized ileum, were about the same, the action mechanism of butylidenephthalide seemed to differ from that of papaverine which inhibited tonic contraction more selectively than phasic contraction. Thus, butylidenephthalide possesses a nonspecific antispasmodic action, the mechanism of action being different from that of papaverine. The further analysis of structure-activity suggested that alkyl substitution at C-3 increased the inhibitory activity probably due to an increase in lipid soly (Ko et al., 1977). The 3-double bond was also an important structural feature for the inhibitory effect. Butylidenephthalide was more active than ligustilide, possibly due to the presence of aromatic character in butylidenephthalide. In addition, seven racemic ligustilide dimers were isolated and purified from *Angelica sinensis*, and identified as the smooth muscle relaxants for treating menstrual disorder, urgent premature birth and hypertension were claimed.  $IC_{50}$  value of a ligustilide dimer tested for the smooth muscle contraction inhibition was 31.8 M vs. 49.9 M for butylidenephthalide control (Kanita et al., 1995).

According to the study by Tao et al. (1984), ligustilide had remarkable antiasthmatic effect in vivo and in vitro experiments. When injected into guinea pigs intraperitoneally at a dose of 0.14 ml/kg, the asthmatic reaction induced by acetylcholine and histamine was immediately impeded with a potency approximately equal to the action of aminophylline (50 mg/kg). Lung overflow experiment showed that an intravenous injection of ligustilide (0.08 ml/kg) into the anesthetic guinea pig caused complete or partial block of the reaction of histamine at the dose of 2 - 10  $\mu$ g/kg. ligustilide also exhibited antispasmodic effect on isolated trachea strip of the guinea pig contracted by acetylcholine, histamine and barium chloride, and a relaxation effect on trachea strip under normal tension. Addition of propranolol did not affect those actions (Tao et al. 1984).

## **B. Effect on Skeletal Muscle**

Three phthalide compounds (ligustilide, cnidilide and senkyunolide) were extracted from the rhizome of *Cnidium officinale*, and the centrally acting muscle-relaxant effect was investigated on the crossed extensor reflex in anesthetized rats. The results showed that these 3 compounds (administered i.p.) could depress the reflex response. Their depressive potencies were almost the same, and their potencies were also the same or somewhat weaker than that of mephenesin. Since no curare-like action was observed, the muscle relaxation induced by these phthalide compounds was considered to be due to a central action (Ozaki et al., 1989).

### **1.5.2.4 Regulation on Microcirculation**

*Ligusticum chuanxiong* rhizoma has been widely used for activating blood circulation and removing blood stasis in the Chinese medicine. The effects of phthalide dimers from the rhizome of *Ligusticum chuanxiong* were studied on the thoracic aorta, mesenteric arteries and blood viscosity. Four phthalide dimers, tokenolide B, levistolide A, riligustilide and senkyunolide P relaxed KCl-induced contraction on the rat thoracic aorta. These compounds also reduced the KCl-induced perfusion pressure of the rat mesenteric arteries. On the other hand, phthalide dimers, tokenolide B, senkyunolide P and phthalides, senkyunolide, butylphthalide and cnidilide decreased the blood viscosity. These results suggested that phthalide dimers and coniferyl ferulate might be important constituents in the rhizome of *Ligusticum chuanxiong* for activating blood circulation and removing blood stasis (Naito et al., 1995).

Ligustilide is also a main active constituent in the essential oil from the rhizome of *Ligusticum chuanxiong*. The influence of the essential oil on microcirculation in conjunctiva bulbar was compared in rabbits intravenously injected with dextran T500 before and after the ligustilide was decomposed. Results showed that there was no difference between the two types of essential oil in the spasmolysis of venule. But the

effects of the ligustilide-decomposed essential oil were obviously weakened in spasmodic contraction of arteriole, deagglutinating erythrocyte, increasing the number of opened capillary, accelerating the speed of blood flow and enlarging the amount of blood flow in microcirculation (Shi et al., 1995). Thus, ligustilide is probably an active constituent to improve microcirculation.

#### **1.5.2.5 Antiproliferative Effects on Smooth Muscle Cells**

The inhibitory effects of *Cnidium* rhizome-derived phthalides on the competence and progression phases of fetal bovine serum (10%)-induced proliferation were compared in the primary cultures of mouse aorta smooth muscle cells (SMC). Their potencies for the competence inhibition were in the order of senkyunolide L > senkyunolide H > senkyunolide J > senkyunolide I > ligustilide = senkyunolide A > butylidenephthalide. The order of their potencies for the progression inhibition was parallel with that for the competence inhibition. Senkyunolide L was considered to be formed during the extraction of *cnidium*. These results demonstrated that the (Z)-6,7-dihydroxy isomer of the dihydroligustilide derivatives was essential for the anti-competent effect on the proliferation of the SMC in primary culture. Senkyunolide H in *cnidium* rhizome may be a prototype of a new anti-atherosclerotic drug (Kobayashi et al., 1993). The IC<sub>50</sub> values of senkyunolide H, senkyunolide A, ligustilide and butylidenephthalide derived from *cnidium* were below 0.1, 1.52, 1.68 and 3.25 g/mL, respectively (Kobayashi et al., 1992).

#### **1.5.2.6 Essence for Food Additive**

Most phthalides are of favorable aroma odor. The following aroma phthalides were identified from the essential oil of the fruit, leaf, stem, tuber, and root of celery (*Apium graveolens*): butylidenephthalide, butylphthalide, ligustilide, and 3-isobutylidene-3a, 4-dihydrophthalide (3a,4-dihydroisobutylidenephthalide) (Fehr, 1979). 4 aroma phthalides were also found in the different organs of *Apium graveolens* rapaceum

(celeriac) (Fehr, 1981). These natural aroma phthalides are available for the essence of food additive.

### **1.5.2.7 Insecticidal Effect**

The insecticidal activity of two phthalides from *Angelica acutiloba* was investigated and compared with that of rotenone (Miyazawa et al., 2004). Z-butylidenephthalide and Z-ligustilide exhibited LC<sub>50</sub> values of 0.94, 2.54,  $\mu\text{mol/mL}$  respectively of a diet concentration against larvae of *D. melanogaster*. Against both sexes (males/females, 1:1) of adults (5-7 days old), Z-butylidenephthalide showed the most potent activity with a LD<sub>50</sub> value of 0.84  $\mu\text{g/adult}$ . Z-butylidenephthalide is a more active insecticide than rotenone (LD<sub>50</sub> = 3.68  $\mu\text{g/adult}$ ) and has the potential as a novel insect control agent. However, Z-ligustilide was inactive against adults. The structure-activity relationship of phthalides isolated indicated that the aromaticity appeared to play an important role in the activity of both larvae and adults.

## **1.5.3 Clinical Application of Derivatives of 3-alkylphthalide**

### **1.5.3.1 Treatment of Essential Oil of *Angelica sinensis* for Irregular Menstruation and Amenorrhoea**

*Angelica sinensis* is one of the most important traditional Chinese medicines used for tonifying blood and treating female irregular menstruation and amenorrhoea. Ligustilide has long been regarded as the main bioactive chemical constituent of *Angelica sinensis* (Lin et al., 1979) and effective for the treatment of primary and secondary dysmenorrhea in clinic (Gao et al., 1988). The clinical study indicated that the essential oil of rhizomes of *Angelica sinensis*, the main constituent of which was ligustilide (purity not indicated), generally reduced the syndrome of dysmenorrhea in 2 h after oral administration and significantly relieved or eliminated it in 6-24 h. After the treatment of three consecutive cycles (each cycle with 3-7 days) of ligustilide (150

mg/time×3 per day, i.g.) during menstruation period, 20.54% of patients obtained significant effective results and did not recur in 3 months, and 76.79% attenuated the pain of patients. In addition, ligustilide was more effective for primary than secondary dysmenorrhea.

### **1.5.3.2 Treatment of Butylphthalide for Acute Ischemic Stroke**

3-butylphthalide (NBP) is a bioactive constituent first isolated from *Apium graveolens* in the nineteenth century in Europe. In the past decade, systemic studies have been carried out on the treatment of NBP for acute moderate ischemic stroke (Chang and Wang, 2003; Chong and Feng, 1999; Hu and Li, 2004; Xu and Feng, 1999). Cui et al reported the results of their multicentric randomized study of synthesized NBP in the treatment of acute moderate ischemic stroke (Cui et al., 2005). Presently, NBP has been approved for the treatment of acute ischemic stroke.

To assess the efficacy and safety of NBP soft capsules in the treatment of acute ischemic stroke, researchers had two groups divided in the clinical trial. Multicentric, randomized, parallel controlled and open study was performed in group I (144 patients) and multicentric opened study was performed in group II (299 patients). Patients were orally administrated 200 mg NBP per time, 4 times daily. The administrative duration was 20 days. The controlled group was administrated with placebo. All patients were simultaneously treated with compound injection of Danshen. The national rating scale score (NRSS) and activities of daily living (ADL) were used for evaluation in the study. Remarkable clinical improvement was found in 73.1% patients (group I) and 63.9% (group II) respectively. There was a significant difference between the two groups on NRSS and ADL assessments on the 11th and 21st days after treatment respectively. Increase of alanine aminotransferase (ALT) and aspartic transaminase (AST) were the main side effects in this study. The incidence of abnormal liver function was 1.4% in group I and 8.7% in group II. ALT and AST returned to normal after stop of medications. Diarrhea was found in one patient for 3 days after taking the

medication, which disappeared after 3 days. The results in the present study indicated that NBP should be regarded as an effective and safe medication in the treatment of acute moderate ischemic stroke without severe side effects.

## 1.6 Primary Properties of Ligustilide

3-butylidene-4,5-dihydrophthalide (ligustilide) is a volatile oil with a color of light yellow and a flavor. It was first isolated from the roots of *Ligusticum acutilobum* of Umbelliferae plant in 1960 (Mitusubishi et al., 1960), and its structure identified the next year (Fig 1.2, Mitusubishi et al., 1961). Late studies showed that ligustilide actually was a characteristic phthalide component of numerous Umbelliferae plants and has been considered as the main biologically active component of many important medical plants, such as *Radix Angelica sinensis* (Lin et al., 1979), *Ligusticum wallichii* (Wang et al., 1984), *Ligusticum chuangxiang* (Naito et al. 1996), and *Cnidium officinale* (Bohrmann et al., 1967). Moreover the roots of *Angelica sinensis* was the more important available source of natural ligustilide for over 50% of its essential oil comprises of ligustilide (Fang et al., 1979; Li et al., 2001). Natural ligustilide of the roots of *Angelica sinensis* has E- and Z- two configurations (structures shown in Fig 1.2) and Z-configuration content is 10 times as much as the E-form (Li et al., 2001).

Ligustilide is a lipophilic compound with an oil/water partition coefficient of (logP) 2.87, molecular weight 190, and is soluble in organic solvents, ethanol, DMSO, ethyl acetate *etc.* At room temperature, ligustilide is an unstable liquid compound due to the active dihydrobenzene, which can be changed to other phthalides through oxidation, isomerization, dimerization, *etc.* It was reported that more than 30 phthalides exist in the roots of *Angelica sinensis* (Lin et al., 1998). It was also reported that the pure ligustilide in CHCl<sub>3</sub> kept in a brown bottle was stable for a year with or without butylated hydroxyanisole (Hisayuki and Ikunori, 1992). The stability of ligustilide with solvent effect and its relationship with solvent effect were studied for the

preservation of ligustilide (Zhou and Li, 2001). Ligustilide was more stable in cyclohexane and chloroform than in air. The isomerization rate of ligustilide was remarkably decreased by 1.6% and 6.7% in cyclohexane and chloroform respectively, and 58% in air was. The results showed that the stability of ligustilide was greatly improved with the solvent effect, and keeping ligustilide in a proper organic solvent helped its preservation.

## **1.7 OBJECTIVES**

This thesis will investigate the neuroprotective effect and mechanism of Z-ligustilide (LIG) from *Radix Angelica sinensis* on cerebral ischemia.

### **1.7.1 Part 1**

This study aims to:

- 1) Determine the transepithelial transport of LIG across Caco-2 monolayers *in vitro*.
- 2) Identify the effects of temperature, extracellular calcium and P-gp inhibitor-cyclosporin A on the apparent permeability coefficients ( $P_{app}$ ) of LIG across Caco-2 monolayers.

These two sets of results will indicate the absorption of LIG in *in vivo* intestine while orally administrated, and elucidate its principal mechanism of intestinal absorption. These *in vitro* pharmacokinetic data will provide the information for designing the dosage regimen of LIG *in vivo*.

### **1.7.2 Part 2**

In order to determine the antioxidant activity of LIG, its scavenging ability on free

radicals DPPH is examined. And the inhibitory effects on lipid peroxidation are also investigated in the automatic oxidation of linoleic acid and enzyme/non-enzyme induced lipid peroxidation in rat brain mitochondria. Studies show that antioxidant may prevent oxidative injury. In this part, the protection of LIG is evaluated on C6 glioma cell damage induced by hydrogen peroxide and the effect on apoptotic process associated with oxidative stress is also studied.

### **1.7.3 Part 3**

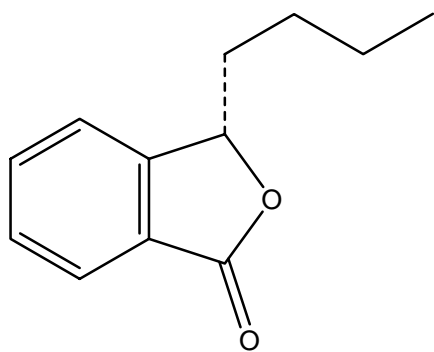
Oxidative stress plays an important role in ischemic brain damage, and the severity and reversibility of the ischemic damage depend on the degree and duration of the flow reduction. Studies indicate that mild ischemic insult causes neuronal death mainly by the apoptosis pathway, and lipophilic antioxidants have been shown to be a beneficial therapy for cerebral ischemic damage. In this part, we investigate the dose-dependent neuroprotection of postischemic application of LIG on transient forebrain ischemia in mice, as well as the mechanisms associated with antioxidation and anti-apoptosis. The results will elucidate whether LIG, a potential antioxidant *in vitro*, also has a potent antioxidant activity *in vivo*, and whether it can protect neurons against mild ischemic insult in brain.

### **1.7.4 Part 4**

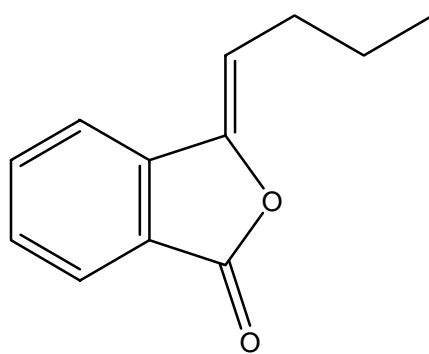
Focal cerebral ischemia, which occurs in a wide variety of clinical settings, affects restricted brain regions and forms an ischemic core and penumbra. The outcome of cerebral ischemia is different in the ischemic core and penumbra due to the different degree and duration of the flow reduction. The neurons in the ischemic core mainly undergo a rapid necrotic death whereas those in the penumbra appear to have a delayed death process of apoptosis. And the switch between these two cell death forms mainly depends on the energy state in the ischemic area (Onténiente et al., 2003). Moreover, the ischemic core will expand if anti-ischemic intervention is delayed. To explore the

neuroprotection of LIG in focal cerebral ischemia, we investigate the effects of postischemic application of LIG on the infarct volume, the neurologic behavior, the number of necrotic or apoptotic neurons in the ischemic penumbra and core after reperfusion following transient MCAO as well as its anti-apoptosis, anti-inflammation and hypothermia properties associated with the mechanisms of delayed brain damage. Findings obtained from these studies provide information for the administration proposal of LIG *in vivo*. In addition, *in vitro* and *in vivo* results will first support the basis for the potential therapeutic application of LIG for cerebral ischemia.

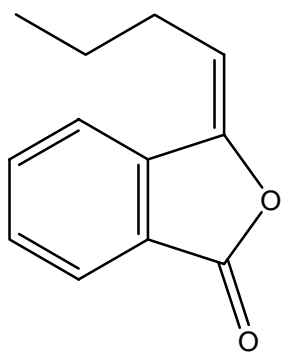
(1) 3-alkylphthalides



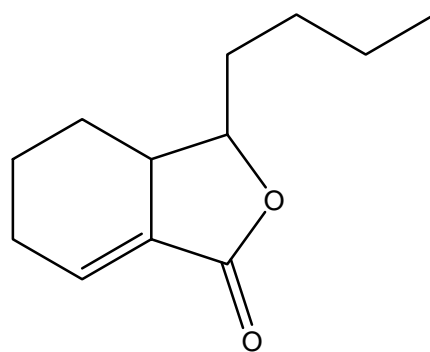
3-n-Butylphthalide (1)



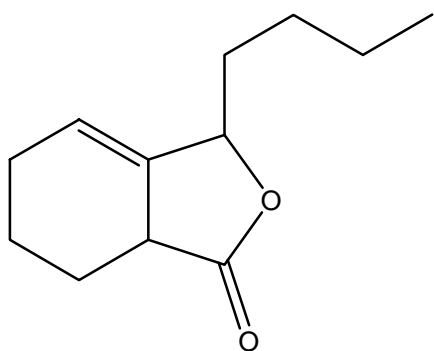
Z-Butylidenephthalide (2)



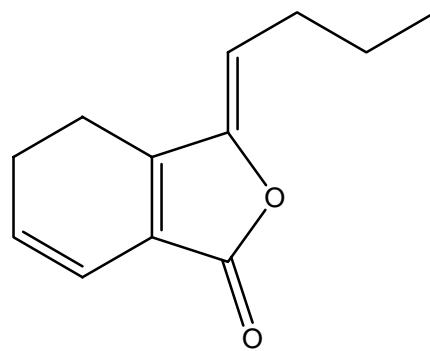
(E)-Butylidenephthalide (3)



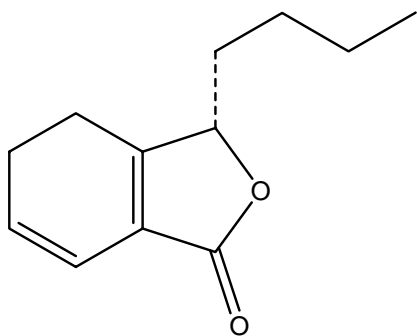
Neocnidilide (4)



Sedanolidide (5)

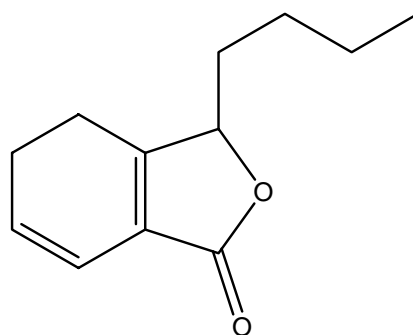


Z-Ligustilide (6)



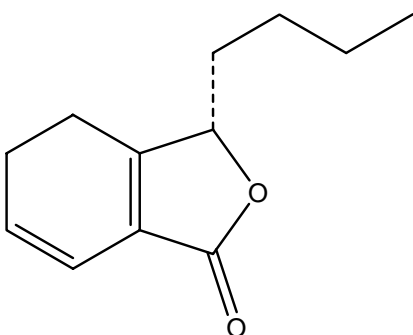
3-n-Butyl-4,5-dihydrophthalide

(7)



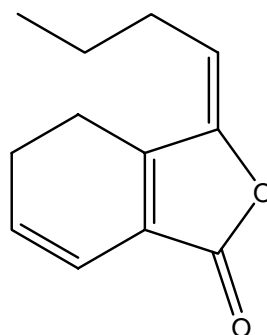
Sedanenolide

(8)



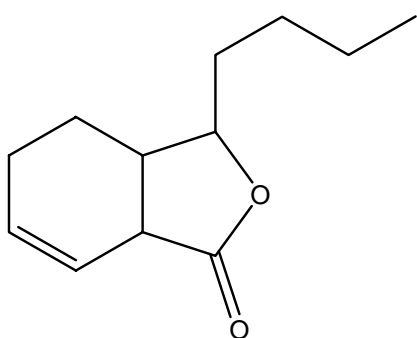
(3S)-3,8-Dihydroxyligustilide  
(Senkyunolide, Senkyunolide A)

(9)



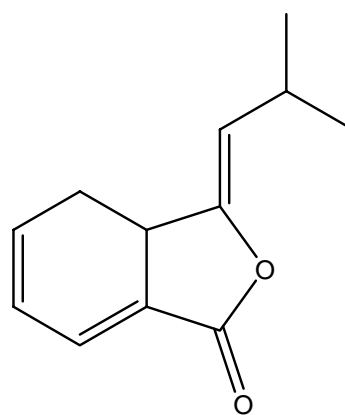
E-Ligustilide

(10)



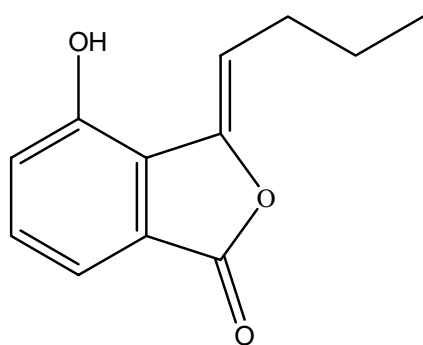
Cnidilide

(11)

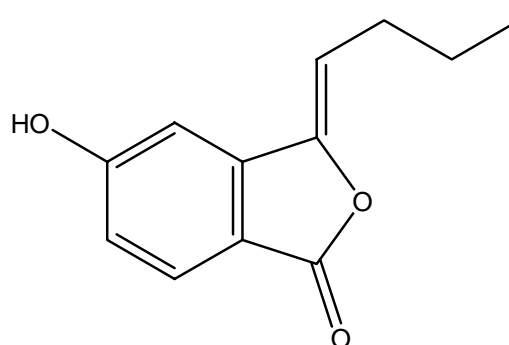


3a,4-Dihydroisobutylidenephthalide (12)

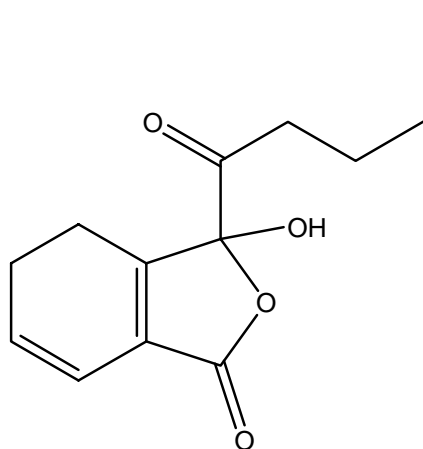
(2) Mono- or bi-hydroxy derivatives of 3-alkylphthalide



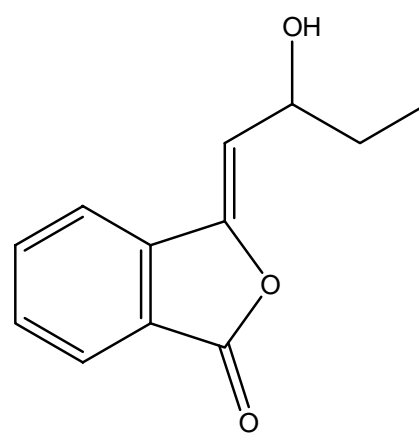
Senkyunolide B (13)



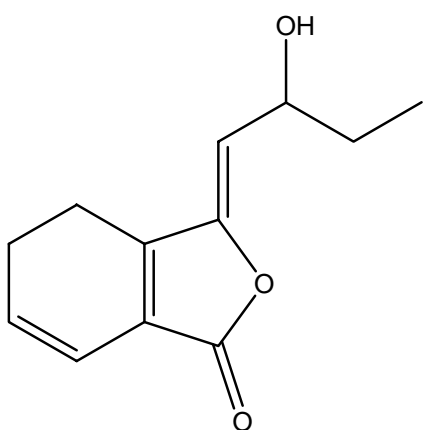
Senkyunolide C (14)



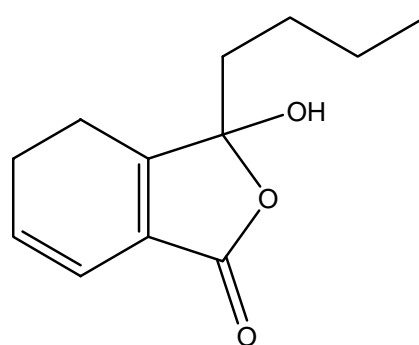
Senkyunolide D (15)



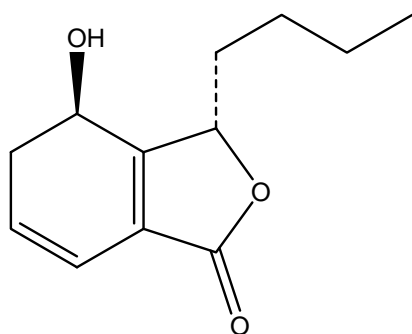
Senkyunolide E (16)



Senkyunolide F (17)

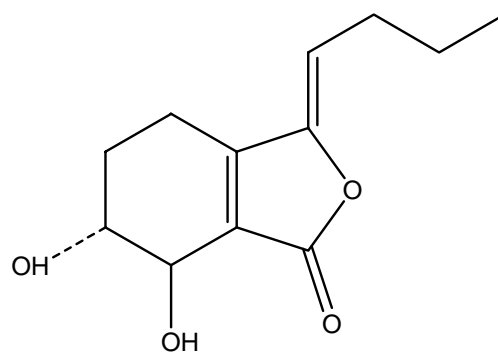


Senkyunolide G (18)



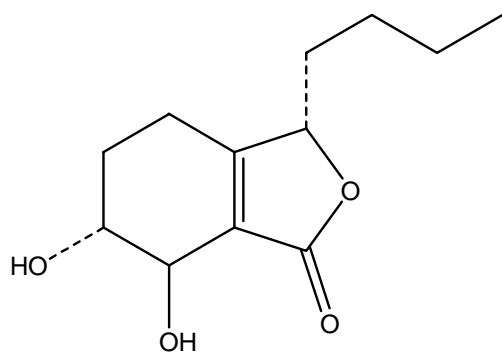
Senkyunolide K

(19)



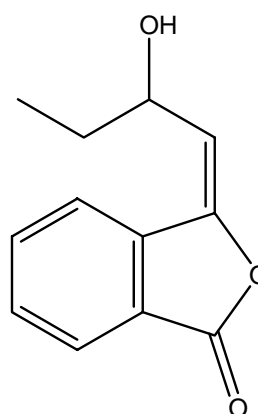
S-Senkyunolide I

(20)



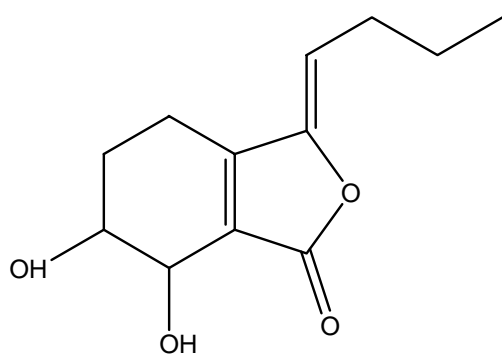
Senkyunolide J

(21)



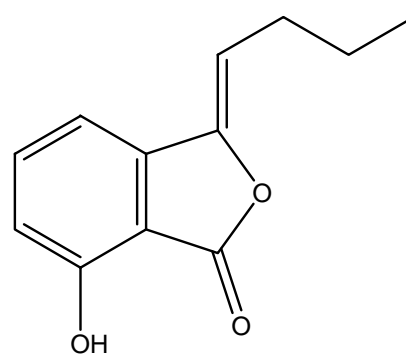
E-Senkyunolide E

(22)

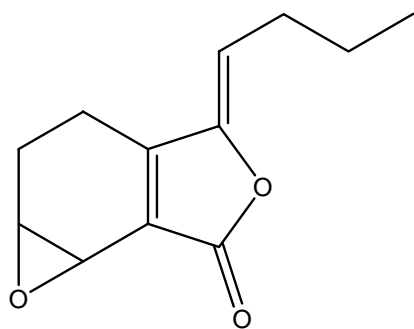


Senkyunolide H

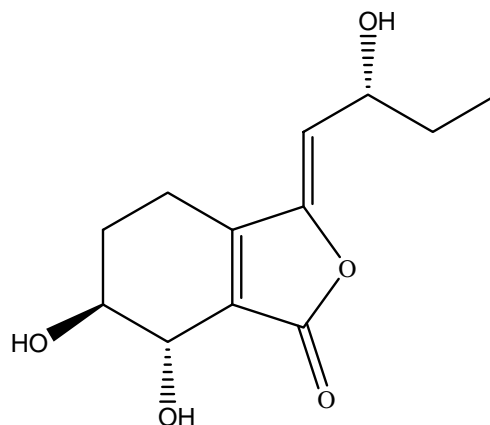
(23)



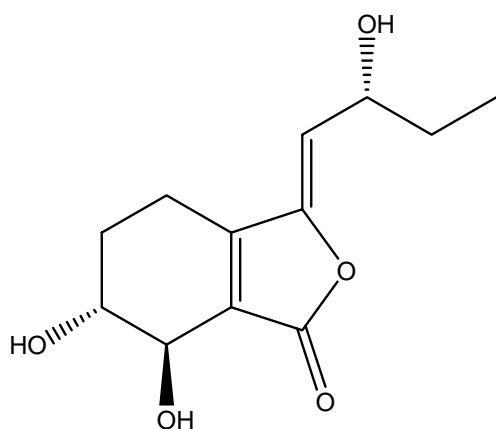
3-Butylidene-7-hydroxyphthalide (24)



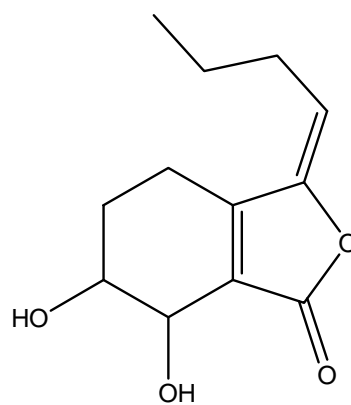
Z-6,7-Epoxyiligustilide (25)



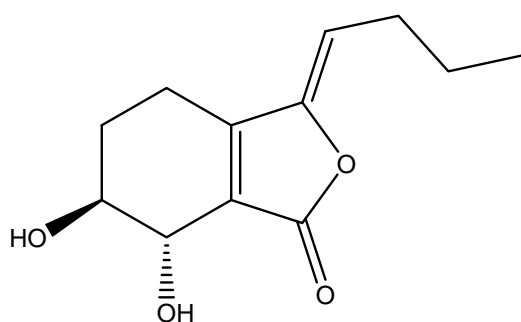
Senkyunolide R (26)



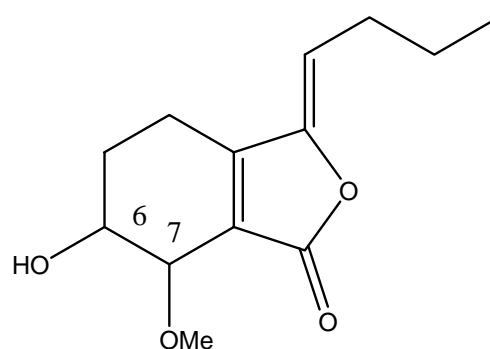
Senkyunolide S (27)



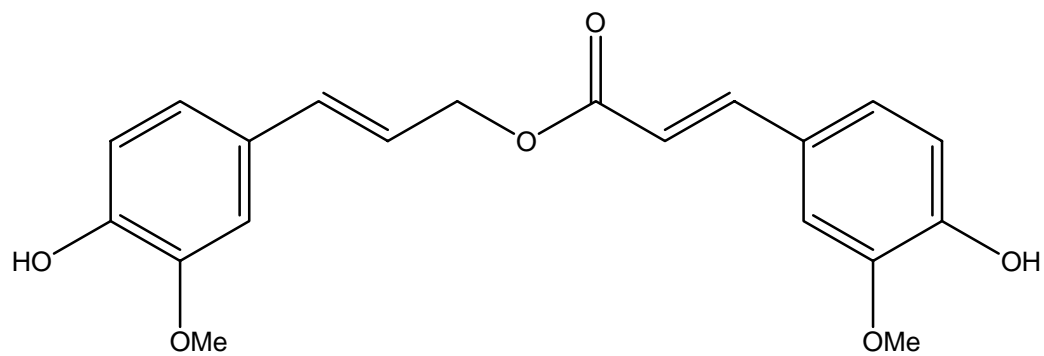
E-6,7-Dihydroxy dihydroiligustilide (28)



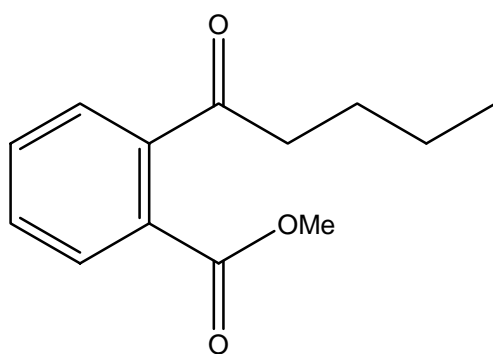
R-Senkyunolide I (29)



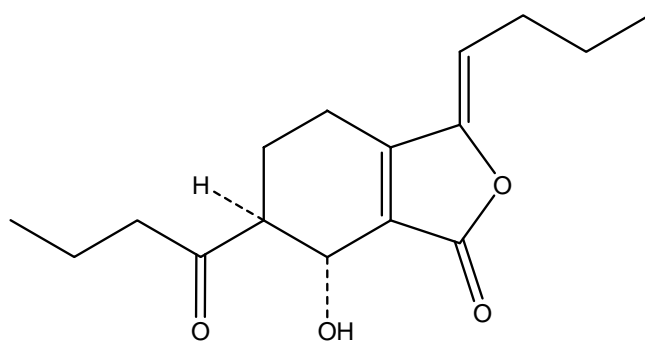
Z-6-Hydroxy-7-methoxy-dihydroiligustilide (30)



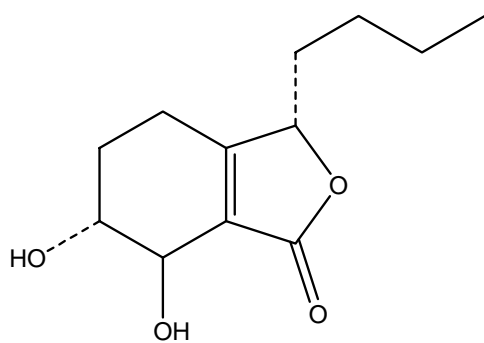
Coniferyl ferulate ( 31)



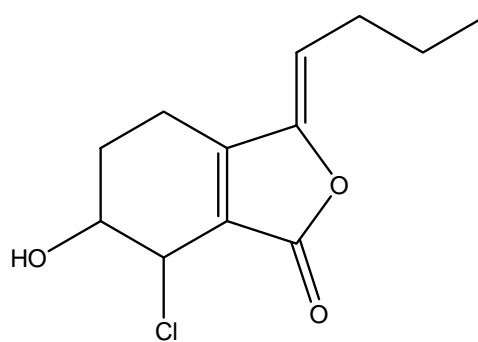
2-(1-Oxopentyl)-  
benzoic acid methyl ester (32)



Senkyunolide M (33)

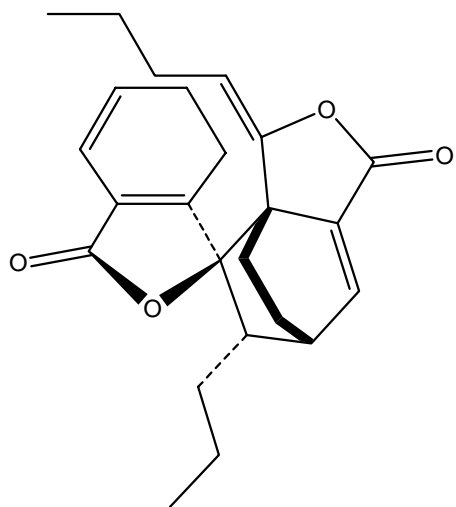


Senkyunolide J (34)

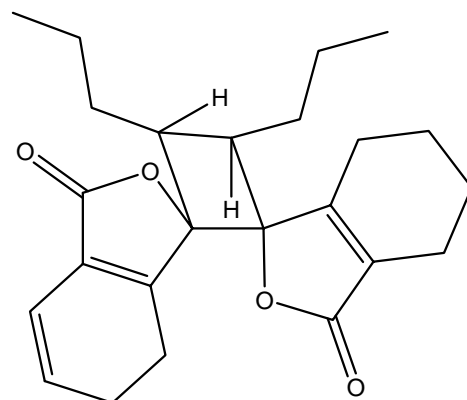


Senkyunolide L (35)

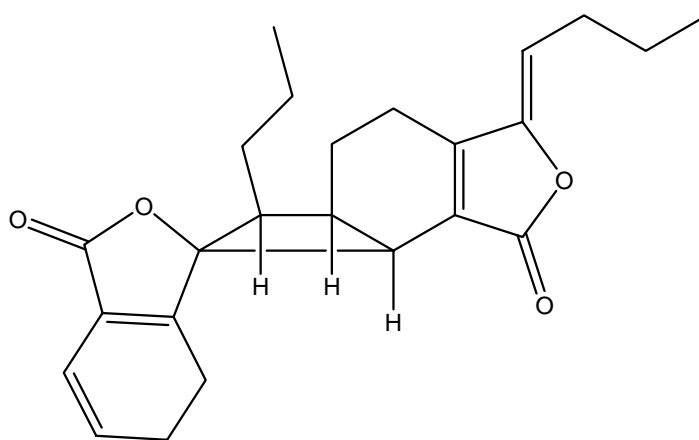
(3) Demeric derivatives of 3-alkylphthalide



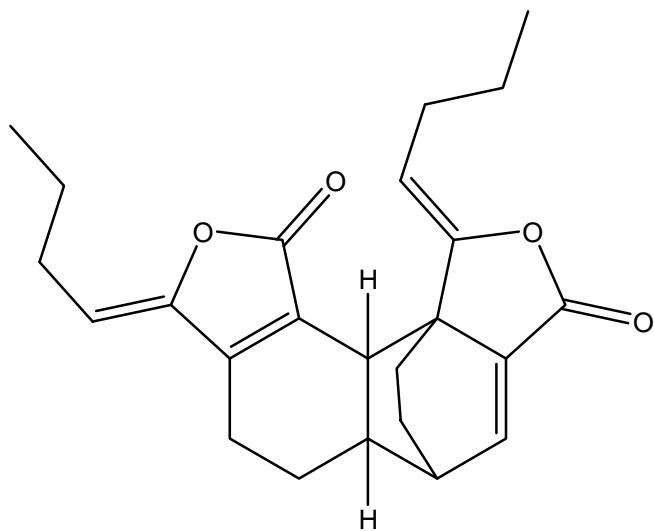
Angeolide (36)



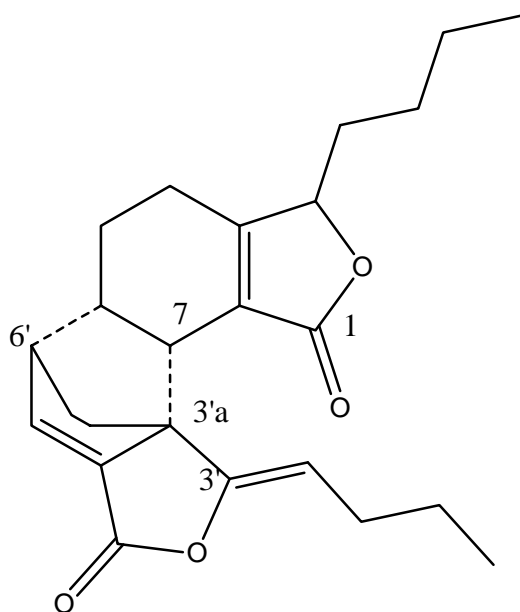
Angelicolide (37)



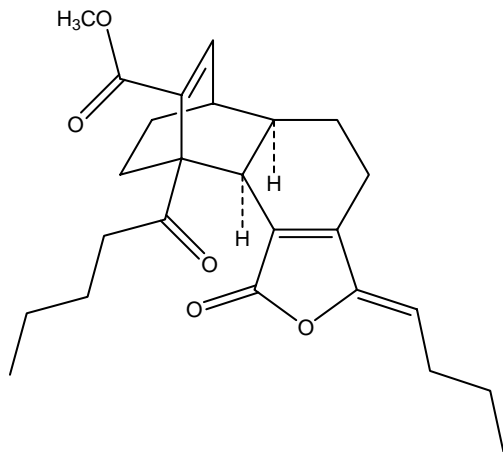
Riligustilide (38)



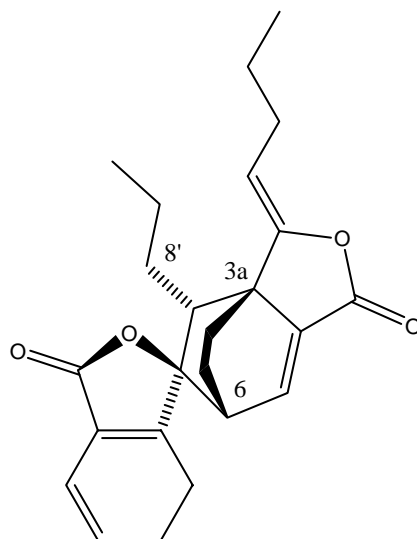
Levistolide A (E) (39)  
 Levistolide B (Z) (40)



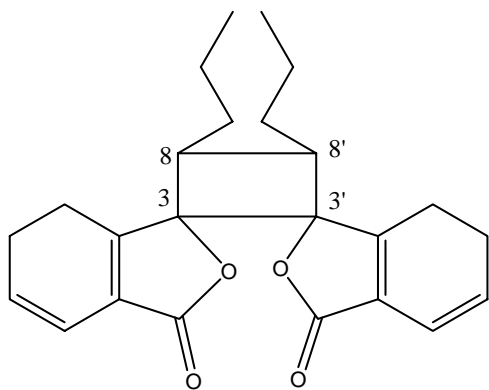
Z-3,8-Dihydro-6,6',7,3a'-diligustilide (41)



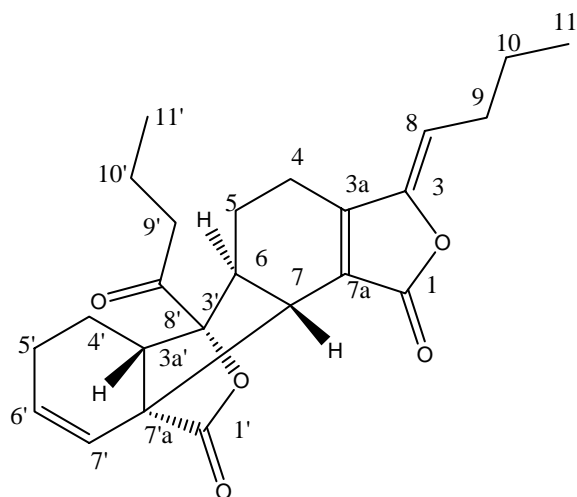
Wallichilide (42)



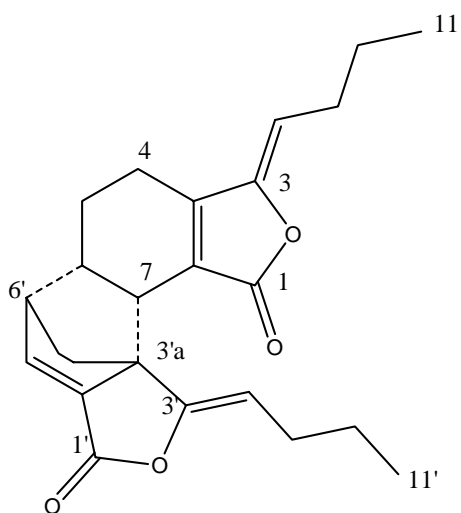
Z-Ligustilide dimer E-232 (43)



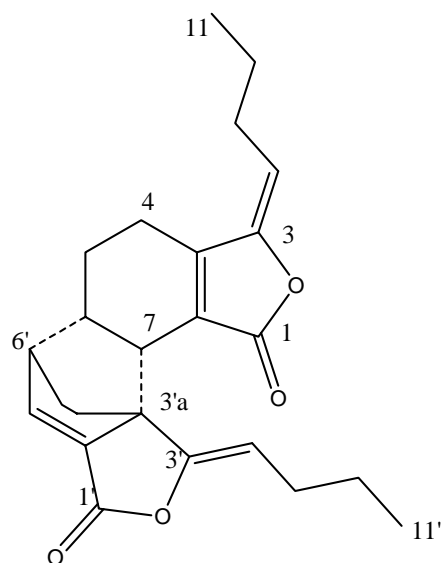
Z,Z'-3.3',8.8'-Diligustilide (44)



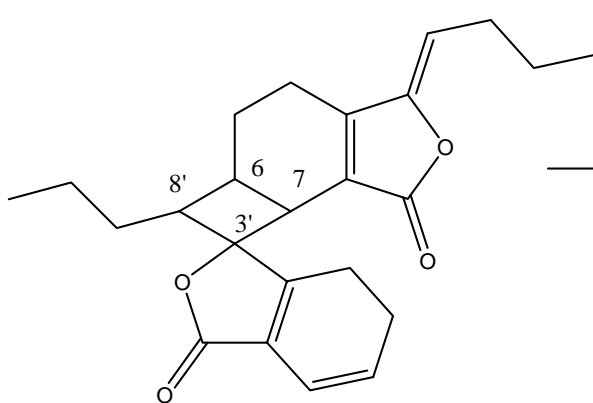
Z-3',8',3'a,7'a-Tetrahydro-6,3',7,7'a-diligustilide-8'-one (45)



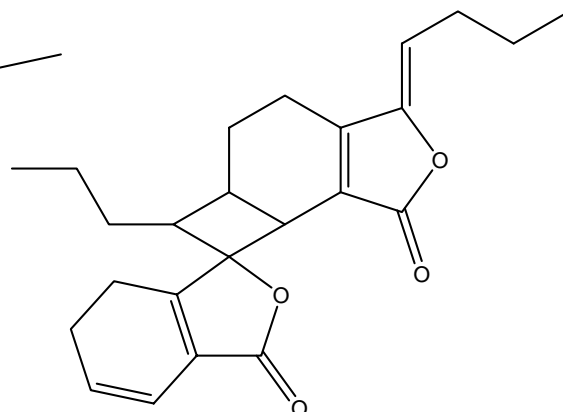
Z,Z'-6,6',7,3'a-Diligustilide (46)



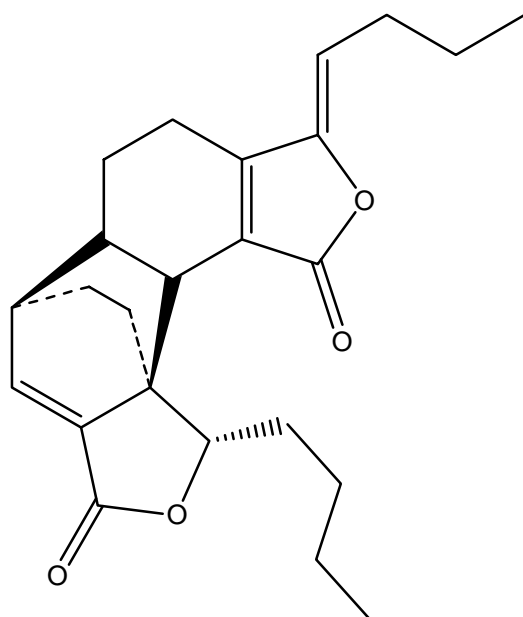
E,Z'-6,6',7,3'a-Diligustilide (47)



Z,Z'-6,8',7,3'-Diligustilide (48)

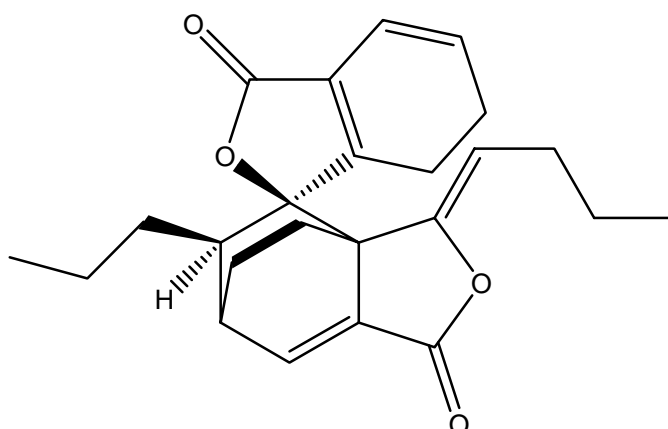


Angelicide (49)



(3Z)-(6R,7R,3'S,3a'S,6'R)-  
3',8'-Dihydro-6,6':7,3a'-biligustilide (50)

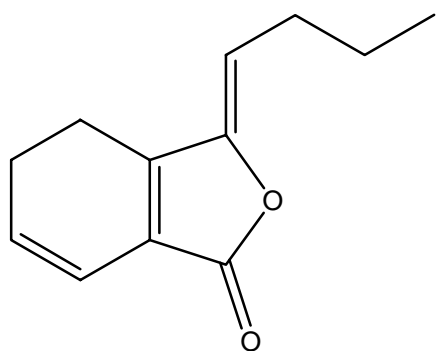
(Senkyunolide P)



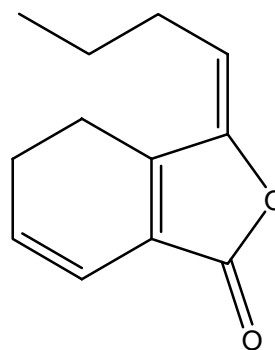
(3'Z)-(3RS,8SR,3a'RS,6'SR)-3,3a':8,6'-biligustilide (51)

( Tokinolide B)

**Figure 1-1.** The structures of 3-alkylphthalides and their derivatives. (1). 3-alkylphthalides (structure number 1-12); (2). Mono- or bi-hydroxy derivatives of 3-alkylphthalide (structure number 13-35); (3). Demeric derivatives of 3-alkylphthalide (structure number 36-51).



Z-Ligustilide



E-Ligustilide

**Figure 1-2.** The configuration structures of ligustilide.

## CHAPTER 2

### MATERIALS, APPARATUS AND METHODS

#### 2.1 MATERIALS

##### 2.1.1 Reagents and Analysis Kits

2,2-diphenyl-1-picrylhydrazyl (DPPH)	Sigma Chemical Co. USA
2-mercaptoethanol	Bio-Rad Technology Ltd., USA
2-Thiobarbituric acid	Sigma Chemical Co. USA
3-(4,5-dimethylthiazol-2-yl)-2,5-diphenyltetrazolium bromide (MTT)	Sigma Chemical Co. USA
100 bp DNA Ladder	Sigma Chemical Co. USA
Acrylamide, electrophoresis grade	Bio-Rad Technology Ltd., USA
Agarose	Bio-Rad Laboratories, USA
Agarose standard low- <i>Mr</i> (100bp)	Bio-Rad Technology Ltd., USA
Aminopropyltriethoxysilane	Beijing Zhong Shan Co., China
Ammonium thiocyanate	Merck, Germany
Aprotinin	Sigma Chemical Co. USA
Ascorbic acid	Sigma Chemical Co. USA
Ascorbic acid	Sigma Chemical Co. USA
Bovine serum albumin (BSA)	Sigma Chemical Co., USA
Bromophenol blue	Sigma Chemical Co. USA
Chloroform	Sigma Chemical Co., USA
Cyclosporine A	Sigma Chemical Co., USA

DAB kit	VECTOR, Burlingame, USA.
D-Glucose	Sigma Chemical Co. USA
Dimethyl sulfoxide (DMSO)	Sigma Chemical Co. USA
Dithiothreitol	Sigma Chemical Co. USA
DMEM medium	Gibco, USA
ECL Western blotting analysis system (RPN 2108)	Amersham Pharmacia Biotech, USA
EDTA	Sigma Chemical Co., USA
Ethanol	Sigma Chemical Co., USA
Ethidium bromide	Bio-Rad Technology Ltd., USA
FeSO <sub>4</sub>	Sigma Chemical Co. USA
Fetal bovine serum	Hyclone, USA
Glycerol	Sigma Chemical Co. USA
Goat anti -caspase-8 polyclonal antibody	Santa Cruz Biotechnology, USA
Kit of GSHPx activity assay	Jianchen Bioengineering Co, China.
H <sub>2</sub> O <sub>2</sub> (30%, w/v)	Riedel-de Haen, Germany
Hank's balance salt solution (HBSS)	Invitrogen, CA, USA
HEPES	Sigma Chemical Co., USA
HEPES-KOH	Sigma Chemical Co. USA
Hoechst 33342	Fluka, Switzerland
Horseradish peroxidase-conjugated anti-goat secondary antibody	Santa Cruz Biotechnology, CA, UAS
Horseradish peroxidase-conjugated anti-mouse secondary antibody	Amersham Biosciences, England

Horseradish peroxidase-conjugated anti-rabbit secondary antibody	Santa Cruz Biotechnology, CA, UAS
Isoamyl alcohol	Sigma Chemical Co., USA
Isopropyl alcohol	Tedia, USA
KCl	Sigma Chemical Co. USA
Kit of caspase-3 activity assay	KeyGen Biotech corporation limited, China
Kit of Caspase-8 activity assay	KeyGen Biotech corporation limited, China
Kit of <i>in situ</i> Cell Death Detection, POD (TUNEL)	Roche, Germany
Kit of iNOS activity assay	Jianchen Bioengineering Co, Nanjing, China
Kit of NO content assay	Jianchen Bioengineering Co, Nanjing, China
Kodak XOMAT AR films	Eastman Kodak, USA
Leupeptin	Sigma Chemical Co. USA
Linoleic acid (18:2)	Sigma Chemical Co. USA
Kit of malondialdehyde (MDA) content assay	Jianchen Bioengineering Co, China.
Methanol	Sigma Chemical Co. USA
MEM non-essential amino acid solution (100×)	Sigma Chemical Co. USA
MgCl <sub>2</sub>	Sigma Chemical Co. USA
Mouse anti- OX42 monoclonal antibody	Serotec, Oxford, UK
Mouse anti-Bax monoclonal antibody	Santa Cruz Biotechnology, USA
Mouse anti-Bcl-2 monoclonal antibody	Santa Cruz Biotechnology, USA

Mouse anti-cytochrome c monoclonal antibody	Santa Cruz Biotechnology, USA
Mouse anti- $\beta$ -actin monoclonal antibody	Sigma Chemical Co., USA
Mouse anti- iNOS monoclonal antibody	BD Biosciences Pharmingen, USA
NADPH	Sigma Chemical Co., USA
Na-EDTA	Sigma Chemical Co. USA
N-butanol	Sigma Chemical Co. USA
Paraformaldehyde	Sigma Chemical Co. USA
Penicillin-streptomycin	Gibco, USA
Pepstatin	Sigma Chemical Co. USA
Phenol	Sigma Chemical Co., USA
Phenylmethyl sulfonyl fluoride (PMSF)	Sigma Chemical Co. USA
Plastic culture flask	Falcon, Franklin UAS
Polyacrylamide	Amresco, USA
Polycarbonate membrane transwells <sup>TM</sup>	Corning Costar Corp. Acton, UAS
Polyvinylidene fluoride (PVDF)	Millipore Corporation, USA
Prestained protein marker	Bio-Rad Laboratories, CA, USA
Proteinase K	Sigma Chemical Co. USA
Rabbit anti- cleaved caspase-3 polyclonal antibody	Cell Signaling Technology, Inc. USA
RNase A	Sigma Chemical Co. USA
Kit of SOD activity assay	Jianchen Bioengineering Co, China.
Sodium deoxycholate	Sigma Chemical Co., USA
Sodium dodecyl sulfate (SDS)	Bio-Rad Technology Ltd., USA
Sodium orthovanadate	Sigma Chemical Co., USA

SP Reagent	Zhongsan Bioengineering Co, China.
Sucrose	Sigma Chemical Co. USA
TEMED	Bio-Rad Technology Ltd., USA
Trichloroacetic acid	Sigma Chemical Co. USA
Triphenyltetrazolium chloride	Sigma Chemical Co. USA
Tris	Bio-Rad Technology Ltd., USA
Trypsin	Gibco, USA
Tween-20	Sigma Chemical Co. USA
Tween-80	Sigma Chemical Co. USA

### 2.1.2 Apparatus

Boiling water bath	Grand Instruments, USA
Freezer (-80 °C)	Czech Republic HETO HOLTEN AS, Denmark
Freezing microtome (model CM1510)	Leica, Germany
Gel Media System	Media Cybernetics, Inc. USA
Gel-pro Analyzer software	Media Cybernetics, Inc. USA
Incubator (model TC2323)	Shel LAB, USA
Leica microscope (Model DRIMB)	Leica, Germany
Microcentrifuge	Eppendorf, Germany
Microtiter plate reader	Bio-Rad Technology Ltd., USA
Millicell-ERS system (Cat #.MERS 000 01)	Millipore Corporation, USA

Minigel apparatus	Bio-Rad Technology Ltd.,USA
Modular 1100 series chromatograph	Agilent Technologies, Germany
pH meter (Model 701 digital)	Orion research, USA
Rotor–stator homogenizer	IKA-Labortechnik., Germany
Sonicator, Branson Sonifier 250	Branson Inc., USA
UV-visible spectrometer	GBC, Australia

### **2.1.3 Animals**

In this project, mice and rats were used to investigate the neuroprotection of Z-ligustilide on cerebral ischemia injury. The use of animals was approved by the Department of Health of Hong Kong, the Animal Ethics Committee of The Hong Kong Polytechnic University and Shenzhen Institute of The Hong Kong Polytechnic University. The rats were supplied by the Animal House of The Hong Kong Polytechnic University or Shenzhen Institute of The Hong Kong Polytechnic University. To eliminate the existence of any sex-related differences in response to Z-ligustilide, the male ICR and Sprague-Dawley (SD) rats were selected for all experiments. All the animals were housed in pairs in stainless steel rust-free cages at  $21\pm 2^{\circ}\text{C}$ . The rooms were in a light-dark cycle of 12 hours of light (7:00 to 19:00) and 12 hours of dark (from 19:00 to 7:00). All the animals were fed the Laboratory Rodent Diet (PMI, Brentwood, MO. Catalog# 5001, containing protein 28%, fat 12.1%, fiber 5.3%, Carbohydrate 59.8% and 270 ppm iron) ad libitum and plenty of distilled water was supplied at all times.

## **2.2 GENERAL METHODS**

### **2.2.1 Cell Culture**

### **2.2.1.1 Cell Culture Medium, Solutions and Reagents**

#### **(1) Milli-Q water**

All the solutions for cell culture and medium were made with Milli-Q water.

#### **(2) Cell culture medium**

Dulbecco's Modified Eagle Medium (DMEM), powder (Gibco, NY, USA).

Fetal Bovine Sera (FBS), qualified, heat inactivated (Hyclone, UT, USA).

MEM non essential amino acid solution (100 ×) (Sigma Chemical Co. USA).

#### **(3) Cell culture solution**

Phosphate-Buffered Saline (PBS) (1×), liquid (Catalogue Number: 20012) pH 7.2 ± 0.05 (Invitrogen, CA, USA)

Hank's Balanced Salt Solution (HBSS) (1×), liquid (Catalogue Number: 14175) (Invitrogen, CA, USA)

Trypsin (2.5%, 10×) (Gibco, NY, USA)

Trypan blue solution (Fluka, Buchs, Switzerland)

### **2.2.1.2 Trypan Blue Staining of Cell**

(1) Cell were placed in complete medium without serum and diluted to an approximate

concentration of  $1 \times 10^5$  to  $2 \times 10^5$  cells per ml. 0.5 ml of this cell suspension was placed in a screw cap test tube, to which was added 0.1 ml of 0.4% Trypan Blue Stain.

(2) The solution was mixed thoroughly and allowed to stand 5 min at 15-30 °C.

(3) A hemocytometer was filled with cell solution for cell counting. Non-viable cells were observed with the stain, and viable cells were not stained.

### **2.2.1.3 Cryopreservation of Cells**

- (1) The cultured cells were detached from the substrate using dissociation agents. This was done as gently as possible to minimize damage to the cells.
- (2) The detached cells were placed in a complete growth medium and established a viable amount of cells.
- (3) The re-suspended cells were centrifuged at  $\sim 200 \times g$  for 5 min and withdrawn the supernatant down to the smallest volume without disturbing the cells.
- (4) The cell pellet was resuspended in freezing cold medium to a concentration of  $5 \times 10^6$  to  $1 \times 10^7$  cells/ml.
- (5) Aliquot of the cells solution was placed into cryogenic storage vials. The vials were put on ice or in a  $4^\circ\text{C}$  refrigerator, and freezing began within 5 min.
- (6) The cells were slowly frozen at a rate of  $1^\circ\text{C}/\text{min}$ . This could be done by programmable coolers or by placing the vials inside an insulated box placed in a  $-70^\circ\text{C}$  to  $-90^\circ\text{C}$  freezer, then transferred for storage in liquid nitrogen.

### **2.2.1.4 Thawing of Cryopreserved Cells**

Cryopreserved cells are fragile and require gentle handling. The cells were thawed quickly and placed directly into complete growth medium. If the cells were particularly sensitive to cryopreservation (DMSO or glycerol), they were centrifuged to remove cryopreservative and then placed into growth medium.

The following were the suggested procedures for thawing the cryopreserved cells.

- (1) Remove cells from storage and thaw quickly in a  $37^\circ\text{C}$  water bath.
- (2) Place 1 or 2 ml of frozen cells in  $\sim 25$  ml of complete growth medium. Mix very gently.
- (3) Centrifuge cells at  $\sim 80 \times g$  for 2 to 3 min.
- (4) Discard supernatant.

- (5) Gently resuspend cells in complete growth medium and perform a viable cell count.
- (6) Culture the cells. Cell density should be at least  $3 \times 10^5$  cells/ml.

#### Direct Plating Method:

- ✓ The cells from storage are thawed quickly in a 37 °C water bath.
- ✓ The thawed cells are directly placed in a flask with complete growth medium. 1 ml of frozen cells is added to 10 to 20 ml of complete medium to make a suspension cell density of at least  $3 \times 10^5$  cells/ml.
- ✓ The cells are cultured for 12 to 24 hours, and the medium replaced with fresh complete growth medium to remove cryopreservatives.

#### **2.2.1.5 Caco-2 Cell Culture**

Frozen human colon adenocarcinoma cells (Caco-2 cells) were obtained from the American Type Culture Collection (ATCC, Rockville, MD, USA) at passage 38. As per accompanying ATCC guidelines, the cells were grown in Dulbecco's modified Eagle's medium (DMEM, Gibco), supplemented with 10% (v/v) heat-inactivated fetal bovine serum (FBS), 1% nonessential amino acid, and 100 U/ml of sodium penicillin G and 100 µg/ml of streptomycin sulfate (Hidalgo et al., 1989; Hilgers et al., 1990). The medium was changed every 2 days. The subculture was prepared by removing the medium, adding 1-3 ml of fresh 0.25% trypsin/1mM EDTA solution for 10 to 15 min, and the trypsin solution removed. Fresh medium was added, aspirated and dispensed until the cells were detached. Then the cells were transferred to a 15 ml centrifuge tube containing 3-5 ml of fresh medium and centrifuged at 1000 rpm for 5 min at 4 °C. The supernatant was discarded and the pellet triturated in 2 ml of fresh medium. The cell number was determined by trypan blue exclusion under the microscope, and the required number of cells placed into the flasks (for maintenance), and in six-well polycarbonate membrane Transwells™ or 6-well plates. All the apparatus and mediums used for cell culture were sterilized before use. Cells from passage 40-50

were used for the transport experiments.

#### **2.2.1.6 C6 Glioma Cell Culture**

C6 Glioma cell line was obtained from the American Type Culture Collection (ATCC). The cells were grown in Dulbecco's modified Eagle's medium (DMEM, Life Technologies), supplemented with 10% (v/v) heat-inactivated FBS and 100 U/ml of sodium penicillin G and 100 µg/ml of streptomycin sulfate. The medium was changed every 3 days. The subculture was prepared by removing the medium, adding 1-3 ml of fresh 0.25% trypsin or 2 mM EDTA solution (for protein extraction) for several minutes, and the trypsin solution removed. The culture was allowed to stand at room temperature for 10 to 15 min. Fresh medium was added, aspirated and dispensed until the cells were detached. Then the cells were transferred to a 15 ml centrifuge tube containing 3-5 ml of fresh medium and centrifuged at 1000 rpm for 5 min at 4 °C. The supernatant was discarded and the pellet triturated in 2 ml of fresh medium. The cell number was determined by trypan blue exclusion under the microscope, and the required number of cells placed into the flasks (for maintenance), and in 6-well plates or 96-well plates. All the apparatus and mediums used for cell culture were sterilized before use.

### **2.2.2 Methods of Molecule Biology**

#### **2.2.2.1 DNA Preparation**

##### **(1) Principle**

The DNA was isolated from the brain tissue using phenol/chloroform/isoamyl alcohol for the detection of fragmented DNA by agarose gel electrophoresis. The relative purity of the isolated DNA was assessed spectrophotometrically and the ratio of A260 nm to A280 nm was 1.8 for all preparations.

## **(2) Procedure**

- (A) Fresh tissues were homogenized in 10 volume of ice-cold TE buffer containing 10 mM Tris-HCl, pH 8.0, 1 mM EDTA.
- (B) After centrifugation at 4000 rpm 5 min at 4 °C, the supernatants were discarded.
- (C) Resuspend the pellets in 500 µl ice-cold TE buffer and centrifuge again.
- (D) Aspirate media, resuspend pellet in 500 µl ice-cold TE buffer.
- (E) Centrifuge sample again and lyse pellets by adding 500 µl ice-cold lysis buffer containing 10 mM Tris-HCl, pH 7.4, 1 mM EDTA, 1% SDS.
- (F) Samples were digested at 37 °C for 1h, after the addition of 0.02 mg/ml RNase A.
- (G )The Digestion was continued for 3 h at 55 °C, followed by the addition of 0.1mg/ml proteinase K.
- (H) Extract by adding an equal volume of phenol:chloroform:isoamyl alcohol (25:24:1) to the sample and vortexing for a few seconds to properly mix the solutions. Spin the tube at 12000 rpm for 3 min at room temperature. Carefully remove the top aqueous phase and transfer to a clean tube.
- (I) Repeat step (H).
- (J) Add an equal volume of chloroform:isoamyl alcohol (24:1) to the sample and mix briefly by vortexing. Spin the tube at 12000 rpm for 3 min at room temperature. Remove the top aqueous layer and place in a new tube.
- (K) Precipitate the DNA by adding 5 M NaCl to a final concentration of 300 mM and add 2 volume of 100% ethanol. Leave overnight at 4 °C.
- (L) Spin samples at 12000 rpm for 10 min at room temperature. Carefully aspirate the ethanol off and wash the DNA pellet with 1 ml of 70% ethanol. Dislodge the pellet by inverting several times so that the ethanol can remove any excess salts.
- (M) Spin samples at 12000 rpm for 10 min at room temperature. Dry the pellet by placing it in a Speedvac evaporator and spin for a couple of minutes.
- (N) Resuspend the dried DNA pellet by adding 100ul of TE buffer and flicking the tube a few times. The sample solution was kept at 4 °C until used.

(O) Determine the purity of samples by measuring the absorbance at 260 nm and 280 nm.

(P) Measure the absorbance of samples at 260 nm and 280 nm. The ratio of A<sub>260</sub>nm to A<sub>280</sub> nm was 1.8 for all preparations. The concentration of the sample was calculated as follows:

$$\text{DNA concentration } (\mu\text{g/ul}) = A_{260} \times \text{diluted times} \times 50/1000$$

#### **2.2.2.2 Detection of Fragmented DNA by Agarose Gel Electrophoresis**

##### **(1) Principle**

Classical apoptotic cell death can be defined by certain morphological and biochemical characteristics that distinguish it from other forms of cell death. A biochemical hallmark of apoptosis is the cleavage of chromatin into small fragments, including oligonucleosomes, that when seen in electrophoresed gels are described as “DNA ladders” (Wyllie 1980; Zakeri et al., 1993). In apoptotic cells, DNA is cleaved by an endonuclease that fragments the chromatin into nucleosomal units, which are multiples of about 180-bp oligomers and appear as a DNA ladder when run on an agarose gel (Arends et al., 1990). Determining whether a cell exhibits DNA fragmentation can provide information about the type of cell death occurred and the pathway activated in the dying cell.

##### **(2) Procedure**

All solutions and glassware were sterilized. The electrophoresis tank was treated with detergent solution, rinsing with ddH<sub>2</sub>O, drying with 70% ethanol.

(A) Prepared 2 % agarose gel: Add 2 g agarose to 100 ml of 0.5 × TBE running buffer (45 mM Tris boric acid, 1 mM EDTA) and heat in microwave until dissolved.

(B) Sample preparation: the DNA samples were added to the 6×DNA loading dye (10 mM EDTA, 0.25% bromphenol blue, 40% sucrose ).

(C) Electrophoresis:

- The gel was equilibrated in 0.5 × TBE gel running buffer for at least 30 min.
- Equivalent amounts of DNA samples (10 µg) were added to the wells of the gel, and the gel electrophoresed at 100 V until the bromophenol blue dye migrated approximately two thirds of the way down the gel (2 h).
- DNA bands were visualized by ethidium bromide staining (0.5 µg/ml). Gel pictures were taken by UV transillumination with a Canon Camera.

The DNA samples were analyzed in a 2 % agarose gel using Gel Media System and Gel-pro Analyzer software (Meida Cybernetics, Silver Spring, MD, USA). The expected sizes for the positions of DNA fragmentation were shown compared to the 100-bp DNA ladder marker. DNA fragmentation values were normalized for vehicle-treated controls and expressed in units relative to these controls.

### **2.2.2.3 Protein Preparation and Determination**

#### **(1) Total Protein Preparation**

Tissue samples were washed in ice-cold PBS, and homogenized in 10 volume of ice-cold lysis buffer containing 50 mM Tris-Cl (PH 8.0), 1mM EDTA, 150 mM NaCl, 0.1% SDS, 0.5% sodium deoxycholate, 1mM PMSF, 1 µg/ml aprotinin, 1 µg/ml leupeptin, 1 µg/ml pepstatin, 1% Triton-X-100. After centrifugation of homogenate at 10,000 × g for 30 min at 4 °C, the supernatant was collected and stored at –20 °C until used.

#### **(2) Cytosolic Protein Preparation**

Tissue samples were washed in ice-cold PBS, and homogenized in 10 volumes of lysis

buffer containing 20 mM Hepes-KOH, pH 7.5, 10 mM KCl, 1.5 Mm MgCl<sub>2</sub>, 1 mM Na-EDTA, 1 mM Na-EGTA, 1 mM dithiothreitol, 1 mM PMSF, 250 mM sucrose, 1 µg/ml aprotinin, 1 µg/ml leupeptin, 1 µg/ml pepstatin, and then centrifuged at 750×g for 10 min at 4 °C. The harvested supernatant was again centrifuged at 10,000×g for 10 min at 4 °C, and the supernatant was collected and stored at –20 °C until used.

**(3) Protein Determination (Protein assay kit, Bio-Rad, USA)**

(A) The dye reagent was prepared by diluting 1 part of Dye Reagent Concentrate with 4 parts of distilled, deionized (DDI) water. This was filtered through Whatman #1 filter to remove particulates. This diluted reagent may be used for approximately 2 weeks when kept at room temperature.

(B) Five dilutions (40, 80, 120, 160, 200 µg/ml) of a protein standard were prepared which were representative of the protein solution to be tested.

(C) 100 µl of each standard and sample solution was placed into a clean, dry test tube; 5.0 ml of diluted dye reagent was added into each tube and vortexed. The sample solutions were assayed in duplicate.

(D) The samples were incubated at room temperature for at least 5 min. Because absorbance would increase over time, samples should be incubated at room temperature for no more than 1 h.

(E) Absorbance was measured at 595 nm.

The protein concentration was adjusted to 2-4 mg/ml and the fractions (containing 40 µg protein) in aliquots stored at –70 °C.

#### 2.2.2.4 Western Blot

##### (1) Principle

Western- or immunoblotting is a commonly employed technique for the detection of protein antigens in complex mixtures. It is highly sensitive and can detect as little as picograms of protein with antibodies of known specificity. Samples are first separated by SDS-polyacrylamide gel electrophoresis. The separated proteins are then transferred to a membrane. These membranes are incubated with an antibody specific for the protein of interest that binds to the protein band immobilized on the membrane. The antibody is then visualized with a detection system that is usually based on a secondary protein binding to Ig chains, which are linked to chemiluminescent substrate reaction.

##### (2) Procedure

###### (A) Polyacrylamide gel electrophoresis and transfer

###### a) Polyacrylamide gel electrophoresis

Forty micrograms total protein were diluted in a 2× sample buffer (50 mM Tris, pH 6.8, 2% SDS, 10% glycerol, 0.1% bromophenol blue, and 5% β-mercaptoethanol) and heated for 5 min at 95 °C before SDS-PAGE on a 15% gel for Bax, Bcl-2, cytochrome c, cleaved caspase-3 and caspase-8 or a 7.5% gel for iNOS. Electrophoresis was conducted by running the stacking gel at 100V for about 15-20 min and running the separating gel at 200V for about 40-50 min.

###### b) Transferring gel

- The gel was disassembled from the plates carefully, the stacking gel was removed and the position marked by the notching of one corner.
- The gel was washed in the transfer buffer for 15 min.
- The PVDF membrane and the filter paper were cut to fit the dimension of gel size.

- The filter paper and fiber pads were soaked in transfer buffer for at least 15 min.
- The cassette was assembled as follows: white (+), fiber pads, filter paper, membrane, gel, filter paper, fiber pads, gray (-). Avoid the bubble by rolling a glass rod.
- The pre-chilled transfer buffer and frozen Bio-ice cooling Unit were placed in the electrophoresis tank.
- The transfer unit was allowed to stand at 4 °C overnight for 12-16 h with 30 voltages and gentle agitation.
- After transferring, the blot was put on a clean filter paper, and stained with commassie blue to check the quality of transfer.
- The blots were either used immediately or stored.

c) Immunoblotting (ECL western blotting analysis system, RPN 2108)

The membrane was blocked with 5% blocking reagent (Amersham Biosciences, England) in Tris buffered solution (TBS, 20mM Tris, 137mM NaCl, pH 7.6) containing 0.1% Tween 20 (TBS-T) for 2 h at RT or overnight at 4 °C. The membrane was rinsed in three changes of TBS-T, incubated once for 15 min and twice for 5 min in fresh washing buffer, and then incubated with primary antibody for 2 h at RT or overnight at 4 °C, the concentration of primary antibodies was maintained according to the instruction of products. After three washes in washing buffer, the membrane was incubated for 2 h in horseradish peroxidase-conjugated second antibody, washed three times in TBS-T solution, and then developed using enhanced chemiluminescence (ECL Western blotting analysis system kit, Amersham Biosciences, England). The blot was exposed to XOMAT AR films (Eastman Kodak, Rochester, NY, USA). The films were scanned on a UMAX PowerLook Scanner (UMAX Technologies, Fremont, CA, USA) using Photoshop 5.0 software (Adobe Systems, Seattle, WA, USA), and optical density of each band was determined using Gel-pro Analyzer software (Media Cybernetics, Silver Spring, MD, USA). To ensure even loading of the samples, the same membrane was probed with mouse anti- $\beta$ -actin monoclonal antibody (Sigma-Aldrich, MO) at 1:5000 dilutions.

## 2.2.3 Methods of Biochemistry and Chemistry

### 2.2.3.1 MTT Assay

#### (1) Principle

3-(4, 5-dimethylthiazolo-2-yl)-2, 5-diphenyletertrazolium bromide (MTT) assay was used to investigate the effect of the iron chelators, DFO, BP and FeCl<sub>3</sub> on cell growth. This is one of the most commonly used methods for measuring cell proliferation and neural cytotoxicity. It is widely believed that MTT is reduced by active mitochondria in living cells (Denizot and Lang, 1986; Hansen et al., 1989; Liu et al., 1997; Mosmann, 1983). Thus, increases obtained in the MTT assay at A570 nm indicate increases in the number of viable cells. It is performed in 96-well microtiter plates. In this study, MTT assay is performed according to Liu et al. (Liu et al., 1997).

#### (2) Materials

- (A) 5 mg/ml of MTT solution is prepared by dissolving 50 mg MTT in 10 ml of 0.9% NaCl and warmed at 60 °C to dissolve.
- (B) Solubilization solution: 5% iso-butyl alcohol, 10% HCl and 10% sodium dodecyl sulfate.

#### (3) Procedure

- (A) The cells of 90 µl (approximately 10<sup>4</sup> cells) per well were plated in culture medium at 37 °C.
- (B) After 24 h, 10 µl of test samples at the designed concentrations or volume-matched vehicle as control were added to the wells.
- (C) After incubation for 24 h, 20 µl of 5 mg/ml MTT were added to each well.
- (D) 4 h later, 100 µl of a solubilization solution was added and the absorbance values

determined at 570 nm, in the next day, by using an automatic microtiter plate reader (Bio-Rad Laboratories Inc.). 640 nm was used as the reference wavelength.

### **2.2.3.2 DPPH Free Radical Scavenging Assay**

#### **(1) Principle**

Many antioxidant assays use accelerated oxidative conditions in lipid systems by using high temperature and a high oxygen supply. The risk of degradation with such conditions during these tests is high for many antioxidants. In addition, this condition itself provokes lipid oxidation and such tests are not always representative of the natural oxidation in food and human tissues.

The 2, 2-diphenyl-1-picrylhydrazyl radical (DPPH) scavenging assay is widely used for its simplicity, ease, speed and sensitivity without the risk of thermal degradation of the molecules tested, despite its biological irrelevance (Blois, 1958; Cakir et al.; 2003). The purple color DPPH is a relatively stable in alcoholic media and reacts with free radicals or other hydrogen donors, which result in a discolored DPPHH (Fig.2-1). The presence of antioxidant leads to the disappearance of these radical chromogens. The rate of discoloration can be monitored to evaluate the antioxidant capacity to donate hydrogen during a free radical attack.

#### **(2) Procedure**

- (A) A 0.1 mM solution of DPPH (90% purity, Sigma Chemical Co. USA) in ethanol was prepared and 1 ml of this was added to every 3 ml of various concentrations of sample solutions in ethanol.
- (B) After 30 min incubation at room temperature, the absorbance of the reaction mixtures were measured spectrophotometrically at 517 nm.
- (C) A decreasing of the DPPH solution absorbance indicates an increase of the DPPH radical-scavenging activity. This activity was calculated by using the following

equation:

$$\text{Reduction (\%)} = \{1 - (\text{At}/\text{Ai})\} \times 100$$

where At represents absorbance at measuring time, and Ai represents absorbance at initial time.

(D) The DPPH solution without tested samples was used as control.

### 2.2.3.3 Ferric Thiocyanate Assay

#### (1) Principle

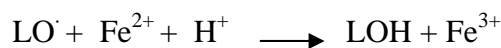
Antioxidant assays use accelerated oxidative conditions in lipid systems by using high temperature and a high oxygen supply. However, many antioxidants can undergo degradation in such circumstance and the conditions are far away from the natural lipid oxidation that occurs in nature, including in food and human tissue.

Ferric thiocyanate assay in linoleic acid model system is the method to quantify conjugated diene hydroperoxides (LOOH) in lipid autooxidation. It has been widely used for understanding the free radical process conducive to LOOH. Through autooxidation, linoleic acid (18:2) produces hydroperoxides (LOOHs) during incubation (37-40 °C). As a result of an one-electron reduction of LOOH, ferrous ion ( $\text{Fe}^{2+}$ ) is oxidized to ferric ion ( $\text{Fe}^{3+}$ ) and lipid alkoxyl radicals ( $\text{LO}^\cdot$ ) are produced (Labeque and Marnett, 1987; Mihaljevic et al., 1996) as follows:



Reactive lipid alkoxyl radicals ( $\text{LO}^\cdot$ ), is produced by hemolytic cleavage of LOOH.

Very reactive alkoxy radicals (LO $\cdot$ ) can further react with another ion, solvent molecules (RH) and LOOH.



The oxidation of ferric ion (Fe $^{3+}$ ) makes complexation with thiocyanate for improving the sensitivity in the spectrophotometric measurement of antioxidant activity. The ferrous oxidation method has been found simpler than iodometry (complexation of iodine with iodide to enhance the spectroscopic property of the reaction product) due to the lower sensitivity of ferrous ion to spontaneous oxidation by oxygen, as compared to the high susceptibility to oxidation iodine solution.

### (3) Procedure

To determine antioxidant activity in an oil-in-water system, the thiocyanate method was applied with modification (Mihaljevic et al., 1996). The amount of peroxides formed in the emulsion during incubation was determined spectrophotometrically by measuring absorbance at 500 nm. A high absorbance indicates a high peroxides formation and a low antioxidant activity. A linoleic acid pre-emulsion was from 3 ml linoleic acid which was vortexed with 3 ml Tween-20 in 200 ml potassium phosphate buffer (40 mM, pH 7.0). One ml of LIG solution was added to the pre-emulsion, and the final volume of the reaction mixture was brought to 25 ml with potassium phosphate buffer. While the mixture was incubated in conical flasks in the dark at 37 °C, aliquots of 0.1 ml from the mixture were periodically taken. The degree of oxidation was measured according to the thiocyanate method by adding 5 ml 75% ethanol, 0.1 ml ammonium thiocyanate (30%, w/v), and 0.1 ml ferrous chloride (0.1%, w/v) to every 0.1 ml reaction mixture. Precisely 5 min after the addition, the absorbance of the peroxide value was measured at 500 nm (Cintra 10e UV-visible

spectrometer, GBC, Australia) against 75% ethanol contained in a reference cell. All test data were averages of triplicate analyses.

The inhibition ratio (%) was calculated according to following formula:

$$\text{Inhibition (\%)} = (1-A1/A) \times 100$$

Where A was the absorbance of the control at 500 nm and A1 was the absorbance of the test samples at 500 nm. Control was incubated with linoleic acid but without the tested samples.

#### **2.2.3.4 Thiobarituristic Acid Reactive Substances Assay**

##### **(1) Principle**

Thiobarituristic acid reactive substances (TBARS) assay is the method to quantify the TBARS formed in the colorimetric reaction of thiobarituristic acid with malondialdehyde (MDA), a secondary product of peroxidation of polyunsaturated fatty acids with three or more double bonds (Janero, 1990; Ohkawa et al., 1979).

Thiobarituristic acid and MDA react to form a Schiff base adduct (Fig 2-2) to produce a chromogenic product that can be easily measured by employing spectrophotometric method. Following the TBARS assay, lipid peroxidation is determined spectrophotometrically by measuring the absorbance at 535 nm (Ohkawa et al., 1979). A high absorbance indicates a high peroxides formation.

Lipid peroxidation can take place on both polyunsaturated fatty acid and triglycerides through a chain reaction mechanism which initiates either the enzymatic and nonenzymatic mechanisms. The neuronal membrane lipids are particularly susceptible to oxidation because of their elevated polyunsaturated fatty acid content and relatively

poorly developed antioxidant defense systems.

## (2) Procedure

### (A) Preparation of Rat Cerebral Cortex Mitochondria

Male SD rats weighing 180-200 g were anesthetized with chloral hydrate (400 mg/kg) and then decapitated. The cerebral cortex was removed, washed in ice-cold PBS and homogenized in buffer solution (20 mM Hepes-KOH, pH 7.5, 10 mM KCl, 1.5 mM MgCl<sub>2</sub>, 1 mM Na-EDTA, 1 mM Na-EGTA, 1 mM dithiothreitol, and 0.1 mM phenylmethylsulfonyl fluoride) containing 250 mM sucrose by using a glass homogenizer at 4 °C, and then centrifuged twice at 750g for 10 min at 4 °C. The harvested supernatants were again centrifuged at 10,000g for 10 min at 4 °C, and the resulting mitochondrial pellets were resuspended in PBS and stored at -80 °C until used.

### (B) Determination of Protein Concentration of Brain Mitochondria

Please refer to Chapter 2.2.2.3.

### (C) Assay of Lipid Peroxidation in Rat Cerebral Brain Cortex Mitochondria

10 µl various concentrations of LIG dissolved in ethanol and 100 µl of mitochondria suspension (3 mg protein/ml) were mixed and adjusted to 380 µl with PBS, then incubated at 37 °C for 10 min, lipid peroxidation was induced by adding newly prepared different agents (20 µl of 1 mM NADPH, or 10µl of 2 mM ascorbic acid and 10 µl of 25 µM FeSO<sub>4</sub>), and then incubated at 37 °C for 30 min in a water bath. TBARS was measured as previously described (Gao et al., 1999; Guo et al., 1996). The reaction was stopped by the addition of 400 µl of ice-cold 2.8% trichloroacetic acid. 1 ml of 0.67% 2- thiobarbituric acid was added, and samples were incubated in a water bath at 95 °C for 60 min. After cooling the sample with tap water, 2.0 ml of the mixture of methanol and n-butanol (15:85, v/v) were added and the mixture was then

vigorously shaken. After centrifugation at 3000 rpm for 30 min, the absorbance of the organic layer (upper layer) was measured at 532 nm.

The results were expressed as the mean  $\pm$  SD of absorbance/mg protein. The inhibition ratio (%) was calculated according to following formula:

$$\text{Inhibition (\%)} = \left( \frac{A - A_1}{A_1} \right) \times 100$$

Where A was the absorbance of the control at 535 nm and A1 was the absorbance of the test samples at 535 nm. Control was incubated with a volume-matched ethanol solution but without the tested samples.

### **2.2.3.5 HPLC Measurement of LIG**

#### **(1) Analysis Method**

A High Performance Liquid Chromatographic assay was used to analyze the LIG content in the stability and transport studies of LIG (Li et al., 2002)

#### **(A) Chromatographic Equipment**

An Agilent 1100 Series HPLC System (Agilent Technologies, Waldbronn, USA), equipped with a vacuum degasser, a quaternary pump, a 100-position autosampler, a diode array detector (DAD) detector. HPLC grade methanol and isopropyl alcohol were purchased from Sigma (St. Louis, MO) and Tedia (Fairfield, USA), respectively.

#### **(B) Analysis Condition**

For chromatographic analyses, an Alltima C<sub>18</sub> column (5 $\mu$ m, 150mm  $\times$  4.6 mm) with a compatible guard column (C<sub>18</sub>, 5 $\mu$ m, 7.5mm  $\times$  4.6 mm) was used. The LIG peak was detected at a UV absorbance wavelength of 280 nm. The mobile phase consisted of

methanol : 5% isopropyl alcohol in distilled deionized water (60:40). The mobile phase was filtered through a 0.2  $\mu\text{m}$  filter and degassed by sonication in vacuum for 20 min. The flow rate of the mobile phase was set at 1 ml/min. Sample was injected on the column for analysis.

### (C) Sample Preparation

It was reported that 2% DMSO did not affect the cell monolayer during the transport experiment (Caloni, 2002). Thus lipophilic LIG was first dissolved in DMSO and then further diluted in assay buffer in order to achieve the final test concentration of 2% DMSO. The LIG solution for Caco-2 transport study and stability was prepared fresh in the assay buffer on the day of the experiment, which is a HBSS buffer at pH 7.4 containing 10 mM HEPES and 25 mM D-Glucose (Hidalgo et.al, 1989; Hilgers et al., 1990). All the samples for experiments were clean, that can be injected onto the column without any extraction procedure. All samples were stored at  $-80\text{ }^{\circ}\text{C}$  in freezer, and analyzed within a week after experiments.

## **(2) HPLC Assay of LIG**

### (A) Calibration Curves

Standard curves were obtained by the injection of standard solutions in triplicate at the LIG concentration of 1.00, 0.75, 0.50, 0.25, 0.10, 0.05, 0.025 mM. These standards were prepared by diluting the LIG solution in an assay buffer containing 2% DMSO. These standards were prepared afresh daily and were randomly interspersed among the experimental samples during the analysis. A 10  $\mu\text{l}$  sample was injected onto column and the chromatographic run time was set at 14 min.

### (B) Intra- and Inter-day Variability

The accuracy and precision of the method was determined by performing intra- and inter-day variability in the peak area and peak retention. For intra-day variability of LIG, the same sample was injected five times on the same day of analysis. For

inter-day variability of LIG, the same sample was injected on five different days.

### **2.2.3.6 Measurement of Malondialdehyde Content and the Activities of SOD and GSHPx (MDA and the Activities of SOD and GSHPx assay kits, Jianchen Bioengineering Co, Nanjing, China)**

#### **(1) Estimation of Lipid Peroxidation**

Malondialdehyde (MDA) content, an indicator of lipid peroxidation, was measured as the procedure described previously (Janero, 1990; Ohkawa et al., 1979). Brain tissues were homogenized in 10 times (w/v) 0.1 M sodium phosphate buffer (pH 7.4). To every 0.1 ml of the above sample, the following reagents were added: acetic acid (20%) 1.5 ml (pH 3.5), thiobarbituric acid (0.8%) 1.5 ml, and sodium dodecyl sulfate (8.1%) 0.2 ml. The mixture was heated at 100 °C for 60 min, and then cooled with tap water. After the addition of 5ml of n-butanol/pyridine (15:1 v/v) and 1ml distilled water, the reaction mixture was vigorously shaken. After centrifugation at 4000 rpm for 10 min, the organic layer was withdrawn and absorbance was measured at 532 nm using a spectrophotometer and quantification was done based on the standard curve generated by using authentic MDA.

#### **(2) Measurement of Activities of SOD and GSHPx**

The procedure was carried out using commercially available kits (Jianchen Bioengineering, Nanjing, Jiangsu Province, PR China). The assay for SOD activity was based on its ability to inhibit the oxidation of oxymine by  $O_2^-$  produced from the xanthine-xanthine oxidase system. One unit of SOD activity was defined as the capability of reducing the absorbance at 550 nm by 50%. The assay of GSHPx activity was determined by quantifying the rate of oxidation of the reduced glutathione (GSH) to the oxidized glutathione (GSSG) by  $H_2O_2$  catalyzed by GSHPx. One unit of GSHPx was defined as the activity that reduced the level of GSH by 1  $\mu$ M in 1 min per

milligram protein. Protein concentration in the sample was determined by the method of Bradford.

#### **2.2.3.7 Measurement of NO content and iNOS activity (NO content and iNOS activity assay kits, Jianchen Bioengineering Co, Nanjing, China)**

##### **(1) Determination of NO Content**

The NO content was measured according to a commercially available kit (Jianchen Bioengineering Co, Nanjing, China). This assay was based on the nitrite measurement, an indicator of NO production, by Griess reaction (Green et al., 1982). NO, once released, is rapidly converted to nitrite and nitrate in the aqueous medium. The ratio of the nitrate and nitrite concentrations may vary substantially on the biological fluids and tissues. Because the Griess reagent does not react with nitrate, nitrate must be converted to nitrite by incubation with nitrate reductase and nicotinamide adenine dinucleotide at room temperature. Nitrite can react with color reagents, and then the absorbance of the solution was measured at 540 nm. Changes of the absorbance at 540 nm were calculated by subtracting the average absorbance value of the blank wells, and NO concentration was determined on the basis of NO standard curve.

The ipsilateral hemispheres were homogenated in normal saline (1:9, w/v) at 4 °C, and centrifuged at 4000×g for 20 min. The NO content in supernatants was measured spectrophotometrically at 540 nm according to the manufacturer's instruction. Nitrite concentrations were calculated by regression analysis of a standard curve using sodium nitrite as a standard and expressed as  $\mu\text{mol}$  per milligram protein. Protein concentration in the sample was determined by the method of Bradford.

##### **(2) Determination of iNOS Enzyme Activity**

It is apparent that the NOS isozymes can be catalogued into at least two types of NOS.

One (cNOS) is constitutive,  $\text{Ca}^{2+}$ /calmodulin dependent, which releases NO for short periods in response to receptor or physical stimulation. This type of NOS isozyme exists in neurons and endothelial cells of blood vessels. Another type (iNOS) is expressed in many cells such as macrophages, neutrophils, hepatocytes and Kupffer cells, chondrocytes. It can also be synthesized in endothelial cells of blood vessels. It is inducible,  $\text{Ca}^{2+}$  independent. Both types of NOS are P450-type oxygenase using NADPH, flavin adenine dinucleotide, flavin mononucleotide, and tetrahydrobiopterin as cofactors (Marletta 1989; Marletta 1993; Stuehr and Griffith 1992).

The enzyme activity of iNOS was measured according to a commercially available kit (Jianchen Bioengineering Co, Nanjing, China). This assay was based on the oxidation of oxyhaemoglobin to methaemoglobin by NO in the  $\text{Ca}^{2+}$ -free reaction mixture (Knowles et al., 1990). The ipsilateral hemispheres were homogenated in normal saline (1:9, w/v) at 4 °C, and centrifuged at 4000×g for 20 min. iNOS activity in supernatants was measured spectrophotometrically at 530 nm according to the manufacturer's instruction, and one enzyme unit was expressed as 1 nM of NO formed in 1 min per milligram protein. Protein concentration in the sample was determined by the method of Bradford.

#### **2.2.3.8 Measurement of Caspase-like Activities (caspase activity assay kits, KeyGen, Nanjing, China)**

##### **(1) Cytosolic Protein Preparation**

Please refer to 2.2.2.3.

##### **(2) Caspase-like activity assay**

Caspase-8 and Caspase-3 activities were measured using colorimetric assay kits essentially according to the manufacturer's instruction (KeyGen Biotech corporation

limited, Nanjing, China). This assay was based on the ability of the active enzyme to cleave the chromophore from the caspase substrate. Fifty micrograms of cytosolic protein were diluted in a 50  $\mu$ l of lysis buffer, and then added to a 50  $\mu$ l reaction buffer, and transferred to a 96 well flat-bottom microplate. To each reaction well, 5  $\mu$ l of caspase 8 colorimetric substrate (IETD-pNA) or caspase-3 colorimetric substrate (DEVD-pNA) were added. The plate was incubated for 4 h at 37 °C. Levels of released *p*-nitroanilide (pNA) were evaluated by measuring optical density at 405 nm with a Model 550 microplate reader (Bio-Rad Lab., Hercules, CA, USA). Caspase-like activities were expressed as the percentage of optical density unit of sham-operated control group.

## **2.2.4 Histochemical Methods**

### **2.2.4.1 Microscopic Analysis of Nuclear Fragmentation**

#### **(1) Principle**

Morphological changes of cells can be observed at the light microscopic level using nucleic acid-binding dyes. Hoechst 33342 is an obvious choice because it is known to produce relatively good stoichiometric DNA staining when preserving cell viability (Foglieni et al., 2001). It is a vital DNA staining that binds preferentially with A-T base-pairs. Hoechst 33342 has the highest permeability into living cells and shows the highest retention on the DNA (Haraguchi et al., 1999). The Hoechst 33342 morphological analysis is chosen as a gentle nondestructive method in which the classic morphology of early and late apoptotic cells, as well as early membrane permeability changes can be reliably evaluated on intact cells. Non-apoptotic cells show dim nonhomogeneous nuclear staining whereas apoptotic cells were brightly stained, and the classic progression of chromatin condensation and nuclear fragmentation were visible (Maciorowski et al., 1998; Seigel and Campbell, 2004; Tanaka et al., 2002).

## **(2) Procedure**

C6 cells were grown in 6-well plates at a density of  $1.0 \times 10^6$  cells /well for 24 h and then incubated with various concentrations of LIG for 24 h before  $H_2O_2$  (final concentration 500  $\mu$ M) for another 24 h. Then cell media was removed, and the cells were gently washed with PBS and fixed with 4% paraformaldehyde in 0.1 M phosphate buffer (pH7.4) for 1 h at room temperature. After washing with PBS, nuclei were stained with 5  $\mu$ g/ml Hoechst 33342 (Fluka, Industriestrasse 25 CH-9471 Buchs SG, Switzerland) dissolved in sterile water for 15 min. The cells were washed with PBS and viewed under an inverted fluorescence microscope (Leica, Wetzlar, Germany).

### **2.2.4.2 TTC Staining of Infarct Brain Tissue**

#### **(1) Principle**

Triphenyltetrazolium chloride (TTC) staining is a commonly used method to quantify experimental brain infarctions (Bederson et al., 1986a; Belayev et al., 1999). TTC is a reagent for oxidative enzymes. It can accept a proton from succinate dehydrogenase in the inner membrane of the mitochondria which reduces it to its red insoluble form formazan, therefore, an area with inactive enzymes, and the infarction, is not stained and appears pale. The major advantages of TTC staining over other histopathologic staining methods are its low cost, technical simplicity, and reproducibility. But TTC staining may overestimate the infarct area by including enzymatically inactive but vital brain tissue.

#### **(2) Procedure**

(A) TTC staining:

At the end of the experiment, the animals were reanesthetized and received intracardiac perfusion with 0.9% normal saline prior to the removal of their brains. The brains were chilled at  $-80^{\circ}\text{C}$  for 4 min to harden the tissues slightly. Seven coronal sections were made at bregma levels from +4.7 mm to -7.3 mm (2 mm each) by a tissue slicer onto an ice-cold plate. The sections were placed in a 2% solution of TTC (Sigma, St. Louis, MO) dissolved in normal saline and stained for 30 min at  $37^{\circ}\text{C}$  in the dark. The sections were then washed twice with saline and fixed in 10% phosphated-buffered formalin at  $4^{\circ}\text{C}$  overnight.

#### (B) Detection of Infarction Volume

The caudal face of each section was scanned using a flatbed color scanner, and the infarct areas from each brain section was measured using Pro-plus 4.5 image analyses software (Image J, Bethesda, MD). The total volume of infarction was calculated from the sum of the infarct areas (seven sections in all)  $\times$  thickness (2 mm). The infarct volume was expressed as a percentage of the total volume from the ipsilateral hemisphere.

### **2.2.4.3 Hematoxylin and Eosin Staining**

#### **(1) Principle**

Hematoxylin and Eosin (HE) Staining is a very common histological procedure. It is used to stain any cell types, from bone tissues to brain tissue. The resulting sections have two colors-blue due to hematoxylin and pink due to eosin. Hematoxylin is a basic stain; thus it preferentially binds to acidic structures (e.g. nucleic acids, giving the nuclei and cytoplasmic structures containing RNA a very dark bluish black appearance). Most other cytoplasmic structures (ones that do not contain acidic molecules) preferentially bind to Eosin, and appear pink. The result is a pink (light) background dotted with blue (dark). The stark contrast between pink and blue allows for most cell structures to be seen clearly under light microscope.

## **(2) Procedure**

- (A) 5 µm paraffin sections are mounted on glass slides and allowed to dry overnight to ensure adherence.
- (B) Paraffin-embedded sections are dewaxed by immersion in xylene for 10min, followed by a further 10 min in fresh xylene.
- (C) Rinse sections in two changes of 100% ethanol and air dry.
- (D) Rinse in 95%, 80%, 70% ethanol and distilled water.
- (E) Stain in Harris hematoxylin solution for 10 min, then wash in distilled water.
- (F) Differentiate in 1% HCl in ethanol for 30 sec, then wash in distilled water. Rinse sections in 1% ammonia, and distilled water.
- (G) Counterstain with 0.25% Eosin for 30 sec to 1 min, then wash in distilled water.
- (H) Dehydrate by immersion in 70%, 80%, 95% and two changes of 100% ethanol (1 min each).
- (I) Mount in resin dissolved in xylene.
- (J) View under a light microscope, where nuclei are stained blue and cytoplasm appear pink.

### **2.2.4.4 Immunohistochemical Method**

#### **(1) Principle**

Immunohistochemistry (IHC) is the localization of antigens in tissue sections by the use of labeled antibodies as specific reagents through antigen-antibody interactions that are visualized by a marker such as fluorescent dye, enzyme, radioactive element or colloidal gold.

With the development of immunohistochemistry techniques, enzyme labels such as peroxidase (Nakane and Pierce, 1967) and alkaline phosphatase (Mason and Sammons, 1978) have been introduced. Since immunohistochemistry involves specific antigen-

antibody reaction, it has an apparent advantage over traditional special and enzyme staining techniques that identify only a limited number of proteins, enzymes and tissue structures. Therefore, immunohistochemistry has become a crucial technique in many areas of research.

## **(2) Procedure**

### **(A) Tissue Processing**

Animals were deeply anaesthetized and perfused through the left cardiac ventricle with normal saline, followed by a fixative consisting of 4% paraformaldehyde in 0.1M phosphate buffer (pH 7.4). The tissue was embedded in OCT and cut at 10  $\mu\text{m}$  thickness on a freezing microtome (Leica), and then mounted on aminopropyltriethoxysilane (APES)-coated slides. If not used immediately, the paraffinized sections were stored at room temperature, and the freezing sections at  $-80\text{ }^{\circ}\text{C}$  until needed.

### **(B) IHC Method**

The immunohistochemical procedure was carried out using a labeled streptavidin-biotin technique. The frozen slices (10  $\mu\text{m}$ ) were obtained on a freezing microtome (Leica, Germany) and placed on APES-coated slides. The slides were washed in PBS and reacted with 0.3%  $\text{H}_2\text{O}_2$  in methanol to quench any endogenous peroxidase activity for 20 min. After washing, the sections were blocked with 5% normal goat serum containing 0.3% Triton-X-100 for 20 min at room temperature to block the non-specific binding of antibodies. After incubation with the primary antibody diluted in PBS 30 min at  $37\text{ }^{\circ}\text{C}$ , and then overnight at  $4\text{ }^{\circ}\text{C}$ , the sections were washed three times and incubated with the biotinylated secondary antibody for 1 h at

room temperature. After three rinses in PBS, the sections were incubated with SP Reagent (Zhongsan Bioengineering Co, China.) for 60 min at 37 °C, and incubated with DAB (0.5mg/ml) and 3% H<sub>2</sub>O<sub>2</sub>. Finally the sections were counterstained with hematoxylin. For each case, 0.01 M PBS was used as a substitute for the primary antibody for the negative control groups. No positive staining was seen in any of these control sections. Quantitative determination of the number of positive cells in the penumbra of focal ischemia was respectively made on anatomically-matched sections for each group. Six randomly-selected microscopic fields (× 400 magnification) were analyzed from two matched slides for each animal, and expressed as the number/high power field.

#### **2.2.4.5 TUNEL Staining (DNA fragmentation detection kit, Roche, Germany)**

##### **(1) Principle**

Classical apoptotic cell death can be defined by certain morphological and biochemical characteristics that distinguish it from other forms of cell death. A biochemical hallmark of apoptosis is the cleavage of chromatin into small fragments, which not only can be analyzed by agarose gel electrophoresis (Wyllie 1980; Zakeri et al., 1993) but also detected by in site DNA nick end labeling in tissue sections (Gavrieli et al., 1992; Labat-Moleur et al., 1998). Although the distinct “ladder” of DNA bands representing multiples of 180-200 bp correlates with the early morphological signs of apoptosis, DNA fragmentation assay cannot be applied to tissue sections. The method of terminal deoxynucleotidyl transferase (TdT)-mediated dUTP-biotin nick end labeling (TUNEL) is widely used to detect and quantifying apoptosis in tissue sections. This method is based on the specific binding of TdT to

3'-OH ends of DNA, ensuing a synthesis of a polydeoxynucleotide polymer. After the exposure of nuclear DNA on histological sections by proteolytic treatment, TdT was used to incorporate biotinylated deoxyuridine at sites of DNA breaks. The signal was amplified by avidin-peroxidase, enabling conventional histochemical identification by light microscopy. Although two types of TUNEL-positive cells were observed: apoptotic cells showing nuclear condensation and fragmentation as well as apoptotic bodies around the nuclear membrane without cytoplasmic staining and necrotic cells showing necrotic characteristics with uncondensed chromatin and more diffuse light cytoplasmic labeling (Charriaut-Marlangue et al., 1996b; Li et al., 1995), the identification and semi-quantitation of apoptotic cells were available based on the outcome of TUNEL staining.

## **(2) Procedure**

- (A) Paraffin sections (5  $\mu\text{m}$ ) are mounted on APES-coated glass slides and allowed to dry overnight to ensure adherence.
- (B) Paraffin-embedded sections are dewaxed by heating at 60 °C for 10 min, washing with xylene for 5 min, followed by a further 5 min in fresh dewaxing agent.
- (C) Rinse sections in 95% and 70% ethanol for 3 min each wash, and distilled water.
- (D) For formaldehyde-fixed sections, digest with proteinase K diluted to a final concentration of 20  $\mu\text{g/ml}$  for 15 min at room temperature.
- (E) Wash in sterile distilled water four times, rinse in 70%, 90%, and 95% alcohol and air dry.
- (F) Rinse the slides twice with PBS at RT. Let excess fluid drain off.
- (F) Prepare 50  $\mu\text{l}$  TUNEL reaction mixture for each section and incubate at 37 °C for 1 h in a moist chamber.
- (G) Terminate the reaction by washing sections in PBS three times (5 min for each wash).
- (H) Block endogenous peroxidase activity with methanol containing 3%  $\text{H}_2\text{O}_2$  for 10 min at room temperature. Wash three times in distilled water and once in PBS (5

min for each wash).

- (J) Add 50  $\mu$ l Converter-POD, pre-diluted 1:2 in blocking solution and incubate for 30 min at 37 °C in a moist chamber.
- (K) Wash in PBS three times (5 min for each wash)
- (L) Add 50  $\mu$ l DAB substrate solution and incubate for 5-10 min at room temperature. Wash in water; lightly counterstain with hematoxylin; dehydrate by immersion in 70%, 90%, 95%, and two changes of 100% ethanol (5 min each); clear in xylene; and mount in resin.
- (M) View under a light microscope, where apoptotic cells show brown apoptotic bodies as well as nuclear condensation and fragmentation, necrotic cells appear uncondensed chromatin and more diffuse light cytoplasmic labeling, and normal cell nuclei appear blue.

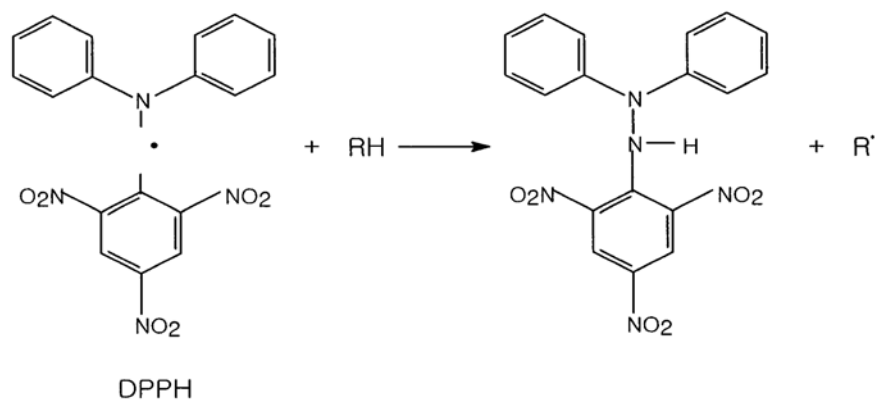


**Figure 2-1.** Reaction of DPPH<sup>•</sup> with a hydrogen donor.

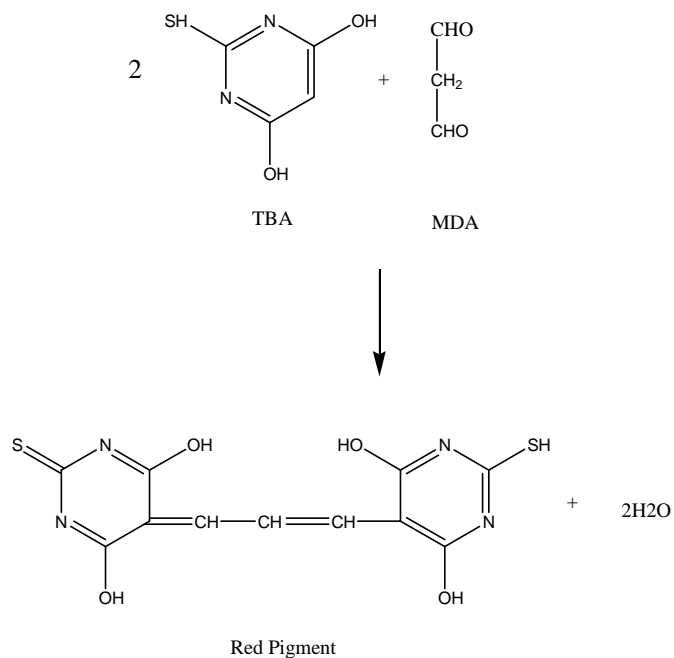


**Figure2-2.** Reaction between TBA and MDA to yield the TBA-MDA adduct.

## CHAPTER 3

# TRANSEPITHELIAL TRANSPORT OF Z-LIGUSTILIDE ACROSS CACO-2 MONOLAYERS

### 3.1 ABSTRACT

Oral administration is the most important and preferred route for small molecular weight conventional drugs. The overall bioavailability of an orally administered drug mainly depends on the physicochemical properties of the drug, as well as the morphological and biochemical state of the intestinal epithelium. Therefore, the present investigation focused on the transepithelial permeation of lipophilic Z-ligustilide (LIG), using the human colonic cell line Caco-2 as a model of human intestinal absorption. In addition, the effects of temperature, extracellular calcium and P-glycoprotein (P-gp) inhibitor-cyclosporin A on the LIG transport were also observed. Apparent permeability coefficients ( $P_{app}$ ) for the apical-to-basolateral (AP-BL) flux were  $(4.0 \pm 0.5) \times 10^{-6}$  cm/sec. Differences in the  $P_{app}$  between AP-BL and BL-AP directions were not statistically significant at both 37 °C and 4 °C. And cyclosporin A at 10  $\mu$ M and extracellular calcium had no effect on  $P_{app}$  for AP-BL transport of LIG. These data suggested efficient absorption of LIG through small intestine *in vivo*, and transcellular passive diffusion might be the principal mechanism of oral absorption for LIG.

## KEY WORDS:

Z-ligustilide, phthalide, Caco-2 monolayer, absorption in intestine, *Radix Angelica sinensis*

## 3.2 INTRODUCTION

Z-ligustilide (LIG), a volatile and liquid compound first isolated from the root of *Ligusticum acutilobum* in 1960 (Mitsuhashi et al., 1960), is a characteristic phthalide component of Umbelliferae plants and has been considered as the main bioactive component of many important medical plants, such as *Radix Angelica sinensis* (Lin et al., 1979), *Ligusticum wallichii* (Wang et al., 1984), *Ligusticum chuangxiong* (Naito et al., 1996), and *Cnidium officinale* (Bohrmann et al., 1967). There is no doubt that understanding the pharmacokinetics of LIG is useful for designing the ideal dosing regimens in pharmacological studies and future clinical applications. So far, however, no related studies have been reported, mostly due to the unstable property and limitation of pure sample preparation.

The Caco-2 cell line, derived from the human colon cancer cells, has become an established in vitro model for the prediction of drug absorption in the human intestine. When cultured on semipermeable membranes, Caco-2 cells differentiate into a highly functionalized epithelial barrier with remarkable morphological and biochemical similarity to the small intestinal columnar epithelium (Pinto et al., 1983). The

membrane transport properties of compounds can thereby be assessed using these differentiated cell monolayers (Artursson, 1990). The apparent permeability coefficients (Papp) obtained from Caco-2 cell transport studies have been shown to correlate to human intestinal absorption (Artursson et al., 1996; Rubas et al., 1993). The growth and maintenance of Caco-2 cell line is simple, cost-effective and available for the test of limited amount of sample. The present study was designed to investigate the transport of LIG extracted from *Radix Angelicae Sinensis* across caco-2 monolayers *in vitro* in order to indicate the absorption of LIG in *in vivo* intestine and the possible mechanisms.

### **3.3 MATERIALS AND METHODS**

#### **3.3.1 Materials**

##### **3.3.1.1 Materials**

Unless otherwise stated, all chemicals were obtained from Sigma chemical company, St. Louis, MO, USA. HPLC grade methanol was purchased from Honeywell International Inc., Muskegon, USA and isopropyl alcohol was from Tedia company, Fairfield, USA. Dulbecco's Modified Eagle Medium (DMEM), trypsin, and penicillin-streptomycin were purchased from Gibco, Grand Island, NY, USA. Heat-inactivated fetal bovine serum was from Hyclone, Logan, UT, USA. Six-well Polycarbonate membrane Transwells<sup>TM</sup> were purchased from Corning Costar

Corporation Acton, MA, USA (0.3  $\mu\text{m}$  pore size, 4.71  $\text{cm}^2$ ). Plastic culture flasks were from Falcon, Becton Dickinson, Franklin Lakes, NJ, USA.

### **3.3.1.2 LIG Preparation**

*Radix Angelica sinensis*, known as Danggui in Chinese, was purchased from the Danggui cultivating base of the Good Agricultural Practice in Min Xian County, Gansu Province, China. Its identity was confirmed by comparison to descriptions of characteristics and appropriate monograph in Chinese Pharmacopoeia (The State Pharmacopoeia Commission of People's Republic of China, 2000). LIG was extracted, separated and purified from *Radix Angelica sinensis* (Oliv.) Diels in our laboratory, with match number: 040608. Purified LIG was identified by electron impact ionisation (EI) MS,  $^1\text{H}$  NMR and  $^{13}\text{C}$  NMR spectrometric techniques. The purity was found to be > 99% based on the percentage of total peak area by HPLC analysis.

## **3.3.2 Methods**

### **3.3.2.1 HPLC Assay of LIG**

A High Performance Liquid Chromatographic (HPLC) assay was used to analyze the LIG content in stability and the transport studies of LIG (Li et al., 2002).

#### **(1) Analysis Condition**

Chromatographic analysis were performed on an Agilent 1100 Series HPLC System (Agilent Technologies, Waldbronn, USA), equipped with a vacuum degasser, a quaternary pump, a 100-position autosampler, and a DAD detector. HPLC grade water, methanol and isopropyl alcohol were used for HPLC analysis. For chromatographic

analyses, an Alltima C<sub>18</sub> column (5µm, 150mm × 4.6 mm) with a compatible guard column (C<sub>18</sub>, 5µm, 7.5mm × 4.6 mm) was used. The LIG peak was detected at a UV absorbance wavelength of 280 nm. The mobile phase consisted of methanol : 5% isopropyl alcohol in distilled deionized water (60:40). The mobile phase was filtered through a 0.2 µm filter and degassed by sonication in vacuum for 20 min. The flow rate of the mobile phase was set at 1 ml/min. Typically, 10 µl of sample was injected on the column for analysis.

## **(2) Sample Preparation**

It was reported that 2% DMSO did not affect the cell monolayer during the transport experiment (Caloni et al., 2002). Thus lipophilic LIG was first dissolved in DMSO and then further diluted in an assay buffer in order to achieve the final test concentration of 2% DMSO. LIG solution for stability, variability and transport study and was prepared afresh in an assay buffer on the day of the experiment, which is HBSS buffer at pH 7.4 containing 10 mM HEPES and 25 mM D-Glucose (Hidalgo et al., 1989). All the samples for experiments were clean, that can be injected onto the column without any extraction procedure. All samples were stored at -80 °C in the freezer (Czech Republic HETO HOLTEN AS, Denmark ), and analyzed within a week after experiments.

## **(3) Calibration Curves**

Standard curves were obtained by the injection of standard solutions in triplicate at

LIG concentrations of 1.00, 0.75, 0.50, 0.25, 0.10, 0.05, 0.025 mM. These standards were prepared by diluting LIG solution in the assay buffer containing 2% DMSO. These standards were prepared afresh daily and were randomly interspersed among the experimental samples during analysis. A 10  $\mu$ l sample was injected onto column and the chromatographic run time was set at 14 min. The retention time of LIG was 9.02 min.

#### **(4) Intra and Inter-day Variability**

The precision of the method was determined by performing intra and inter-day variability in peak area and retention time. For intra-day variability of LIG, the same sample was injected five times (10  $\mu$ l) on the same day of analysis. For inter-day variability of LIG, the same sample was injected in five different days.

#### **3.3.2.2 Stability Studies of LIG in Assay Buffer**

The stability of LIG was determined by adding 5 ml of 0.5 mM LIG solution in a plastic centrifuge tube maintained at 37 °C on the shaker of an orbital Incubator (Shel LAB, USA). Samples of 10  $\mu$ l were removed at regular time intervals, and directly injected onto HPLC column. The chromatographic peak areas of samples were measured at the period of 2 h.

#### **3.3.2.3 Preparation of Caco-2 Monolayers**

### **(1) Caco-2 Cell Culture**

Please refer to chapter 2.

When reaching 70~80% confluence, cells were applied for the subsequent studies.

### **(2) Preparation of Caco-2 Monolayers**

Caco-2 cell monolayers were established by using a 21-day culture method (Ranaldi et al., 2003). When cells reached about 80% confluence, they were seeded on polycarbonate membrane filters inside a six-well Costar Transwell at a density of  $6.4 \times 10^4$  cells/cm<sup>2</sup>. Each transwell insert was placed in a 35-mm well of a culture plate with 2.6 and 1.5 ml of culture medium on the basal side and apical side, respectively. Culture media were replaced every 48 h for the first 7 days and every 24 h thereafter. Cells grown in these Transwell insert became confluent in 5-7 days but were allowed to mature until 21 days.

### **(3) Assessment of Caco-2 Monolayers Integrity**

The monolayers integrity was assessed by the inverted light microscopy and the measurement of transepithelial electric resistance (TEER). After seeding cells into transwell inserts, TEER was measured every 3 days by using the Millicell-ERS voltohmmeter fitted with 'chopstick' electrodes (Millipore Co., Bedford, MA, USA). The TEER values were calculated according to the following equations:

$$\text{TEER } (\Omega \cdot \text{cm}^2) = (R_{\text{total}} - R_{\text{blank}}) \times A$$

Where  $R_{\text{total}}$  is the measured resistance.  $R_{\text{blank}}$  is the resistance of inserts without cells.

A is the growth surface area. The confluent monolayers which exhibited TEER values over  $600 \Omega \cdot \text{cm}^2$  were used in the transport experiments (Asano et al., 2003). Monolayer integrity during the transport experiment was determined by measuring the TEER before and after drug addition.

#### **3.3.2.4 Transport Studies of LIG Across Caco-2 Monolayers**

##### **(1) Transport Experiment Procedure**

To begin the transport experiment, Caco-2 monolayers were washed three times with an assay buffer (previously warmed to  $37^\circ\text{C}$ ) and incubated with an assay buffer (1.5 ml in donor and 2.6 ml in receiver) for 30 min at  $37^\circ\text{C}$ . Then the buffer in the donor compartment (representing the lumen of intestine) was aspirated and replaced with a 1.5 ml fresh buffer containing LIG at 1.5 mM concentration. The Transwell was placed on the shaker of an incubator at  $37^\circ\text{C}$ . At time points of 20, 40, 60, 90, and 120 min, samples of  $50 \mu\text{l}$  were removed from the receiver (representing the blood of intestine) and replaced with an equal volume of fresh assay buffer. Sample aliquots were transferred in sampler vials and stored at  $-80^\circ\text{C}$  for HPLC analysis. All experiments were conducted in triplicate.

##### **(2) Transport of LIG Across Caco-2 Monolayers under Different Conditions**

To understand the absorption and potential mechanisms of LIG in intestine *in vivo*, the

transport characteristics of LIG were studied under different conditions.

### **(A) Temperature Dependency of LIG Transport in Bidirections**

To determine the effect of temperature on the absorption and secretion of LIG in cell monolayers, transport studies were conducted in both AP-to-BL and BL- to-AP directions at 37 °C and 4 °C respectively.

### **(B) Effects of Additives on LIG Transport**

a) For a study which aimed at determining the effect of P-gp on LIG transport, a LIG solution containing 10 µM cyclosporin A was selected for the apical medium. The transport experiments were then initiated as described above.

b) To study the possibility of LIG transport by paracellular route (through the intercellular spaces), the monolayers were preincubated with calcium-free assay buffer containing 2.5 mM EDTA in two sides for 45 min, then the transport studies were initiated in a calcium-free assay buffer as described above.

### **(3) Sample Analysis**

LIG content in the samples was determined by HPLC as previously described. On the day of analysis, 10 µl of the samples were injected onto the HPLC column to obtain a concentration within the range of LIG standard curves.

#### **(4) Data Calculations**

Transport studies were performed at a LIG concentration of 1.5 mM under different experimental conditions. The apparent permeability coefficient,  $P_{app}$ , was expressed as  $\text{cm/s} \times 10^6$  (Artursson, 1990). It was obtained by plotting the cumulative amount of compound transported ( $Q$ ) versus time ( $T$ ) and determining the linear appearance rate (slope,  $\Delta Q/\Delta T$ ) of the compound on the receiver side. The appearance rate was determined by analyzing the linear part of the curve using a linear regression fitting:  $Q = aT + b$ , where  $a$  is the slope, which equals  $\Delta Q/\Delta T$ , and  $b$  is the intercept. The  $P_{app}$  value was obtained by the formula  $P_{app} = (\Delta Q/\Delta T)/(AC_0)$ , where  $\Delta Q/\Delta T$  is expressed in millimoles per second,  $A$  is the surface area of the cell monolayers (in  $\text{cm}^2$ ), and  $C_0$  is the initial concentration of the LIG on the donor side (in  $\text{mM}/\text{cm}^3$ ).

#### **3.3.2.5 Statistic Analysis**

The statistical analysis was performed using SPSS 10.0. Data was presented as the mean  $\pm$  SD. The difference between the means was determined by One-Way ANOVA followed by a Student-Newman-Keuls test for multiple comparisons. Differences with  $P < 0.05$  were considered significant.

### **3.4 RESULTS**

#### **3.4.1 HPLC Assay of LIG**

#### **3.4.1.1 Calibration Curves (Fig. 3-1, Fig.3-2)**

The calibration curve was fitted by plotting the mean of the three peak areas ( $y$ ) against the concentration of LIG ( $x$ ). A sample chromatogram is shown in Fig.3-1 and a standard curve is shown in Fig.3-2. The results for the calibration curve showed good linearity ( $r = 0.9995$ ) over the concentration range of 0.025~1.000 mmol/L, with an equation of  $y=1861.6x + 40.174$ .

#### **3.4.1.2 Intra and Inter-day Variability (Tab. 3-1, Tab. 3-2)**

Intra and inter-day variability of the HPLC assay of LIG is shown in Tab.3-1 and Tab. 3-2. Both the Intra-day and inter-day variability were found to be minimal (relative standard deviation, RSD, less than 3% in all cases). Consequently, these results indicated that the method was reliable within the analytical ranges.

#### **3.4.2 Assessment of Caco-2 Monolayers Integrity (Fig. 3-3, Fig.3-4)**

Caco-2 cells grown on a transwell insert became confluent in 5-7 days. The maturation of tight junctions during intestinal cell differentiation is a crucial factor in the establishment and maintenance of the differentiated polarized epithelial cell phenotype. TEER measures predominantly the ionic conductance of the paracellular pathway in the epithelial monolayer, and is therefore widely regarded as an important

indicator of monolayer integrity. The TEER of cell monolayers was monitored at set days from day 7 until day 21 after seeding. As shown in Fig. 3-3, the TEER of Caco-2 monolayers gradually increased with time of differentiation reaching a plateau value at about day 16 after seeding. In addition, TEER was not changed significantly before and after the LIG addition, indicating no effect on the monolayer integrity during the transport experiment.

### **3.4.3 Stability Studies of LIG in Assay Buffer (Fig.3-5)**

LIG is an unstable volatile oil. Therefore, one of the difficulties involved in studying the transport of LIG is the lack of information on its stability under transport studies. The finding in this study demonstrated that LIG was almost stable (> 94%) in assay buffer at pH 7.4 (Fig. 3-5). This suggests the degradation of LIG under transport conditions across caco-2 monolayers is thus insignificant.

### **3.4.4 Transport of LIG Across Caco-2 Monolayers**

#### **3.4.4.1 Temperature Dependency of LIG Transport in Bidirections of Caco-2 Monolayers (Fig.3-6, Fig. 3-7)**

The transport of both apical and basolateral loading of LIG was linear with time for up to 2 h at 37 °C or 4 °C (Fig. 3-6). The  $P_{app}$  for AP-BL or BL-AP flux of LIG were  $(4.0 \pm 0.5) \times 10^{-6}$  cm/sec or  $(4.1 \pm 0.7) \times 10^{-6}$  cm/sec at 37 °C , and  $(3.2 \pm 0.4) \times 10^{-6}$  cm/sec or  $(3.5 \pm 0.2) \times 10^{-6}$  cm/sec at 4 °C respectively (Fig. 3-7). The difference in  $P_{app}$  between bi-directional transport of LIG was not statistically significant, and also not

temperature- dependent ( $P > 0.05$ ).

#### **3.4.4.2 Effects of Additives on LIG Transport Across Caco-2 Monolayers (Fig 3.8, Fig 3.9)**

The effects of cyclosporin A and extracellular calcium on LIG transport gave further information on its characteristics of transport across Caco-2 monolayers. As shown in Fig. 3-8 and Fig 3.9, cyclosporin A, an inhibitor of P-gp transporter, and calcium-free assay buffer in apical medium did not show any significant effect on the permeation of LIG in AP-BL direction ( $P > 0.05$ ). Thus P-gp was not involved in the LIG transport, and also the possibility of paracellular transport pathway of LIG could be ruled out.

### **3.5 DISCUSSION**

As the gastrointestinal tract represents the first barrier of *in vivo* absorption, the transepithelial permeation in *in vitro* Caco-2 monolayers is widely used to predicate compound absorption in human small intestine. Studies have shown a good correlation between the permeability in the Caco-2 monolayers and the oral absorption in humans (Artursson et al., 1996; Rubas et al., 1993). The present data showed that the apical-to-basal Papp of LIG was  $4.0 \times 10^{-6}$  cm/sec. According to previous studies (Artursson and Karlsson, 1991; Pade and Stavchansky, 1998; Yee, 1997), a Papp value in Caco-2 monolayers of  $> 1 \times 10^{-6}$  cm/sec should, in general, be associated with

efficient intestinal absorption in humans. Moreover, it was reported that the Papp of highly lipophilic compounds in Caco-2 monolayers could be underestimated because of a considerable retention by the Caco-2 monolayers and non-specific binding to the transwell surface (Krishna et al., 2001). In physiological condition, highly lipophilic drugs exist in a protein-bound form with serum proteins such as albumin. The protein-binding ability enhances the solubility of such drugs to the serum that might facilitate their absorption into blood. Of greater importance as a potential predictor of oral absorption is the apical-to-basal Papp. Therefore, the finding in this study suggests good oral absorption of LIG in *in vivo* small intestine.

For most small molecule drugs, passive diffusion or active (or carrier-mediated) transport are their main mechanisms of intestinal absorption. With simple diffusion, the rate of transport increases directly in proportion to the concentration gradient, and low temperature may decrease the diffusion rate to some extent. On the other hand, the active transport rate depends on the functional state of carrier proteins, and thus can be inhibited by low temperature. Based on the present findings regarding the comparison between AP-BL and BL-AP flux at a physiological temperature (37 °C) and low temperature (4 °C), it appeared that the transepithelial transport of LIG in bidirections of Caco-2 monolayers was be a passive diffusion process. In addition, it was reported that apical membranes of Caco-2 cells expressed high level of P-gp (Hunter et al., 1993). Therefore, we further examined whether P-gp, an ATP-dependent efflux pump (Anderle et al., 1998), was involved in the transport of LIG. Our results showed that

addition of Cyclosporin A, a P-gp inhibitor, did not significantly increase the Papp of LIG across the Caco-2 monolayers, suggesting that LIG was not a substrate for P-gp. Moreover, passive diffusion involves two parallel routes: the transcellular route (across the membranes) and the paracellular route (through the intercellular spaces). It was reported that low calcium medium could loosen the tight junction of caco-2 monolayers, then enlarging the intercellular space and increasing compound transport by paracellular route (Artursson and Magnusson, 1990). In this study, the Papp of LIG was not significantly changed with Ca<sup>2+</sup>-free media in the Caco-2 monolayers. Thus, the opening of the tight junctions in monolayers had no effect on the transport of LIG, indicating that LIG transported across the Caco-2 cell monolayer predominately via the transcellular pathway.

In conclusion, the data generated in this study suggests excellent absorption of LIG through small intestine *in vivo*. Moreover, transcellular passive diffusion may be the principal mechanism of the oral absorption for LIG.

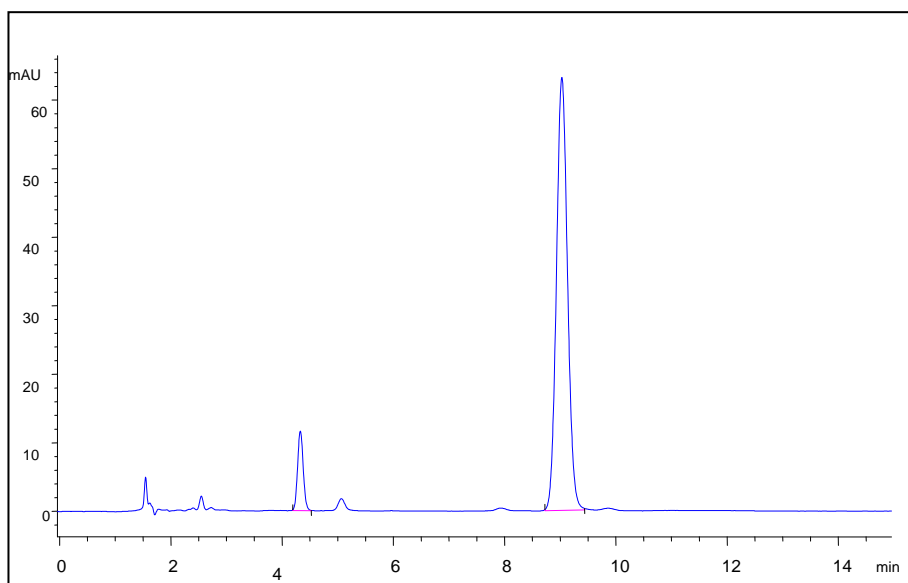


**Figure 3-1.** A typical HPLC profile of LIG recorded at 280 nm. (Analytical column: Alltima C<sub>18</sub>, 5 $\mu$ m, 150mm $\times$ 4.6 mm; guard column: C<sub>18</sub>, 5 $\mu$ m, 7.5mm $\times$ 4.6 mm; mobile phase: methanol-5% isopropyl alcohol (60:40); flow rate: 1.0 ml/min; temperature: ambient.) The retention time of LIG is 9.02 min under the condition described above.

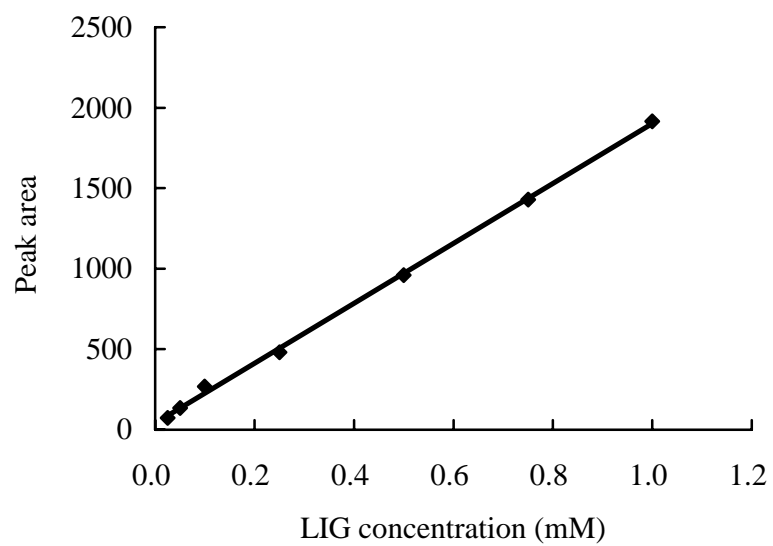


**Figure 3-2.** LIG standard curve. A calibration curve fitted by plotting the mean of the three peak areas ( $y$ ) against the concentration of LIG ( $x$ ) gave the following regression equation:  $y=1861.6x + 40.174$  with determination coefficient  $r = 0.9995$ .

**Table 3-1.** Intra-Assay variability in the HPLC analysis of LIG

Parameter	Mean±SD	% RSD	No. of peaks
LIG peak area (same standard)	812 ±14	1.7	5
LIG retention time	8.73 ± 0.03 min	0.3	5

**Table 3-2.** Inter-Assay variability in the HPLC analysis of LIG

Parameter	Mean±SD	% RSD	No. of days
LIG peak area (same standard)	842 ±18	2.1	5
LIG retention time	8.91 ± 0.17 min	1.9	5

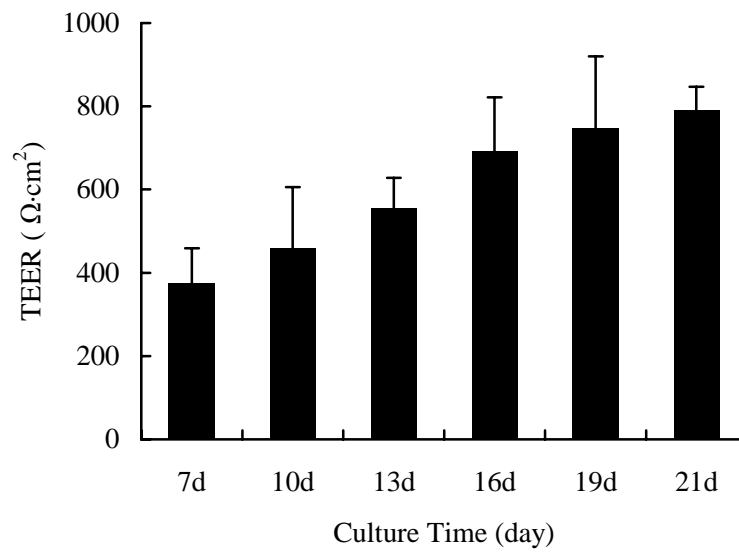


**Figure 3-3.** The TEER values of Caco-2 cells during differentiation. The data represent mean  $\pm$  SD ( $n = 24$ ).

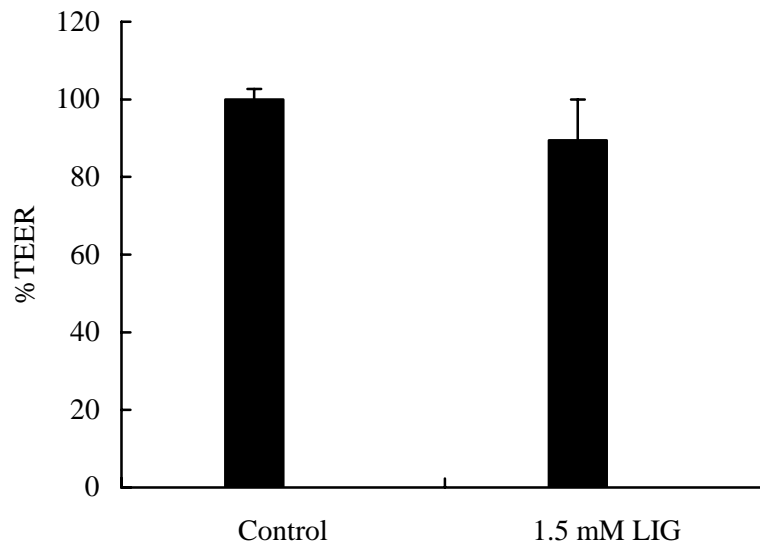


**Figure 3-4.** The percent change of TEER values of Caco-2 monolayers before (Control) or after addition of the LIG solution (1.5 mM LIG). The data represent mean  $\pm$  SD ( $n = 3$ ).

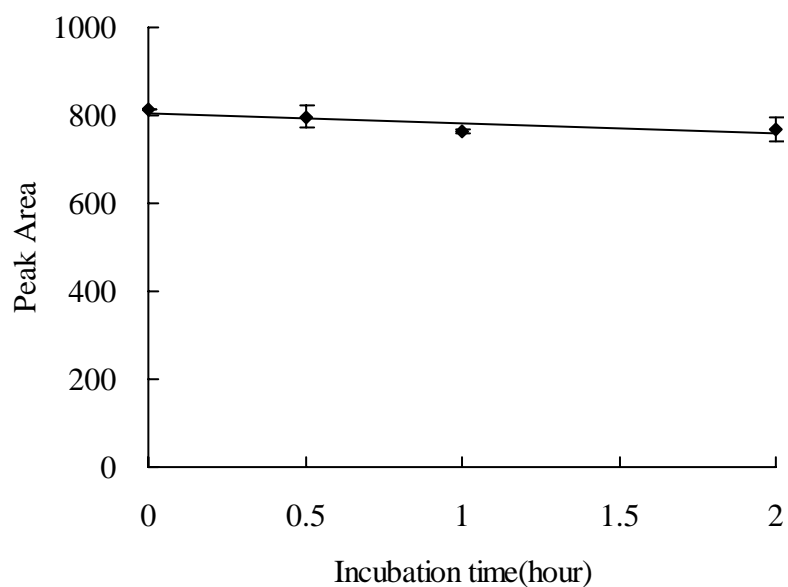


**Figure 3-5.** The stability of 0.5 mM LIG in pH 7.4 HBBS buffer, measured as the chromatographic peak areas. The data represent the mean  $\pm$  SD ( $n = 3$ ).

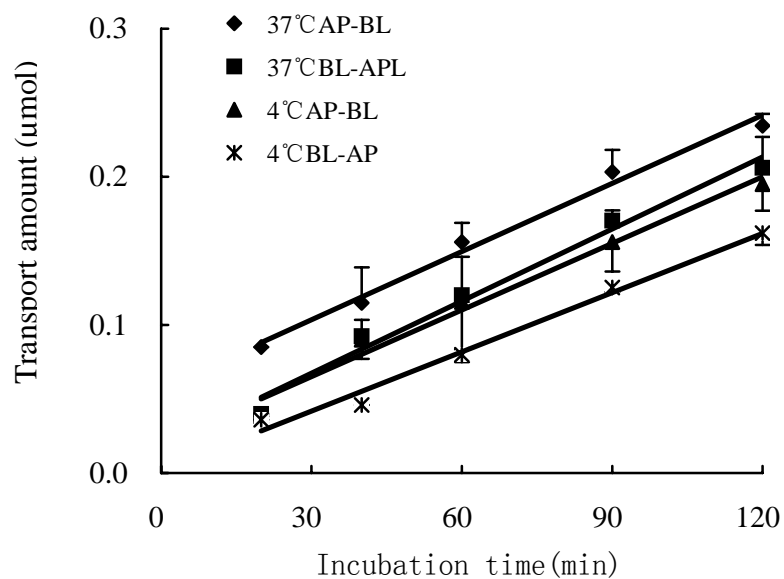


**Figure 3-6.** The transport profile of LIG in bidirections across the Caco-2 monolayers at 37 °C or 4 °C. The data represent the mean  $\pm$  SD ( $n = 3$ ).

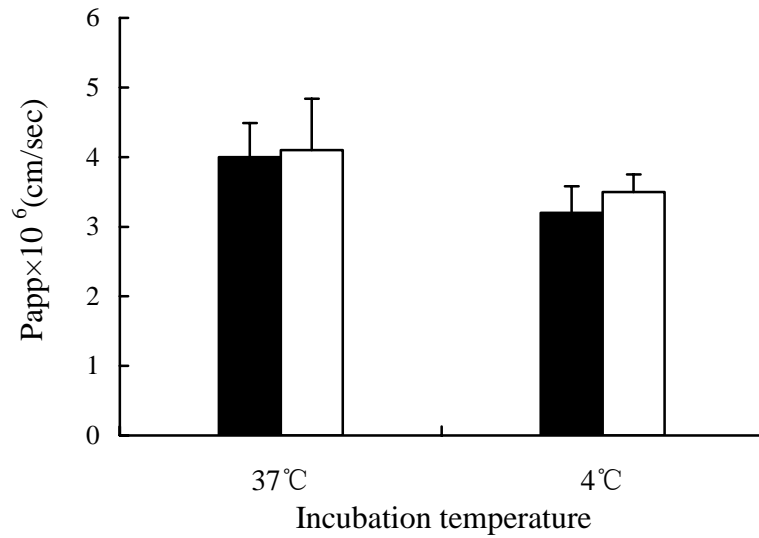


**Figure 3-7.** The effect of temperature on the permeability of LIG in AP-BL (■) or BL-AP (□) direction across the Caco-2 monolayers. The data represent the mean ± SD ( $n = 3$ ).

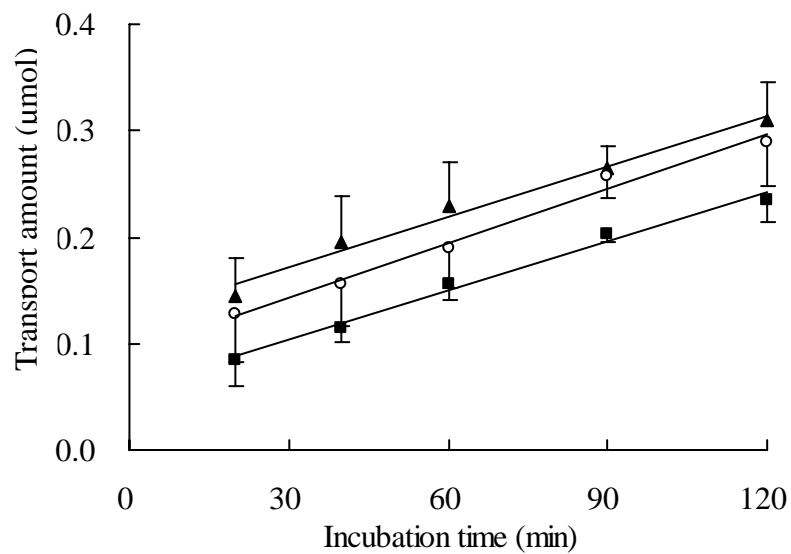


**Figure 3-8.** The transport profile of AP-BL of LIG across the Caco-2 monolayers in the assay buffer (■), 10 μM Cyclosporin A (▲), or calcium -free assay buffer (○) in the apical medium. The data represent the mean ± SD ( $n = 3$ ).

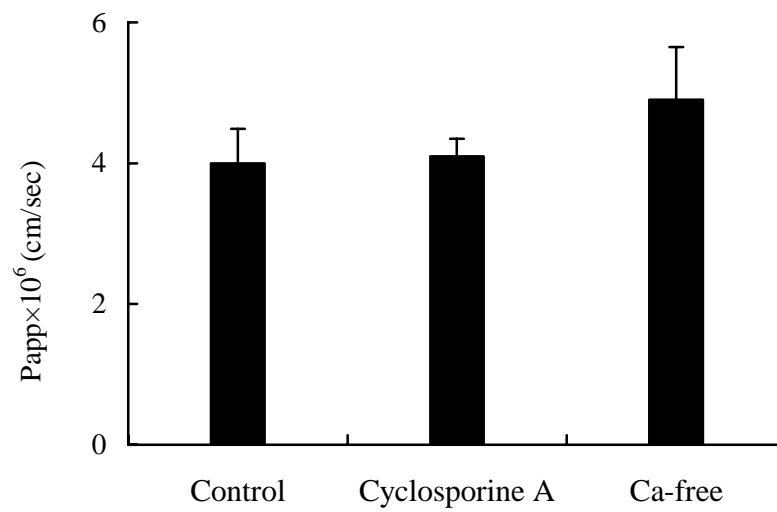


**Figure 3-9.** The permeability of AP-BL flux of LIG in the Caco-2 monolayers in the presence or absence of additives in the apical medium. The data represent the mean  $\pm$  SD ( $n = 3$ ).

## CHAPTER 4

# ANTIOXIDANT PROPERTIES AND PROTECTIVE EFFECTS OF Z-LIGUSTILIDE ON HYDROGEN PEROXIDE-INDUCED OXIDATIVE DAMAGE IN C 6 CELLS

### 4.1 ABSTRACT

The free radical scavenging and antioxidant activities of Z-Ligustilide (LIG) of *Radix Angelica sinensis* were examined for the 2,2-diphenyl-1-picrylhydrazyl (DPPH) stable free radical scavenging activity, and for the inhibition of lipid peroxidation. LIG at concentrations of 5, 20, 80  $\mu$ M could scavenge DPPH radical and inhibit linoleic acid autooxidation,  $\text{Fe}^{2+}$ /ascorbic acid or NADPH-induced lipid peroxidation of rat cerebral cortex mitochondria in a concentration-dependent manner. Moreover, the protective effect of LIG against hydrogen peroxide-induced oxidative damage in the rat C6 glioma cells was investigated by measuring cell viability via MTT, and Hoechst 33342 staining for nuclear fragmentation. Following 4 h cell exposure to hydrogen peroxide, a marked reduction in cell survival was observed, which was significantly and concentration-dependently prevented by 24 h pretreatment with LIG at 0.5-50  $\mu$ M. In separate experiments, LIG also significantly and concentration-dependently attenuated the apoptotic chromatin-condensation and

nuclear fragmentation induced by a 24 h treatment with hydrogen peroxide in the C6 cells. Taken together, these results suggest that LIG shows a relevant antioxidant activity both in *in vitro* chemical systems and oxidative stress-induced cell injury model, by means of scavenging free radicals, inhibiting lipid peroxidation and preventing oxidative injury. Furthermore, protection for oxidative damage of LIG may be of values in disorders in which oxidative stress is implicated.

**KEY WORDS:**

Z-ligustilide, Phthalide, *Radix Angelica sinensis*, Antioxidant, Free radical, DPPH, Hydrogen peroxide, C6 cell

## **4.2 INTRODUCTION**

It is generally accepted that oxidative injury plays an important role in the development of tissue damage and pathological events in various chronic diseases (Cheeseman, 1993; Delanty and Dichter, 2001; Reiter 1995). Oxygen centered free radicals, known as reactive oxygen species (ROS), are one of the major sources of primary catalysts that initiate oxidation in living organism. Normal aerobic respiration in mitochondria, stimulated polymorphonuclear leukocytes, macrophages and peroxisomes are the main endogenous sources of ROS in organisms. Exogenous sources of ROS include tobacco smoke, certain pollutants, organic solvents and

pesticides (Davies, 1995; Halliwell and Gutteridge, 1989). ROS are continuously produced during normal physiologic events, and are scavenged respectively by endogenous SOD, GSHPx, and catalase. Other antioxidants, including GSH, ascorbic acid, and vitamin E are also likely to be involved in the detoxification of free radicals (Halliwell et al., 1992). In pathological conditions such as cerebral ischemia/reperfusion, however, ROS are overproduced and can cause the inactivation of detoxification systems, consumption of antioxidants, and the failure to adequately replenish them. As a result of the dysfunction of the antioxidant defense, ROS attack membrane lipids, modify proteins and damage DNA. Therefore, due to the potential application of potent antioxidants against various oxidative stress-related disorders, up to now, many compounds or drugs have been screened for their possible antioxidant activity. There is an increasing interest in the antioxidant effects of compounds derived from herbs which could be relevant in relation to their role in health and disease and concerns about the toxic effects of synthetic antioxidants (Schwarz et al., 2001).

As described as in Chapter 3, Z-Ligustilide (LIG) is a characteristic phthalide component of many important medical plants. The analysis of its chemical structure suggests that LIG may give rise to an antioxidant activity due to the active dihydrobenzene and conjugated double-bonds. Although studies have showed its multiple pharmacological actions including antiasthmatic, spasmolytic and insecticidal actions (Miyazawa et al., 2004; Tao et al., 1984), and a mild inhibition on

the central nervous system (Matsumoto et al., 1998; Xie et al., 1985), there is so far no report related to the antioxidant effect of LIG.

The present study was carried out to determine the antioxidant activity of LIG in different lipid peroxidation systems, its property as a free radical scavenger, and even further, to assess its protective effects against oxidative injury in C6 cells induced by hydrogen peroxide.

### **4.3 MATERIALS AND METHODS**

#### **4.3.1 Materials**

##### **4.3.1.1 Materials**

Unless otherwise stated, all chemicals were obtained from Sigma Chemical Company, St. Louis, MO, USA. Amonium thiocyanate was purchased from Merck, Darmstadt, Germany. Hoechst 33342 was obtained from Fluka, Industriestrasse, Buchs SG, Switzerland. H<sub>2</sub>O<sub>2</sub> (30%, w/v) was purchased from Riedel-de Haen, Seelze, Germany. C6 glioma cells were obtained from the American Tissue Culture Collection (ATCC), Rockville, MD, USA. DMEM, trypsin, and pencillin-streptomycin were purchased from Gibco, Grand Island, NY, USA. Heat-inactivated FBS was from Hyclone, Logan, UT, USA. Plastic culture flasks and plates were from Falcon,

Franklin Lakes, NJ, USA. All chemicals and solvents used were of the highest available grade.

#### **4.3.1.2 LIG Preparation**

LIG was extracted, separated and purified from *Radix Angelica sinensis* (Oliv.) Diels in our laboratory, with match number: 041008 (containing LIG > 98.5%). Before application, various concentrations of LIG solution were freshly prepared by dissolving it in proportional solvent according to the experimental requirement.

### **4.3.2 Methods**

#### **4.3.2.1 DPPH Radical Scavenging Assay**

The scavenging activity on DPPH (Sigma Chemical Co. USA) radicals of LIG was measured according to the previous method (Blois et al., 1958) with minor modification. A 0.1 mM solution of DPPH in ethanol was prepared and 1 ml of this was added to every 3 ml of various concentrations of LIG solutions in ethanol (5, 20, or 80 mM concentration). After 30 min incubation at room temperature, the absorbance of the reaction mixtures were measured at 517 nm (UV-visible spectrometer, GBC, Australia). Decreasing of the DPPH solution absorbance indicates an increase of the DPPH radical-scavenging activity. This activity was calculated by

using the following equation:

$$\text{Reduction (\%)} = \{1 - (A_t/A_i)\} \times 100$$

where  $A_t$  represents absorbance at the measuring time, and  $A_i$  represents absorbance at the initial time.

The DPPH solution without tested samples was used as control.

#### **4.3.2.2 Measurement of Autooxidation in Linoleic Acid**

To determine the antioxidant activity in an oil-in-water system, the thiocyanate method was applied with modification (Mihaljevic et al., 1996). The amount of peroxides formed in the emulsion during incubation is determined spectrophotometrically by measuring absorbance at 500 nm. A high absorbance indicates a high peroxides formation and a low antioxidant activity. A linoleic acid (Sigma Chemical Co. USA) pre-emulsion from 3 ml linoleic acid was vortexed with 3 ml Tween-20 (Sigma Chemical Co. USA) in 200 ml potassium phosphate buffer (40 mM, pH 7.0). One ml LIG solution (5, 20, 80 mM concentration) was added to the pre-emulsion, and the final volume of the reaction mixture was brought to 25 ml with a potassium phosphate buffer. While the mixture was incubated in conical flasks in the dark at 37°C, aliquots of 0.1 ml from the mixture were periodically taken. The degree of oxidation was measured according to the thiocyanate method by adding 5 ml 75% ethanol, 0.1 ml ammonium thiocyanate (30%, w/v), and 0.1 ml ferrous chloride (0.1%,

w/v) to every 0.1 ml of the reaction mixture. Precisely 5 min after the addition, the absorbance of peroxide value was measured at 500 nm (UV-visible spectrometer, GBC, Australia) against 75% ethanol contained in a reference cell. All test data were averages of triplicate analyses.

The inhibition ratio (%) was calculated according to following formula:

$$\text{Inhibition (\%)} = (1 - A1/A) \times 100$$

Where A was the absorbance of the control at 500 nm and A1 was the absorbance of the test samples at 500 nm. Control was incubated with linoleic acid but without the tested samples.

#### **4.3.2.3 Assay for Lipid Peroxidation of Rat Cerebral Cortex Mitochondria**

To determine the effect of LIG in preventing enzymatic and non-enzymatic lipid peroxidation in mitochondria, lipid peroxidation was measured by the described method (Guo et al., 1996). The formation of the 2-thiobarbituric acid reactive substances (TBARS) in mitochondria suspension was initiated with  $\text{Fe}^{2+}$ /ascorbate system or NADPH, and then determined spectrophotometrically by measuring absorbance at 535 nm (UV-visible spectrometer, GBC, Australia). A high absorbance indicates a high peroxides formation and a low antioxidant activity.

##### **(1) Preparation of Rat Cerebral Cortex Mitochondria**

Please refer to chapter 2.

## **(2) Determination of Protein Concentration of Brain Mitochondria**

Please refer to Chapter 2.

## **(3) Lipid Peroxidation Assay in Brain Mitochondria**

Please refer to chapter 2.

### **4.3.2.4 C6 Glioma Cell Culture**

Please refer to chapter 2.

When cells reached 70~80% confluence, they were applied for the subsequent studies.

### **4.3.2.5 Assessment of Cell Viability**

Cell viability was evaluated by a morphological observation with a phase-contrast light microscope and a MTT assay (Denizot and Lang, 1986; Hansen et al., 1989; Mosmann, 1983; Liu et al., 1997). The MTT assay measures the metabolic reduction of MTT to formazan (blue) by mitochondrial dehydrogenases, which are active only in living cells. Before experiments, the cells were trypsinized, and cell concentration was assessed by using a hemocytometer. The cells were diluted into 2000 cells/100  $\mu$ l in DMEM with 10% FBS and then seeded on a 96-well plate at 100  $\mu$ l/well. In the following day, LIG was added to the wells (final concentration 0.5, 5, 25, 50  $\mu$ M) and incubated for 24 h before the addition of hydrogen peroxide ( $H_2O_2$ , final concentration

500  $\mu$ M). Following 4 h of treatment, the plates were viewed under a phase-contrast light microscope (Leica, Wetzlar, Germany). Images were obtained using a 10 $\times$  lens. For MTT assay, 20  $\mu$ l of 5 mg/kg MTT were added to each well, and the plate was incubated for 4 h at 37  $^{\circ}$ C. All culture media were then removed and the coloured formazan dissolved in 100  $\mu$ l DMSO. The absorbance at 570 nm of each aliquot was determined by using an automated 550 microtiter plate reader (Bio-Rad, USA). The cell viability in each well was assessed by the colorimetric change and presented as percentage of the control cells.

#### **4.3.2.6 Microscopic Analysis of Nuclear Fragmentation**

To investigate the effect of LIG on H<sub>2</sub>O<sub>2</sub>-induced cells apoptosis, the morphological changes in H<sub>2</sub>O<sub>2</sub>-treated nuclear fragmentation were observed by a fluorescence microscopy after being stained with Hoechst 33342 (Foglieni et al., 2001; Maciorowski et al., 1998). C6 cells were grown in 6-well plates at a density of 1.0 $\times$ 10<sup>6</sup> cells /well for 24 h and then incubated with various concentrations of LIG (final concentration 0.5, 5, 25, 50  $\mu$ M) for 24 h before H<sub>2</sub>O<sub>2</sub> ( final concentration 500 $\mu$ M ) for another 24 h. Then the cell media was removed, and the cells were gently washed with PBS and fixed with 4% paraformaldehyde in 0.1 M phosphate buffer (pH7.4) for 1 h at room temperature. After washing with PBS, nuclei were stained with 5  $\mu$ g/ml Hoechst 33342 (Fluka, Buchs SG, Switzerland) dissolved in sterile water for 15 min. The cells were washed with PBS and viewed under an inverted fluorescence microscope (Leica,

Wetzlar, Germany). Images were obtained by using a 40× lens. Non-apoptotic cells showed dim nonhomogeneous nuclear staining whereas apoptotic cells were brightly stained, and the classic progression of chromatin condensation and nuclear fragmentation was visible.

### **4.3.3 Statistical Analysis**

The statistical analyses were performed by using SPSS 10.0. Data are presented as mean ± SD. The difference between means was determined by ONE-Way ANOVA followed by a Student –Newman-Keuls test for multiple comparisons. Differences with  $P < 0.05$  were accepted as significant and  $P$  values  $< 0.01$  very significant. The correlation was analyzed using Pearson’s bivariate correlations with the SPSS version 10.0 statistical software program.

## **4.4 RESULTS**

### **4.4.1 DPPH Radical Scavenging Activity (Fig. 4-1, Fig. 4-2)**

DPPH is a stable free radical in aqueous or ethanol solution. In order to evaluate the free radical scavenging activity by using the test samples, the change of the optical density of DPPH radicals was monitored. Any scavenging action means that the compound has the ability to provide a hydrogen atom to DPPH radical, which results

in the decoloration and decrease in absorbance of DPPH in solution (Blois, 1958; Cakiret al., 2003). As shown in Fig. 4-1, the addition of the different concentration of LIG solution decreased the absorbance and reached a steady state after 30 min. LIG scavenged DPPH radical at a concentration-dependent manner. The free radical scavenging activities of 5, 20 and 80 mM LIG were 7.5%, 50.2% and 69.8 %, respectively (Fig. 4-2).

#### **4.4.2 Inhibition on Autooxidation in Linoleic Acid (Fig. 4-3, Fig. 4-4)**

The antioxidant activity of LIG was also determined by the thiocyanate assay. The amount of peroxides formed in emulsion during incubation (37 °C) was determined spectrophotometrically by measuring the absorbance at 500 nm after adding ammonium thiocyanate and ferrous ion. A high absorbance indicates a high peroxides formation. As shown in Fig. 4-3, the peroxidation of linoleic acid emulsion gradually increased during a 120 h reaction process. LIG concentration-dependently inhibited the peroxidation of linoleic acid over the total time course, and showed the maximal inhibition at 96 h incubation. The inhibition ratio of 5, 20 and 80 mM of LIG were 27.1%, 55.0%, and 68.6%, respectively (Fig.4-4).

#### **4.4.3 Inhibition on Lipid Peroxidation of Rat Cerebral Cortex Mitochondria (Fig. 4-5, Fig. 4-6)**

The TBARS contents in mitochondria suspension increased significantly when incubated with  $\text{Fe}^{2+}$ /ascorbate (non-enzymatically lipid peroxidation initiation system) and NADPH (enzymatically lipid peroxidation initiation system). LIG at concentrations of 5, 20, 80 mM attenuated  $\text{Fe}^{2+}$ /ascorbate and NADPH-induced lipid peroxidation in a dose-dependent manner (Fig. 4-5, Fig. 4-6). At a concentration of 80 mM LIG showed 45% and 52% of inhibitions in non-enzymatic and enzymatic system, respectively.

#### **4.4.4 Protection on C6 Cells Against Hydrogen Peroxide-induced Cytotoxicity (Fig. 4-7, Fig. 4-8)**

As shown in Fig 4-7, the C6 cells exhibited a marked decrease in cell number and most cells demonstrated a round shape, some of which were lysed or replaced by debris after a 24 h exposure to 500  $\mu\text{M}$   $\text{H}_2\text{O}_2$ . However, when the C6 cells were preincubated with various concentrations of LIG before the application of  $\text{H}_2\text{O}_2$ , a significant increase in cell number was found and most of the cells recovered their characteristic shape.

The loss of cell viability in culture was measured by the reduction of MTT activity of cells. The survival rate of C6 was about 53% when the cells were treated with 500  $\mu\text{M}$   $\text{H}_2\text{O}_2$  for 24 h. The viability of C6 cells pretreated with LIG at 0.5, 5, 25 and 50  $\mu\text{M}$  24 h before exposure to  $\text{H}_2\text{O}_2$  (500  $\mu\text{M}$ ) were increased in a statistically significant

fashion to  $70 \pm 7$ ,  $81 \pm 17$ ,  $92 \pm 9$ , and  $88 \pm 11\%$ , respectively (Fig. 4-8). Cells treated with  $50 \mu\text{M}$  of LIG alone for 24 h showed no obvious change in their viability.

#### **4.4.5 Prevention of Hydrogen Peroxide-induced Apoptosis in C6 Cells (Fig. 4-9)**

After staining with Hoechst 33342, the C6 cells were assessed as having undergone apoptosis by a fluorescence microscopy. The occurrence of apoptosis was differentiated by morphological observation after staining with Hoechst 33342. By means of a fluorescence microscopy, the C6 cells positively stained with Hoechst 33342 showed condensed and fragmented nuclei typical of  $\text{H}_2\text{O}_2$ -induced apoptotic cell death (Fig. 4-9). However, LIG ( $0.5$ - $50 \mu\text{M}$ ) significantly prevented  $\text{H}_2\text{O}_2$ -induced apoptotic cell death in a dose-dependent manner.

## **4.5 DISCUSSION**

Antioxidants can be defined as the compounds, which inhibit or delay, but are not able to prevent oxidation completely. Because many factors affect oxidation, such as oxygen pressure, temperature, metal catalysts and fat composition, the value of antioxidant activity varies depending on the oxidation condition and the assay used. We used four different *in vitro* systems and a cell condition to the determination of the antioxidant potency of LIG. In the present study, we found that LIG extracted from

*Radix Angelica sinensis* had dose-dependent antioxidative activity in various *in vitro* experiments. The potent ability to scavenge DPPH free radicals demonstrated the direct radical scavenging activity of this compound. Furthermore, LIG significantly inhibited the autooxidation of linoleic acid, and both enzymatic NADPH-dependent and non-enzymatic Fe<sup>2+</sup>/ascorbate-dependent lipid peroxidation in rat cerebral cortex mitochondria.

Hydrogen peroxide (H<sub>2</sub>O<sub>2</sub>) is a major precursor of ROS generated *in vivo*. It is able to cross biologic membranes and induce cellular damages by the formation of ·OH free radicals and readily damaging biological molecules, which can ultimately lead to an apoptotic cell death (Sur et al., 2003). Morphologically, apoptosis is characterized by intact plasma membranes and cellular organelles, nuclear condensation, DNA fragmentation and the formation of apoptotic bodies (Kerr et al., 1972). Apoptosis can be monitored experimentally in several ways. Fixed cells can be stained with nucleic acid fluorochromes or detected by TUNEL labeling of breaks at 3-OH ends in DNA strands. However, TUNEL labeling lacks specificity for apoptosis since DNA strand breaks are also seen in necrotic cell death (Labat-Moleur et al., 1998; Mangili et al., 1999). Hoechst 33342 binds preferentially with DNA rich in thymidine and adenine base pairs and is widely used as a marker for DNA condensation and/or fragmentation that accompanies apoptotic cell death in various cell types (Foglieni et al., 2001; Maciorowski et al., 1998). We also found in the present study that the nuclear condensation and fragmentations of the C6 cells were detected by the fluorescent cell

marker H33342 in H<sub>2</sub>O<sub>2</sub>-treated C6 cells, which was attenuated by LIG pretreatment. In addition, hydrogen peroxide decreased C 6 cell viability and its cytotoxic effect was significantly prevented in the presence of LIG in cell cultures. According to these results, it may be said that the protection effect of LIG on H<sub>2</sub>O<sub>2</sub>- induced cell damage, at least in part, is related to its antioxidant activity in lipid peroxidation and free radical scavenging activity. Furthermore, LIG showed significant antioxidant activity at lower dose in cell model than *in vitro* systems, which is likely that LIG, a highly lipophilic small molecule compound (log P = 2.86, molecular weight = 190) may be of a good affinity for cell membranes and can be efficiently uptake by cells. Therefore, further analysis of antioxidation activity of LIG in *in vivo* is good for the study after the oral administration due to its probably remarkable absorption in small intestine as described in Chapter 3.

In conclusion, the present study shows that LIG exerts a potent antioxidant activity in *in vitro* systems and significant protection on H<sub>2</sub>O<sub>2</sub> -induced oxidative injury in C6 cells. These results suggest that LIG may be of values in disorders where oxidative stress is greatly implicated.

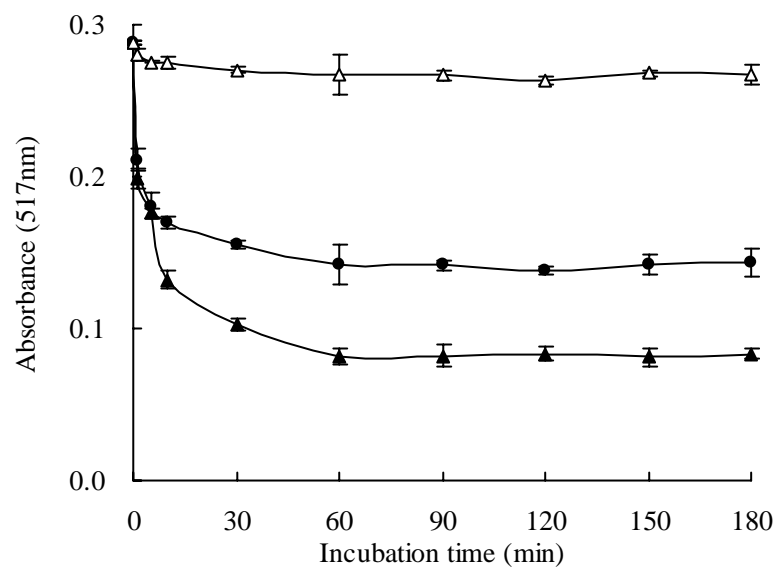


**Figure 4-1.** The scavenging effect of LIG on DPPH radical. The free radical scavenging activity was measured by the degree of decoloration of a DPPH solution. The indicated concentration of LIG was added to a 100  $\mu$ M ethanolic solution of DPPH. Decoloration percentage was measured at the indicated incubation time at 25  $^{\circ}$ C. Each value represents the average obtained in three different experiments in each of which four measurements were made. The data points without error bar indicate that standard deviation is too small to be seen. Key: ( $\Delta$ ) 5 mM LIG, ( $\bullet$ ) 20 mM LIG, ( $\blacktriangle$ ) 80 mM LIG.

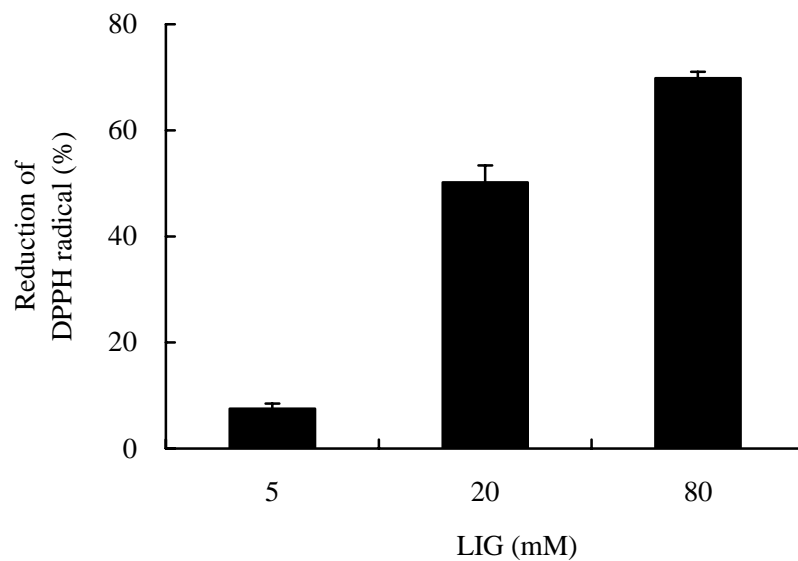


**Figure 4-2.** The percentage reduction of the DPPH radical by LIG. The free radical scavenging activity was measured after 180 min incubation at 25 °C. Each value represents the average obtained in three different experiments in each of which four measurements were made.

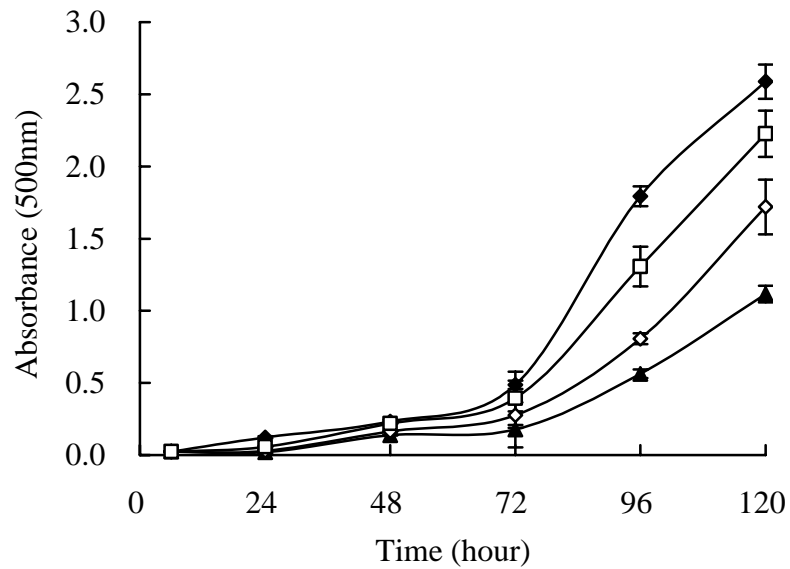


**Figure 4-3.** The antioxidant activity of LIG on the oxidation of linoleic acid emulsion. The activity was determined by the thiocyanate method. The indicated concentration of LIG or volume-matched vehicle was added to the linoleic acid emulsion. The amount of peroxides was measured in the linoleic acid emulsion at the indicated incubation time at 37 °C. Each value represents the average obtained in three different experiments performed in triplicate. Key: (◆) control; (□) 5 mM LIG; (◇) 20 mM LIG; (▲) 80 mM LIG.

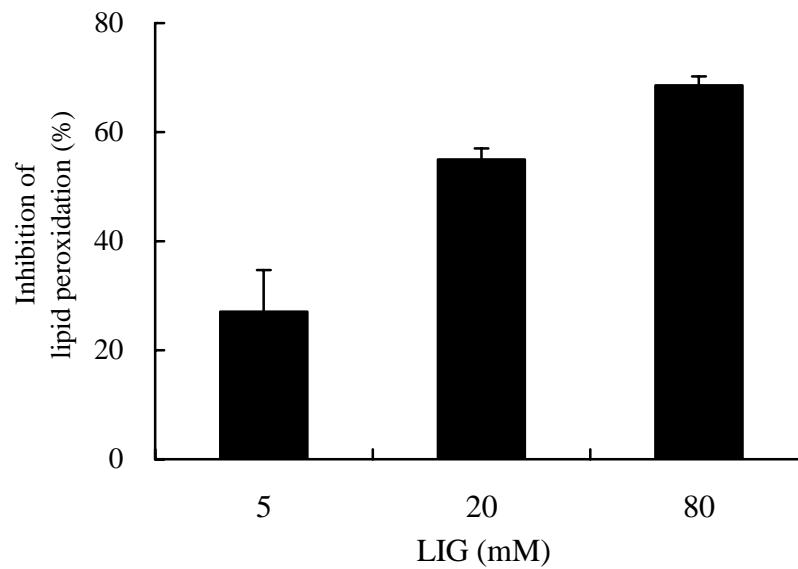


**Figure 4-4.** The percentage inhibition of the lipid peroxidation of LIG in the linoleic acid emulsion. The free radical scavenging activity was measured after a 96 h incubation at 37 °C. Values represent mean  $\pm$  SD ( $n = 4$ ). Each value represents the average obtained in three different experiments.

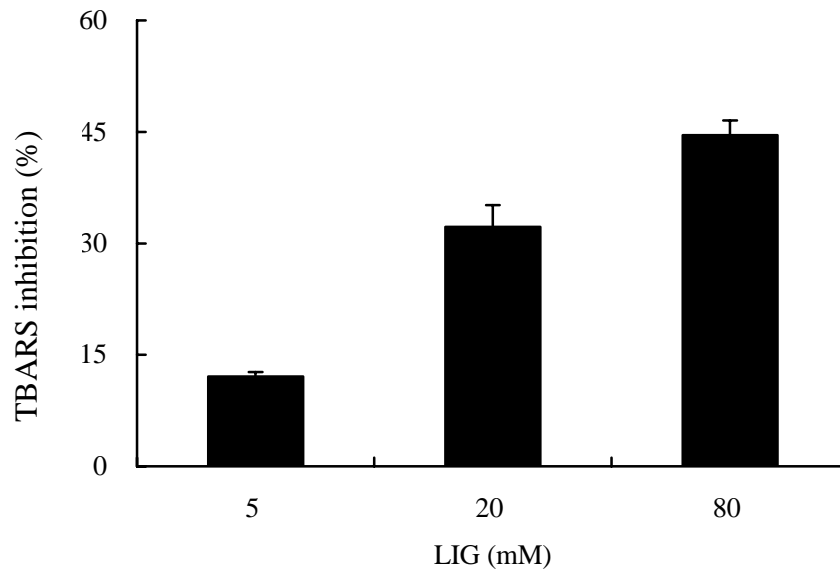


**Figure 4-5.** The inhibition effect of LIG on  $\text{Fe}^{2+}$ /ascorbate-induced lipid peroxidation in rat cerebral cortex mitochondria. Brain mitochondria (3 mg of protein /ml) were incubated with the  $\text{Fe}^{2+}$ /ascorbate acid generating system, in the presence of 10  $\mu\text{l}$  of the indicated concentrations of LIG or just the control solvent for 30 min at 37 °C. TBARS was measured as described in materials and methods. Values represent mean  $\pm$  SD ( $n = 4$ ). Each value represents the average obtained in three different experiments performed.

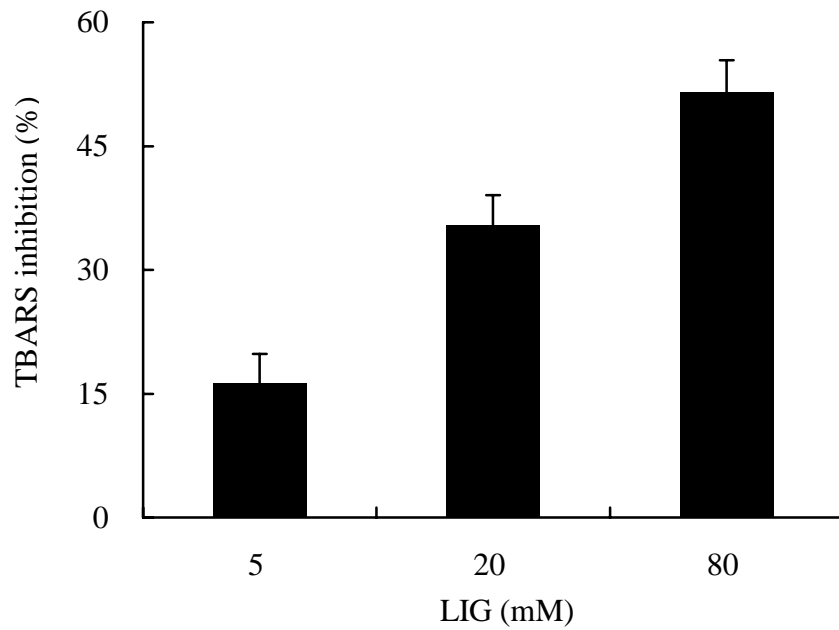


**Figure 4-6.** The inhibition effect of LIG on the NADPH-dependent lipid peroxidation in rat cerebral cortex mitochondria. Brain mitochondria (3 mg of protein/ml) were incubated with the NADPH generating system, in the presence of 10  $\mu$ l of the indicated concentrations of LIG or just the control solvent for 30 min at 37 °C. TBARS was measured as described in materials and methods. Values represent mean  $\pm$  SD ( $n = 4$ ).

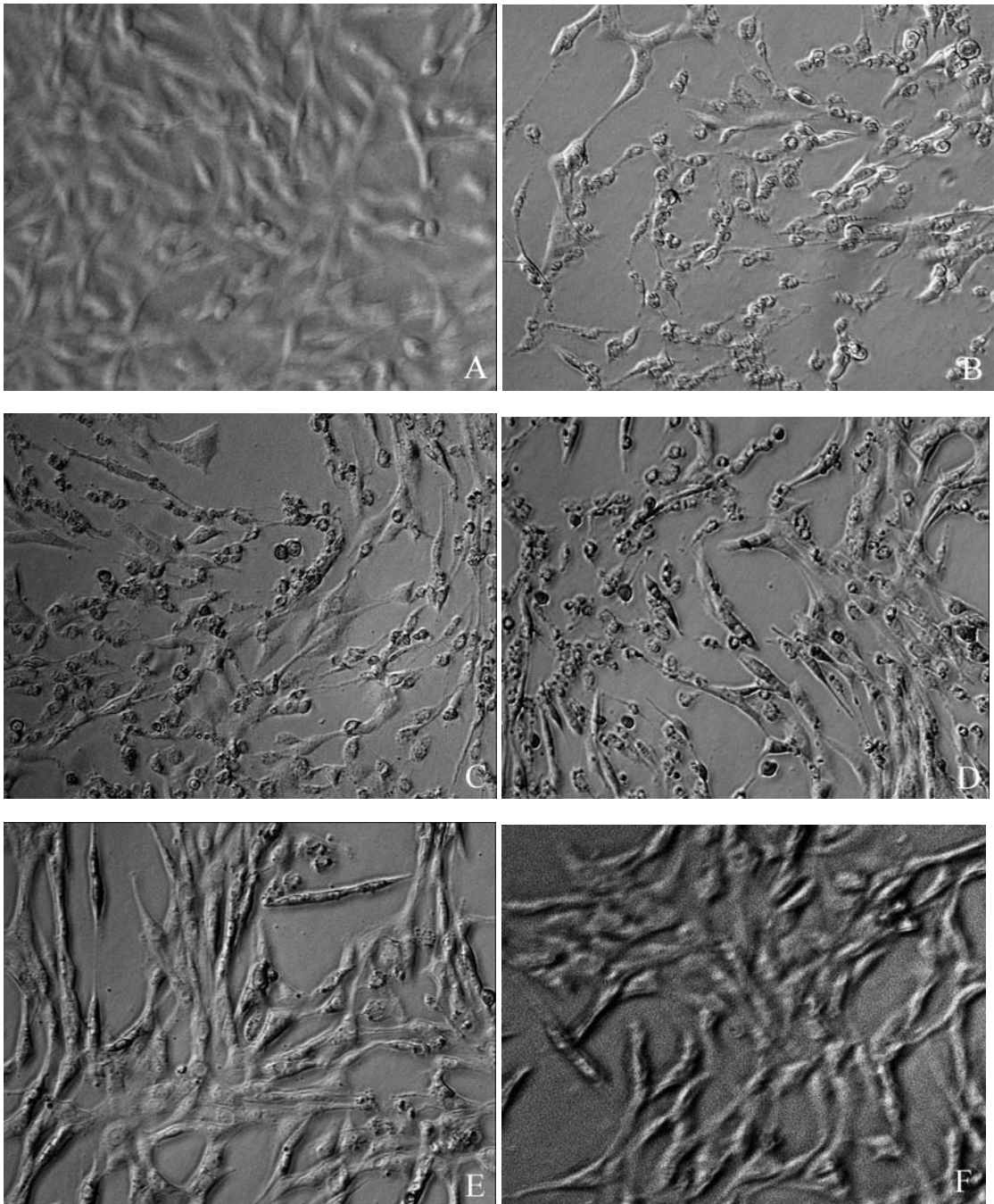


**Figure 4-7.** Representative photomicrographs showing the protective effect of LIG on H<sub>2</sub>O<sub>2</sub>-induced C6 cell injury. The C6 cells were incubated in the presence of the various indicated concentrations of LIG for 24 h and then 500 μM H<sub>2</sub>O<sub>2</sub> for another 24 h. A: normal cells, B: H<sub>2</sub>O<sub>2</sub> -treated cells which showed a significant decrease in cell number and most of them demonstrated the round shape, C-F: LIG (final

concentration of 0.5, 5, 25 and 50  $\mu\text{M}$ , respectively) prevented  $\text{H}_2\text{O}_2$ -induced cell injury in a concentration-dependent manner. 100-fold magnification.

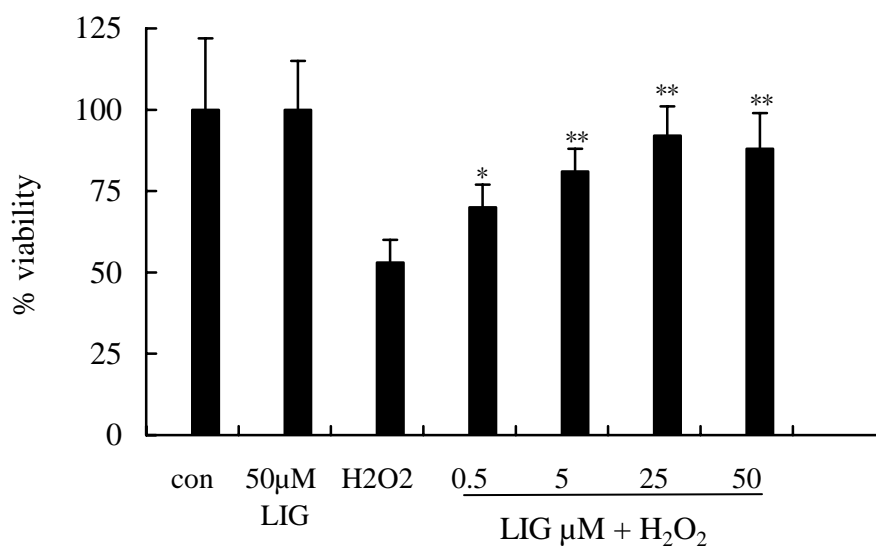


**Figure 4-8.** The protective effect of LIG on  $\text{H}_2\text{O}_2$ -induced cytotoxicity in C6 cells with the MTT assay. The C6 cells were incubated in the presence of the various indicated concentrations of LIG for 24 h and then 500  $\mu\text{M}$   $\text{H}_2\text{O}_2$  for another 24 h.  $\text{H}_2\text{O}_2$ -treated cells showed greatly reduction in cell viability. LIG prevented  $\text{H}_2\text{O}_2$ -induced cytotoxicity in a dose-dependent manner. Each value is the mean  $\pm$  SD ( $n = 6$ ) expressed as a percentage of control cultures. \* $P < 0.05$ , \*\* $P < 0.01$  vs the group of  $\text{H}_2\text{O}_2$  treatment.

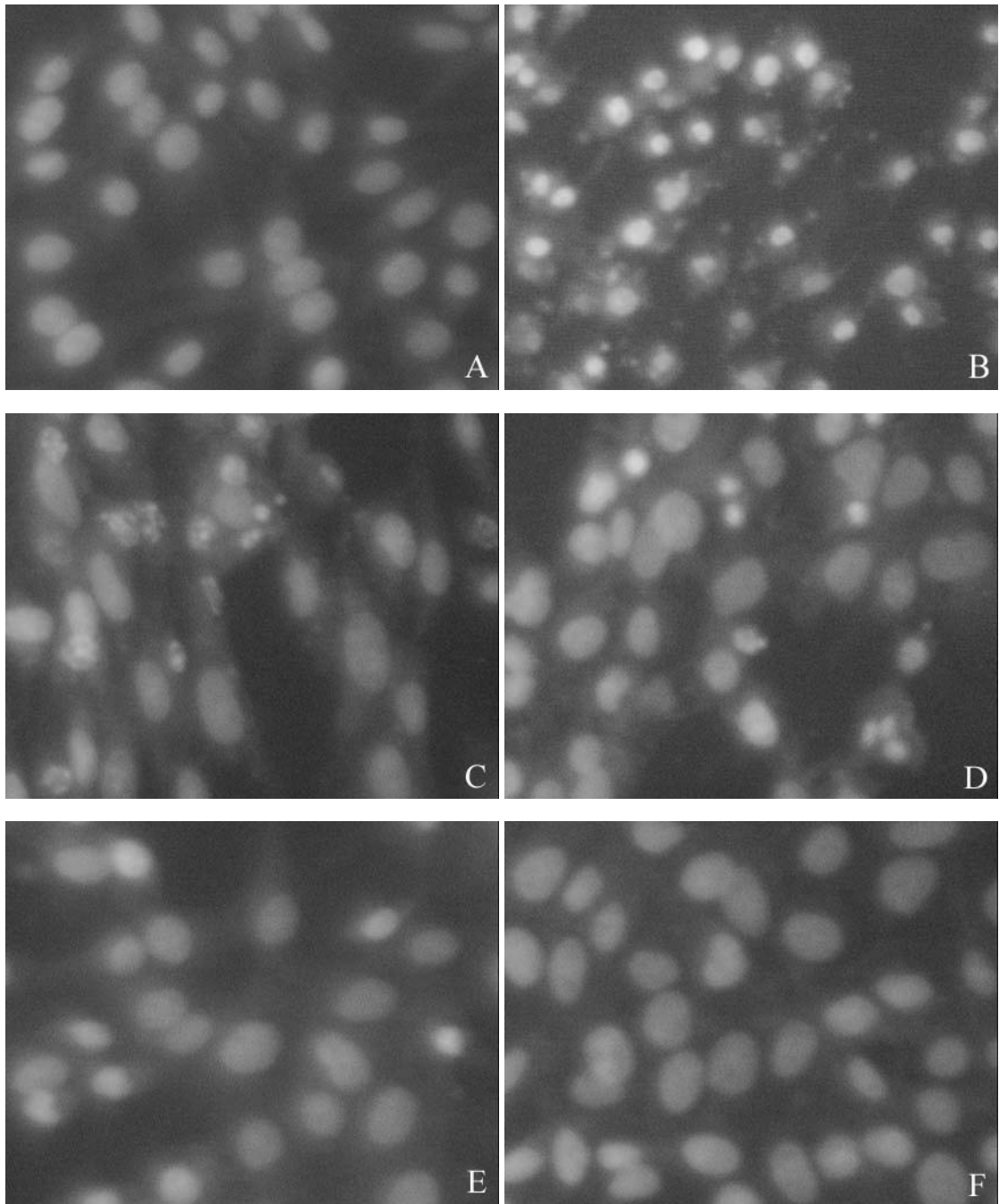


**Figure 4-9.** The effect of LIG on  $H_2O_2$ -induced apoptotic cell death in the C6 cells with Hoechst 33342 staining. The C6 cells were incubated in the presence of the various indicated concentrations of the tested samples for 24 h and then  $500 \mu M H_2O_2$  for another 24 h. A: normal cells, B: the  $H_2O_2$ -treated cells which showed chromatin condensation and/or nuclear fragmentation, C-F: LIG (final concentration of 0.5, 5, 50, and 500  $\mu M$ ).

25 and 50  $\mu\text{M}$ , respectively) prevented  $\text{H}_2\text{O}_2$ -induced apoptotic cell death in a dose-dependent manner. Original magnification:  $\times 400$ .

## **CHAPTER 5**

# **NEUROPROTECTION OF Z-LIGUSTILIDE AGAINST FOREBRAIN ISCHEMIA IN MICE MEDIATED BY ANTIOXIDATION AND ANTIAPOPTOSIS**

### **5.1 ABSTRACT**

Literature suggests that lipid-soluble antioxidants probably have greater efficacious neuroprotective potency in cerebral ischemia because of their potential ability to cross the blood-brain barrier and their presence in neuronal membrane structures where lipid peroxidation can be halted. Findings in chapter 4 showed that lipophilic Z-ligustilide (LIG) was a novel potent antioxidant in various *in vitro* ROS systems and could protect C6 cells against hydrogen peroxide-induced oxidative injury. And the transepithelial permeation characteristics of LIG in Caco-2 monolayer model, as demonstrated in chapter 3, indicated the excellent absorption potential of LIG through small intestine *in vivo*. These results, plus the accumulating evidences on the interaction of oxidative stress and ischemic brain injury, suggest that oral administration of LIG might be beneficial for the treatment of cerebral ischemia. Therefore, the present study investigated the antioxidative activity, anti-apoptotic effect, and potential neuroprotection by postischemic treatment with orally administrated LIG on forebrain ischemia in ICR mice. A forebrain ischemic model

was produced by a 0.5 h bilateral common carotid artery occlusion (BCCAO) in the ICR mice (8-10 weeks old). LIG or the vehicle was orally administrated at the start of reperfusion and subsequently once daily. As determined at 5 d after ischemia, the treatment with LIG (20 or 80 mg/kg, p.o.) significantly prevented neuronal damage in the hippocampal CA1 and cortex, LIG treatment also dose-dependently decreased the level of MDA and increased the activities of the antioxidant enzymes GSHPx and SOD in ischemic brain tissues. In addition, LIG provided a great increase in Bcl-2 expression as well as a significant decrease in Bax immunoreactivity, cytosolic cytochrome c release, cleaved caspase-3 expression and caspase-3 activity. The findings of ischemic brain samples from vehicle-treated group, which showed markedly increase in the number of TUNEL positive cells as well as the ladderized feature of DNA fragmentation, were greatly suppressed by the treatment with LIG. Taken together, these results first presented the neuroprotective effect of LIG in forebrain ischemic brain injury, which may be associated, at least partly, with its antioxidant properties and the suppression of apoptotic mitochondrial pathway.

**KEY WORDS:**

Z-ligustilide, phthalides, neuroprotection, cerebral ischemia, apoptosis, oxidative stress, Bcl-2, Bax, caspase-3, cytochrome c, neuronal death

**5.2 INTRODUCTION**

As postmitotic cells, neurons are almost incapable of division and regeneration, and therefore largely irreplaceable once they die. It is reported that ischemic stroke is the third leading cause of death in major industrialized countries and also a major cause of long-lasting disability (Bonita R, 1992). Approximately 20% of stroke patients do not survive the first month and >30% who are alive 6 months later will be dependent on others (Warlow, 1998). Ischemia stroke therefore has major repercussions not only for the survivor but also for the family and society as a whole. In the past 20 years, numerous studies have identified several key biochemical and cellular events that lead to ischemic neuronal degeneration (Chan, 2001; Leist and Nicotera, 1998; Onteniente et al., 2003), and oxidative stress is widely regarded as an important role among these various factors contributing to ischemic brain damage (Chan, 1996; Chan, 2001). Cerebral ischemia/reperfusion enhances the formation of ROS in the brain tissues. An excessive production of ROS, such as superoxide anion, hydroxyl radical, hydrogen peroxide, and nitric oxide, may directly attack bio-macromolecules, including proteins, membrane lipids and DNA, and induce neuronal necrosis. A particularly important aspect of oxidative stress in neurons is the lipid peroxidation in that neuronal membrane have plenty of polyunsaturated fatty acids. In addition, oxidative stress resulting from ROS production may also affect the cellular signaling pathway and gene expression and be implicated in apoptosis following brain ischemia (MacManus and Linnik, 1997 ). The endogenous antioxidant enzymes, such as SODs, GSHPx and catalase, are known to scavenge ROS, and neuroprotective effects of these free radical scavengers during ischemia/reperfusion have been variously demonstrated (Chan,

2001).

Recent investigations have shown that ischemic severity might affect the pathological process of cell death, and mild insults are more likely to induce apoptosis (Du et al., 1996; Leist and Nicotera, 1998; Onteniente et al., 2003). When the regional cerebral blood flow (rCBF) drops below 10% of the control values, such as in the core of the lesion in a focal stroke, cells die through the energy-independent pathway within a few minutes or hours that mainly include a necrotic process. In the remaining arterial territory, or penumbra, rCBF levels are kept at up to 40% of the control values due to retrograde perfusion by anastomosis from the adjacent arteries. In this area, ATP levels remain high enough to allow for apoptosis, an energy dependent mechanism, and cell death is delayed by hours or even days. Transient forebrain ischemia by occluding the bilateral common carotid artery is one of the models of low-perfusing cerebral ischemia, which mainly results in neuronal injury through the energy-dependent mitochondrial apoptotic mechanism. Hippocampal pyramidal neurons have been shown to be the major target of an ischemic insult in this model (Kogure et al., 1993; Koistinaho and Hokfelt, 1997; Matsunaga et al., 2003).

As shown in chapter 3 and 4, LIG, a highly lipophilic compound absorbable through small intestine, was a novel potent antioxidant in various ROS systems and hydrogen peroxide-induced cell oxidative injury model *in vitro*. However it remains uncertain whether LIG has any antioxidant activity *in vivo* and can protect the brain against

ischemic injury by its oral administration. The present study was carried out to determine the effect of LIG on forebrain ischemia-induced neuronal damage in mice, as well as the mechanisms associated with the antioxidation and anti-apoptosis.

## **5.3 MATERIALS AND METHODS**

### **5.3.1 Materials**

#### **5.3.1.1 Chemicals**

Unless otherwise stated, all chemicals were obtained from Sigma chemical company, St. Louis, MO, USA. Agarose, Tris, ethidium bromide and prestained protein marker were purchased from Bio-Rad Laboratories, Hercules, CA, USA. Polyacrylamide was from Amresco, Solon Industrial Parkway Solon, Ohio, USA. ECL Western blotting analysis system was from Amersham Biosciences, England. The mouse monoclonal antibodies against cytochrome c, Bcl-2 and Bax were from Santa Cruz Biotechnology, Santa Cruz, CA, USA. The rabbit anti-caspase-3 polyclonal against cleaved caspase-3 was from Cell Signaling technology, Inc. Beverly, MA, USA. The kit of *in situ* Cell Death Detection, POD, was purchased from Roche, Mannheim, Germany. The SP reagent and DAB kit were from Zhongshan Bioengineering Co, China and VECTOR, Burlingame, USA, respectively. The kits of MDA, SOD and GSHPx activity assay were from Jianchen Bioengineering Co, Nanjing, China. The kit

of caspase-3 activity (KGA210) colorimetric assay was purchased from KeyGen Biotech Corporation Limited, Nanjing, China.

#### **5.3.1.2 Animal Preparation**

Male ICR mice weighing 24 to 26 g (8~10 weeks old) were housed at  $20 \pm 1^\circ\text{C}$ , with relative humidity at  $55 \pm 15\%$  and a 12-h lighting cycle (08:00-20:00 h), and allowed access to food and water ad libitum. Mice were used in experiments following the adjustment to these conditions for 1 week, and were fasted overnight before experiments but had free access to water. Animal care was in compliance with the Chinese regulations on the protection of animals used for experimental and other scientific purposes.

#### **5.3.1.3 Drug Preparation**

LIG (purity over 98 %) was prepared from our own laboratory and stored at  $-20^\circ\text{C}$ . Before the application, LIG was diluted into 2 and 8 mg/ml with 3% Tween-80. Mice were orally administrated a drug solution in a dose of 20 or 80 mg/kg, or a volume-matched vehicle.

### **5.3.2 Methods**

### **5.3.2.1 Murine Forebrain Ischemic Model**

The Forebrain ischemia-reperfusion model of mouse was induced by a 0.5 h occlusion of the bilateral common carotid arteries (BCCAO) and 5 days of reperfusion. The operation of BCCAO was improved based on previous reports (Kitagawa et al., 1998; Matsunaga et al., 2003). Male ICR mice were anesthetized through the intraperitoneal injection of chloral hydrate (350 mg/kg). Core body temperatures were maintained at  $37 \pm 0.5$  °C with a feedback-regulated heating pad. Both the common carotid arteries were exposed through a midline incision in the neck. The forebrain ischemia was induced by the occlusion of BCCAO with microaneurysm clips. After 30 min ischemia, the bilateral carotid clamps were removed and complete reperfusion was allowed for 5 days. An exposure of the bilateral common carotid arteries without BCCAO was used to produce the sham-operated animals. After surgery, the wound was sutured and the mice were returned to their cage with free access to water and food. The animals were placed on a thermostatically controlled warming plate to maintain body temperature at 37 °C during the ischemic insult and until the animals regained their righting reflex after reperfusion. It was reported that this warming procedure successfully maintained both the rectal and brain temperature of the animals at over 35.5 °C (Hall et al., 1993).

### **5.3.2.2 LIG Treatment Schedule**

After 30 min of ischemia, the animals were randomly allocated to the following experimental groups (n = 14 in each group): the sham-operation group, the vehicle-treated control group, the LIG low dose group and the high dose group. LIG was orally administrated (20 or 80 mg/kg) at the start of reperfusion after 30 min of ischemia and again once daily during the period of 5 day reperfusion. The sham-operation group received an administration of a volume-matched vehicle. The administrated volume was kept constant at 10 ml/kg.

### **5.3.2.3 Brain Tissue Preparation**

#### **(1) Brain Tissue Preparation for Biochemical and Western blot Analyses**

During the 5 days of reperfusion, the animals were deeply reanesthetized through the intraperitoneal injection of chloral hydrate (400 mg/kg) and received an intracardiac perfusion with the phosphate-buffered saline (pH 7.2) until the effluent was cleared of blood. The brain was then quickly removed, frozen by suspension over liquid nitrogen, and cut into coronal blocks. The section at bregma +0.62 to -1.46 mm was then used directly or stored at -80 °C until used.

#### **(2) Brain Tissue Preparation for Histochemistry**

During the 5 days of reperfusion, the animals were reanesthetized through the intraperitoneal injection of chloral hydrate (400 mg/kg) and received an intracardiac perfusion with 100 ml of PBS (pH 7.2), followed by 100 ml of 4% paraformaldehyde

in PBS (pH 7.4). The brain was removed, postfixed for 24 h in the same fixative solution, and the section at bregma  $-1.46$  to  $-3.52$  mm was then embedded in paraffin.

#### **5.3.2.4 Estimation of Neuronal Loss**

The paraffinized sections ( $5\ \mu\text{m}$ ) were taken and mounted on glass slides and deparaffinized by heating at  $70\ ^\circ\text{C}$  for 10 min. Slices were washed twice with xylene for 5 minutes, 95% and 70% ethanol for 3 minutes in each wash, and PBS. The slices were stained with HE as described in Chapter 2. The cerebral cortex and hippocampal CA1 were viewed under a light microscope (Leica, Wetzlar, Germany). The total images of the hippocampus were obtained by using a  $4\times$  lens, and the local pictures of the cortex and hippocampus were obtained using a  $40\times$  lens. Neurons which had shrunken cell bodies with surrounding empty spaces were identified as damaged and excluded. All normal appearing CA1 pyramidal neurons in a  $0.5$  mm length of the CA1 region were counted bilaterally and then averaged. Animals which showed significant asymmetry in regard to the CA1 neuronal counts ( $>50\%$  difference between hemispheres) were discarded. The average of the right and left neuronal densities was regarded as the neuronal cell density of each mouse. The values of neuronal density were expressed as the mean value/ $0.5$  mm (Kirino et al., 1986).

#### **5.3.2.5 Measurement of Antioxidant Enzyme Activities**

The sections obtained at the level of bregma +0.62 to -1.46 mm were subjected to enzyme activity analyses. The procedure was carried out using commercially available kits (Jianchen Bioengineering, Nanjing, Jiangsu Province, PR China). The assay for SOD activity was based on its ability to inhibit the oxidation of oxyamine by  $O_2^-$  produced from the xanthine-xanthine oxidase system. One unit of SOD activity was defined as the capability of reducing the absorbance at 550 nm by 50%. The assay of GSHPx activity was determined by quantifying the rate of oxidation of the reduced GSH to the GSSG by  $H_2O_2$  catalyzed by GSHPx. One unit of GSHPx was defined as the activity that reduced the level of GSH by  $1\mu M$  in 1 min per mg protein.

#### **5.3.2.6 Estimation of Lipid Peroxidation**

The sections obtained at the level of bregma +0.62 to -1.46 mm were subjected to the measurement of the tissue contents of MDA, an indicator of lipid peroxidation. The procedure was carried out as described previously (Ohkawa et al., 1979). Brain tissues were homogenized in 10 times (w/v) 0.1 M sodium phosphate buffer (pH 7.4). To every 0.1ml of the above sample, the following reagents were added: acetic acid (20%) 1.5 ml (pH 3.5), thiobarbituric acid (0.8%) 1.5 ml, and SDS (8.1%) 0.2 ml. The mixture was heated at 100 °C for 60 min, and then cooled with tap water. After the addition of 5 ml of n-butanol/pyridine (15:1 v/v) and 1ml of distilled water, the reaction mixture was vigorously shaken. After centrifugation at 4000 rpm for 10 min, the organic layer was withdrawn and absorbance was measured at 532 nm using a

spectrophotometer and quantification done based on the standard curve generated by using vigorously authentic malondialdehyde.

### **5.3.2.7 Western Blot Analyses**

#### **(1) Total Protein Extraction**

Brain tissues were washed in ice-cold PBS, and homogenized in 10 time volume of ice-cold lysis buffer containing 50 mM Tris-Cl (PH 8.0), 1mM EDTA, 150mM NaCl, 0.1% SDS, 0.5% sodium deoxycholate, 1mM PMSF, 1 µg/ml aprotinin, 1 µg/ml leupeptin, 1 µg/ml pepstatin, 1% Triton-X-100. After the centrifugation of the homogenate at  $10,000 \times g$  for 30 min at 4 °C, the supernatant was collected and stored at -20 °C until used.

#### **(2) Cytosolic Protein Extraction**

Brain tissues were washed in ice-cold PBS, and put into 10 volumes of lysis buffer containing 20 mM Hepes-KOH, pH 7.5, 10 mM KCl, 1.5 Mm MgCl<sub>2</sub>, 1 mM Na-EDTA, 1 mM Na-EGTA, 1 mM dithiothreitol, 1 mM PMSF, 250 mM sucrose and then centrifuged at  $750 \times g$  for 10 min at 4 °C. The harvested supernatant was again centrifuged at  $10,000 \times g$  for 10 min at 4 °C, and the supernatant was collected and stored at -20 °C until used.

#### **(3) Protein Concentration Determination**

Please refer to chapter 2.

#### **(4) Western Blot Analyses**

Total protein samples were used to determine the Bax and BCL-2 expression and cytosolic samples used to assay the cytochrome c and cleaved the caspase-3 expression.

Forty micrograms protein were diluted in a  $2 \times$  sample buffer (50 mM Tris, pH 6.8, 2% SDS, 10% glycerol, 0.1% bromophenol blue, and 5%  $\beta$ -mercaptoethanol). After being heated for 5 min at 95 °C, the samples were first separated by 15% SDS-polyacrylamide gel electrophoresis, and subsequently transferred to a polyvinylidene difluoride membrane (Amersham Biosciences, England). Membranes were blocked with 5% blocking reagent (Amersham Biosciences, England) in TBS (pH 7.6) containing 0.1% Tween-20 (TBS-T) for 2 h at room temperature or overnight at 4 °C. The membrane was rinsed in three changes of TBS-T, incubated once for 15 min and twice for 5 min in a fresh washing buffer, and then incubated with primary antibody for 2 h at room temperature or overnight at 4 °C. The concentrations of primary antibodies for blotting are mouse anti-Bax and anti-Bcl-2 monoclonal antibodies (1:100, Santa Cruz Biotechnology, CA), mouse anti-cytochrome c monoclonal antibody (1:500, Santa Cruz Biotechnology, CA) and rabbit anti-caspase-3 polyclonal (1:1000, Cell Signaling technology, recognizes cleaved caspase-3). After three washes in a washing buffer, the membrane was incubated for 2

h in a horseradish peroxidase-conjugated anti-mouse secondary antibody (1:2000, Amersham Biosciences, England) or horseradish peroxidase-conjugated anti-rabbit secondary antibody (1:5000, Santa Cruz Biotechnology, CA), and developed using enhanced chemiluminescence (ECL western blotting analysis system kit, Amersham Biosciences, England). The blot was exposed to XOMAT AR films (Eastman Kodak, Rochester, NY). The films were scanned on a UMAX PowerLook Scanner (UMAX Technologies, Fremont, CA, USA) using Photoshop 5.0 software (Adobe Systems, Seattle, WA, USA) , and the optical density of each band was determined by using Gel-pro Analyzer software (Media Cybernetics, Silver Spring, MD, USA). To ensure even loading of the samples, the same membrane was probed with the mouse anti- $\beta$ -actin monoclonal (Sigma-Aldrich, MO) at 1:5000 dilutions. The specific band is normalized with  $\beta$ -actin and expressed as a percentage of normal level in the sham-operated group.

#### **5.3.2.8 Caspase-3 Activity Assay**

Caspase-3 activity of brain tissues was measured using colorimetric assay kits essentially according to the manufacturer's instruction (KeyGen Biotech corporation limited, Nanjing, China). This assay was based on the ability of the active enzyme to cleave the chromophore from the caspase substrate. Fifty micrograms of cytosolic protein was diluted in a 50  $\mu$ l of lysis buffer, added to a 50  $\mu$ l reaction buffer, and transferred to a 96 well flat-bottom microplate. To each reaction well, 5  $\mu$ l of caspase 3

colorimetric substrate (DEVD-pNA) were added. The plate was incubated for 4 h at 37 °C. Levels of released *p*-nitroanilide (pNA) were evaluated by measuring the optical density at 405 nm with a Model 550 microplate reader (Bio-Rad Lab., Hercules, CA, USA). Caspase-like activities were expressed as the percentage of optical density unit of the sham-operated control group.

#### **5.3.2.9 TUNEL Staining**

The terminal deoxynucleotidyltransferase (TdT)-mediated dUTP-biotin nick end-labeling (TUNEL) method was employed for the *in situ* detection of apoptotic cells in the tissue sections with an *in situ* Cell Death Detection Kit, POD (Roche, Mannheim, Germany) (Gavrieli et al., 1992). The 5- $\mu$ m thick slices were placed on APES- treated slides and deparaffinized by heating at 60 °C for 10 min. Slices were washed twice with xylene for 5 min, 95% and 70% ethanol for 3 min in each wash, and double-distilled water. They were then treated with 20  $\mu$ g/ml proteinase K (Sigma Chemical Co) for 15 min at room temperature and washed 4 times with distilled water and PBS. The slides were incubated in TUNEL reaction mixture at 37 °C for 60 min. The reaction was terminated by stopping the buffer for 30 min at 37 °C. After washing 3 times with PBS for 5 min each, the endogenous peroxidase was inactivated by covering the sections with 3% H<sub>2</sub>O<sub>2</sub> in methanol for 10 minutes at room temperature. The slides were treated by Converter-POD for 30 min at 37 °C, washed again with PBS, and visualized by the DAB Chromagen. Negative control slides were prepared,

with distilled water substituted for the TdT enzyme in the preparation of working the TdT buffer. Coronal sections stained with the TUNEL method were counterstained with hematoxylin. The labeling target of the TUNEL method was the new 3'-OH DNA ends generated by DNA fragmentation. Using the TUNEL staining, there were two distinct patterns of TUNEL positive staining, TUNEL-positive apoptotic cells and TUNEL-positive necrotic cells, as reported previously (Charriaut-Marlangue and Ben-Ari, 1995; Charriaut-Marlangue et al., 1996a; Charriaut-Marlangue et al., 1996b). The slides were viewed under a light microscope (Leica, Germany). The TUNEL-positive apoptotic cells were defined as showing a condensation and fragmentation of nuclei and apoptotic bodies around the nuclear membrane without cytoplasmic a staining. Other TUNEL-positive cells were weakly labeled, showing a diffused cytoplasmic staining and a lack of nuclear condensation, and were considered to be necrotic cells. The number of TUNEL-positive apoptotic cells were counted in six microscopic fields ( $\times 400$  magnification), respectively and expressed as the number/high power field.

#### **5.3.2.10 DNA Fragmentation Assay**

The sections obtained at the level of bregma +0.62 to -1.46 mm were subjected to the determination of laddering of DNA fragmentation. For oligonucleosomal fragmentation of genomic DNA, fresh brain tissues (about 100 mg) were homogenized with 1ml ice-cold TE, washed with TE two times, and then lysed in 1ml of lysis buffer

(containing 10 mM Tris-HCl, pH 7.4, 1 mM EDTA, 1% SDS). After addition of RNase A to 0.02mg/ml, the sample was digested at 37 °C for 1h. Digestion continued for 3 h at 55 °C, followed by the addition of proteinase K to 0.1 mg/ml. The fragmented DNA was extracted and purified by the method of phenol-chloroform-isoamyl alcohol. Equivalent amounts of DNA (10 µg) were added to 6×loading dye (10 mM EDTA, 0.25% bromphenol blue, 40% sucrose), and loaded into each lane of the 2% agarose gel electrophoresed in 0.5 × TBE buffer for 2 h at 100V. DNA was visualized by ethidium bromide staining. Gel pictures were taken by Gel Media System (Media Cybernetics, Silver Spring, MD, USA). The expected sizes of the positions of DNA fragmentation were shown compared to the 100-bp DNA ladder marker. DNA fragmentation was quantified by an analysis software using Gel-pro Analyzer software (Media Cybernetics, Silver Spring, MD, USA). The values were normalized for vehicle-treated ischemic controls and expressed in units relative to these controls.

#### **5.3.2.11 Statistical Analysis**

The statistical analysis were performed using SPSS 10.0. Data were presented as mean ± SD. The difference between the means was determined by One-Way ANOVA followed by a Student-Newman-Keuls test for multiple comparisons. Differences with  $P < 0.05$  were considered significant.

## **5.4 RESULTS**

#### **5.4.1 Neuronal Protection (Fig. 5-1)**

To determine the effect of LIG on cerebral ischemia-induced neuronal damage, HE staining was used to detect the intact neuron cells in the cortical and hippocampal CA1 areas. On the fifth day after 30 min of ischemia, numerous neuronal loss or damage could be found in the cortex and hippocampal CA1 of the vehicle-treated group whereas there was not abnormality in the sham-operated group (Fig. 5-1 A-F). In contrast, postischemic treatment with LIG produced dose-dependent protection on ischemia-induced neuron damage (Fig. 5-1 H-J). Quantificative analysis showed that 80 mg/kg LIG had significant neuroprotection on the CA1 neurons when compared to the vehicle-treated ischemic group ( $P < 0.01$  vs. Fig. 5-1 K).

#### **5.4.2 Antioxidant Potential (Fig. 5-2)**

To answer whether the neuroprotective effect of LIG was associated with any the antioxidant effect as suggested by our in vitro observations in chapter 4, we measured the tissue contents of MDA, an indicator for lipid peroxidation, and the activities of SOD and GSHPx. Results showed that the cerebral tissue levels of SOD (Fig. 5-2A) and GSHPx (Fig. 5-2B) activities were significantly decreased in the vehicle-treated ischemic group at 5 day reperfusion after 30 min of BCCAO ( $P < 0.05$  vs. sham-operated controls), whereas LIG treatment restored the reduction in these antioxidant enzymes in a dose-dependent manner. 80 mg/kg LIG could recover the

levels of SOD and GSHPx activities to near the sham-operated levels, and these changes reached statistic significance as compared to the vehicle-treated ischemic group ( $P < 0.01$  or  $P < 0.05$  vs. ischemic controls, respectively; Fig. 5-2A and B). Consistent with this effect of LIG on the antioxidant enzymes, LIG treatment at a dose level of 80 mg/kg also significantly attenuated the increases in MDA contents after ischemia/reperfusion ( $P < 0.05$  vs. ischemic controls; Fig. 5-2C).

#### **5.4.3 Expression of Bcl-2 and Bax (Fig. 5-3, Fig. 5-4)**

To evaluate whether any anti-apoptosis mechanism was involved in the anti-infarction effect of LIG, several methods were used in the present study. We detected the effect of LIG on pro- and anti-apototic proteins including Bcl-2 and Bax expression by immunoblot. As shown in Fig. 5-3 and Fig. 5-4, at 5 d after 30 min of BCCAO, Bcl-2 expression was weak while Bax expression was intensely immunoreactiv. The treatment by orally administrating LIG markedly and dose-dependently increased Bcl-2 ( $P < 0.01$  at the doses of 20 and 80 mg/kg) and decreased Bax expression ( $P < 0.05$  or  $P < 0.01$  at 20 or 80 mg/kg) in forebrain ischemic tissues.

#### **5.4.4 Cytochrome C Release (Fig. 5-5)**

To test the effect of LIG on the cytosolic release of cytochrome c in forebrain ischemia, western blot analyses was used for the cytosolic cytochrome c expression of brain

tissues. As shown in Figure 5.5, brain samples obtained from the sham-operated control mice showed traces of cytochrome c protein level (relatively density = 1). Samples obtained from ischemic brain tissues of mice subjected to 0.5 h BCCAO/5 d reperfusion revealed an over 1.7-fold increases (relatively density =  $2.76 \pm 0.83$ ) in the cytosolic cytochrome c expression, which were dose-dependently reduced to  $2.34 \pm 0.29$  or  $1.28 \pm 0.36$  relative density by the postischemic treatment with 20 or 80 mg/kg LIG. As compared to the vehicle-treated control mice, 80 mg/kg LIG significantly inhibited the cytochrome c release from mitochondria in forebrain ischemia ( $P < 0.05$ ).

#### **5.4.5 Activation of Caspase 3 (Fig. 5-6, Fig. 5-7)**

To further confirm the anti-apoptosis mechanism of the neuroprotective effect of LIG on forebrain ischemia, cleaved caspase 3 expression and caspase 3 activity of brain tissues were assayed. As shown in Figure 5-6 and Fig. 5-7, cleaved caspase 3 expression and caspase 3 activity were significantly increased in the ischemic control group as compared to the sham-operated control ( $P < 0.05$ ), which were significantly and dose-dependently inhibited by the postischemic treatment with LIG ( $P < 0.05$  or  $P < 0.01$  at 20 or 80 mg/kg). These results showed that LIG could significantly inhibit caspase 3 activation following transient forebrain ischemia.

#### **5.4.6 Formation of Apoptotic-positive Cells (Fig. 5-8)**

To ask whether LIG inhibits neuronal apoptotic death in forebrain ischemia, TUNEL-positive apoptotic cells were identified in situ via TUNEL staining in the infarct cortex. As shown in Fig 5-8, no TUNEL-positive cells were observed in the nonischemic cerebral cortex of the sham-operated control group. At 0.5 h reperfusion after 5 d BCCAO, TUNEL-positive cells were markedly increased in the ischemic cortex. The apoptotic cells were identified by the condensation and fragmentation of nuclei and/or apoptotic bodies around the nuclear membrane and considered to be mainly neurons based on the morphologic characteristics. After the treatment of LIG, the apoptotic cells were dose dependently reduced in the ischemic cortex, and 80 mg/kg LIG significantly suppressed the increase in the number of apoptotic neuron when compared to the vehicle-treated control group ( $P < 0.05$ ).

#### **5.4.7 Formation of DNA Fragmentation (Fig5-9)**

Oligonucleosomal DNA fragmentation is known as a hallmark of apoptosis. Thus, to confirm the antiapoptotic effect of LIG, DNA fragmentation was measured by gel electrophoresis. Fig 5-9 showed the segmented DNA at 180- to 200-bp internals, reflecting the activity of endonuclease cleavage of DNA at the internucleosomal site in the forebrain ischemia mice at 5 days after 30 min of BCCAO. No laddering was detected in the sham-operated animals and significant laddering was seen in samples from the vehicle-treated mice. Treatment with LIG (20 or 80 mg/kg, p.o.) strongly suppressed the ladder feature of DNA fragmentation by 45% and 62 % ( $P < 0.05$  or

$P < 0.01$ , respectively).

## **5.5 DISCUSSION**

The first objective of the present study was to determine the effect of LIG treatment on transient forebrain ischemic brain injury by an oral administration of LIG. It has been reported that less than 10% of neuronal death was observed in the hippocampal CA1 area after 3 days of reperfusion to 5 min of BCCAO ischemia (Ding et al., 2004), and maturation of brain damage, especially in the hippocampal CA1 region, occurred 6–7 days after reperfusion following a 10-min BCCAO forebrain ischemia (Smith et al., 1984). We observed in the present experiments that about 50% neuronal death developed in the CA1 region after 30 min of forebrain ischemia with 5 days recovery in mice, suggesting that neuronal damage is a function of the ischemic duration. In comparison with the vehicle-treated group, the post-ischemic treatment with LIG showed an excellent dose-dependent protection in the cortical and hippocampal areas. And further semi-quantification of the intact neuronal density in the vulnerable hippocampal CA1 demonstrated that LIG could provide excellent neuroprotective effect at a dose level of 80 mg/kg ( $P < 0.01$  vs. ischemic control group). As the main active constituent of many important medical plants, various pharmacological activities of LIG had been reported as reviewed in chapter 1. The data presented here provided the first experimental evidence about the potential neuroprotective effect of LIG for cerebral ischemia-induced brain injury. In this study, the body temperature of

mice was controlled in a normal range during the experimental procedure and LIG was orally administered after reperfusion. Recent studies demonstrated that intra-ischemic hypothermia resulted in the significant protection in to ischemic brain damage whereas post-ischemic hypothermia was not effective in reducing the lesion size early after ischemia (Pabello et al., 2004). Therefore the potential effects of hypothermia or the improvement in the cortical blood flow, two physiological factors substantially affecting the outcome of ischemic brain injury, should be excluded from the primary mechanism of this compound.

An antioxidant effect may be one of the underlying mechanisms by which LIG protected against ischemia/reperfusion brain injury based on its antioxidant activity in various *in vitro* ROS model. Our previous results showed that LIG was a free radical scavenger capable of reducing DPPH, and inhibiting the lipid peroxidation of linoleic acid and rat brain mitochondria in a dose-dependent manner. Moreover, LIG could promote cell survival and attenuate chromatin condensation and nuclear fragmentation in H<sub>2</sub>O<sub>2</sub>-induced oxidative damage in the C6 cells. Although the precise biochemical process of the interaction between LIG and ROS is not understood, the analyses based on the structure characteristics suggests that active dihydrobenzene and conjugated double bonds are likely to be responsible for the antioxidant properties of LIG. Consistent with its role as an antioxidant *in vitro*, we observed in this study that the treatment of LIG attenuated the increases in the cerebral contents of the lipid peroxidation marker MDA, and restored the tissue levels of SOD and GSHPx

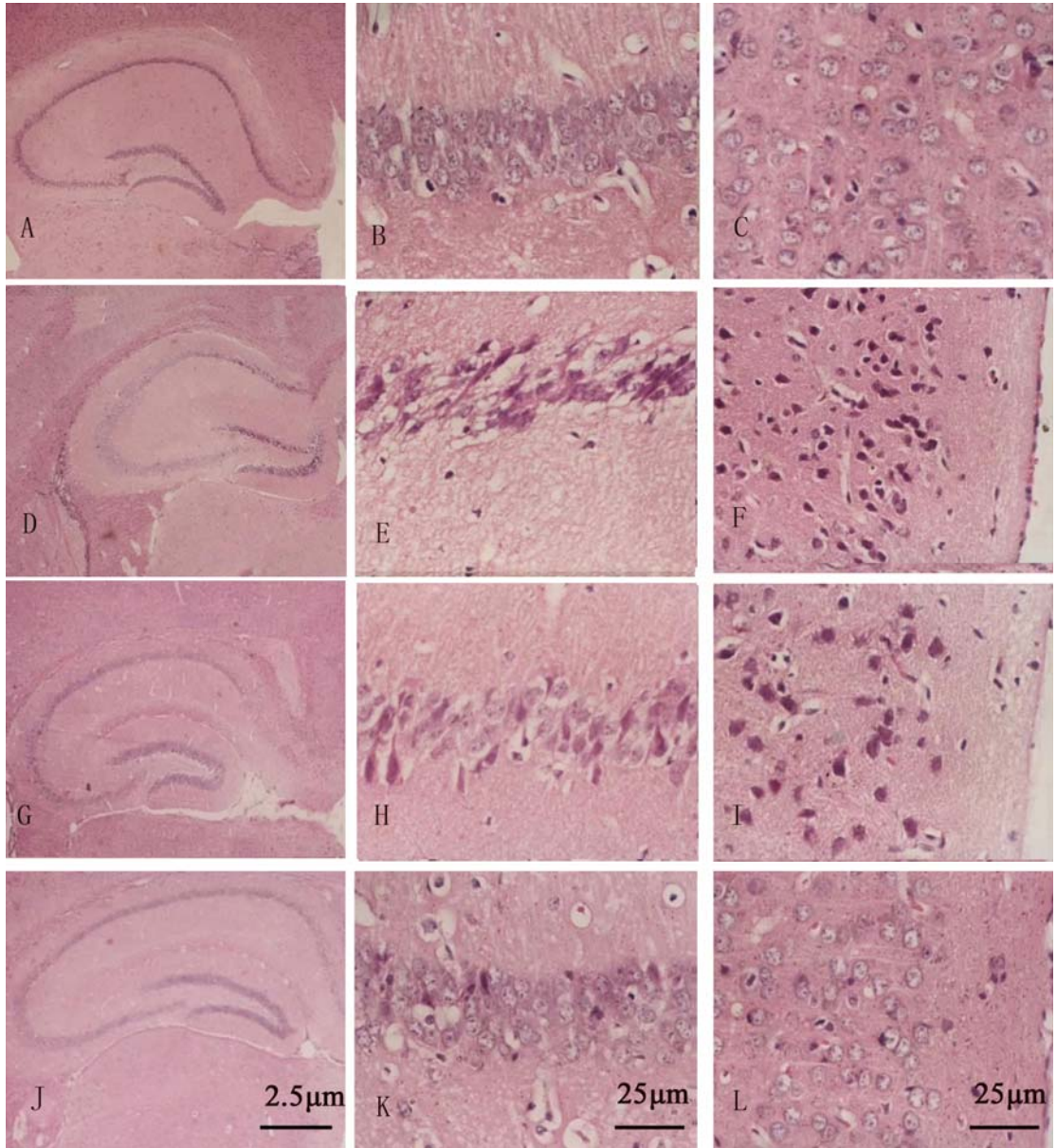
activities in the ischemic brain tissues. As main endogenous antioxidants, SOD can catalyze the dismutation of the superoxide anion, and GSHPx may mediate the breakdown of hydrogen peroxide (Chan, 2001). Therefore, LIG is potentially beneficial for neuronal recovery from ischemic brain injury by increasing the endogenous antioxidant activities and scavenging ROS in the ischemic brain tissues. However, further study is needed to determine whether its effect on the activities of antioxidant enzymes is based on the direct enhancement of the enzymes activities or is just secondary, due to the decreased accumulation of ROS in tissues by LIG, and, consequently, had a decreased consumption of antioxidant enzymes.

Another pharmacological property of LIG that could contribute to its neuroprotective effect in ischemic brain injury is the anti-apoptosis effect. One of the principal findings of this work is that LIG significantly inhibited the mitochondria-dependent caspase apoptosis pathway following transient forebrain cerebral ischemia and apoptosis in the cortical area. Caspases are aspartate-specific cysteine proteases and exist as zymogens in cells. There are two main caspase pathways during the development of apoptosis of cerebral ischemia: the mitochondrial pathway and the death receptor Fas pathway (Benchoua et al., 2001; Benchoua et al., 2002; Cecconi, 1999). The energy-independent Fas pathway, involving the stimulation of the members of the tumor necrosis factor-receptor (TNF-R) super family and the main initiator caspase-8, has been reported to be mainly implicated in the cell death following severe insults, such as the core of focal brain ischemia. The energy-dependent mitochondrial pathway

of apoptosis is mainly involved in mild ischemic insult, and can be initiated by imbalance between antiapoptotic (e.g. Bcl-2) and proapoptotic (e.g. Bax) members of the Bcl-2 family. Studies show that cerebral ischemia induces an up-regulation of Bax expression parallel to a Bcl-2 down-regulation within the ischemic neurons (Isenmann et al., 1998; Krajewski et al., 1995). Bax-like proteins are then translocated from cytoplasm into mitochondria and may rupture the outer mitochondrial membrane or induce the formation of a channel complex for cytochrome c release (Desagher and Martinou, 2000). This complex with a protein apoptotic protease-activating factor-1 (Apaf-1) and together they activate the main caspase initiator procaspase-9 of mitochondrial pathway, which goes on to cleave the down-stream executor procaspase-3, thus initiating the proteolytic cascade involved in apoptosis. In addition, anti-apoptotic Bcl-2 protein localizes predominantly to the outer mitochondrial membrane, which acts on mitochondria with a resultant unopposed action of Bax. Our results showed that LIG increased Bcl-2 expression together with a significant decrease in Bax expression in the ischemic brain tissue. In addition, LIG significantly inhibited the cytosolic cytochrome c release, cleaved caspase-3 expression and caspase-3 activity, the number of TUNEL-positive apoptotic cell and the ladderized feature of DNA fragmentation. These results demonstrated for the first time that LIG could inhibit mitochondria-dependent apoptosis involved in cerebral ischemia. Recent studies have revealed that antioxidants attenuated ischemic neuronal apoptosis by inhibiting the cytochrome c release (Kim et al., 2000; Namura et al., 2001), and the overexpression of SOD-1 reportedly has protective effects against

ischemia–reperfusion injury through blocking the cytosolic release of cytochrome c and reducing apoptosis after cerebral ischemia (Fujimura et al., 2000). These observations are consistent with our results that LIG, a new lipophilic antioxidant, has neuroprotective effect through the antiapoptotic effect in ischemic brain.

In conclusion, LIG shows a potent protection against ischemic brain injury in a murine transient forebrain ischemia model after an oral administration. This neuroprotection of LIG is, at least in part, derived from its antioxidant and antiapoptotic effect through the mitochondria dependent caspase pathway. The present data first suggest that LIG may be a promising therapeutic agent for the potential treatment of cerebral ischemic disorders.



## K

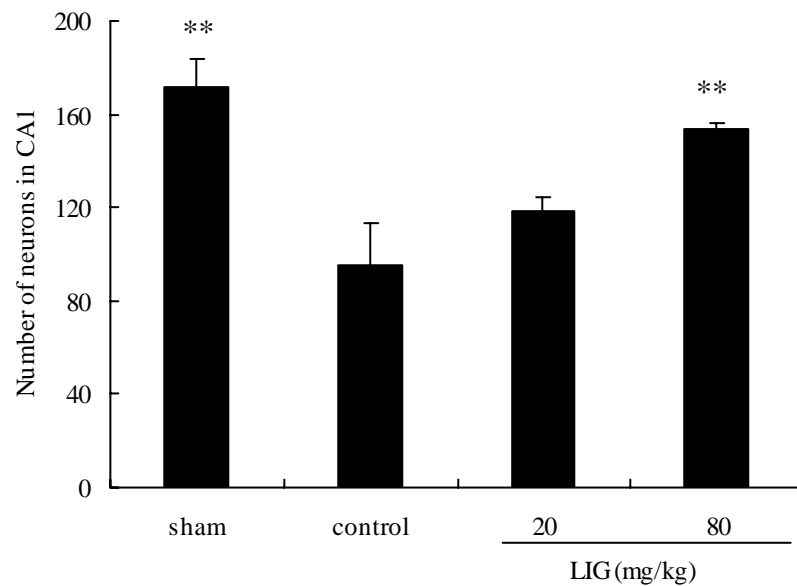
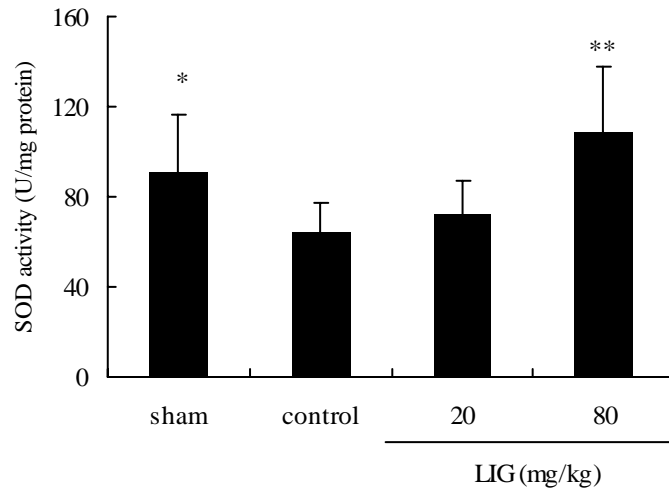
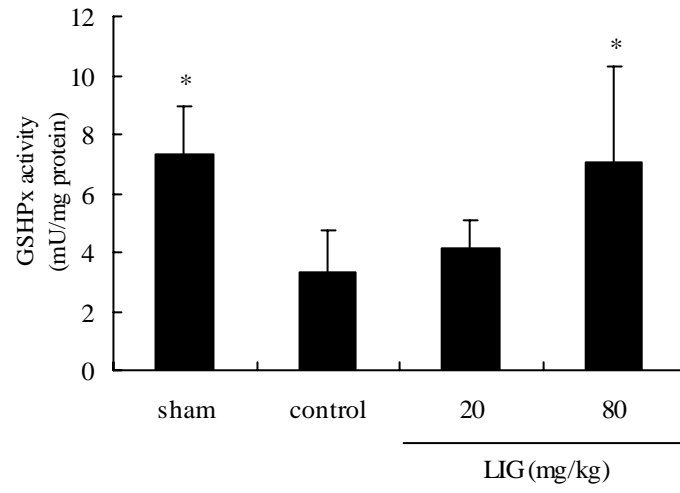


**Figure 5-1.** The effect of LIG to salvage on the cerebral neurons in the forebrain ischemia/reperfusion mice. HE staining was performed as described in Materials and Methods. Animals received the treatment of an orally administrated LIG, or a volume-matched vehicle at the start of reperfusion and again daily in the subsequent 5 days. A-C: the total hippocampal CA1 and the cortex of the sham-operated control, D-F: the total hippocampal CA1 and the cortex of the vehicle-treated ischemic control, G-I: the total hippocampal CA1 and the cortex of 20 mg/kg LIG, H-J: the total hippocampal CA1 and the cortex of 80 mg/kg LIG. Lower panel (K) represents the analyses of normal neurons in a neuronal cell density per 0.5 mm linear length of the CA1 subfield ( $\times 400$  magnification). Results represent the mean  $\pm$  SD of six animals of each group.  $**P < 0.01$  versus the vehicle-treated control group.

**A**



**B**



**C**

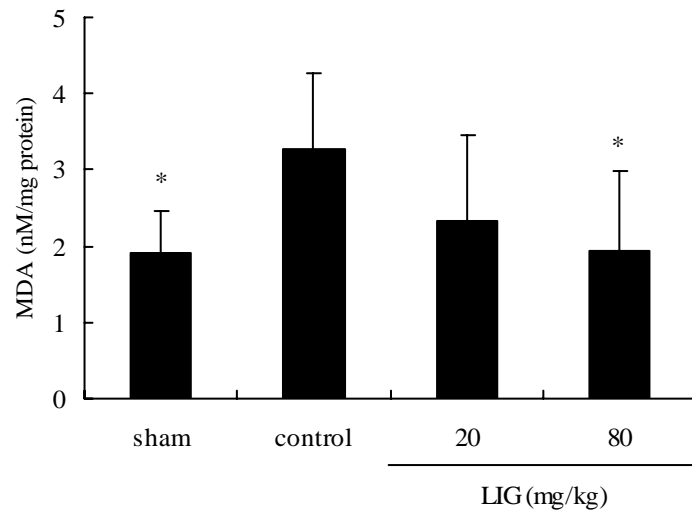


**Figure 5-2.** The antioxidative effects of LIG in the ischemic brain tissue of mice subjected to 30 min of BCCAO/ 5 d reperfusion. The data represent the mean  $\pm$  SD ( $n = 6$ ). Animals received the treatment of the orally administrated LIG, or volume-matched vehicle at the start of reperfusion and again daily in the subsequent 5 days. A. The effect of LIG on the level of SOD of the ischemic brain tissue. B. The effect of LIG on the activity of GSHPx of the ischemic brain tissue. C. The effect of LIG on the MDA content of the ischemic brain tissues. \* $P < 0.05$ , \*\* $P < 0.01$  versus the vehicle-treated control group.

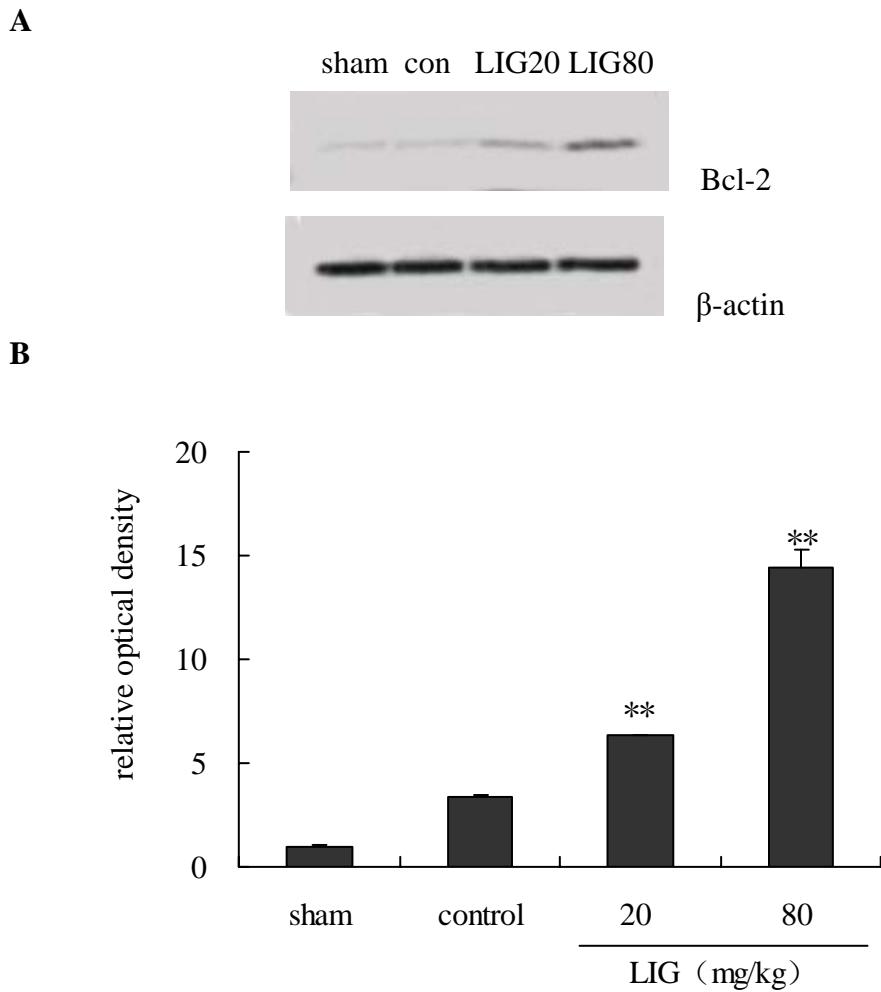
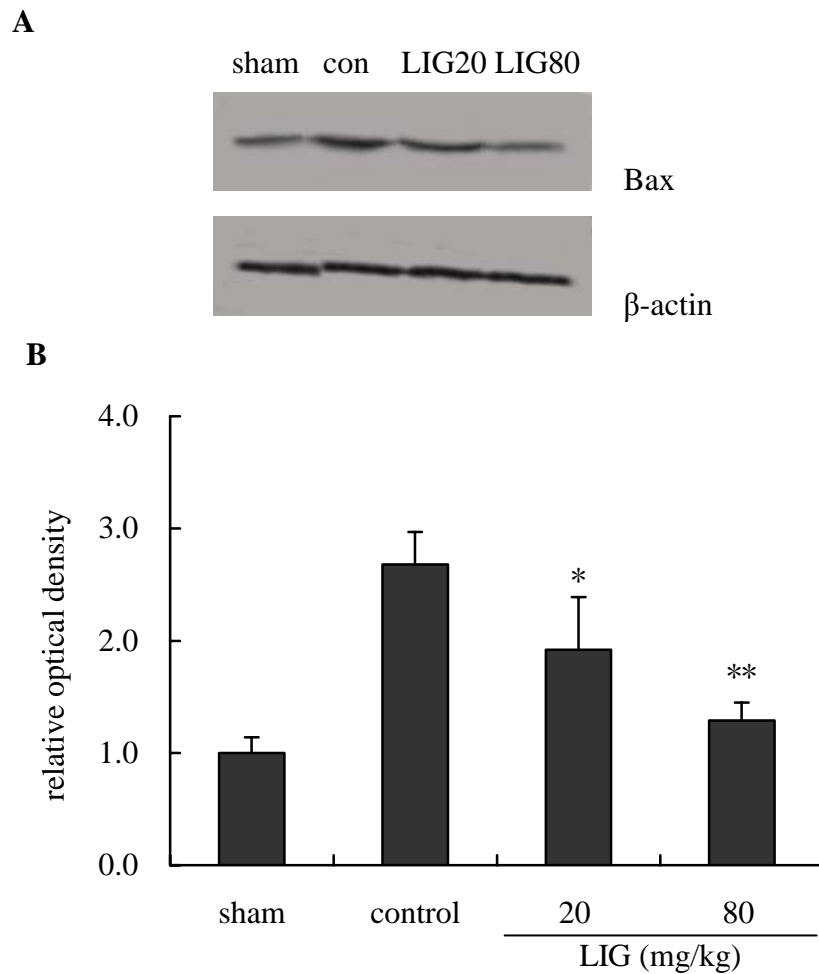
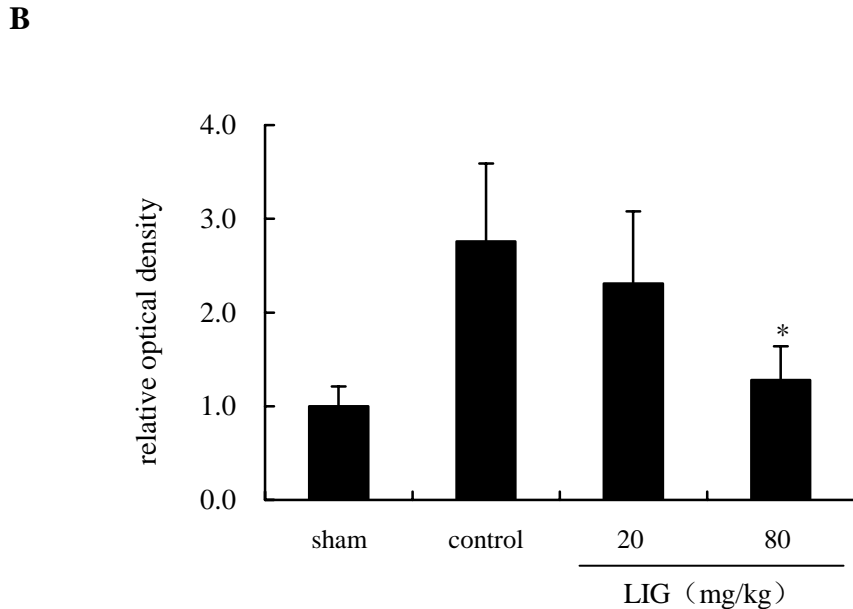
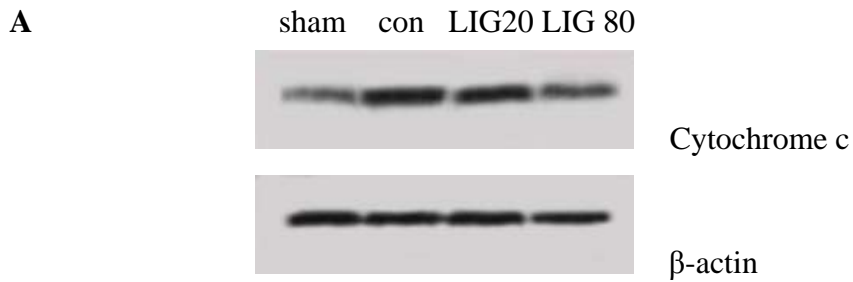


Figure 5-3. Effect of LIG on Bcl-2 expression in the ischemic brain tissues of mice subjected to 30min of BCCAO/5 d reperfusion. Animals received LIG (20 or 80 mg/kg, orally administrated) or a volume-matched vehicle (control) at the start of reperfusion and again daily in subsequent 5 days. Western blot analysis was performed as described in Materials and Methods. A: The expected molecular weight of Bcl-2 ~26 kDa and  $\beta$ -actin ~43 kDa bands appearing on each gel. B: Quantification of the effect of LIG on the expression of Bcl-2 in the ischemia-reperfusion brain. Expression values were normalized for  $\beta$ -actin and expressed as a percentage of sham group. Results are expressed as mean  $\pm$  SD of 3 separate experiments. \*\* $P < 0.01$  versus the control group.



**Figure 5-4.** The effect of LIG on Bax expression in the ischemic brain tissues of mice subjected to 30min of BCCAO/5 d reperfusion. Animals received LIG (20 or 80 mg/kg, orally administrated) or a volume-matched vehicle (control) at the start of reperfusion and again daily in the subsequent 5 days. Western blot analysis was performed as describes in Materials and Methods. A: The expected molecular weight of Bax ~20 kDa and  $\beta$ -actin ~43 kDa bands appearing on each gel. B: Quantification of the effect of LIG on the expression of Bax in the ischemia-reperfusion brain. Expression values were normalized for  $\beta$ -actin and expressed as a percentage of the sham group. Results are expressed as the mean  $\pm$  SD of 3 separate experiments. \* $P$  <0.05, \*\* $P$  <0.01 versus the control group.



**Figure 5-5.** The effect of LIG on the cytosolic cytochrome c expression in the ischemic brain tissue subjected to 30min of BCCAO /5 d of reperfusion. Animals received LIG (20 or 80 mg/kg, orally administrated) or volume-matched vehicle (control) at the start of reperfusion and again daily in the subsequent 5 days. Western blot analysis was performed as describes in Materials and Methods. A: The expected molecular weight of the cytochrome c ~11 kDa and  $\beta$ -actin ~43 kDa bands appearing on each gel. B: Quantification of the effect of LIG on the expression of cytosolic cytochrome c in the ischemia-reperfusion brain. The expression values were normalized for  $\beta$ -actin and expressed as a percentage of the sham group. Results are expressed as the mean  $\pm$  SD of 3 separate experiments. \* $P$  < 0.05 versus the control group.

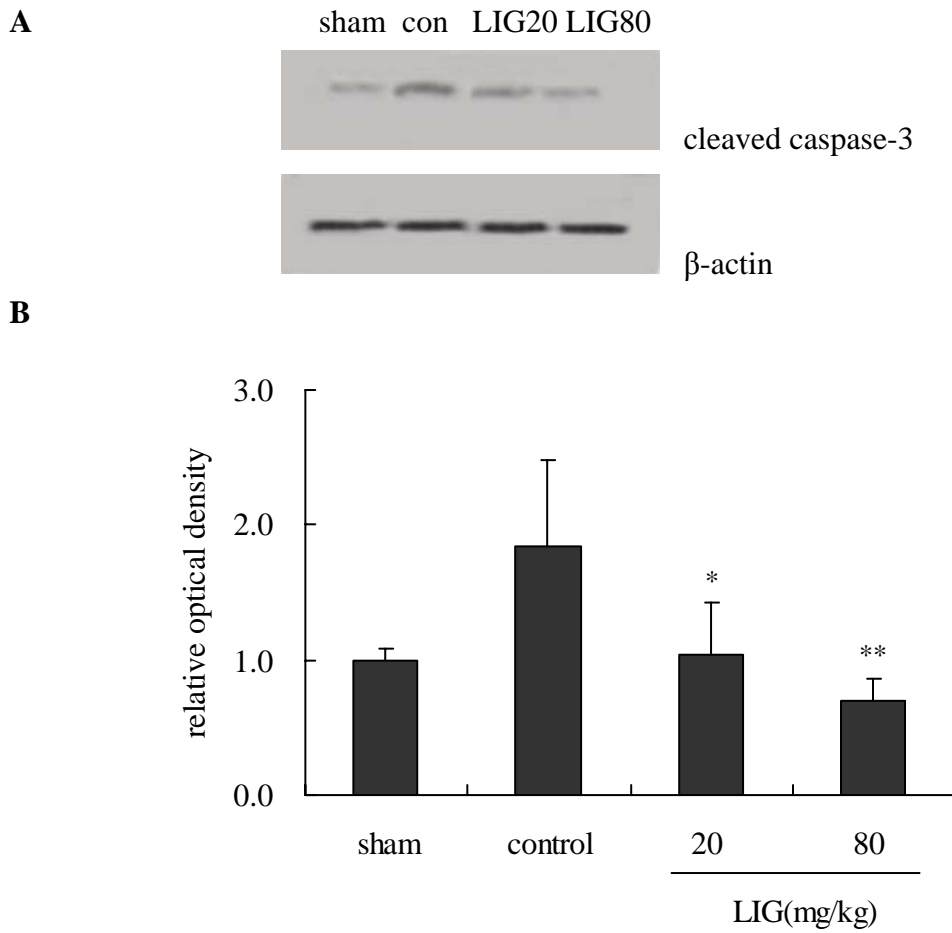


**Figure 5-6.** The effect of LIG on the expression of cleaved caspase-3 in the ischemic brain tissue of mice subjected to 30min of BCCAO /5 d of reperfusion. Animals received LIG (20 or 80 mg/kg, orally administrated) or the volume-matched vehicle (con) at the start of reperfusion and again daily in the subsequent 5 days. Western blot analysis was performed as described in Materials and Methods. A: The expected molecular weight of cleaved caspase-3 ~19 kDa and  $\beta$ -actin ~43 kDa bands appearing on each gel. B: Quantification of the effect of LIG on the expression of cleaved caspase-3 in ischemia-reperfusion brain. Expression values were normalized for  $\beta$ -actin and expressed as a percentage of the sham group. Results are expressed as the mean  $\pm$  SD of 3 separate experiments. \* $P < 0.05$ , \*\* $P < 0.01$  versus the control group.

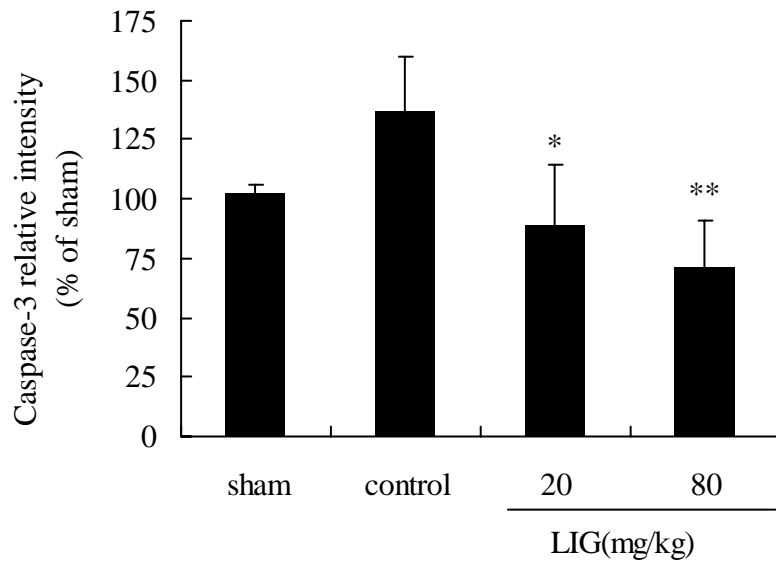
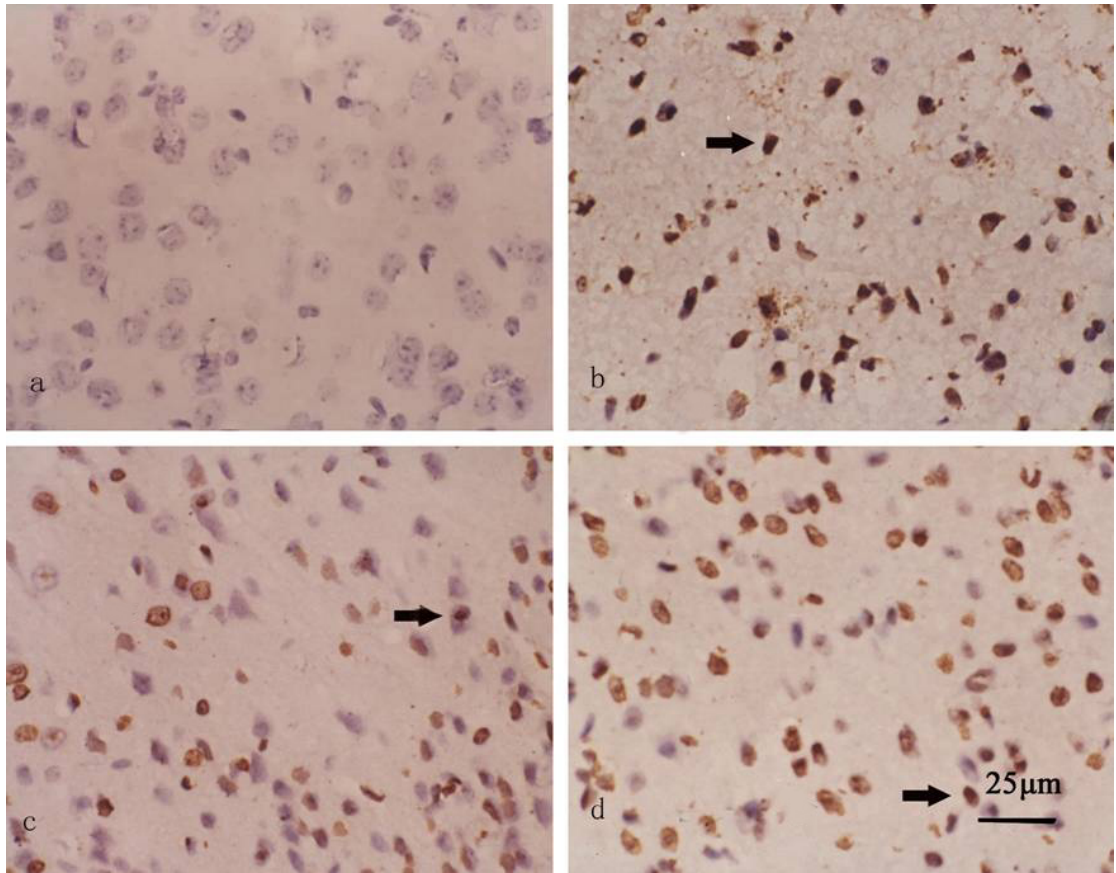


**Figure 5-7.** The inhibition of caspase-3 activity in the ischemic brain tissue by the treatment of LIG on mice subjected to 30 min of BCCAO/5 days reperfusion. Animals received LIG (20 or 80 mg/kg, orally administered) or volume-matched vehicle (control) at the start of reperfusion and again daily in subsequent 5 days. The activity of caspase 3 was measured as described in Materials and Methods. Caspase activity was expressed as the optical density unit percent of the sham-operated control group at 405 nm. Data shown are the mean  $\pm$  SD ( $n = 6$ ). \* $P < 0.05$ , \*\* $P < 0.01$  versus the vehicle-treated control group.

**A**



**B**

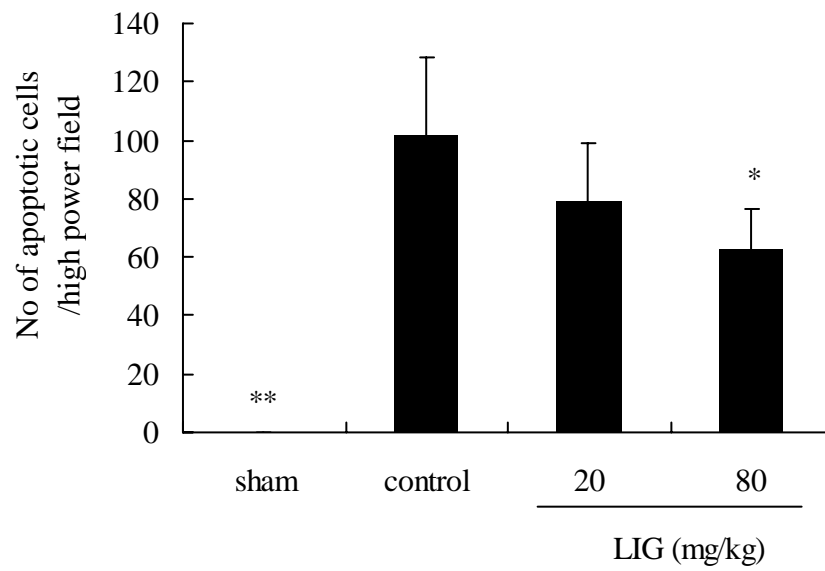
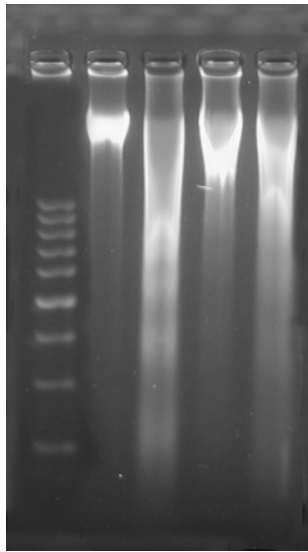


**Figure 5-8.** The effect of LIG on the development of the apoptotic cells in the ischemic cortex of mice subjected to 30 min of BCCAO /5 days of reperfusion. (A) Representative photographs of TUNEL staining in the cerebral cortex. TUNEL-positive apoptotic cells exhibit condensation and fragmentation of nuclei and apoptotic bodies around the nuclear membrane without cytoplasmic staining (arrow). a: sham-operated control, b: vehicle-treated control, c and d: 80 or 20 mg/kg LIG orally administered at the start of reperfusion and the subsequent 5 days. The magnification was 400 ×. (B) Quantification of the apoptotic cells in the ischemic cortex. Results represent the means ± SD of four animals of each group. \* $P < 0.05$ , \*\* $P < 0.01$  versus the vehicle-treated control group.

**A**

M sham con LIG80 LIG20



**B**

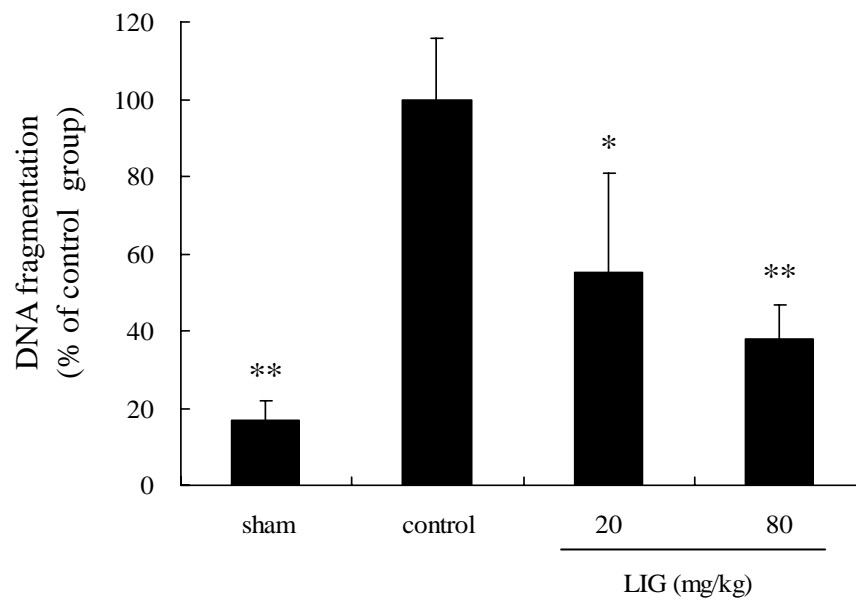


**Figure 5-9.** The effect of LIG on the formation of DNA laddering in the ischemic brain of mice subjected to 30 min of BCCAO/ 5 d reperfusion. The internucleosomal DNA-fragmentation was analysed electrophoretically as described in Methods.

Animals were divided into the sham-operated control (sham), and the vehicle-treated control (con), LIG-treated groups at doses of 20 or 80 mg/kg LIG, orally administered at the start of reperfusion and again daily in subsequent 5 days. M represents the 100-bp DNA ladder marker. A: representative findings of the agarose gel electrophoresis showing DNA laddering. B: The results of densitometric analysis representing mean $\pm$  SD of four animals. \* $P < 0.05$ , \*\* $P < 0.01$  versus the control group.

## **CHAPTER 6**

# **Z-LIGUSTILIDE THERAPY PROTECTS BRAIN AGAINST BOTH APOPTOSIS AND NECROSIS IN FOCAL CEREBRAL ISCHEMIA IN RATS**

### **6.1 ABSTRACT**

Previous studies demonstrated that Z-ligustilide (LIG) showed significant neuroprotective effect in forebrain ischemic injury in mice, which might be associated at least in part with its antioxidant properties and the suppression on the mitochondria-dependent caspase apoptotic mechanism. The transient middle cerebral artery occlusion (MCAO) is generally accepted as the model that most closely duplicates focal ischemic stroke in human patients, in which complex processes involving mixed types of cell death, containing both necrotic and apoptotic cell death, are involved in neuronal death following focal ischemic stroke. Therefore, in the current study, we investigated the potential neuroprotective effect of LIG in focal cerebral ischemia in rats.

Male SD rats weighing 250–300 g were used in this study. Focal cerebral ischemia (2 h) was induced in the anesthetized rats by MCAO with an intra-luminal suture through the internal carotid artery. At the completion of ischemia, the rats were scored and

randomly divided into 3 groups based on the neurobehavioral scores. At 0 and 4 h after 2 h of MCAO, LIG (20 or 80 mg/kg) was orally administered twice. The sham-operated and vehicle-treated control animals received volume-matched vehicle. At 24 h of reperfusion, the rats were scored for neurological deficits again, and then sacrificed. The infarct volume in the brain was assessed by 2,3,5-triphenyl tetrazolium chloride (TTC). Brain sections were immunostained for the expression of OX42. The inducible nitric oxide synthase (iNOS) and cytosolic release of cytochrome c, cleaved caspase-3 and caspase-8 expression were analyzed by immunoblot. The brain tissues of ischemic hemispheres were used to detect the activities of iNOS, caspase-3 and caspase-8 as well as the NO level via colorimetry. The number of apoptotic and necrotic cells were determined by TUNEL staining in the brain sections.

Our results revealed that postischemic treatment with LIG could prevent the development of the infarct volume following the transient MCAO. Twenty-four hours after MCAO, the brain infarct volume was reduced by 70% and 90% following treatment with LIG at the dose levels of 20 or 80 mg/kg, respectively. The reduction in the brain infarct volume in all the LIG-treated groups was accompanied by a significant decrease in the observed neurological deficit ( $P < 0.01$  vs. vehicle-treated control group). Additionally, postischemic treatment with LIG significantly diminished the increase in the number of apoptotic and necrotic cells in the penumbra region ( $P < 0.01$  vs. vehicle-treated group), and necrotic cells in the ischemic core ( $P < 0.05$  vs. vehicle-treated group), whereas there was no statistically difference in the

number of apoptotic cells in the ischemic core between the LIG-treated groups and the vehicle-treated group. The findings of the samples from the ischemic hemisphere, which showed a markedly increased expression of iNOS, cytosolic cytochrome c, cleaved caspase-3 and caspase-8, were significantly reversed by treatment with LIG. In addition, microglial activation was detected by immunohistochemistry at 24 h after ischemia, which was significantly decreased by treatment of LIG ( $P < 0.05$  vs. vehicle-treated group). Consistent with the changes of the above protein expression, the LIG-treated groups also significantly reduced the activities of iNOS, caspase-3 and caspase-8 ( $P < 0.05$  or  $P < 0.01$  at 20 or 80 mg/kg vs. vehicle-treated group, respectively) and the NO level ( $P < 0.05$  at 80 mg/kg vs. vehicle-treated group) in the ischemic hemisphere. These data suggest that LIG significantly attenuates ischemic brain injury in this focal ischemia/reperfusion model. This protective effect may be attributed to the prevention of both necrotic and apoptotic death by suppressing the apoptotic mechanisms, including mitochondrial pathway and death receptor pathway, as well as the activated inflammatory cells-induced inflammatory responses besides its antioxidant action as described in chapter 5.

**KEY WORDS:**

Z-ligustilide, acute stroke, focal cerebral ischemia, neuronal cell death, apoptosis, necrosis, phthalides

## 6.2 INTRODUCTION

Many patients with acute stroke have an area of the severely affected brain tissue, the ischemic core, irreversibly damaged. The brain tissue surrounding the ischemic core, the penumbra, has potential to recover its function under favorable conditions provided by therapeutic intervention. Depending on the occlusion period of the cerebral artery, the ischemic core that shows rapid cell death may enlarge and the penumbral zone that shows gradual cell death may reduce its size. It has been recognized that the ischemic core cells mainly undergo necrosis as well as energy-independent apoptosis because of the marked decrease in energy supply followed by injury in the plasma membranes, whereas the penumbral zone mainly exhibits delayed injury features of energy-dependent apoptosis (Benchoua et al., 2001; Li et al., 1998). Although many different signaling pathways are reported to be involved in apoptosis, in all cases the final pathway resulting in the cell death is the activation of a family of proteases (caspases) (Endres et al., 1998; Harrison et al., 2001; Raff, 1998). It has been shown that caspase-3 is the main apoptotic effector, which can be activated through two major upstream pathways. The first one is via the release of cytochrome c from the mitochondria into the cytoplasm, which consequently binds to procaspase-9 and Apaf-1, and forms an apoptosome. The apoptosome cleaves caspase-9 and the latter further cleaves caspase-3 (Ding et al., 2004; Ferrer and Planas, 2003; Green and Reed, 1998). The second pathway is via the binding of Fas to the Fas-associated death domain, which activates procaspase-8 and further activates

caspase-3 (Northington et al., 2001; Padosch et al., 2003).

In addition, cerebral ischemia induces a marked response of resident microglia and hematopoietic cells, including monocytes and macrophages, and elicits a strong intrinsic inflammatory response in the ischemic area (Clark et al., 1994; Komine-Kobayashi et al., 2004). There is increasing evidence that post-ischemic inflammation contributes to ischemic damage by many mechanisms. Inducible NOS (iNOS), which is not normally present in healthy tissue, can be induced by cytokines in activated brain glial, vascular cells and infiltrating neutrophils following ischemic stress (Marletta, 1993; Samdani et al., 1997). Once expressed, iNOS is continuously active and leads to a long-lasting (several hours to days) NO generation compared to cNOS-dependent NO synthesis, which lasts only a few minutes. Furthermore, the iNOS produces much greater amounts of NO (in micromolar range) than either nNOS or eNOS (picomolar levels) (Ogden and Moore, 1995). Therefore, the toxic amounts of NO produced by iNOS greatly contribute to cerebral ischemia damage. In addition, resident brain glials are also involved in the inflammatory response. Microglial cells are rapidly activated in response to the pathological stimuli, including ischemic insult (Gerhmann et al., 1992). In the early phase of activation the resting microglial cells undergo morphological changes. Four to six hours after ischemia, microglial cells retract their processes and assume an ameboid morphology that is typical of activated microglia (Gerhmann et al., 1992; Komine-Kobayashi et al., 2004). They proliferate and migrate to the site of neuronal damage. The activated microglial cells play a

central role in the in the expansion of ischemic damage by removing the neuronal debris (Mabuchi et al., 2000).

Our previous *in vitro* results showed that LIG was a potent antioxidant in various ROS system, and could protect the cultured cells against H<sub>2</sub>O<sub>2</sub>-induced injury. After treatment with LIG in BCCAO-induced forebrain ischemic model in mice, where apoptosis was the main cell death process, the neuroprotective effect of LIG has been demonstrated to be at least in part due to its antioxidant and anti-apoptotic mechanisms. In stroke patients, spontaneous recanalization often occurs within hours or days after the initial occlusion and often induces this reperfusion injury. Moreover, the restoration of blood flow with tissue-plasminogen activator (t-PA) in the acute phase proves to be an effective strategy for treating ischemic stroke in clinic, which also faces the potential risk of inducing reperfusion injury. Therefore, transient cerebral ischemia induced by MCAO is generally regarded as one of the most common models of cerebral stroke, in which the middle cerebral artery is occluded, resulting in damage to the cerebral cortex and striatum in that hemisphere (Longa et al., 1989). In the current study, we investigated the mode of neuroprotective action of LIG in transient MCAO ischemic rats with special attention to the apoptosis pathways and the inflammatory response leading to cell death.

### **6.3 Materials and Methods**

### **6.3.1 Materials**

#### **6.3.1.1 Chemicals**

Unless otherwise stated, all chemicals were obtained from Sigma chemical company, St. Louis, MO, USA. Agarose, Tris, ethidium bromide and prestained protein marker were purchased from Bio-Rad Laboratories, Hercules, CA, USA. ECL Western blotting analysis system was from Amersham Biosciences, England. The monoclonal antibodies against cytochrome c and polyclonal antibody against caspase-8 were obtained from Santa Cruz Biotechnology (Santa Cruz, CA, USA). The monoclonal antibody against OX42 was from Serotec (Oxford, UK). The polyclonal antibody against cleaved caspase-3 was from Cell Signaling technology, Inc. Beverly, MA, USA. The kit of *in situ* Cell Death Detection, POD, was purchased from Roche, Mannheim, Germany. The ABC Reagent and DBA kit were from VECTOR, Burlingame, USA. The kits of iNOS activity and NO content assay were from Jianchen Bioengineering Co, Nanjing, China. The kits of caspase-8 (KGA312) and caspase-3 (KGA210) activity assay were purchased from KeyGen Biotech corporation limited, Nanjing, China.

#### **6.3.1.2 Animal Preparation**

Male SD rats weighing 220–250 g (8 weeks old) were obtained from the Experimental

Animal Center of the Guangzhou Chinese Medical University (Guangzhou, China). Animals were housed in stainless steel cages (three rats per cage), and given distilled water and laboratory chow (PMI, Brentwood, MO.Catalog# 5001) ad libitum. Rats were maintained under controlled conditions with temperature at  $20 \pm 1$  °C, relative humidity at  $55 \pm 15\%$  and a 12-h lighting cycle (08:00 – 20:00 h). Rats were used in experiments following adjustment to these conditions for at least 1 week, and were fasted overnight before experiments but had free access to water. Animal care was in compliance with the Chinese regulations on protection of animals used for experimental and other scientific purposes.

### **6.3.1.3 Drug Preparation**

LIG (purity > 98 %) was prepared from our own laboratory and stored at  $-20$  °C. Before the application, LIG was diluted into 2 and 8 mg/ml with 3% Tween-80. Rats were orally administrated a drug solution in a dose of 20 or 80 mg/kg, or a volume-matched vehicle.

## **6.3.2 Methods**

### **6.3.2.1 Focal Cerebral Ischemia Model**

The focal ischemia model of rat was induced by the occlusion of middle cerebral

artery (MCAO) for 2 h and reperfusion for 24 h. The operation of MCAO was improved based on Longa et al. (Longa et al., 1989). SD rats were anesthetized through the intraperitoneal injection of chloral hydrate (300 mg/kg). Core body temperatures were monitored and maintained at  $37 \pm 0.5$  °C with a feedback-regulated heating pad. The left common carotid artery (CCA) and the left external carotid artery were exposed by means of a midline neck incision. The distal CCA, the external carotid artery and the pterygopalatine artery were ligated with a 4-0 suture. A 4-0 monofilament nylon suture (its tip coated with poly-lysine) was placed into a guide sheath (30 mm in length) and inserted through arteriotomy of the CCA and then gently advanced into the internal carotid artery to a point of 17 mm distal to the carotid bifurcation. Mild resistance to the advancement indicated that the monofilament had entered the anterior cerebral artery, occluding the origin of the MCA. To establish reperfusion after 2 h, the guide sheath and the suture were removed. The CCA was then ligated distal to the arteriotomy. Finally, the neck incision was closed by suturing. Sham rats underwent the entire initial surgical procedure with the insertion of the filament into the internal carotid artery, but the filament was not advanced to occlude the MCA. It was completely withdrawn 2 h after insertion, i.e. the procedures were similar to those followed in animals subjected to the MCA occlusion.

### **6.3.2.2 Neurological Deficit Scores**

The neurological status of each rat after 2 h of MCAO/ 24 h of perfusion was blindly

evaluated according to the neurological examination grading system described previously (Bederson et al., 1986b; Menzies et al., 1992). A scale of 0 to 4 was used to assess the motor and behavioral changes after 2 h MCAO. This test consisted of the following maneuvers: the rats were suspended from the tail approximately 30 cm above the floor and their forelimb posture was noted. Normal animals extended both forelimbs toward the floor and were assigned a score of 0. When the forelimb contralateral to the side of the MCAO was consistently flexed during the suspension and there was no other abnormality, the rat was scored 1. The rats were then placed on the absorbent pads and they were gently held by the tail. If the animals showed an apparent decrease in grip in the contralateral forelimb when pulled by the tail, then they were assigned a score of 2. Thereafter and while still being held by the tail, the rats were allowed to move freely and observed for circling behavior. Rats that moved spontaneously in all directions but established a monodirectional circling toward the paretic side when given a slight jerk of the tail were scored 3. Rats that showed a consistent spontaneous contralateral circling were scored 4. Animals that showed a higher clinical score also showed all features of the lower grades. This neurological evaluation was completed within a few minutes.

All animals showing grade 0-3 were excluded from this study. The grade 4 animals, i.e. those showing consistent circling clockwise were the majority, constituting about 90% of the animals originally subjected to MCAO. The neurological status of the ischemia-reperfusion rats was blindly estimated after a 2-h occlusion and then a 24-h

reperfusion.

### **6.3.2.3 Experimental Treatment Schedule**

After 2 h of MCA occlusion, the animals were randomly allocated to the following experimental groups (n = 14 – 16 per group) based on the neurological scores: the sham operation group, the control group, the LIG low dose group and high dose group. At the start and again at 4 h of reperfusion after 2 h of focal ischemia, the rats received an oral administration of LIG (20 or 80 mg/kg) or volume-matched vehicle. The administrated volume was kept constant at 10 ml/kg.

### **6.3.2.4 Measurement of Body Temperature**

It was reported that the temperature in the brain was 0.5 °C lower than the rectal temperature and the brain temperature was well correlated with the core body temperature (Noor et al., 2003). Since the insertion of a temperature probe may result in a physical injury to the brain which would confound our infarct volume measurements, we therefore elected to use rectal temperature and correlated it to the resultant brain temperature.

Core body temperature was measured in the conscious rats prior to anesthesia using a rectal probe (Electronic Temperature Monitor DT-02C rectal probe; Huang Zhou

Hua-An Instruments Inc., Huang Zhou, Zhei Jiang, China). The probe was inserted 3.5 cm and it took approximately 5 sec to reach a stable temperature. During the 2 h intra-ischemic period, body temperature was sustained at 37 °C in the transient MCAO rats. In order to examine the effect of LIG on the postischemic temperature following a 2 h ischemia, body temperature was monitored in the conscious rats at 1, 5, and 24 h after reperfusion, respectively, while LIG was orally administrated at the start of reperfusion and again at 4 h of reperfusion.

#### **6.3.2.5 Estimation of Ischemic Infarction Size**

Triphenyltetrazolium chloride (TTC) staining is used to quantify experimental brain infarction (Bederson et al., 1986a; Belayev et al., 1999). At 24 h of reperfusion following 2 h of MCAO, the animals were reanesthetized through the intraperitoneal injection of chloral hydrate (300 mg/kg) and received intracardiac perfusion with 0.9% normal saline. For morphometric study, the brain was then quickly removed, frozen by suspension over liquid nitrogen to slightly harden the tissue, and cut into 2-mm thick coronal sections by a tissue slicer onto an ice-cold plate. The distances of the infarct rims from the midline were determined on the brain slices from the coronal block of samples. The brains were sectioned at bregma levels +4.7, +2.7, +0.7, -1.3, -3.3, -5.3 and -7.3 mm (seven sections). The sections were placed in a 2% solution of TTC in normal saline at 37 °C for 30 min in dark and then fixed in 10% phosphated-buffered formalin at 4 °C overnight. The caudal sides of all the TTC-stained section were

scanned using a color flatbed scanner, and the infarct areas from each brain section was measured using Pro-plus 4.5 image analyses software (Image J, Bethesda, MD, UAS). The total volume of infarction was calculated from the sum of the infarct areas (seven sections in all)  $\times$  thickness (2 mm). The infarct volume was expressed as a percentage of the total volume to the ipsilateral hemisphere.

#### **6.3.2.6 Brain Tissue Preparation**

##### **(1) Brain Tissue Preparation for Analyses of Enzyme Activity and Western blot**

At 24 h of reperfusion, the animals were reanesthetized through the intraperitoneal injection of chloral hydrate (400 mg/kg) and received intracardiac perfusion with 100 ml of phosphate-buffered saline (pH 7.2). The brain was then quickly removed, frozen by suspension over liquid nitrogen, and cut into two hemispheres or 2-mm thick coronal sections. The section 3 and section 4 were then stored at  $-80^{\circ}\text{C}$  until used.

##### **(2) Brain Tissue Preparation for Histochemistry**

At 24 h of reperfusion, the animals were reanesthetized through the intraperitoneal injection of chloral hydrate (400 mg/kg) and received intracardiac perfusion with 100 ml of phosphate-buffered saline and followed by 100 ml of 4% paraformaldehyde in phosphate-buffered saline (pH 7.4). The brain was removed, postfixed 24 h in the same fixative solution, and cut into 2-mm thick coronal sections. The section 3 was then embedded in paraffin and the section 4 stored in liquid nitrogen until used.

The distances of the infarct rims from the midline were determined on the slices of the coronal blocks of samples dissected for measurement of the intact areas. The region of the lateral cortex between 3- and 4- mm distance from the midline of the coronal section 4, which falls within the border of the infarction in the vehicle-treated animals, was spared in the LIG-treated animals and can be considered part of the ischemic penumbra (Fig 6-1). Ischemic core was defined as the infarct region of the lateral cortex in both the vehicle- and LIG-treated animals.

#### **6.3.2.7 Western Blot Analyses**

The coronal section 3 (at bregma level +0.7 to -1.3 mm) of ischemic ipsilateral hemisphere was used for Western blot assays.

##### **(1) Cytosolic Protein Extraction**

The stored tissue was put into 10 times volume of lysis buffer containing 20 mM HEPES-KOH, pH 7.5, 10 mM KCl, 1.5 mM MgCl<sub>2</sub>, 1 mM Na-EDTA, 1 mM Na-EGTA, 1 mM dithiothreitol, and 1 mM PMSF and, 250 mM sucrose and then centrifuged at 750×g for 10 min at 4 °C. The harvested supernatant was again centrifuged at 10,000×g for 10 min at 4 °C, and the supernatant was collected and stored at -20 °C until used.

## **(2) Protein Concentration Determination**

Please refer to chapter 2.

## **(3) Western Blot Analyses**

Forty micrograms protein were diluted in 2×sample buffer (50 mM Tris, pH 6.8, 2% SDS, 10% glycerol, 0.1% bromophenol blue, and 5% β-mercaptoethanol). After heated for 5 min at 95 °C, the samples were loaded into a 15% SDS-polyacrylamide gel for cytochrome c, cleaved caspase 3 and 8 or 7.5% gel for iNOS, which were subsequently transferred to the polyvinylidene difluoride membrane (Amersham Biosciences, England). Membranes were blocked with 5% blocking reagent (Amersham Biosciences, England) in TBS-T for 2 h at room temperature or overnight at 4 °C. The membrane was rinsed in three changes of TBS-T, incubated once for 15 min and twice for 5 min in a fresh washing buffer, and then incubated with the primary antibody for 2 h at room temperature or overnight at 4 °C. The concentrations of primary antibodies for blotting are goat anti-caspase-8 polyclonal (1:100, Santa Cruz Biotechnology, CA; recognizes both pro- and cleaved caspase-8), rabbit anti-caspase-3 polyclonal (1:1000, Cell Signaling technology, recognizes cleaved caspase-3), mouse anti-cytochrome c monoclonal antibody (1:500, Santa Cruz Biotechnology, CA), and mouse anti-iNOS monoclonal antibody (1: 2500, BD Biosciences Pharmingen, USA). After three washes in the washing buffer, the membrane was incubated for 2 h in a horseradish peroxidase-conjugated anti-goat secondary antibody (1:5000, Santa Cruz Biotechnology, CA), or horseradish

peroxidase-conjugated anti-rabbit secondary antibody (1:5000, Santa Cruz Biotechnology, CA), horseradish peroxidase-conjugated anti-mouse secondary antibody (1:2000, Amersham Biosciences, England) and developed using enhanced chemiluminescence (ECL western blotting analysis system kit, Amersham Biosciences, England). The blot was exposed to XOMAT AR films (Eastman Kodak, Rochester, NY). The films were scanned on a UMAX PowerLook Scanner (UMAX Technologies, Fremont, CA, USA) using Photoshop 5.0 software (Adobe Systems, Seattle, WA, USA), and the optical density of each band was determined using Gel-pro Analyzer software (Media Cybernetics, Silver Spring, MD, USA). To ensure even loading of the samples, the same membrane was probed with the mouse anti- $\beta$ -actin monoclonal (Sigma-Aldrich, MO) at 1:5000 dilutions. The specific band is normalized with  $\beta$ -actin and expressed as a percentage of the normal level in the sham-operated group.

#### **6.3.2.8 Caspase-like Activity Assay**

The coronal section 4 (at bregma level  $-1.3$  mm to  $-3.3$  mm) was used for the determination of the enzyme activity. Caspase-8 and Caspase-3 activities were measured using colorimetric assay kits essentially according to the manufacturer's instruction (KeyGen Biotech corporation limited, Nanjing, China). This assay was based on the ability of the active enzyme to cleave the chromophore from the caspase substrate. Fifty micrograms of cytosolic protein were diluted in  $50$   $\mu$ l of lysis buffer,

added to 50 µl reaction buffer, and transferred to a 96 well flat-bottom microplate. To each reaction well, 5 µl of caspase 8 colorimetric substrate (IETD-*p*NA) or caspase 3 colorimetric substrate (DEVD-*p*NA) were added. The plate was incubated for 4 h at 37 °C. Levels of released *p*-nitroanilide (*p*NA) were evaluated by measuring optical density at 405 nm with a Model 550 microplate reader (Bio-Rad Lab., Hercules, CA, USA). Caspase-like activities were expressed as the percentage of the optical density unit of the sham-operated control group.

#### **6.3.2.9 Immunohistochemical Examination**

The frozen sections obtained at the level of bregma –1.3 to –3.3 mm (section 4) were subjected to XO42 immunohistochemical analysis. The immunohistochemical procedure was carried out using a labeled streptavidin-biotin technique. The frozen slices (10 µm) were obtained on a freezing microtome (Leica, Germany) and placed on APES-coated slides. The slides were washed in PBS and reacted with 0.3% H<sub>2</sub>O<sub>2</sub> in methanol to quench any endogenous peroxidase activity for 20 min. After washing, the sections were blocked with 5% normal goat serum containing 0.3% Triton-X-100 for 20 min at room temperature to block the non-specific binding of antibodies. After incubation with the primary mouse anti-OX42 monoclonal antibody (Serotec, Oxford, UK) at a dilution of 1:100 in PBS 30 min at 37 °C, and then overnight at 4 °C, the sections were washed three times and incubated with the biotinylated anti-mouse secondary antibody at a dilution of 1:200 for 1 h at room temperature. After three

rinses in PBS, the sections were incubated with ABC Reagent (VECTOR, Burlingame, USA) for 60 min at 37°C, and incubated with DAB (0.5mg/ml) and 3% H<sub>2</sub>O<sub>2</sub>. Finally the sections were counterstained with hematoxylin. For each case, 0.01 M PBS was used as a substitute for the primary antibody for the negative control groups. No positive staining was seen in any of these control sections. Quantitative determination of the number of OX42 positive cells in the penumbra of focal ischemia was respectively made on anatomically-matched sections for each group. Six randomly-selected microscopic fields (× 400 magnification) were analyzed from two matched slides for each animal, and expressed as the number/high power field.

#### **6.3.2.10 NO Content Measurement**

The NO content was measured according to a commercially available kit (Jianchen Bioengineering Co, Nanjing, China). This assay was based on a nitrite measurement, an indicator of NO production, by Griess reaction (Green et al., 1982). NO, once released, is rapidly converted to nitrite and nitrate in the aqueous medium. The ratio of the nitrate and nitrite concentrations may vary substantially on the biological fluids and tissues. Because the Griess reagent does not react with nitrate, nitrate must be converted to nitrite by incubation with nitrate reductase and nicotinamide adenine dinucleotide at room temperature. Nitrite can react with color reagents, and then the absorbance of the solution was measured at 540 nm. Changes of the absorbance at 540 nm were calculated by subtracting the average absorbance value of the blank wells,

and NO concentration was determined on the basis of NO standard curve.

The ipsilateral hemispheres were homogenated in normal saline (1:9, w/v) at 4 °C, and centrifuged at 4000×g for 20 min. The NO level in the supernatant was measured spectrophotometrically at 540 nm according to the manufacturer's introduction. Nitrite concentrations were calculated by regression analysis of a standard curve using sodium nitrite as a standard and expressed as μM per milligram protein. Protein concentration in the sample was determined by the method of Bradford.

#### **6.3.2.11 Determination of iNOS Activity**

The enzyme activity of iNOS was measured according to a commercially available kit (Jianchen Bioengineering Co, Nanjing, China). This assay was based on the oxidation of oxyhaemoglobin to methaemoglobin by NO in the Ca<sup>2+</sup>-free reaction mixture (Knowles et al., 1990). The ipsilateral hemispheres were homogenated in normal saline (1:9, w/v) at 4 °C, and centrifuged at 4000×g for 20 min. iNOS activity in the supernatants was measured spectrophotometrically at 530 nm according to the manufacturer's introduction, and one enzyme unit was expressed as 1 nM of NO formed in 1 min per one milligram protein. Protein concentration in the sample was determined by the method of Bradford.

#### **6.3.2.12 TUNEL Staining**

### **(1) TUNEL Staining Procedure**

Please refer to chapter 5.3.2.10.

### **(2) Analyses of TUNEL Staining**

The TUNEL-positive apoptotic cells were defined as showing a condensation and fragmentation of nuclei and apoptotic bodies around the nuclear membrane without the cytoplasmic staining. Other TUNEL-positive cells were weakly labeled, showing a diffused cytoplasmic staining and a lack of nuclear condensation, and were considered to be necrotic cells. Quantitative determinations of the intact cells, apoptotic and necrotic cells in the penumbra or core region of focal ischemia were respectively made on anatomically-matched sections for each group (Charriaut-Marlangue and Ben-Ari, 1995; Charriaut-Marlangue et al., 1996a; Charriaut-Marlangue et al., 1996b; Furuichi et al., 2004; Gavrieli et al., 1992). Six randomly-selected microscopic fields ( $\times 400$  magnification) were analyzed from two matched slides for each animal, and expressed as number/high power field.

### **6.3.2.13 Statistical Analysis**

The statistical analysis were performed using SPSS 10.0. Data are presented as the mean  $\pm$  SD. The difference between the means was determined by One-Way ANOVA followed by a Student-Newman-Keuls test for multiple comparisons. Differences with

$P < 0.05$  are considered significant.

## **6.4 RESULTS**

### **6.4.1 Infarction Size in Ischemic Rats (Fig 6-2, Fig 6-3)**

At 24 h of reperfusion following 2 h of ischemia, all rats treated with the vehicle solution developed obviously visible infarctions in the territory supplied by the MCA, which were mainly located in the cerebral cortex and the striatum as a distinct pale-stained area. The percentage of the infarct volume of ipsilateral hemisphere was  $46.3 \pm 7.1\%$ , which was drastically attenuated by post-ischemic treatment with LIG (Fig 6-2). After two oral administrations of 20 or 80 mg/kg LIG at 0 and 4 h of reperfusion following 2 h of ischemia, the infarction development areas were dose-dependently and significantly prevented, and the percent of the infarct volume were reduced to  $13.0 \pm 4.3\%$  and  $4.5 \pm 3.8\%$ , respectively ( $P < 0.01$ , Fig 6-3).

### **6.4.2 Body Temperature Changes following Transient MCAO (Fig 6-4)**

Since hypothermia had been shown to ameliorate ischemic brain injury, the modulation of LIG was evaluated to determine its effect on postischemic temperature and whether this contributes to the neuroprotection of LIG in cerebral ischemia. As shown in Fig. 6-3, the core body temperature at baseline prior to anesthesia between the vehicle- or LIG-treated groups appeared to have no significant differences ( $P > 0.05$ ). In the vehicle-treated group during the 24 h reperfusion following ischemia, the

body temperature showed slight hyperthermia with about an 1 °C increase compared with the baseline level whereas postischemic treatment with 20 or 80 mg/kg LIG caused body temperature to return to near the baseline but did not induce hypothermia.

#### **6.4.3 Neurological Deficit Scores (Fig 6-5)**

To detect the effect of LIG on the neurological function in the transient focal cerebral ischemia rats, the neurological deficit scores were evaluated for each group before and after the treatment of LIG. In this present study, all rats showed normal postural reflex (score = 0) before intervention. None of the sham-operated animals showed any motor-behavioral abnormalities as described in the neurological examination grading system (Fig. 6-5). At 2 h MCAO, the rats scored 4, i.e. those showing a consistent circling clockwise, constituted the majority of the operated animals. The grade 4 rats were randomly treated with orally administrated LIG (20 or 80 mg/kg) or a volume-matched vehicle at 0 h and 4 h of reperfusion. By the reevaluation after the 24 h reperfusion, early neurological abnormalities almost persisted in the animals of the vehicle-treated group. However, all LIG-treated rats significantly attenuated the motor-behavioral abnormalities ( $P < 0.01$ , vs. vehicle-treated group, Fig. 6-5). After the treatment of LIG, the neurological scores were decreased to  $1.92 \pm 0.69$  and  $1.29 \pm 0.73$  at the doses of 20 or 80 mg/kg LIG, respectively. The results of the behavioral deficits conformed to the change in the ischemic infarction volumes in the ipsilateral hemisphere (Fig. 6-4, Fig. 6-5).

#### **6.4.4 Cytosolic Release of Cytochrome C (Fig 6-6)**

To test the effect of LIG on the cytosolic cytochrome c release in focal cerebral ischemia, Western blot analyses were used for the cytosolic cytochrome c expression of the ipsilateral brain tissues. As shown in Figure 6.6, brain samples obtained from the sham-operated control rats showed traces of cytochrome c protein level (relative density = 1). Samples obtained from the ipsilateral hemisphere of rats subjected to 2 h MCAO/24 h reperfusion revealed an over 3.5-fold increases in cytosolic cytochrome c expression, which were dose-dependently reduced to a  $3.14 \pm 0.52$  or  $2.43 \pm 0.83$  relative density by treatment with 20 or 80 mg/kg LIG, respectively. As compared with the ischemic control rats ( $4.45 \pm 0.21$ ), 80 mg/kg LIG significantly inhibited the cytochrome c release from mitochondria in focal cerebral ischemia ( $P < 0.01$ ).

#### **6.4.5 Activation of Caspase-3 and Caspase-8 (Fig 6-7, Fig 6-8, Fig 6-9)**

To elucidate the neuroprotective mechanism of LIG in MCAO rats, cleaved caspase 3 and caspase 8 expression of the ipsilateral hemisphere of brain were assayed. As shown in Fig 6-7 and Fig 6-8, brain samples obtained from the sham-operated control rats showed a weak expression of cleaved caspase 8 and caspase 3, which were significant increased by a 2 h focal ischemia. The treatment with LIG significantly decreased the expression of the cleaved caspase 3 and caspase 8 ( $P < 0.05$  or  $P < 0.01$  at dose of 20 or 80 mg/kg, respectively).

To further confirm the effects of LIG on the caspase enzymes, the activities of caspase 3 and caspase 8 were assayed. As shown in Figure 6-9, brain samples obtained from the sham-operated control rats showed low caspase 3 and caspase 8 activities. Samples obtained from the ipsilateral hemisphere of MCAO rats subjected to 2 h of ischemia/24 of reperfusion revealed an over 3-fold increase in the caspase 3 activity and an over 5-fold increase in the caspase 8 activity, which were significantly and dose dependently inhibited by treatment with 20 or 80 mg/kg LIG ( $P < 0.01$ ). Taken together, LIG could significantly inhibit the activation of caspase 8 and caspase 3 after focal cerebral ischemia.

#### **6.4.6 Induction of iNOS (Fig 6-10, Fig 6-11, Fig 6-12)**

To understand whether the neuroprotection of LIG was involved in the iNOS-derived NO mechanism in focal stroke, the effect of LIG was studied on the iNOS expression and activity in MCAO/reperfusion rats. As shown in Fig 6-10, the results showed that the expression of iNOS were weakly detected by immunoblot in the brain tissues from the sham-operated group, and the enzyme activity of iNOS was also very low (Fig 6-11). At 24 h reperfusion after 2 h MCAO, a significant expression of iNOS was observed in vehicle-treated group, and iNOS activity was greatly increased to about 4 - fold in the vehicle-treated control group as the sham-operated group (Fig 6-11). Treatment of rats with LIG dose-dependently and significantly suppressed iNOS expression (80 mg/kg vs. vehicle-treated group), and also enzyme activity ( $P < 0.05$  or

$P < 0.01$  at 20 or 80 mg/kg vs. vehicle-treated group, respectively).

To further confirm the effect of LIG on iNOS/NO pathway, the content of NO, the product-catalyzed by NOS, was assayed by the Griess reaction. As shown in Fig 6-12, NO content in the sham-operated group was in a low level whereas that of the ipsilateral ischemic hemisphere was significantly increased in the vehicle-treated animals ( $P < 0.01$ ), which was dose-dependently reduced by the oral administration of LIG (Fig 6-9). As compared to the vehicle-treated group, LIG at the dose level of 80 mg/kg significantly reduced NO content ( $P < 0.05$ ).

These results suggested that the suppression of NO production by LIG might be due to both the suppression of iNOS protein expression and the direct inhibition of iNOS enzyme activity. The present study indicated that LIG could attenuate the inflammatory responses involving the iNOS-derived NO mechanism in focal brain ischemia.

#### **6.4.7 Activation of Microglia (Fig. 6-13)**

To further evaluate the effect of LIG on inflammatory responses in ischemia-reperfusion, an immunohistochemical study was carried out using OX42 as a maker of activated microglia. No intense immunoreactive cells were observed in the nonischemic cerebral cortex of the sham-operated control group.

OX42-immunoreactive microglial cells were markedly detected in the brain ischemic zone subjected to 2 h ischemia/ 24 h reperfusion in rats, which were dose dependently reduced by the treatment of LIG. In the infarct penumbra, 80 mg/kg LIG significantly suppressed the increase in the number of OX42 positive microglial cells ( $P < 0.01$  vs vehicle-treated group).

#### **6.4.8 Formation of TUNEL-positive Cells (Fig. 6-14)**

To answer whether LIG inhibits neuronal death in the ischemia-reperfusion brain of MCAO rats, necrotic and apoptotic cells were identified in situ via TUNEL staining in the infarct cortex. As shown in Fig 6-14A, no TUNEL-positive cells were observed in the nonischemic cerebral cortex of the sham-operated control group. At 24 h reperfusion after 2 h MCAO, TUNEL-positive cells were markedly increased in the infarct cortex. There were two types of TUNEL-positive cells: some showing signs of apoptotic death, with a condensation and fragmentation of nuclei and/or apoptotic bodies around the nuclear membrane but without the cytoplasmic staining, and others showing signs of necrotic death, with an uncondensed nuclear chromatin and a diffused light cytoplasmic labeling. The number of apoptotic and necrotic cells were semi-quantitatively determined in the ischemic penumbra and core regions in the cerebral cortex, respectively. As shown in Fig 6-14 B, the number of apoptotic cells was twice as many as the necrotic cells in the ischemic penumbra of the vehicle-treated group 24 h after the end of ischemia. There was a significant and

dose-dependent reduction in the number of apoptotic cells ( $P < 0.01$  at 20 or 80 mg/kg vs. vehicle-treated group) and also a significant and dose-dependent reduction of necrotic cells in the penumbra of the LIG-treated groups ( $P < 0.01$  at 80 mg/kg vs. vehicle-treated group).

Results in Fig 6-15 showed that the effect of LIG on cell death in the ischemic core of the cerebral cortex. No TUNEL-positive cells were observed in the nonischemic cerebral cortex of the sham-operated control group (Fig 6-15A). The number of necrotic neurons was about twice as many as the apoptotic cells in the ischemic core of the vehicle-treated group. After treatment with LIG, TUNEL-positive cells, including both apoptotic and necrotic cells, were significantly decreased in the ischemic core of the cerebral cortex ( $P < 0.05$  vs vehicle-treated group, Fig 6-15B).

## **6.4 DISCUSSION**

In the present study, we first demonstrated that treatment of LIG significantly protected the brain against cerebral ischemic injury in rats as evidenced by the reduction in the infarct volume and improvement in neurological function 24 h after focal ischemia. Post-ischemic treatment with an oral administration of LIG decreased  $70 \pm 10 \%$  and  $90 \pm 8 \%$  of the infarct volume in focal stroke at the dose level of 20 or 80 mg/kg, respectively. Consistent with the effective protection on the infarction volume, the LIG-treated groups significantly reduced the neurological deficit scores at

doses of 20 or 80 mg/kg when compared with the vehicle-treated group ( $P < 0.01$ ).

There are two different kinds of cell death, necrosis and apoptosis, involved in rat focal cerebral ischemia (Li et al., 1998). Necrosis is a passive form of cell death involving morphological changes such as cytoplasmic eosinophilia, whereas apoptosis is an active form of cell death involving cell shrinkage, nuclear/cytoplasmic condensation, margination of chromatin and DNA fragmentation. Recent evidence suggests that complex processes involving mixed types of cell death, containing both necrotic and apoptotic cell death, are involved in the neuronal death following ischemic stroke (Barinaga, 1998). In our focal ischemia model, two types of TUNEL-positive neurons were observed in the ischemic cerebral cortex: one was cells showing nuclear condensation and fragmentation as well as apoptotic bodies around the nuclear membrane without cytoplasmic staining and the other showing necrotic characteristics with uncondensed chromatin and a more diffused light cytoplasmic labeling, in agreement with previous reports by others (Charriaut-Marlangue et al., 1996b; Li et al., 1995). Postischemic treatment with LIG significantly reduced the number of TUNEL-positive apoptotic and necrotic cells in the ischemic penumbra and core areas in the cerebral cortex when compared with the vehicle-treated group. This is the first study to our knowledge demonstrating that LIG could suppress both apoptotic and necrotic cell death in the gradually expanding area of cortical damage.

It is well known that two major distinct apoptotic pathways of caspases have been

demonstrated for their involvement in ischemia/reperfusion injury (Namura et al., 1998; Noshita et al., 2001; Velier et al., 1999). One involves the activation of caspase-8 from cell surface receptors linked via death domains to caspase cascade activation and cell death; the other is the cytochrome *c*-dependent mitochondrial pathway of apoptosis. Both pathways lead to the activation of caspase-3 and finally result in apoptosis (Budihardjo et al., 1999). To determine which pathway of caspase-3 activation is inhibited by LIG, we measured the cytochrome *c* release as well as the expression of cleaved caspase-8 and caspase-3 and the enzyme activities of caspase-8 and caspase-3 at 24 h reperfusion following 2 h ischemia. Consistent with previous reports, our observation supported that caspase-3 could be activated by the cytochrome *c* and caspase-8 pathway following focal cerebral ischemia. A dose of 80 mg/kg significantly decreased the cytochrome *c* release ( $P < 0.05$ ). Doses of 20 or 80 mg/kg LIG significantly decreased the cleaved caspase-8 and caspase-3 expression as well as their activities compared with the vehicle-treated group ( $P < 0.01$ ). These data are in agreement with the significant reduction in the infarct size and improvement in the neurobehavioral function in all LIG-treated animals 24 h after the insult. Therefore, neuroprotection mediated by the treatment of LIG may be associated with a potential apoptotic pathway, dependent of the cytochrome *c* and possibly caspase-8, to suppress caspase-3 activation and subsequent apoptosis.

Recent study suggested that apoptosis and necrosis cell death may share a common initial activation after cerebral ischemia (Benchoua et al., 2001). The ultimate choice

between apoptosis and necrosis depends on the energetic state of the affected cells (Leist et al., 1997; Nicotera et al., 1998). In the ischemic core, the ATP concentration is severely reduced (Folbergrová et al., 1992); this decreased ATP level may abort energy-dependent apoptotic cascades and favor necrotic cell death as well as energy-independent apoptotic cell death (Lei et al., 2004; Onténiente et al., 2003). Thus, the pharmacological intervention probably changes the cell death pattern from necrosis to apoptosis by delaying energy depletion. Our data showed that treatment with LIG significantly reduced the number of necrotic cells in the ischemic cortical core when compared with the vehicle-treated group. Thus, a potential explanation for the prevention of LIG on the cell necrosis is LIG-induced the shift from necrosis to apoptosis via delaying energy depletion. Although further study is needed to elucidate the detailed mechanism of LIG, a potential shift from necrosis to apoptosis induced by LIG treatment may have clinical relevance because it may expand the time-therapy window following cerebral ischemia and allow the antiapoptotic agents to rescue the neurons in the ischemic core.

In addition, studies demonstrate that inflammatory reaction may play an important role in the necrotic process following cerebral ischemia (Chan, 2001; Del Zoppo et al., 2000). In the focal ischemic brain, activated microglia/macrophages are the major source of inflammatory mediators and an induction of the iNOS expression was observed in the activated microglia (Mabuchi et al., 2000; Marletta, 1993; Samdani et al., 1997). Once expressed, iNOS is continuously active and leads to toxic amounts of

NO generation, which greatly contributes to cerebral ischemia injury by the formation of highly reactive peroxynitrite to neurons (Fukuyama et al., 1998; Samdani et al., 1997) as well as the increasing glutamate-induced excitotoxicity to neurons (Bal-Price and Brown, 2001). In addition to its association with apoptosis, therefore, LIG may involve the regulation of inflammatory responses in ischemic brain injury. In the present study, we observed the effect of LIG on the NO level, iNOS expression and activity, and the microglia activation in the ischemic brain tissues. Microglial activation was detected by OX42 immunohistochemistry, a reliable and sensitive marker of microglial activation (Abraham and Lazar, 2000). Our results indicated that cerebral ischemia markedly activated microglia, induced the increase of iNOS expression and activity, and NO level 24 h after ischemia, which were significantly suppressed with LIG treatment. This study suggested that LIG might obtain neuroprotective effect via efficiently blocking the activation of NO/iNOS pathway and the microglia induced by focal cerebral ischemia in rats.

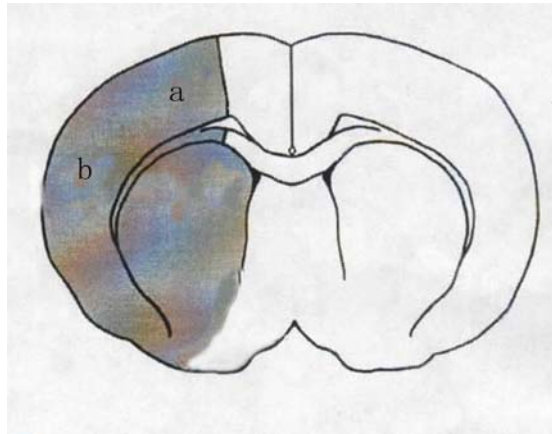
Hyperthermia may worsen the outcome of ischemic stroke in patients and also in animal models. Animal research and clinical studies in patients suffering from focal cerebral ischemia suggest that moderate hypothermia may improve the outcome by attenuating the deleterious metabolic processes in neuronal injury (Reith et al., 1996; Schwab et al., 1998). In MCAO model induced by the intraluminal filament technique, postischemic hyperthermia is related to the ischemic damage to the hypothalamic temperature regulating center (Legos et al., 2002; Zhao et al., 1994).

However, hyperthermia induced by 1.5 h MCAO could be rapidly reversed and approached basal temperature within following 30 min of reperfusion because 90 min ischemia did not produce irreversible damage on hypothalamus (Legos et al., 2002). Several studies have demonstrated that combating hyperthermia by reducing body temperature to 33 °C provides dramatic neuroprotection following focal stroke (Barone et al., 1997; Chen et al., 1992; Corbett et al., 2000; Maier et al., 1998) by multiple mechanisms (Hammer and Krieger, 2003; Legos et al., 2002).

As described in chapters 1.5.2 and 1.5.3, LIG has been shown to be of various bioactivities. Xie and Tao reported that 98 or 196 mg/kg LIG (i.p.) induced a murine body temperature decrease from  $37.9 \pm 0.2$  °C and  $38.1 \pm 0.2$  °C to  $36.8 \pm 0.4$  °C and  $35.9 \pm 0.2$  °C, respectively (Xie and Tao, 1985). In order to determine whether the mild hypothermia of LIG in normal mice was involved in its neuroprotection in the transient MCAO, we measured the effect of LIG on the core body temperature during reperfusion following ischemia. Our results demonstrated that the body temperature through 24 h reperfusion period following 2 h ischemia was only increased by less than 1 °C. The fact that mild spontaneous hyperthermia occurred in this study suggests that 2 h MCAO at 37 °C may not have induced completely irreversible damage on hypothalamus (Legos et al., 2002). In addition, postischemic application of LIG (20 or 80 mg/kg, p.o.) showed no hypothermic effect. The present results rule out the involvement of hypothermia in the neuroprotective mechanism of LIG in ischemia/reperfusion induced brain damage.

In conclusion, the present study first demonstrated that post-ischemic oral administration of LIG could result in neuroprotection by suppressing apoptotic and necrotic death following focal cerebral ischemia in rats. In addition, the novel finding of this study was to provide potential evidence for the molecular mechanism involved in the neuroprotective effect of LIG. Effect of LIG has been associated with the suppression of caspase-3 activation and subsequent apoptosis, associated with both the cytochrome *c* release from mitochondria and the caspase-8 activation following focal stroke, as well as inflammatory responses. Based on the findings in the present study, we propose for the first time that LIG may be a useful intervention for the treatment of focal ischemic brain injury.

**A**



**B**

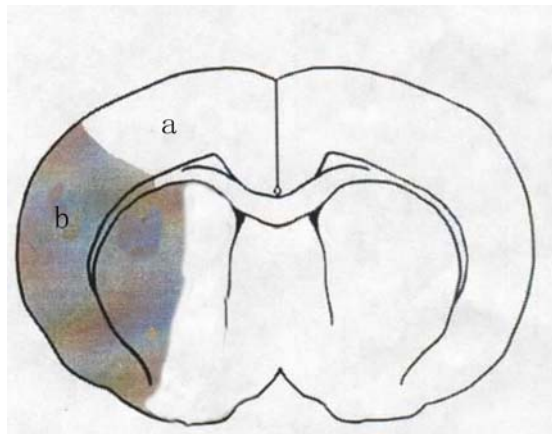


**Figure 6-1.** The location of cerebral infarcts and regions sampled for histological analyses in the focal cerebral ischemic rat. Panels show coronal sections at bregma -1.3 to -3.3 mm from representative (A) the vehicle-treated and (B) the LIG-treated animals, respectively. The infarct tissues are shown in gray. In the ipsilateral (ischemic) hemisphere: a= the region of the dorsolateral cortex at the borders of infarcts in the vehicle-treated animals. This region was typically spared in the LIG-treated animals and can be considered part of the ischemic penumbra. b = the region of the lateral cortex in the ischemic core of infarcts in both the vehicle- and LIG-treated animals.



**Figure 6-2.** Illustrative coronal sections showing the infarct area in the ipsilateral hemisphere of the MCAO rats. The infarct area was stained as a distinct pale-stained area in the rats subjected to 2 h of ischemia/24 h of reperfusion (left) and attenuation of the infarct area by treatment with orally administrated 20 or 80 mg/kg LIG at the start and again at 4 h of reperfusion.

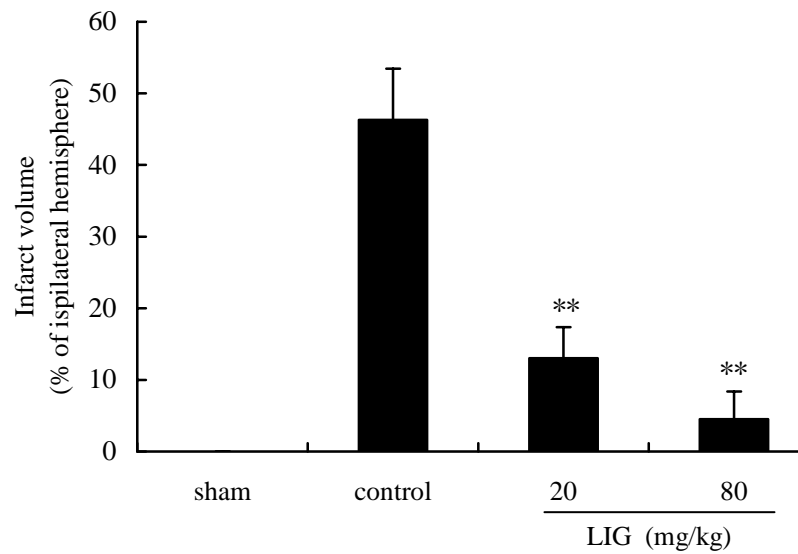


**Figure 6-3.** The dose-dependent inhibitory effect of LIG on the infarct volume of the ischemic hemisphere in rats subjected to 2 h MCAO/24 h reperfusion. Animals received LIG (20 or 80 mg/kg, orally administered) or the volume-matched vehicle (control) at the start and again at 4 h of reperfusion. The infarct volume was significantly decreased by treatment with 20 or 80 mg/kg LIG. Results are expressed as the mean  $\pm$  SD of 4~5 animals. \*\* $P < 0.01$  versus the vehicle-treated control group.

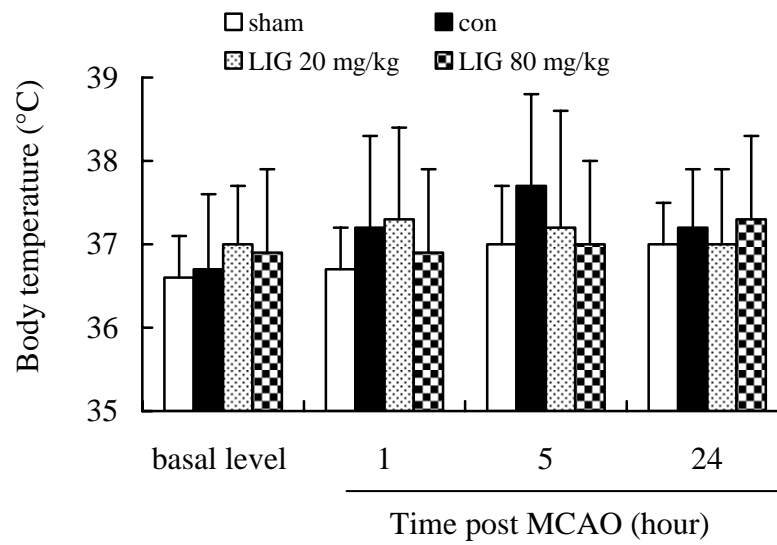


**Figure 6-4.** The effect of LIG on the core body temperature of rats during 24 h of reperfusion following 30 min of MCAO. Rats were treated with either LIG (20, 80 mg/kg) or vehicle immediately following MCAO and again at 4 h postischemia. All data are represented as the mean  $\pm$  SD ( $n = 14\sim 16$ ).

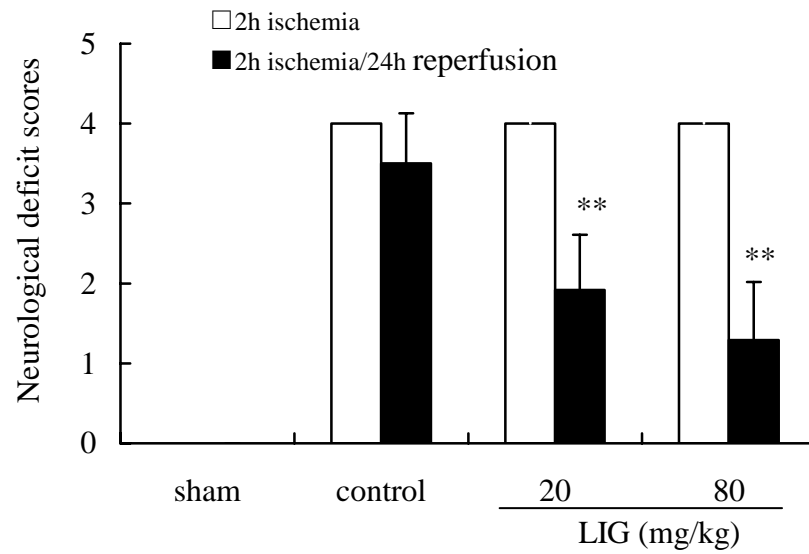


**Figure 6-5.** The dose-dependent inhibitory effect of LIG on the neurological scores of the rats subjected to 2 h MCAO/24 h reperfusion. Animals received LIG (20 or 80 mg/kg, orally administrated) or the volume-matched vehicle (control) at the start and again at 4 h of reperfusion. The neurological deficit scores were significantly decreased by the treatment with 20 or 80 mg/kg LIG. Results are expressed as the mean  $\pm$  SD of 14 ~16 animals. \*\* $P < 0.01$  versus the vehicle-treated control group.

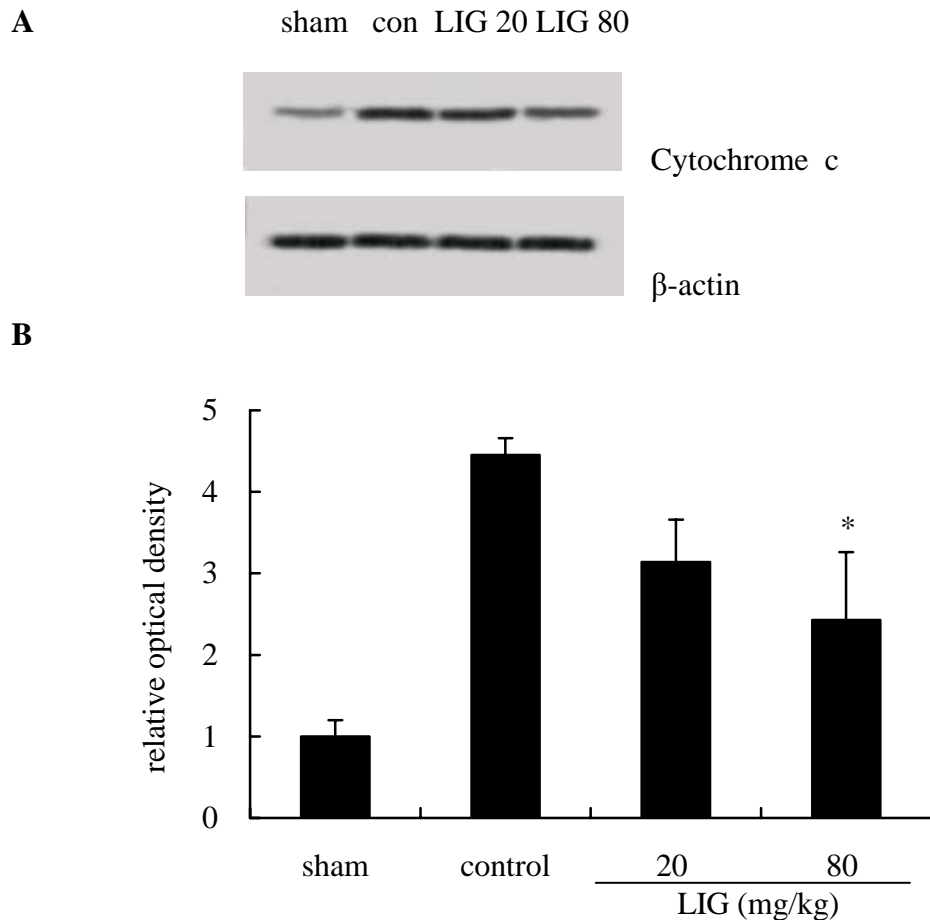


**Figure 6-6.** The effect of LIG on the cytosolic cytochrome c expression in the ischemic brain tissues of rats subjected to 2 h MCAO/24 h reperfusion. Animals received LIG (20 or 80 mg/kg, orally administrated) or the volume-matched vehicle (control) at the start and again at 4 h of reperfusion. Western blot analysis was performed as described in Materials and Methods. A: The expected molecular weight of cytochrome c ~11 kDa and  $\beta$ -actin ~43 kDa bands appearing on each gel. B: Quantification of the effect of LIG on the expression of cytosolic cytochrome c in the ipsilateral hemisphere. Expression values were normalized for  $\beta$ -actin and expressed as a percentage of the sham group value. Results are expressed as the mean  $\pm$  SD of 3 separate experiments. \* $P < 0.05$  versus the vehicle-treated control group.

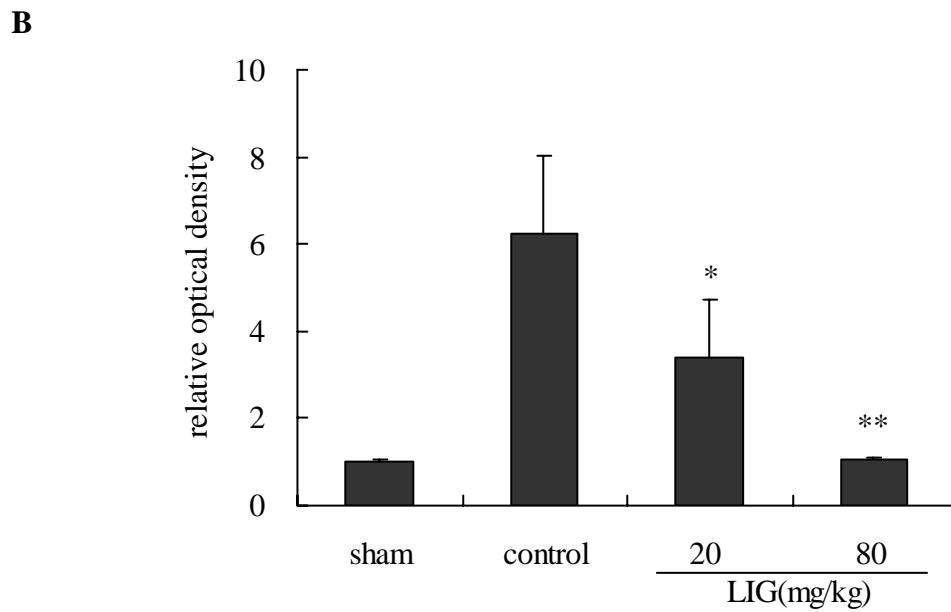
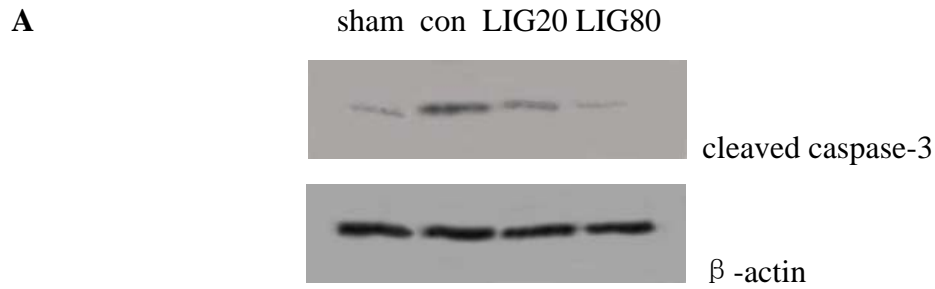


**Figure 6-7.** The effect of LIG on the cleaved caspase-3 expression in the ischemic brain tissues of rats subjected to 2 h MCAO/24 h reperfusion. Animals received LIG (20 or 80 mg/kg, orally administrated) or the volume-matched vehicle (control) at the start and again at 4 h of reperfusion. Western blot analysis was performed as described in Materials and Methods. A: The expected molecular weight of cleaved caspase-3 ~19 kDa and  $\beta$ -actin ~43 kDa bands appearing on each gel. B: Quantification of the effect of LIG on the expression of the cleaved caspase-3 in the ipsilateral hemisphere. Expression values were normalized for  $\beta$ -actin and expressed as a percentage of sham group. Results are expressed as the mean  $\pm$  SD of 3 separate experiments. \* $P < 0.05$ , \*\* $P < 0.01$  versus the vehicle-treated control group.

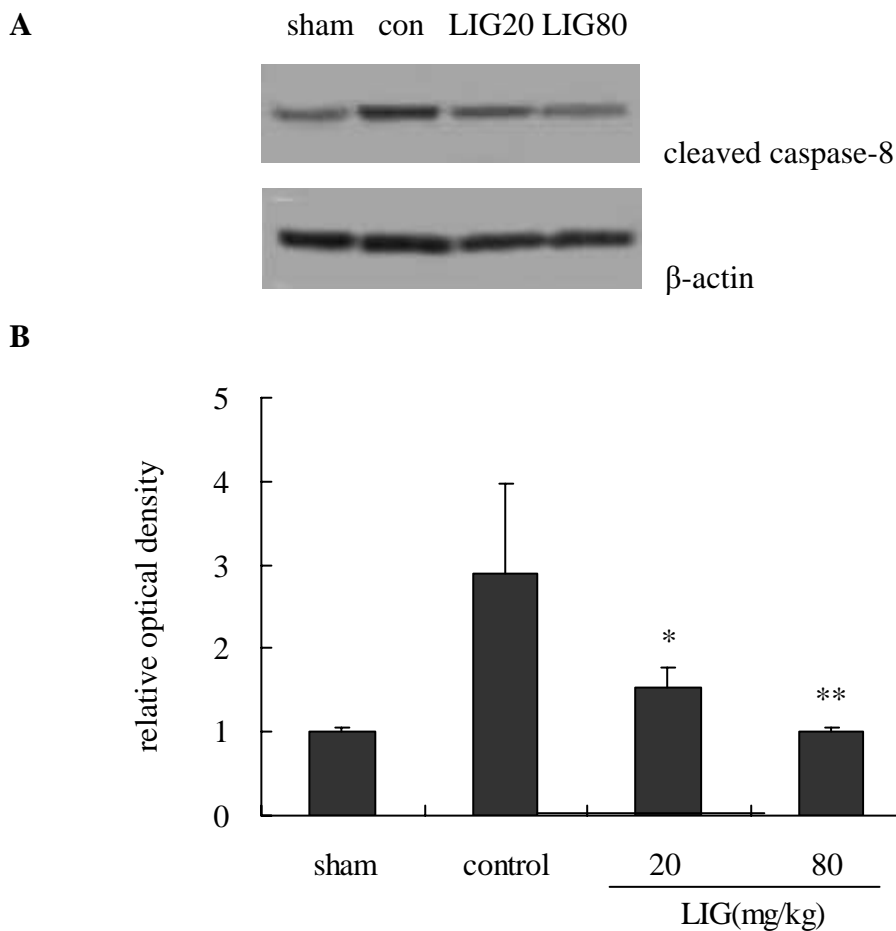


**Figure 6-8.** The effect of LIG on the cleaved caspase-8 expression in the ischemic brain tissues of rats subjected to 2 h MCAO/24 h reperfusion. Animals received LIG (20 or 80 mg/kg, orally administrated) or the volume-matched vehicle (control) at the start and again at 4 h of reperfusion. Western blot analysis was performed as described in Materials and Methods. A: The expected molecular weight of cleaved caspase-8 ~20 kDa and  $\beta$ -actin ~43 kDa bands appearing on each gel. B: Quantification of the effect of LIG on the expression of the cleaved caspase-3 in the ipsilateral hemisphere. Expression values were normalized for  $\beta$ -actin and expressed as a percentage of sham group. Results are expressed as the mean  $\pm$  SD of 3 separate experiments. \* $P < 0.05$ , \*\* $P < 0.01$  versus the vehicle-treated control group.

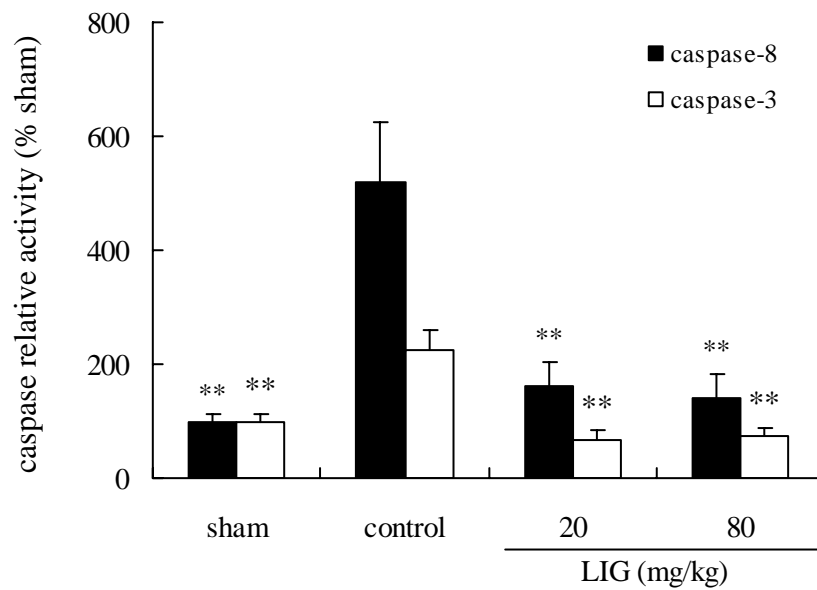


**Figure 6-9.** The inhibition of the caspase-like activities by the treatment of LIG in the ischemic brain tissues of rats subjected to 2 h MCAO/24 h reperfusion. Animals received LIG (20 or 80 mg/kg, orally administrated) or the volume-matched vehicle (control) at the start and 4 h of reperfusion. The activity of the caspase 8 (solid column) or caspase 3 (open column) was measured as described in Materials and Methods. Caspase activity was expressed as the optical density unit percent of the sham-operated control group at 405 nm. Data shown are the mean  $\pm$  SD ( $n = 4$ ). \*\* $P < 0.01$  versus the vehicle-treated control group.

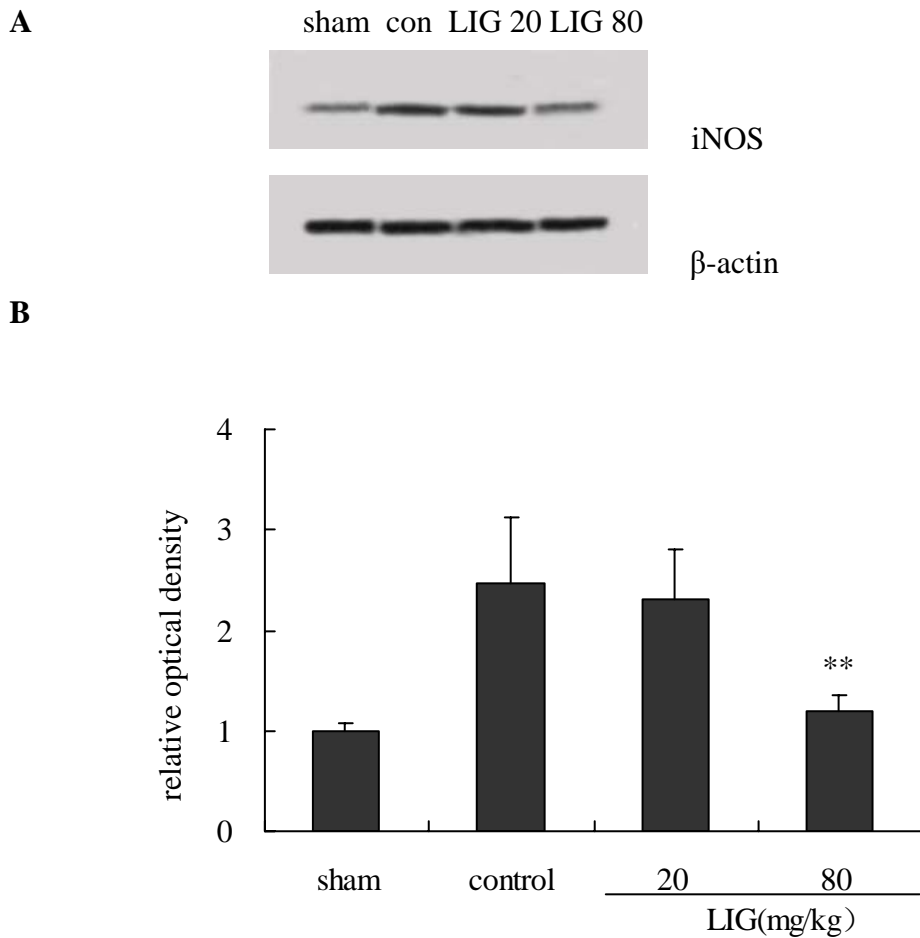


**Figure 6-10.** The effect of LIG on iNOS expression in the ischemic brain tissues of rats subjected to 2 h MCAO/24 h reperfusion. Animals received LIG (20 or 80 mg/kg, orally administrated) or the volume-matched vehicle (control) at the start and again at 4 h of reperfusion. Western blot analysis was performed as described in Materials and Methods. A: The expected molecular weight of iNOS ~130 kDa and  $\beta$ -actin ~43 kDa bands appearing on each gel. B: Quantification of the effect of LIG on the expression of iNOS in the ipsilateral hemisphere. Expression values were normalized for  $\beta$ -actin and expressed as a percentage of sham group. Results are expressed as the mean  $\pm$  SD of 3 separate experiments. **\*\*** $P < 0.01$  versus the vehicle-treated control group.

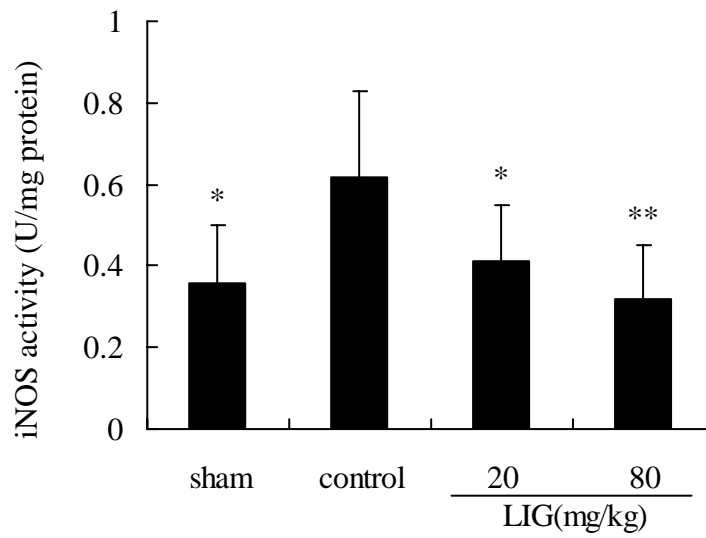


**Figure 6-11.** The effect of LIG on iNOS activity in the ischemic brain tissues of rats after 2 h of MCAO /24 h of reperfusion. Animals received oral administration of LIG (20 or 80 mg/kg) or the volume-matched vehicle at the start and again at 4 h of reperfusion. Results represent the mean  $\pm$  SD ( $n = 6$ ). \* $P < 0.05$ , \*\* $P < 0.01$  versus the vehicle-treated control group.

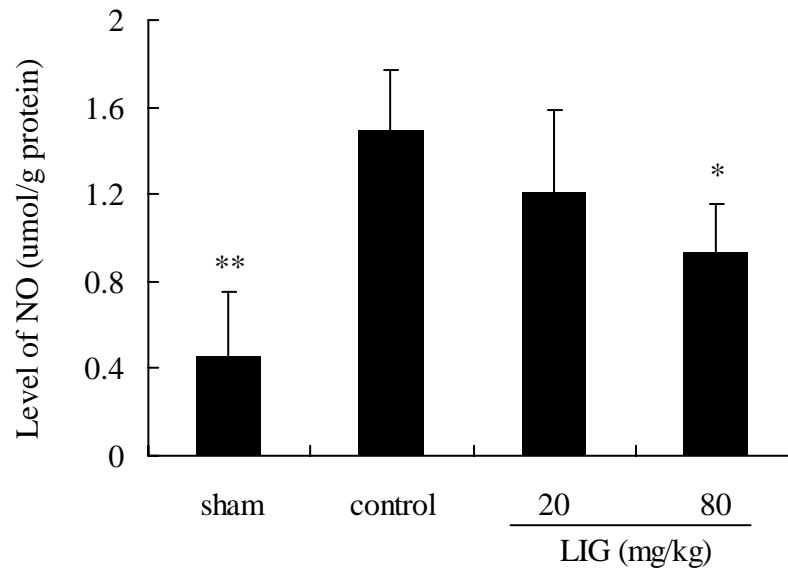
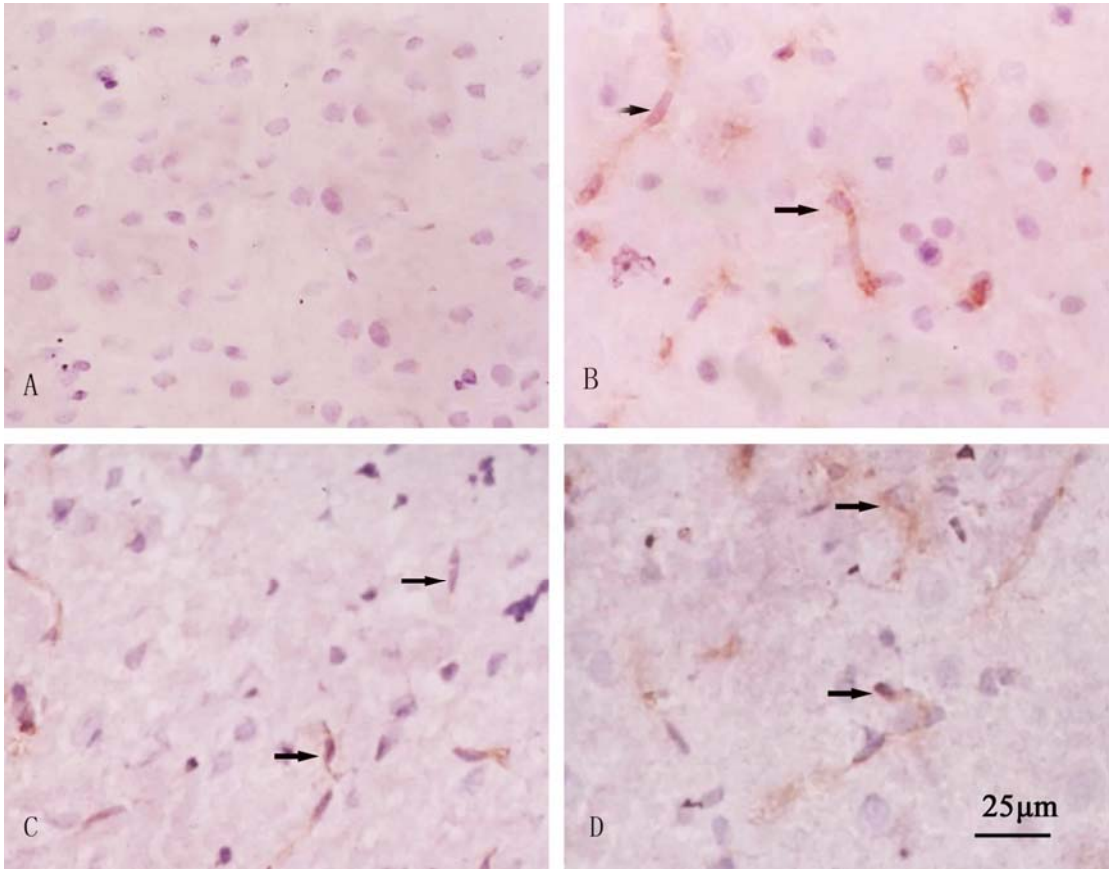


**Figure 6-12.** The effect of LIG on the NO content in the ischemic brain tissues of rats subjected to 2 h of MCAO/24 h of reperfusion. Animals received oral administration of LIG (20 or 80 mg/kg) or the volume-matched vehicle at the start and again at 4 h of reperfusion. The level of NO was analyzed by the Griess reaction described as Methods. Results represent the mean  $\pm$  SD ( $n = 6$ ). \* $P < 0.05$ , \*\* $P < 0.05$  versus the vehicle-treated group.



**E**

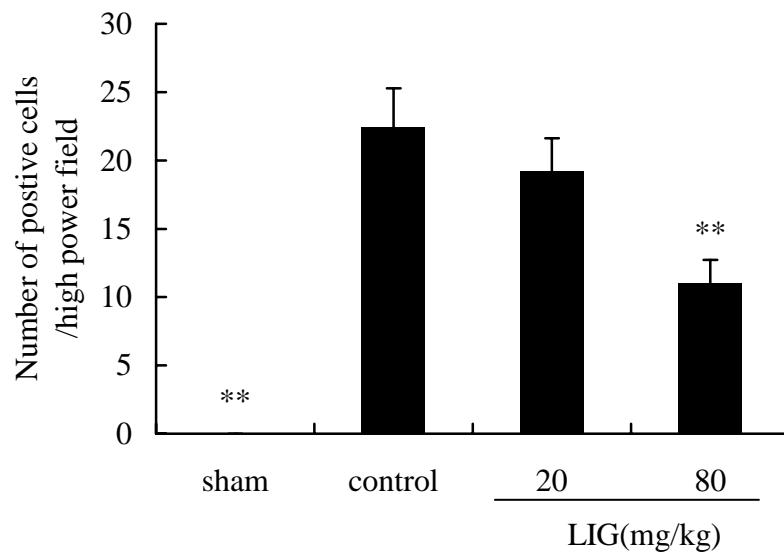
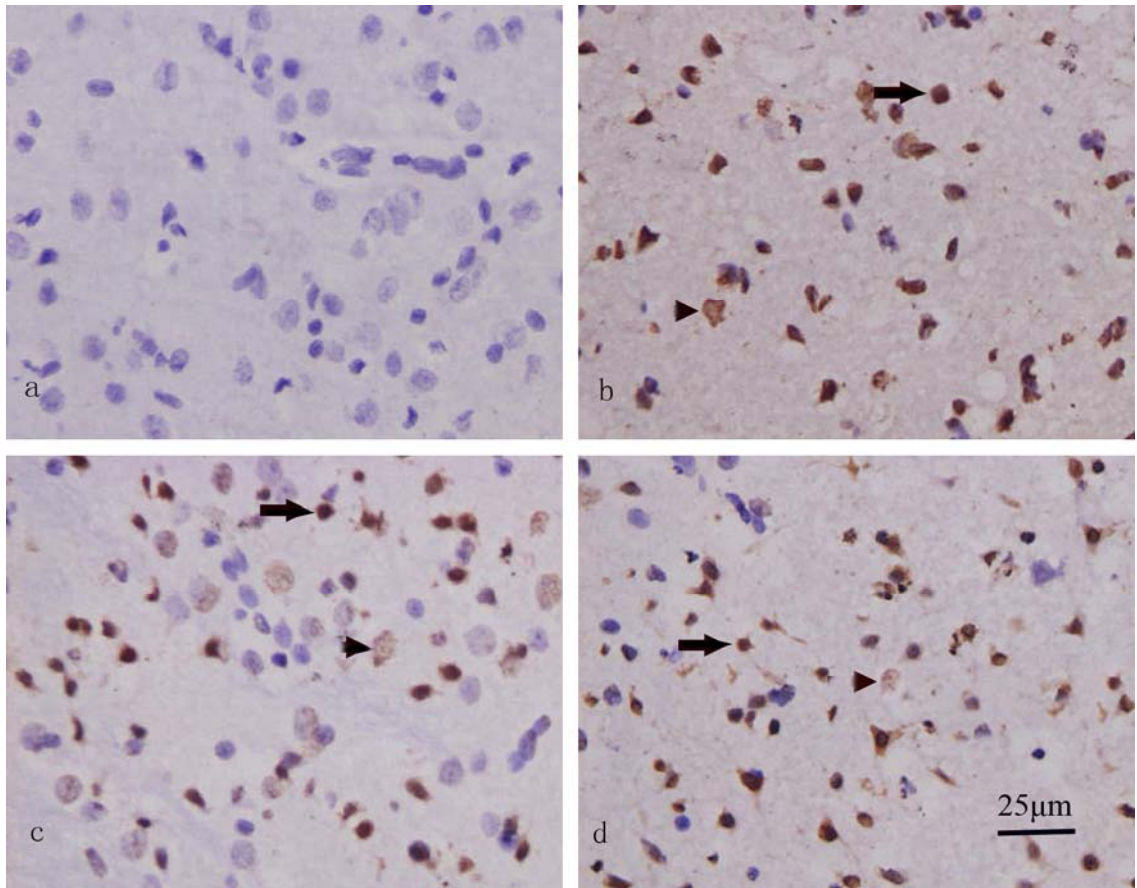


**Figure 6-13.** The effect of LIG on the development of OX42 positive microglial cells within the infarct penumbra of focal ischemic rats subjected to 2 h of ischemia/24 of reperfusion. The cell specific positive staining of OX42 was detected in the activated microglia (arrows). A: the sham-operated control, B: the vehicle-treated control, C and D: 20 or 80 mg/kg LIG orally administrated at the start and again at 4 h of reperfusion. The magnification was 400 ×. Lower panel (E) represents the analyses of activated microglia. Results represent the mean ± SD of four animals of each group. \*\* $P < 0.01$  versus the vehicle-treated control group.

**A**



**B**

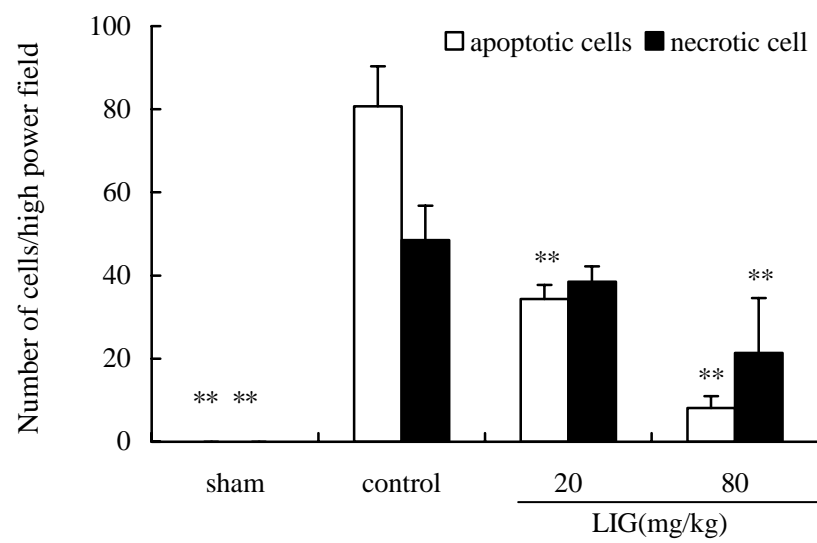
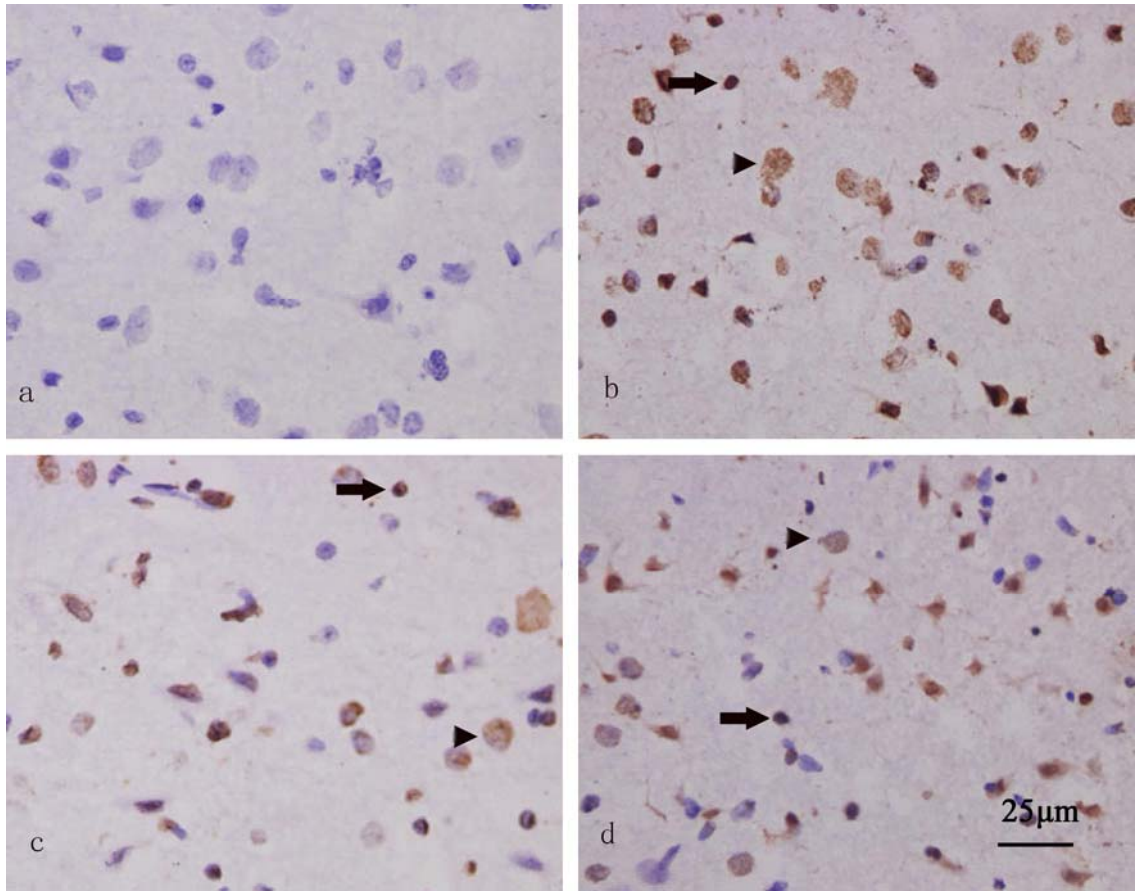


**Figure 6-14.** The effect of LIG on the development of TUNEL-positive cells in the ischemic cortical penumbra of the focal ischemic rats subjected to 2 h of ischemia/24 h of reperfusion. (A) Representative photographs of TUNEL staining in the ischemic cortical penumbra. TUNEL-positive apoptotic cells exhibit a condensation and fragmentation of nuclei and apoptotic bodies around the nuclear membrane without cytoplasmic staining (arrow). TUNEL-positive necrotic cells exhibit a diffused labeling compared to the apoptotic cells, without the fragmentation of nuclei or apoptotic bodies (arrowhead). a: the sham-operated control, b: the vehicle-treated control, c and d: 80 or 20 mg/kg LIG orally administered at the start and again at 4 h of reperfusion. The magnification was 400 ×. (B) Quantification of apoptotic and necrotic cells in the ischemic penumbra. Results represent the mean ± SD of four animals of each group. \* $P < 0.05$ , \*\* $P < 0.01$  versus the vehicle-treated control group.

**A**



**B**

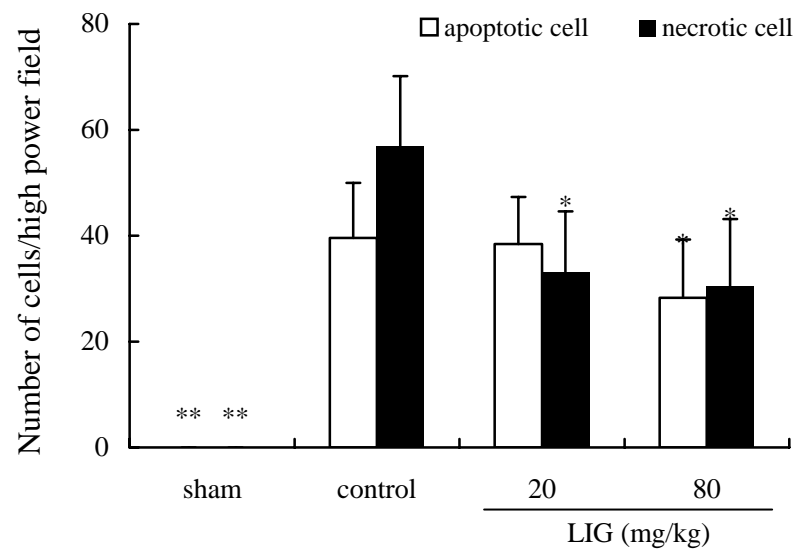


**Figure 6-15.** The effect of LIG on the development of TUNEL-positive cells in the ischemic cortical core of the focal ischemic rats subjected to 2 h of ischemia/24 h of reperfusion. (A) Representative photographs of TUNEL staining in the ischemic cortical core. TUNEL-positive apoptotic cells exhibit a condensation and fragmentation of nuclei and the apoptotic bodies around the nuclear membrane without cytoplasmic staining (arrow). TUNEL-positive necrotic cells exhibit a diffused labeling compared to the apoptotic cells, without a fragmentation of nuclei or apoptotic bodies (arrowhead). a: the sham-operated control, b: the vehicle-treated control, c and d: 80 or 20 mg/kg LIG orally administrated at the start and again at 4 h of reperfusion. The magnification was 400 ×. (B) Quantification of apoptotic and necrotic cells in the ischemic core. Results represent the mean ± SD of four animals of each group. \* $P < 0.05$ , \*\* $P < 0.01$  versus the vehicle-treated control group.

## CHAPTER 7

### GENERAL DISCUSSION

3-alkylphthalide derivatives are a type of natural products which exist in plants. In the past 100 years, studies have been conducted where tens of the derivatives have been isolated from numerous plants, among which butylphthalide, LIG and sedanenolide are the most widely distributed constituents. Most of the 3-alkylphthalide compounds, except butylphthalide, are not stable at room temperature. They can easily have structural arrangements, oxidation, hydrolysis and polyreaction. Therefore, in the past decade, butylphthalide, the only stable 3-alkylphthalide derivative, has been synthesized and its pharmacological activities systemically studied (Chang and Wang, 2003; Chong and Feng, 1999; Hu and Li, 2004; Xu and Feng, 1999). Recently, orally administered butylphthalide was approved for the treatment of acute ischemic stroke patients in China (Cui et al., 2005). With the development of pharmaceutical technology, various methods solving the stability problem of the the unstable compounds are available, which provide the potentiality for the research and development of unstable bioactive compounds (e.g. LIG) as potential drugs. As mentioned in the introduction, LIG administration almost always used intraperitoneal injection in pharmacodynamic studies mostly due to the limitation of pure sample preparation. It is well known that oral administration is the most important and preferred route of administration for small molecular weight conventional drugs.

Therefore, predicting the overall bioavailability of LIG is useful for designing an ideal dosing regimen for pharmacological studies and future clinical applications *in vivo*.

It was reported that the *Papp* obtained from the Caco-2 cell transport studies had been shown to correlate well to human intestinal absorption (Artursson, 1996; Rubas, 1993). A *Papp* value in the Caco-2 monolayers of  $> 1 \times 10^{-6}$  cm/s should, in general, be associated with an efficient intestinal absorption in humans (Artursson, 1991; Pade, 1998; Yee, 1997). The experiments described in chapter 3 demonstrated that the *Papp* of LIG for the AP-BL flux was  $(4.0 \pm 0.5) \times 10^{-6}$  cm/sec on the Caco-2 monolayers. Although it was reported that the *Papp* of highly lipophilic compounds in Caco-2 monolayers could be underestimated because of a considerable retention by the Caco-2 monolayers and non-specific binding to the transwell surface, the data generated in this study suggests that LIG may have good oral absorption *in vivo*. In addition, our results indicated that temperature, P-gp inhibitor cyclosporin A and extracellular calcium had no significant effect on the transepithelial transport. Therefore, we propose that oral administration is a preferred route for LIG in long-term application and transcellular passive diffusion may be the principal mechanism of the oral absorption for LIG.

Stroke remains one of the major causes of death and disability throughout the world. More than 80% of all strokes are a result of cerebral ischemia (Caplan, 1992). Restoration of blood flow by regular thrombolytic therapy can be beneficial but can

also contribute to further brain injury, as in reperfusion injury. During reperfusion, reoxygenation provides oxygen to sustain neuronal viability and also provide oxygen as a substrate for numerous enzymatic oxidation reactions that produce ROS. If these overproduced ROS failed to be scavenged by the endogenous antioxidants such as SOD, GSHPx, catalase, GSH, ascorbic acid and vitamin E, they can attack the lipids of the cell membrane, modify proteins and damage DNA (Halliwell et al., 1992). The endogenous antioxidative defense mechanisms are perturbed as a result of the overproduction of oxygen radicals, consumption of antioxidants, and the failure to adequately replenish them in the ischemic brain tissue. Thus, penetrating-BBB antioxidants are expected to be useful for the treatment of cerebral ischemic damage (Schwarz et al., 2001; Soehle et al., 1998; Traystman et al., 1991). LIG had significant central effects after systemic administration (Matsumoto et al., 1998; Xie and Tao, 1985), which suggests that this lipophilic compound may penetrate BBB. The experiments described in chapter 4 demonstrated that LIG dose-dependently scavenged DPPH radical and also inhibited the automatic oxidation of the linoleic acid or lipid peroxidation of NADPH-dependent or  $\text{Fe}^{2+}$ /ascorbic acid induced rat brain mitochondria at the range of 5 to 80 mM. In addition, LIG significantly protected the C6 glioma cells against  $\text{H}_2\text{O}_2$ -induced oxidative injury by increasing cell viability and attenuating the apoptotic chromatin-condensation and nuclear fragmentation in a concentration-dependent manner at the range of 0.5 to 50  $\mu\text{M}$ . It is interesting that LIG showed a significant antioxidant activity at a lower dose in the cell model than in vitro oxidative systems. A probable explanation is likely that LIG, a highly lipophilic

antioxidant, may be of a good affinity to cell membranes, where peroxidative reactions can be halted. As described in chapter 5, the antioxidant activity of LIG was also observed in the transient forebrain ischemia model in mice. Our results showed that oral administration of LIG dose-dependently decreased the level of MDA, and increased the activities of GSHPx and SOD in the ischemic brain tissues at 5 days postischemia. Although further study is needed to determine whether the increase of these enzyme activities is the result of a direct regulation of LIG or just a secondary consequence to LIG antioxidant effect, we propose that LIG is an orally administrated lipophilic antioxidant, which will probably benefit for the treatment of the disorders associated with oxidative stress, such as ischemic brain damage.

The impact of cerebral ischemia on the structure and function of the brain depends both on the severity and the duration of the flow reduction. Studies demonstrate that there are two different kinds of cell death, necrosis and apoptosis, involved in brain damage. Pharmacological interventions to halt or reverse necrosis or programmed cell death, to enhance the intrinsic autoprotection and repair mechanisms are the promising strategies for the treatment of ischemic brain damage. Since re-establishing the flow in the ischemic area is an available therapy for some stroke patients (The NINDS, 1995) and the late onset of spontaneous reperfusion occurs in 50% of the stroke patients (Saito et al., 1987), ischemia reperfusion models are proposed to be more closely mimic the clinical situation and suitable for the screening of neuroprotective agents (Mhairi Macrae, 1992). The experiments described in chapter 5 demonstrated that

postischemic treatment with LIG could significantly and dose-dependently preserve the CA1 intact neurons and decrease the cortical TUNEL-positive apoptotic cells at 5 days after 30 min forebrain ischemia in mice when compared with the control (vehicle-treated). Our results indicated that this mild forebrain ischemia activated the mitochondria-dependent caspase-3 apoptosis pathway at 5 days after ischemia whereas LIG markedly inhibited the main events involved in this energy-dependent apoptotic pathway. Immunoblot study showed that LIG increased the Bcl-2 expression together with a significant decrease in the Bax expression in the ischemic brain tissues, which were confirmed by the immunohistochemistry study of the anatomic precision in the ischemic brain sections. Meanwhile, LIG decreased the cytosolic cytochrome c expression, caspase-3 expression and activity. Therefore, we propose that the neuroprotection of LIG is, at least in part, derived from its antioxidant and anti-apoptotic effect through the mitochondria dependent caspase-3 pathway.

Focal cerebral ischemia affects restricted brain regions and occurs in a wide variety of clinical settings. It has been found that a mildly ischemic area, the penumbra area, borders the severely ischemic core area (Du et al., 1996). Cells in both the ischemic core and penumbra area probably die through necrosis or a delayed process that involves apoptosis (Furuichi et al., 2004; Onténiente et al., 2003). The experiments described in chapter 6 demonstrated that postischemic treatment with LIG could significantly not only reduce the infarct volume but also improve the recovery of the neurological function of the focal cerebral ischemic brain. TUNEL staining showed

that LIG could decrease both cell apoptosis as well as necrosis in the cortical ischemic penumbra and core. As for the analysis of anti-apoptosis mechanisms for LIG, the immunoblot was used to detect the expression of pro-apoptotic proteins (cytochrom c, cleaved caspase-8 and cleaved caspase-3) and the results showed that LIG could effectively inhibit these protein expression. In addition, the measurement of the enzymatic activity indicated that LIG induced a dose-dependent inhibition on caspase-8 and caspase-3 activities. Therefore, we propose for the first time that the inhibition on both the mitochondria-dependent and Fas death receptor pathways contributes to the neuroprotection of LIG in focal cerebral ischemia.

It is known that inflammatory responses may play an important role in the necrotic procedure of neurons in cerebral ischemia, and participate in the expansion of ischemic brain damage (Chan, 2001; Furuichi et al., 2004). Our results, as well as some previous papers have demonstrated that there was an activation of microglia which showed an increase of the OX-42 immunoreactivity and an upregulation of the NO/iNOS pathway after reperfusion following a transient MCAO (Chan, 2001; Furuichi et al., 2004). In the present study, LIG significantly suppressed the increase in the number of OX-42 positive microglial cells and iNOS expression in ischemic brain tissues, and decreased the iNOS activity and NO level in the ipsilateral hemisphere. Therefore, we propose that the anti-inflammation property is probably involved in the neuroprotection of LIG for cerebral ischemia. In addition, recent study suggests that apoptosis and necrosis may share a common initial activation after cerebral ischemia

(Benchoua et al., 2001). The ultimate choice between apoptosis and necrosis depends on the energetic state of the affected cells (Leist et al., 1997; Nicotera et al., 1998). In the ischemic core, the ATP concentration is severely reduced, which may abort energy-dependent apoptotic cascades and favor necrotic cell death as well as the energy-independent apoptotic cell death (Folbergrová et al., 1992; Lei et al., 2004; Onténiente et al., 2003). The interesting finding in this study is that LIG can significantly decrease the number of necrotic cells in the core. A potential explanation for this anti-necrotic effect LIG is that LIG may improve the energetic state in the ischemic core area, and thus induce the shift from necrosis to apoptosis. Although further study is needed to elucidate the detailed mechanism of LIG, the anti-necrotic effect of LIG may have special clinical relevance because it may expand the time-therapy window following cerebral ischemia and allow neuroprotective agents, such as antiapoptotic agents, to reduce irreversibly ischemic damage in the core.

There are consensus that hyperthermia may aggravate the brain infarction associated with ischemic stroke and that hypothermia reducing body temperature to 33 °C or below provides dramatic neuroprotection following focal stroke (Barone et al., 1997; Chen et al., 1992; Corbett et al., 2000; Maier et al., 1998). In this study, hypothermia is not the main mechanism involved in the neuroprotection of LIG in the reperfusion following cerebral ischemia.

However, the potential mechanisms of action underlying the neuroprotective effect of

LIG in cerebral ischemia injury have not been fully explored in the present study. For example, as introduced in chap 1, LIG exists in many important medical plants such as *Anglica sinsens* and *Ligusticum chuanxiong* . These Umbelliferae plants are often used to invigorate blood circulation in Chinese traditional medicines. Therefore, further study is needed to determine whether LIG can benefit the treatment of cerebral ischemia by improving and restoring blood flow in the ischemic areas.

Taken together, our results demonstrated for the first time that oral administration of LIG had significant neuroprotection for the reperfusion following the transient forebrain and focal ischemia by inhibiting both the necrosis and apoptosis process. And LIG may achieve its neuroprotective effect by antagonizing the following main cytotoxic events of ischemia/reperfusion injury: oxidative stress, apoptosis and inflammation. Therefore, LIG is a promising neuroprotective agent for the treatment of cerebral ischemia. In addition, oxidative stress and apoptosis appear to play a significant role in the neurodegeneration associated with Alzheimer's disease (Moreira et al., 2004; Moreira et al., 2005; Roth, 2001; Shimohama, 2000) and Parkinson's disease (Alexi et al., 2000; Ziv et al., 1994). Thus it is worthwhile to further study the potential efficacy of LIG for the treatment of these neurological degenerative disorders.

In conclusion, LIG has been tested for its efficacy in preventing histological, neurological and biochemical abnormalities following cerebral ischemia damage. Oral

administration of LIG showed significant neuroprotection on both the murine transient forebrain ischemia and rat MCAO models by post-ischemic treatment. We propose that multiple mechanisms, including antioxidant, anti-apoptosis and anti-inflammation, contribute to the efficacy of LIG for ischemic brain damage.

## REFERENCES

- A randomized trial of tirilazad mesylate in patients with acute stroke (RANTTAS).  
(1996) The RANTTAS Investigators. *Stroke* 27:1453-1458.
- Abraham H, Lazar G (2000) Early microglial reaction following mild forebrain ischemia induced by common carotid artery occlusion in rats. *Brain Research* 862: 63-73.
- Adams HP Jr, Bendixen BH, Leira E, Chang KC, Davis PH, Woolson RF, Clarke WR, Hansen MD (1999) Antithrombotic treatment of ischemic stroke among patients with occlusion or severe stenosis of the internal carotid artery: a report of the Trial of Org 10172 in Acute Stroke Treatment (TOAST). *Neurology* 53:122-125.
- Adams HP, Brott TG, Furlan AJ, Gomez CR, Grotta J, Helgason CM, Kwiatkowski T, Lyden PD, Marler JR, Torner J, Feinberg W, Mayberg M, Thies W (1996) Guidelines for thrombolytic therapy for acute stroke: a supplement to the guideline for the management of patients with acute ischemic stroke. A statement for healthcare professionals from a Special Writing Group of the Stroke Council, American Heart Association. *Stroke* 27: 1711-1718.
- Albers GW (1999) Expanding the window for thrombolytic therapy in acute stroke. The potential role of acute MRI for patients selection. *Stroke* 30: 2230-2237.
- Alexi T, Borlongan CV, Faull RL, Williams CE, Clark RG, Gluckman PD, Hughes PE (2000) Neuroprotective strategies for basal ganglia degeneration: Parkinson's and Huntington's diseases. *Progress in Neurobiology* 60:409-70.

- Anderle P, Niederer E, Rubas W, Hilgendorf C, Spahn-Langguth H, Wunderli-Allenspach H, Merkle HP, Langguth P (1998) P-Glycoprotein(P-gp) mediated efflux in Caco-2 cell monolayers: the influence of culturing conditions and drug exposure on P-gp expression levels. *Journal of Pharmaceutical Sciences* 87:757-762.
- Arends MJ, Morris RG, Wyllie AH (1990) Apoptosis: the role of the endonuclease. *American Journal of Pathology* 136:593-608.
- Artursson P (1990) Epithelial transport of drugs in cell culture. I: A model for studying the passive diffusion of drugs over intestinal absorptive (caco-2) cells. *Journal of Pharmaceutical Sciences* 79:476-482.
- Artursson P and Karlsson J (1991) Correlation between oral drug absorption in human and apparent drug permeability coefficients in human intestinal epithelial (Caco-2) cells. *Biochemical & Biophysical Research Communication* 175:880-885.
- Artursson P, Magnusson C (1990) Epithelial transport of drugs in cell culture. II: Effect of extracellular calcium concentration on the paracellular transport of drugs of different lipophilicities across monolayers of intestinal epithelial (Caco-2) cells. *Journal of Pharmaceutical Sciences* 79: 595-600.
- Artursson P, Palm K, Luthman K (1996) Caco-2 monolayers in experimental and theoretical predictions of drug transport. *Advanced Drug Delivery Review* 22:67-84.
- Asano T, Ishihara K, Morota T, Takeda S, Aburada M (2003) Permeability of the flavonoids liquiritigenin and its glycosides in licorice roots and davidigenin, a

- hydrogenated metabolite of liquiritigenin, using human intestinal cell line Caco-2. *Journal of Ethnopharmacology* 89: 285-289.
- Atkinson RP (1998) Ancrod in the treatment of acute ischemic stroke: a review of clinical data. *Cerebrovascular Diseases* 8 (Suppl 1): 23-28.
- Atlante A, Valenti D, Gagliardi S, Passarella S (2000) A sensitive method to assay the xanthine oxidase activity in primary cultures of cerebellar granule cells. *Brain Research Protocols* 6: 1-5.
- Baird AE, Benfield A, Schlaug G, Siewert B, Lovblad KO, Edelman RR, Warach S (1997) Enlargement of human cerebral ischemic lesion volumes measured by diffusion-weighted magnetic resonance imaging. *Annals of Neurology* 41: 581-589.
- Bal-Price A, Brown GC (2001) Inflammatory neurodegeneration mediated by nitric oxide from activated glia-inhibiting neuronal respiration, causing glutamate release and excitotoxicity. *The Journal of Neuroscience* 21:6480-6491.
- Banerjee SK, Gupta BD, Sheldrick WS, Höfle G (1982) Angeolide, a novel Lactone from *Angelica glauca*. *Liebigs Annalen der Chemie* 699-707.
- Banerjee SK, Gupta BD, Sheldrick WS, Höfle G (1984) Lactonic constituents of *Angelica glauca*. *Liebigs Annalen der Chemie* 888-893.
- Bannai S and Tateishi N (1986) Role of membrane transport in metabolism and function of glutathione in mammals. *The Journal of membrane biology* 89: 1-8.
- Barinaga M (1998) Stroke-damaged neurons may commit cellular suicide. *Science* 281:1302-1303.

- Barnwell SL, Clark WM, Nguyen TT, O'Neill OR, Wynn ML, Coull BM (1994) Safety and efficacy of delayed intraarterial urokinase therapy with mechanical clot disruption for thromboembolic stroke. *American Journal of Neuroradiology* 15:1817-1822.
- Baron JC (1999) Mapping the ischemic penumbral with PET: implications for acute stroke treatment. *Cerebrovascular Diseases* 9: 193-201.
- Barone FC, Feuerstein GZ, White RF (1997) Brain cooling during transient focal ischemia provides complete neuroprotection. *Neuroscience and Biobehavioral Reviews* 21:31-44.
- Barton DHR, Juan X de Vries (1963) The constitution of Sedanolid. *Journal of the Chemical Society* 19:1916-1919.
- Bartus RT (1999) The blood-brain barrier as a target for pharmacological modulation. *Current Opinion in Drug Discovery & Development* 2: 152-167.
- Bartus RT, Elliott PJ, Dean RL, Hayward NJ, Nagle RL, Huff MR, Snodgrass PA, Blunt DG (1996) Controlled modulation of BBB permeability using the bradykinin agonist, RMP-7. *Experimental Neurology* 142:14-28.
- Bederson JB, Pitts LH, Germano SM, Nishimura MC, Davis RL, Bartkowski HM (1986a) Evaluation of 2,3,5-triphenyltetrazolium chloride as a stain for detection and quantification of experimental cerebral infarction in rats. *Stroke* 17:1304-1308.
- Bederson JB, Pitts LH, Tsuji M, Nishimura MC, Davis RL, Bartkowski H (1986b) Rat middle cerebral artery occlusion: Evaluation of the model and development of a

- neurologic examination. *Stroke* 17:472-476.
- Belayev L, Busto R, Zhao W, Fernandez G, Ginsberg MD (1999) Middle cerebral artery occlusion in the mouse by intraluminal suture coated with poly-L-lysine: neurological and histological validation. *Brain Research* 833:181-190.
- Benchoua A, Couriaud C, Guegan C, Tartier L, Couvert P, Friocourt G, Chelly J, Menissier-de Murcia J, Onteniente B (2002) Active caspase-8 translocates into the nucleus of apoptotic cells to inactivate poly(ADP-ribose) polymerase-2. *Journal of Biological Chemistry* 277: 34217-34222.
- Benchoua A, Guégan C, Couriaud C, Hosseini H, Sampaio N, Morin D, Onténiente B (2001) Specific caspase pathways are activated in the two stages of cerebral infarction. *The Journal of Neuroscience* 21:7127-7134.
- Bjeldanes LF, Kim IS (1977) Phthalide components of Celery essential oil. *The Journal of Organic Chemistry* 42:2333-2335.
- Blois MS (1958) Antioxidant determinations by the use of a stable free radical. *Nature* 181:1199-1200.
- Blondeau N, Widmann C, Lazdunski M, Heurteaux C (2002) Polyunsaturated fatty acids induce ischemic and epileptic tolerance. *Neuroscience* 109: 231-241.
- Bohrmann H, Stahl E, Mitsuhashi H (1967) Studies of the constituents of Umbelliferae plants. XIII. Chromatographic studies on the constituents of *Cnidium officinale* Makino. *Chemical & Pharmaceutical Bulletin* 15: 1606-1608
- Bonita R (1992) Epidemiology of stroke. *Lancet* 339: 342-344.
- Brandt T, von Kummer R, Muller-Kupfers M, Hacke W (1996) Thrombolytic therapy

- of acute basilar artery occlusion: variables affecting recanalization and outcome. *Stroke* 27:875-881.
- Bratton SB, Cohen GM (2001) Apoptotic death sensor: an organelle's alter ego? *Trends in Pharmacological Sciences* 22: 306-315.
- Brinker G, Franke C, Hoehn M, Uhlenkuken U, Hossmann KA (1999) Thrombolysis of cerebral clot embolism in rat: effect of treatment delay. *Neuroreport* 10: 3269-3272.
- Budihardjo I, Oliver H, Lutter M, Luo X, and Wang X (1999) Biochemical pathways of caspase activation during apoptosis. *Annual Review of Cell and Developmental Biology* 15:269-290.
- Busto R, Dietrich WD, Globus MY, Ginsberg MD (1989) Postischemic moderate hypothermia inhibits CA1 hippocampal ischemic neuronal injury. *Neuroscience Letters* 101:299-304.
- Cakir A, Mavi A, Yıldırım A, Duru ME, Harmandar M, Kazaz C (2003) Isolation and characterization of antioxidant phenolic compounds from the aerial parts of *Hypericum hyssopifolium* L. by activity-guided fractionation. *Journal of Ethnopharmacology* 87:73-83.
- Caldwell MA, Reymann JM, Allain H, Leonard BE, Bentue-Ferrer D, Caloni F, Spotti M, Pompa G, Zucco F, Stamatii A, Angelis ID (2002) Evaluation of fumonisin B<sub>1</sub> and its metabolites absorption and toxicity on intestinal cells line caco-2. *Toxicol* 40:1181-1188.
- Caplan LR (1992) Intracerebral haemorrhage. *Lancet* 339:656-658.

- Carroll M, Beck O (1992) Protection against hippocampal CA1 cell loss by post-ischemic hypothermia is dependent on delay of initiation and duration. *Metabolic Brain Disease* 7:45–50.
- Cassarino DS, Bennett Jr JP (1999) An evaluation of the role of mitochondria in neurodegenerative diseases: mitochondrial mutations and oxidative pathology, protective nuclear responses, and cell death in neurodegeneration. *Brain Research Reviews* 29: 1-25.
- Castillo J, Davalos A, Noya M (1999) Aggravation of acute ischemic stroke by hyperthermia is related to an excitotoxic mechanism. *Cerebrovascular Diseases* 9: 22-27.
- Cecconi F (1999) Apaf1 and the apoptotic machinery. *Cell death and differentiation* 6: 1087-1098.
- Cervantes M, Gonzalez-Vidal MD, Ruelas R, Escobar A, Morali G (2002) Neuroprotective effects of progesterone on damage elicited by acute global cerebral ischemia in neurons of the caudate nucleus. *Archives of Medical Research* 33: 6-14.
- Chan PH (1996) Role of oxidants in ischemic brain damage. *Stroke* 27: 1124-1129.
- Chan PH (2001) Reactive oxygen radicals in signaling and damage in the ischemic brain. *Journal of Cerebral Blood Flow and Metabolism* 21: 2-14.
- Chan PH, Kinouchi H, Epstein CJ, Carlson E, Chen SF, Imaizumi S, Yang GY (1993) Role of superoxide dismutase in ischemic brain injury: reduction of edema and infarction in transgenic mice following focal cerebral ischemia. *Progress in Brain*

Research 96: 97-104.

Chang Q, Wang XL (2003) Effects of chiral 3-*n*-butylphthalide on apoptosis induced by transient focal cerebral ischemia in rats. *Acta Pharmaceutica Sinica* 24: 796-804.

Charriaut-Marlangue C, Aggoun-Zouaoui D, Represa A, Ben-Ari Y (1996a) Apoptotic features of selective neuronal death in ischemia, epilepsy and gp 120 toxicity. *Trends in Neurosciences* 19: 109-114.

Charriaut-Marlangue C, Ben-Ari Y (1995) A cautionary note on the use of the TUNEL stain to determine apoptosis. *Neuroreport* 7: 61-64.

Charriaut-Marlangue C, Margail I, Represa A, Popovici T, Plotkine M, Ben-Ari Y (1996b) Apoptosis and necrosis after reversible focal ischemia: an in situ DNA fragmentation analysis. *Journal of Cerebral Blood Flow and Metabolism* 16:186-194.

Cheeseman KH (1993) Tissue injury by free radicals. *Toxicology & Industrial Health* 9:39-51.

Chen H, Chopp M, Zhang ZG, Garcia JH (1992) The effect of hypothermia on transient middle cerebral artery occlusion in the rat. *Journal of Cerebral Blood Flow and Metabolism* 12:621-628.

Chen YZ, Zhang HD (1984) Analysis of the chemical ingredients of *Angelica sinensis*. *Chemical Journal of Chinese Universities* 5:515-520.

Chen ZL, Strickland S (1997) Neuronal death in the hippocampus is promoted by plasmin-catalyzed degradation of laminin. *Cell* 91: 917-925.

- Cheng Y, Deshmukh M, D'Costa A, Demaro JA, Gidday JM, Shah A, Sun Y, Jacquin MF, Johnson EM, Holtzman DM (1998) Caspase inhibitor affords neuroprotection with delayed administration in a rat model of neonatal hypoxic-ischemic brain injury. *The Journal of Clinical Investigation* 101: 1992-1999.
- Chinese Acute Stroke Trial (CAST) Collaborative Group (1997): randomised placebo-controlled trial of early aspirin use in 20,000 patients with acute ischaemic stroke. *Lancet* 349:1641-1649.
- Choi DW and Rotham SM (1990) The role of glutamate neurotoxicity in hypoxic-ischemic neuronal death. *Annual Review of Neuroscience* 13:171-182.
- Chong Z and Feng YP (1999) Effect of 3-n-butylphthalide on reperfusion induced lipid peroxidation following cerebral ischemia in rats and superoxide radical formation in vitro. *Journal of Chinese Pharmaceutical Science* 8: 95-99
- Chopp M, Li Y, Jiang N, Zhang RL, Probst J (1996) Antibodies against adhesion molecules reduce apoptosis after transient middle cerebral artery occlusion in rat brain. *Journal of Cerebral Blood Flow and Metabolism* 16: 578-584.
- Cichy M, Wray V, Höfle G (1984) Neue Inhaltsstoffe von *Levisticum officinale* Koch (Liebstöckel). *Liebigs Annalen der Chemie* 397-400.
- Clark RK, Lee EV, White RF, Jonak ZL, Feuerstein GZ, Barone FC (1994) Reperfusion following focal stroke hastens inflammation and resolution of ischemic injured tissue. *Brain Research Bulletin* 35: 387-392.
- Connolly ES Jr, Winfree CJ, Springer TA, Naka Y, Liao H, Yan SD, Stern DM, Solomon RA, Gutierrez-Ramos JC, Pinsky DJ (1996) Cerebral protection in

- homozygous null ICAM-1 mice after middle cerebral artery occlusion. Role of neutrophil adhesion in the pathogenesis of stroke. *The Journal of Clinical Investigation* 97: 209-216.
- Corbett D, Hamilton M, Colbourne F (2000) Persistent neuroprotection with prolonged postischemic hypothermia in adult rats subjected to transient middle cerebral artery occlusion. *Experimental Neurology* 163:200-206.
- Cross DT III, Moran CJ, Akins PT, Angtuaco EE, Diringer MN (1997) Relationship between clot location and outcome after basilar artery thrombolysis. *American Journal of Neuroradiology* 18:1221-1228.
- Cui LY, Li SW, Lu CZ, Dong Q, Dong P, Shi LF, Huang JZ, Mao SY, Zhang CD, Cao YP, Nie YX, Wang WZ, Liang QC, Yang XC, Dong WW, Li GQ, Peng GG, Luo ZM, He L, Wan Q, Han JL, Huang RX, Li L, Li CY, Meng ZZ (2005) The multicentric randomized study of dl-3-butylphthalide in the treatment of acute moderate ischemic stroke. *Chinese Journal of Cerebrovascular Diseases* 18:112-115.
- Davies KJ (1995) Oxidative Stress: the paradox of aerobic life. *Biochemical Society Symposium* 61: 1-31.
- Davis SM, Albers GW, Diener HC, Lees KR, Norris J (1997) Termination of Acute Stroke Studies Involving Selfotel Treatment. ASSIST Steering Committed. *Lancet* 349: 32.
- Dawson DA, Wadsworth G, Palmer AM (2001) A comparative assessment of the efficacy and side effect liability of neuroprotective compounds in experimental

- stroke. Brain Research 892: 344-350.
- Del Zoppo G, Ginis I, Hallenbeck JM, Iadecola C, Wang X, and Feuerstein GZ (2000) Inflammation and stroke: putative role for cytokines, adhesion molecules and iNOS in brain response to ischemia. Brain Pathology 10:95-112.
- Del Zoppo GJ, Higashida RT, Furlan AJ, Pessin MS, Rowley HA, Gent M (1998) PROACT: a phase II randomized trial of recombinant prourokinase by direct arterial delivery in acute middle cerebral artery stroke. Stroke 29: 4-11.
- Delanty N, Dichter MA (2000) Antioxidant therapy in neurologic disease. Archives of Neurology 57: 1265-1270.
- Delgado G, Reza-Garduño RG, Toscano RA, Bye R, and Linares E (1988) Secondary metabolites from the roots of *Ligusticum porteri* (Umbelliferae) X-ray structure of Z-6.6',7.3a'-diligustilide. Heterocycles 27:1305-1312.
- Denizot F, Lang R (1986) Rapid colorimetric assay for cell growth and survival. Modifications to the tetrazolium dye procedure giving improved sensitivity and reliability. Journal of Immunological Methods 89:271-277.
- Dereski MO, Chopp M, Knight RA, Rodolosi LC, Garcia JH (1993) The heterogeneous temporal evolution of focal ischemic neuronal damage in the rat. Acta Neuropathologica 85: 327-333.
- Desagher S and Martinou JC (2000) Mitochondria as the central control point of apoptosis. Trends in Cell Biology 10: 369-377.
- Diener HC (1998) Multinational randomised controlled trial of lubeluzole in acute ischaemic stroke. European and Australian Lubeluzole Ischaemic Stroke Study

- Group. *Cerebrovascular Diseases* 8: 172-181.
- Diener HC (1999) Lubeluzole in acute ischemic stroke treatment. Lack of efficacy in a large phase III study with an 8-hour window. *Stroke* 30: 234.
- Diener HC, Hacke W, Hennerici M, Radberg J, Hantson L, De Keyser J (1996) Lubeluzole in acute ischemic stroke. A double-blind, placebo-controlled phase II trial. Lubeluzole International Study Group. *Stroke* 27: 76-81.
- Dietrich WD, Busto R, Watson BD, Scheinberg P, Ginsberg MD (1987) Photochemically induced cerebral infarction. II. Edema and blood-brain barrier disruption. *Acta Neuropathologica* 72: 326-334.
- Ding C, He QP, Li PA (2004) Activation of cell death pathway after a brief period of global ischemia in diabetic and non-diabetic animals. *Experimental Neurology* 188:421-429.
- Dirnagl U, Iadecola C, Moskowitz MA (1999) Pathobiology of ischemic stroke: an integrated view. *Trends in Neurosciences* 22: 391-397.
- Donnan GA, Davis SM, Chambers BR, Gates PC, Hankey GJ, McNeil JJ, Rosen D, Stewart-Wynne EG, Tuck RR (1996) Streptokinase for acute ischemic stroke with relationship to time of administration: Australian Streptokinase (ASK) Trial Study Group. *Journal of American Medicine Association* 276:961-966.
- Du C, Hu R, Csernansky CA, Hsu CY, Choi DW (1996) Very delayed infarction after mild focal cerebral ischemia: a role for apoptosis? *Journal of Cerebral Blood Flow and Metabolism* 16: 195-201.
- Endres M, Namura S, Shimizu-Sasamala M, Waeber C, Zhang L, Gomez-Isla T,

- Hyman BT, Moskowitz MA (1998) Attenuation of delayed neuronal death after mild focal ischemia in mice by inhibition of the caspase family. *Journal of Cerebral Blood Flow and Metabolism* 18: 238-247.
- Enlimomab Acute Stroke Trial Investigators (1997) The Enlimomab Acute. Stroke Trial: final results. *Cerebrovascular Diseases* 7 (Suppl 4): 18.
- Ezura M, Kagawa S (1992) Selective and superselective infusion of urokinase for embolic stroke. *Surgical Neurology* 38: 353-358.
- Fang HJ, Lu RM, Liu GS, Liu TC (1979) Studies on the components of essential oils II. Comparison of the major constituents of the essential oil from two species of Dang gui [*Angelica sinensis* (Oliv.) Diels] and *Levisticum officinale* Koch. *Acta Pharmaceutica Sinica* 14: 617-623.
- Fehr D (1979) Study on the aroma substances of celery (*Apium graveolens* L.). *Pharmazie* 34: 658-662.
- Fehr D (1981) Study on the aroma substances of celery (*Apium graveolens* L.). *Pharmazie* 36: 374-376.
- Ferrer I, Planas AM (2003) Signaling of cell death and cell survival following focal cerebral ischemia: life and death struggle in the penumbra. *Journal of Neuro pathology and Experimental Neurology* 62: 329-339.
- Fink K, Zhu J, Namura S, Shimizu-Sasamata M, Endres M, Ma J, Dalkara T, Yuan J, Moskowitz MA (1998) Prolonged therapeutic window for ischemic brain damage caused by delayed caspase activation. *Journal of Cerebral Blood Flow and Metabolism* 18: 1071-1076.

- Fisher M, Bogousslavsky J (1998) Further evolution toward effective therapy for acute ischemic stroke. *Journal of American Medicine Association* 279:1298-1303.
- Foglieni C, Meoni C, Davalli AM (2001) Fluorescent dyes for cell viability: an application on prefixed conditions. *Histochemistry & Cell Biology* 115: 223-229.
- Folbergrová J, Memezawa H, Smith ML, Siesjö BK (1992) Focal and perifocal changes in tissue energy state during middle cerebral artery occlusion in normo- and hyperglycemic rats. *Journal of Cerebral Blood Flow Metabolism* 12:25-33.
- Forsting M, Reith W, Dorfler A, Meyding-Lamade U, Sartor K (1994) MRI monitoring of experimental cerebral ischaemia: comparison of two models. *Neuroradiology* 36:264 -268.
- Francel PC, Long BA, Malik JM, Tribble C, Jane JA, Kron IL (1993) Limiting ischemic spinal cord injury using a free radical scavenger 21-aminosteroid and/or cerebrospinal fluid drainage. *Journal of Neurosurgery* 79:742 -751.
- Frizzell RT, Meyer YJ, Borchers DJ, Weprin BE, Allen EC, Pogue WR, Reisch JS, Cherrington AD, Batjer HH (1991) The effects of etomidate on cerebral metabolism and blood flow in a canine model for hypoperfusion. *Journal of Neurosurgery* 74:263-269.
- Fujimura M, Morita-Fujimura Y, Murakami K, Kawase M, Chan PH (1998) Cytosolic redistribution of cytochrome c after transient focal cerebral ischemia in rats. *Journal of Cerebral Blood Flow and Metabolism* 18: 1239-1247.
- Fujimura M, Morita-Fujimura Y, Noshita N, Sugawara T, Kawase M, Chan PH (2000) The cytosolic antioxidant copper/zinc-superoxide dismutase prevents the early

- release of mitochondrial cytochrome c in ischemic brain after transient focal cerebral ischemia in mice. *The Journal of Neuroscience* 20: 2817- 2824.
- Fukuyama N, Takizawa S, Ishida H, Hoshiai K, Shinohara Y (1998) Peroxynitrite formation in focal cerebral ischemia-reperfusion in rats occurs predominantly in the peri-infarct region. *Journal of Cerebral Blood Flow Metabolism* 18:123-129.
- Fulbert JC and Cals MJ (1992) Free radicals in clinical biology. Origin, pathogenic effect and defense mechanisms. *Pathologie-biologie* 40:66-77.
- Furlan A, Higashida R, Wechsler L, Gent M, Rowley H, Kase C, Pessin M, Ahuja A, Callahan F, Clark WM, Silver F, Rivera F (1999) Intra-arterial prourokinase for acute ischemic stroke: the PROACT II study: a randomized controlled trial. *Journal of American Medicine Association* 282:2003-2011.
- Furuichi Y, Noto T, Li JY, Oku T, Ishiye M, Moriguchi A, Aramori I, Matsuoka N , Mutoh S, Yanagihara T (2004) Multiple modes of action of tacrolimus (FK506) for neuroprotective action on ischemic damage after transient focal cerebral ischemia in rats. *Brain Research* 1014: 120-130.
- Furukawa K, Fu W, Li Y, Witke W, Kwiatkowski DJ, Mattson MP (1997) The actin-severing protein gelsolin modulates calcium channel and NMDA receptor activities and vulnerability to excitotoxicity in hippocampal neurons. *The Journal of Neuroscience* 17: 8178-8186.
- Gao YM, Zhang H, Duan ZX (1988) Clinical studies of the essential oil (Ligustilide) from rhizome of *Angelica sinensis* for the treatment of 112 patient amenorrhoea. *Journal of Lanzhou Medical College* 1:36-38.

- Gao Z, Huang K, Yang X, Xu H (1999) Free radical scavenging and antioxidant activities of flavonoids extracted from the radix of *Scutellaria baicalensis* Georgi. *Biochimica et Biophysica Acta* 1472: 643-650.
- Gavrieli Y, Sherman Y, Ben-Sasson SA (1992) Identification of programmed cell death in situ via specific labeling of nuclear DNA fragmentation. *The Journal of Cell Biology* 119: 493-501.
- Gerhmann J, Bonnekoh P, Miyazawa T, Hossmann KA, Kreutzberg GW (1992) Immunocytochemical study of an early microglial activation in ischemia. *Journal of Cerebral Blood Flow Metabolism* 12:257-269.
- Gillardon F, Kiprianova I, Sandkuhler J, Hossmann KA, Spranger M (1999) Inhibition of caspases prevents cell death of hippocampal CA1 neurons, but not impairment of hippocampal long-term potentiation following global ischemia. *Neuroscience* 93: 1219-1222.
- Ginsberg MD (2003) Adventures in the pathophysiology of brain ischemia: penumbra, gene expression, neuroprotection. The 2002 Thomas Willis Lecture. *Stroke* 34: 214-223.
- Ginsberg MD, Sternau LL, Globus MY, Dietrich WD, Busto R (1992) Therapeutic modulation of brain temperature: relevance to ischemic brain injury. *Cerebrovascular and Brain Metabolism Reviews* 4:189-225.
- Gong C, Qin Z, Betz AL, Liu XH, Yang GY (1998) Cellular localization of tumor necrosis factor alpha following focal cerebral ischemia in mice. *Brain Research* 801: 1-8.

- Green AR, Cross AJ (1994) The neuroprotective actions of chlormethiazole. *Progress in Neurobiology* 44:463-484.
- Green DR, Reed JC (1998) Mitochondria and apoptosis. *Science* 281:1309-1312.
- Green LC, Wagner DA, Glogowski J (1982) Analysis of nitrite, nitrate, and [<sup>15</sup>N]nitrate in biological fluids. *Analytical Biochemistry* 126:131-138.
- Greenamyre JT and Porter RH (1994) Anatomy and physiology of glutamate in the CNS. *Neurology* 44: S7-13.
- Grond M, Rudolf J, Schmulling S, Stenzel C, Neveling M, Heiss WD (1998) Early intravenous thrombolysis with recombinant tissue-type plasminogen activator in vertebrobasilar ischemic stroke. *Archives of Neurology*. 55:466-469.
- Grotta J (1997) Lubeluzole treatment of acute ischemic stroke. The US and Canadian Lubeluzole Ischemic Stroke Study Group. *Stroke* 28: 2338-2346.
- Guo Q, Zhao B, Li M, Shen S, Xin W (1996) Studies on protective mechanisms of four components of green tea polyphenols against lipid peroxidation in synaptosomes. *Biochimica et Biophysica Acta* 1304: 210-222.
- Hacke W, Kaste M, Fieschi C, Toni D, Lesaffre E, von Kummer R, Boysen G, Bluhmki E, Hoxter G, Mahagne MH (1995) Intravenous thrombolysis with recombinant tissue plasminogen activator for acute hemispheric stroke. The European Cooperative Acute Stroke Study (ECASS). *Journal of American Medicine Association* 274: 1017-1025.
- Haley EC Jr (1998) High-dose tirilazad for acute stroke (RANTTAS II). RANTTAS II Investigators. *Stroke* 29: 1256-1257.

- Hall ED, Andrus PK, Pazara KE (1993) Protective effect of a hypothermic pharmacological agent in gerbil forebrain ischemia. *Stroke* 24: 711-715.
- Halliwell B, Gutteridge JM (1989) *Free radicals in biology and medicine*. Oxford: Clarendon Press, p 23-30.
- Halliwell B, Gutteridge JM, Cross CE (1992) Free radicals, antioxidants, and human disease: where are we now. *The Journal of Laboratory and Clinical Medicine* 119: 598-620.
- Hammer MD, Krieger DW (2003) Hypothermia for Acute Ischemic Stroke: Not just another neuroprotectant. *Neurologist* 9: 280-289.
- Hankey GJ, Sandercock P, Counsell C, Stobbs SL (2005) Low-Molecular-Weight Heparins or Heparinoids Versus Standard Unfractionated Heparin for Acute Ischemic Stroke. *Stroke* 36: 2045-2046.
- Hansen MB, Nielsen SE, Berg K (1989) Re-examination and further development of a precise and rapid dye method for measuring cell growth/cell kill. *Journal of Immunological Method* 119:203-210.
- Hara H, Friedlander RM, Gagliardini V, Ayata C, Fink K, Huang Z, Shimizu-Sasamata M, Yuan J, Moskowitz MA (1997) Inhibition of interleukin-1beta converting enzyme family proteases reduces ischemic and excitotoxic neuronal damage. *Proceedings of the National Academy of Sciences of the United States of America* 94:2007-2012.
- Haraguchi T, Ding DQ, Yamamoto A, Kaneda T, Koujin T, Hiraoka Y (1999) Multiple-color fluorescence imaging of chromosomes and microtubules in living

- cells. *Cell Structure and Function* 24:291-298.
- Haring HP, Berg EL, Tsurushita N, Tagaya M, Del Zoppo GJ (1996) E-selectin appears in nonischemic tissue during experimental focal cerebral ischemia. *Stroke* 27: 1386-1391.
- Harrison DC, Davis RP and Bond BC (2001) Caspase mRNA expression in a rat model of focal cerebral ischemia. *Molecular Brain Research* 89:113-146.
- Hartmann A, Troadec JD, Hunot S, Kikly K, Faucheux BA, Mouatt-Prigent A, Ruberg M, Agid Y, Hirsch EC (2001) Caspase-8 is an effector in apoptotic death of dopaminergic neurons in Parkinson's disease, but pathway inhibition results in neuronal necrosis. *The Journal of Neuroscience* 21: 2247-2255.
- Hidalgo IJ, Raub TJ, Borchardt RT (1989) Characterization of the human colon carcinoma cell line (Caco-2) as a model system for intestinal epithelial permeability. *Gastroenterology* 96: 736-749.
- Hidalgo IJ, Raub TJ, Borchardt RT (1989) Characterization of the human colon carcinoma cell line (Caco-2) as a model system for intestinal epithelial permeability. *Gastroenterology* 96: 736-749.
- Hilgers AR, Conradi RA, Burton PS (1990) Caco-2 cell monolayers as a model for drug transport across the intestinal mucosa. *Pharmaceutical Research* 7: 902-10.
- Himi T, Ishizaki Y, Murota S (1998) A caspase inhibitor blocks ischemia-induced delayed neuronal death in gerbil. *European Journal of Neurosciences* 10: 777-781.
- Hisayuki K, Ikunori S (1992) Evaluation of *Angelicae radix*. I. Purification method and stability of ligustilide. *Hiroshima-ken Eisei Kenkyusho Kenkyu Hokoku* 39:

23-26.

Hommel M (1998) Fraxiparine in ischaemic stroke study (FISS bis). *Cerebrovascular Diseases* 8: A64.

Hon PM, Lee CM, Choang TF, Chui KY, Wong HNC (1990) A Ligustilide dimer from *Angelica Sinensis*. *Phytochemistry* 29:1189-1191.

Horsburgh K, Macrae IM, Carswell H (2002) Estrogen is neuroprotective via an apolipoprotein E-dependent mechanism in a mouse model of global ischemia. *Journal of Cerebral Blood Flow and Metabolism* 22:1189-1195.

Hu DB and Li SW (2004) Effects of vitamin E and 3-n-butylphthalide on the production of NO and the expression of iNOS induced by chronic episodic hypoxia. *Chinese Journal of Neuroscience* 20: 140-144.

Hunter J, Jepson MA, Tsuruo T, Simmons NL, Hirst BH. (1993) Functional expression of P-glycoprotein in apical membranes of human intestinal caco-2 cells. *Journal of Biological Chemistry* 268 :14991-14997.

Iadecola C (1997) Bright and dark sides of nitric oxide in ischemic brain injury. *Trends in Neurosciences* 20: 132-139.

Iadecola C, Salkowski CA, Zhang F, Aber T, Nagayama M, Vogel SN, Ross ME (1999) The transcription factor interferon regulatory factor 1 is expressed after cerebral ischemia and contributes to ischemic brain injury. *Journal of Experimental Medicine* 189: 719-727.

Iadecola C, Zhang F, Casey R, Nagayama M, Ross ME (1997) Delayed reduction of ischemic brain injury and neurological deficits in mice lacking the inducible nitric

- oxide synthase gene. *The Journal of Neuroscience* 17: 9157-9164.
- Ikonomidou C and Turski L (2002) Why did NMDA receptor antagonists fail clinical trials for stroke and traumatic brain injury? *Lancet Neurology* 1: 383-386.
- Imaizumi S, Woolworth V, Fishman RA, Chan PH (1990) Liposome-entrapped superoxide dismutase reduces cerebral infarction in cerebral ischemia in rats. *Stroke* 21: 1312-1317.
- Isenmann S, Stoll G, Schroeter M, Krajewski S, Reed JC, Bahr M (1998) Differential regulation of Bax, Bcl-2, and Bcl-X proteins in focal cortical ischemia in the rat. *Brain Pathology* 8: 49-62.
- Ivacko J, Szaflarski J, Malinak C, Flory C, Warren JS, Silverstein FS, (1997) Hypoxic-ischemic injury induces monocyte chemoattractant protein-1 expression in neonatal rat brain. *Journal of Cerebral Blood Flow and Metabolism* 17: 759-770.
- Janero DR (1990) Malondialdehyde and thiobarbituric acid reactivity as diagnostic indices of lipid peroxidation and peroxidative tissue injury. *Free Radical Biology & Medicine* 9: 515-540.
- Kameyama M (1985) A new model of bilateral hemispheric ischemia in the rat—three vessel occlusion model. *Stroke* 16:489-493.
- Kammersgaard LP, Jorgensen HS, Rungby JA, Reith J, Nakayama H, Weber UJ, Houth J, Olsen TS (2002) Admission body temperature predicts long-term mortality after acute stroke. The Copenhagen Stroke Study. *Stroke* 33: 1759-1762.

- Kammersgaard LP, Jorgensen HS, Rungby JA, Reith J, Nakayama H, Weber UJ, Houth J, Olsen TS (2002) Admission body temperature predicts long-term mortality after acute stroke. The Copenhagen Stroke Study. *Stroke* 33: 1759-1762.
- Kanita T, Tsutsui F, Matsuda M, Yamashita A, Kozaka N, Sekida S, Satake M. Smooth muscle relaxants, their extraction from *Angelica sinensis* and compositions containing the smooth muscle relaxants. [P] JP: 09077666, 1995.
- Kaouadji M, Madeleine PB, Mariotte AM (1983) (Z)-Ligustilidiol, nouveau phthalide hydroxyle isole de *Ligusticum Wallichii*. *Tetrahedron Letters* 24:4675-4676.
- Kaouadji M, Pachtere FD, Pouget C, Albert JC (1986) Three additional phthalide derivatives, an epoxy monomer and two dimers, from *Ligusticum Wallichii* Rhizomes. *Journal of Natural Products* 49:872-877.
- Katsura K, Kristian T and Siesjo BK (1994) Energy metabolism, ion homeostasis, and cell damage in the brain. *Biochemical Society Transactions* 22: 991-996.
- Kawai N, Nakamura T, Okauchi M, Nagao S (2000) Effects of hypothermia on intracranial pressure and brain edema formation: studies in a rat acute subdural hematoma model. *Journal of Neurotrauma* 17:193-202.
- Kawamura S, Suzuki A, Hadeishi H, Yasui N, Hatazawa J (2000) Cerebral blood flow and oxygen metabolism during mild hypothermia in patients with subarachnoid haemorrhage. *Acta Neurochirurgica* 142:1117-1121.
- Kay R, Wong KS, Yu YL, Chan YW, Tsoi TH, Ahuja AT, Chan FL, Fong KY, Law CB, Wong A (1995) Low-molecular-weight heparin for the treatment of acute

- ischemic stroke. *The New England Journal of Medicine* 333:1588-1593.
- Kerr JF, Wyllie AH, Currie AR (1972) Apoptosis: a basic biological phenomenon with wide-ranging implications in tissue kinetics. *British Journal of Cancer* 26: 239-257.
- Kidwell CS, Liebeskind DS, Starkman S, Saver JL (2001) Trends in acute ischemic stroke trials through the 20<sup>th</sup> century. *Stroke* 32: 1349-1359.
- Kim DM, Lee SJ, Kim IC, Kim ST, Byun SM (2000) Asp41-His48 region of streptokinase is important in binding to a substrate plasminogen. *Thrombosis Research* 99:93-98.
- Kim GW, Sugawara T, Chan PH (2000) Involvement of oxidative stress and caspase-3 in cortical infarction after photothrombotic ischemia in mice. *Journal of Cerebral Blood Flow and Metabolism* 20: 1690-1701.
- Kirino T (1982) Delayed neuronal death in the gerbil hippocampus following ischemia. *Brain Research* 239: 57-69.
- Kirino T, Tamura A, Sano K (1986) A reversible type of neuronal injury following ischemia in the gerbil hippocampus. *Stroke* 17:455-459.
- Kitagawa K, Matsumoto M, Yang G, Mabuchi T, Hon M, Yanagihara T (1998) Cerebral ischemia after bilateral carotid artery occlusion and intraluminal structure occlusion in mice: evaluation of the potency of the posterior communicating artery. *Journal of Cerebral Blood Flow and Metabolism* 18: 570-579.
- Knowles RG, Salter M, Brooks SL, Moncada S (1990) Anti-inflammatory glucocorticoids inhibit the induction by endotoxin of nitric oxide synthase in the

- lung, liver and aorta of the rat. *Biochemical Biophysical Research Communications* 172: 1042-1048.
- Ko WC (1980) A newly isolated antispasmodic-butylidenephthalide. *Japanese Journal of Pharmacology* 30: 85-91.
- Ko WC, Lin SC, Yeh CY, Wang YT (1977) Alkylphthalides isolated from *Ligusticum wallichii* Franch and their in vitro inhibitory effect on rat uterine contraction induced by prostaglandin F<sub>2</sub>α. *Taiwan Yixuehui Za Zhi* 76: 669-677.
- Kobayashi M, Fujita M, Mitsuhashi H (1984) Components of *Cnidium officinale* Makino: Occurrence of pregnenolone, coniferyl ferulate, and hydroxyphthalides. *Chemical & Pharmaceutical Bulletin* 32:3770-3773.
- Kobayashi M, Fujita M, Mitsuhashi H (1987) Studies on the constituents of Umbelliferae Plants. XV. Constituents of *Cnidium officinale*: occurrence of pregnenolone, coniferylferulate and hydroxyphthalides. *Chemical & Pharmaceutical Bulletin* 35:1427-1433.
- Kobayashi M, Mitsuhashi H (1987) Studies on the constituents of Umbelliferae Plants. XVII. Structures of three new ligustilide derivatives from *Ligusticum wallichii*. *Chemical & Pharmaceutical Bulletin* 35:4789-4792.
- Kobayashi S, Mimura Y, Naitoh T, Kimura I, Kimura M (1993) Chemical structure-activity of *Cnidium* rhizome-derived phthalides for the competence inhibition of proliferation in primary cultures of mouse aorta smooth muscle cells. *Japanese Journal of Pharmacology* 63: 353-359
- Kobayashi S, Mimura Y, Notoya K, Kimura I, Kimura M (1992) Antiproliferative

effects of the traditional Chinese medicine Shimotsu-To, its component Cnidium rhizome and derived compounds on primary cultures of mouse aorta smooth muscle cells. *Japanese Journal of Pharmacology* 60: 397-401.

Kogure K and Kato H (1993) Altered gene expression in cerebral ischemia. *Stroke* 24: 2121-2127.

Koh JY, Suh SW, Gwag BJ, He YY, Hsu CY, Choi DW (1996) The role of zinc in selective neuronal death after transient global cerebral ischemia. *Science* 272: 1013-1016.

Koistinaho J, Hokfelt T (1997) Altered gene expression in brain ischemia. *Neuroreport* 8: i - viii.

Komine-Kobayashi M, Chou N, Mochizuki H, Nakao A, Mizuno Y, Urabe T (2004) Dual role of Fcγ receptor in transient focal cerebral ischemia in mice. *Stroke* 35: 958-963.

Kondo Y, Ogawa N, Asanuma M, Ota Z, Mori A (1995) Regional differences in late-onset iron deposition, ferritin, transferrin, astrocyte proliferation, and microglial activation after transient forebrain ischemia in rat brain. *Journal of Cerebral Blood Flow and Metabolism* 15: 216-226.

Krajewski S, Mai JK, Krajewska M, Sikorska M, Mossakowski MJ, Reed JC (1995) Upregulation of bax protein levels in neurons following cerebral ischemia. *The Journal of Neuroscience* 15: 6364-6376.

Krieger DW, De Georgia MA, Abou-Chebl A, Sila CA, Katzan IL, Mayberg MR, Furlan AJ (2001) Cooling for acute ischemic brain damage (COOL AID): an open

pilot study of induced hypothermia in acute ischemic stroke. *Stroke* 32:1847-1854.

Krishna G, Chen K, Lin C, Nomeir AA (2001) Permeability of lipophilic compounds in drug discovery using in-vitro human absorption model, Caco-2. *International Journal of Pharmaceutics* 222: 77-89.

Kroemer G, Reed JC (2000) Mitochondrial control of cell death. *Nature Medicine* 6: 513-519.

Kwiatkowski TG, Libman RB, Frankel M, Tilley BC, Morgenstern LB, Lu M, Broderick JP, Lewandowski CA, Marler JR, Levine SR, Brott T (1999) Effects of tissue plasminogen activator for acute ischemic stroke at one year. *The New England Journal of Medicine* 340:1781-1787.

Labat-Moleur F, Guillermet C, Lorimier P, Robert C, Lantuejoul S, Brambilla E, Negoescu A (1998) TUNEL apoptotic cell detection in tissue sections: critical evaluation and improvement. *The Journal of Histochemistry and Cytochemistry* 46:327-334.

Labeque R, Marnett LJ (1987) 10-Hydroperoxy-8, 12-octadecadienoic acid: a diagnostic probe of alkoxyl radical generation in metal-hydroperoxide reaction. *Journal of the American Chemical Society* 109:2828-2829.

Lee JM, Zipfel GJ, Choi DW (1999) The changing landscape of ischaemic brain injury mechanisms. *Nature* 399: A7-A14.

Lees KR (1997) Cerestat and other NMDA antagonists in ischemic stroke. *Neurology* 49 (Suppl. 4): S66-69.

Legos JJ, Mangoni AA, Read SJ, Campbell CA, Irving EA, Roberts J, Barone FC,

- Parsons AA (2002) Programmable microchip monitoring of post-stroke pyrexia: effects of aspirin and paracetamol on temperature and infarct size in the rat. *Journal of Neuroscience Methods* 113: 159-166.
- Lei B, Popp S, Capuano-Waters C, Cottrell JE, Kass IS (2004) Lidocaine attenuates apoptosis in the ischemic penumbra and reduces infarct size after transient focal cerebral ischemia in rats. *Neuroscience* 125: 691-701.
- Leist M and Nicotera P (1998) Apoptosis, excitotoxicity, and neuropathology. *Experimental Cell Research* 239: 183-201.
- Leist M, Single B, Castoldi AF, Kühnle S, Nicotera P (1997) Intracellular adenosine triphosphate (ATP) concentration: a switch in the decision between apoptosis and necrosis. *The Journal of Experimental Medicine* 185:1481-1486.
- Lemaire C, Andreau K, Souvannavong V, Adam A (1998) Inhibition of caspase activity induces a switch from apoptosis to necrosis. *FEBS Letters* 425: 266-270.
- Lesage AS, Peeters L, Leysen JE (1996) Lubeluzole, a novel long-term neuroprotectant, inhibits the glutamate-activated nitric oxide synthase pathway. *The Journal of Pharmacology and Experimental Therapeutics* 279: 759-766.
- Levine S, Sohn D (1969) Cerebral ischemia in infant and adult gerbils, relation to incomplete circle of Willis. *Archives of Pathology & Laboratory Medicine* 87: 315-317.
- Li GS, MA CJ, LIU ZF, LIU K (2001) Extraction of essential oil from *Angelica sinensis* by supercritical-CO<sub>2</sub> fluid in comparison with that by steam distillation. *Chinese Traditional and Herbal Drugs* 32: 581-583.

- Li HX, Ding MY, Yu JY (2002) Separation and Identification of the phthalic anhydride derivatives of *Ligusticum chuanxiong* Hort by GC-MS, TLC, HPLC-DAD, and HPLC-MS. *Journal of Chromatographic Science* 40: 156-161.
- Li PA, He QP, Miyashita H, Howllet W, Siesjo BK, Shuaib A (1999) Hypothermia ameliorates ischemic brain damage and suppresses the release of extracellular amino acids in both normo- and hyperglycemic subjects. *Experimental Neurology* 158: 242-253.
- Li Y, Powers C, Jiang N, Chopp M (1998) Intact, injured, necrotic and apoptotic cells after focal cerebral ischemia in the rat. *Journal of the Neurological Sciences* 156: 119-132.
- Li Y, Sharov VG, Jiang N, Zaloga C, Sabbah HN, Chopp M (1995) Ultrastructural and light microscopic evidence of apoptosis after middle cerebral artery occlusion in the rat. *American Journal of Pathology* 146: 1045-1051.
- Lin LZ, He XG, Lian LZ, Wayne K, Jerry E (1998) Liquid chromatographic-electrospray mass spectrometric study of the phthalides of *Angelica sinensis* and chemical changes of Z-ligustilide. *Journal of Chromatography A* 810: 71-79.
- Lin LZ, He XG, Lian LZ, Wayne K, Jerry E (1998) Liquid Chromatographic-electrospray mass spectrometric study of phthalide *Angelica sinensis* and chemical changes of Z-Ligustilide. *Journal of Chromatography A* 810:71-79.
- Lin M, Zhu GD, Sun QM, Fang QC (1979) Chemical studies of *Angelica sinensis*.

- Acta Pharmaceutica Sinica 14:529-534.
- Lindsberg PJ, Carpen O, Paetau A, Karjalainen-Lindsberg ML, Kaste M (1996) Endothelial ICAM-1 expression associated with inflammatory cell response in human ischemic stroke. *Circulation* 94: 939-945.
- Liu XG and Feng YP (1995) Protective effect of dl-3-n-butylphthalide on ischemic neurological damage and abnormal behavior. *Acta Pharmaceutica Sinica* 30:896-903.
- Liu Y, Peterson DA, Kimura H, Schubert D (1997) Mechanism of cellular 3-(4,5-dimethylthiazol-2-yl)-2,5-diphenyltetrazolium bromide (MTT) reduction. *Journal of Neurochemistry* 69:581-593.
- Lizano S, Johnston KH (1995) Streptokinase-mediated plasminogen activation using a recombinant dual fusion protein construct. A novel approach to study bacterial-host protein interactions. *Journal of Microbiological Methods* 23:261-280.
- Loddick SA, Rothwell NJ (1996) Neuroprotective effects of human recombinant interleukin-1 receptor antagonist in focal cerebral ischaemia in the rat. *Journal of Cerebral Blood Flow and Metabolism* 16: 932-940.
- Loetscher H, Niederhauser O, Kemp J, Gill R (2001) Is caspase-3 inhibition a valid therapeutic strategy in cerebral ischemia? *Drug Discovery Today* 6: 671-680.
- Longa EZ, Weinstein PR, Carlson S, Cummins R (1989) Reversible middle cerebral artery occlusion without craniectomy in rats. *Stroke* 20:84-91.
- Luo YM, Pan JG, Ding KP, Yan ZM (1996) Anticonvulsive constituents in the essential oil of Chaxiong (*Ligusticum sinense* Oliv cv. Chaxiong). *Chinese*

Traditional and Herbal Drugs 27: 456-457.

Lyden P, Brott T, Tilley B, Welch KM, Mascha EJ, Levine S, Haley EC, Grotta J,

Marler J (1994) Improved reliability of the NIH Stroke Scale using video training.

Stroke 25:2220-2226.

Mabuchi T, Kitagawa K, Ohtsuki T, Kuwabara K, Yagita Y, Yanagihara T, Hori M,

Matsumoto M (2000) Contribution of microglia/macrophages to expansion of infarction and response of oligodendrocytes after focal cerebral ischemia in rats.

Stroke 31: 1735-1743.

Maciorowski Z, Delic J, Padoy E, Klijanienko J, Dubray B, Cosset JM, Dumont J,

Magdelenat H, Vielh P (1998) Comparative analysis of apoptosis measured by

Hoechst and flow cytometry in non-Hodgkin's lymphomas. Cytometry 32: 44-50.

MacManus JP, Linnik MD (1997) Gene expression induced by cerebral ischemia. An

apoptotic perspective. Journal of Cerebral Blood Flow and Metabolism 17:

815-832.

Maier CM, Ahern K, Cheng ML, Lee JE, Yenari MA, Steinberg GK (1998) Optimal

depth and duration of mild hypothermia in a focal model of transient cerebral ischemia: effects on neurologic outcome, infarct size, apoptosis, and inflammation.

Stroke 29:2171-2180.

Mangili F, Cigala C, Santambrogio G (1999) Staining apoptosis in paraffin sections.

Advantages and limits. Analytical and Quantitative Cytology and Histology 21:

273-276.

Marletta MA (1989) Nitric oxide biosynthesis and biological significance. Trends in

- Biochemical Sciences 14: 488- 492.
- Marletta MA (1993) Nitric Oxide Synthase: function and mechanism. *Advances in Experimental Medicine and Biology* 338:281-284.
- Martin RL, Lloyd HG and Cowan AI (1994) The early events of oxygen and glucose deprivation: setting the scene for neuronal death? *Trends in Neurosciences* 17: 251-257.
- Martin U, Bader R, Boehm E, Kohnert U, von Moellendorf E, Fischer S, Sponer G (1993) A novel recombinant plasminogen activator. *Cardiovascular Drug Reviews* 11:299-311.
- Martin U, Fischer S, Kohnert U, Rudolph R, Sponer G, Stern A, Strein K (1991) Coronary thrombolytic properties of a novel recombinant plasminogen activator (BM 06.022) in a canine model. *Journal of Cardiovascular Pharmacology* 18:111-119.
- Mason DY, Sammons R (1978) Alkaline phosphatase and peroxidase for double immunoenzymatic labelling of cellular constituents. *Journal of Clinical Pathology* 31:454-460.
- Massieu L, Thedinga KH, McVey M, Fagg GE (1993) A comparative analysis of the neuroprotective properties of competitive and uncompetitive N-methyl-D-aspartate receptor antagonists in vivo: implications for the process of excitotoxic degeneration and its therapy. *Neuroscience* 55: 883-892.
- Matsumoto K, Kohno SI, Ojima K, Tezuka Y, Kadota S, Watanabe H (1998) Effects of methylene chloride-soluble fraction of Japanese Angelica root extract,

- ligustilide and butylidenephthalide, on pentobarbital sleep in group-housed and socially isolated mice. *Life Sciences* 62: 2073-2082.
- Matsunaga M, Ohtaki H, Takaki A, Iwai Y, Yin L, Mizuguchi H, Miyake T, Usumi K, Shioda S (2003) Nucleoprotamine diet derived from salmon soft roe protects mouse hippocampal neurons from delayed cell death after transient forebrain ischemia. *Neuroscience Research* 47: 269-276.
- Menzies SA, Hoff JT, Betz AL (1992) Middle cerebral artery occlusion in rats: a neurological and pathological evaluation of a reproducible model. *Neurosurgery* 31:100-106.
- Mhairi Macrae I (1992) New models of focal cerebral ischemia. *British Journal of Clinical Pharmacology* 34: 302-308.
- Michaelis EK (1998) Molecular biology of glutamate receptors in the central nervous system and their role in excitotoxicity, oxidative stress and aging. *Progress in Neurobiology* 54: 369-415.
- Mihaljevic B, Katusin-Razem B, Razem D (1996) The reevaluation of the ferric thiocyanate assay for lipid hydroperoxides with special considerations of the mechanistic aspects of the response. *Free Radical Biology & Medicine* 21:53-63.
- Minamisawa H, Smith ML, Siesjo BK (1990) The effect of mild hypothermia and hypothermia on brain damage following 5, 10, and 15 minutes of forebrain ischemia. *Annals of Neurology* 28:26-33.
- Minger SL, Geddes JW, Holtz ML, Craddock SD, Whiteheart SW, Siman RG, Pettigrew LC (1998) Glutamate receptor antagonists inhibit calpain-mediated

- cytoskeletal proteolysis in focal cerebral ischemia. *Brain Research* 810:181-199
- Mink RB, Dutka AJ, Hallenbeck JM (1991) Allopurinol pretreatment improves evoked response recovery following global cerebral ischemia in dogs. *Stroke* 22:660-665.
- Mitsuhashi H and Muramatsu T (1964) Studies on the Constituents of Umbelliferae Plants-IX Structure of Cnidilide and Neocnidilide. *Tetrahedron* 20:1971-1982.
- Mitsuhashi H, Nagai U, Muramatsu T (1961) Studies on the constituents of Umbelliferae plants. III. Structure of ligustilide. *Chemical & Pharmaceutical Bulletin* 9:115-119.
- Mitsuhashi H, Nagai U, Muramatsu T, Tashiro H (1960) Studies on the constituents of Umbelliferae plants. II. Isolation of the active principles of Ligusticum root. *Chemical & Pharmaceutical Bulletin* 8:243-245.
- Miyazawa M, Tsukamoto T, Anzai J, Ishikawa Y (2004) Insecticidal effect of phthalides and furanocoumarins from *Angelica acutiloba* against *Drosophila melanogaster*. *The Journal of Agricultural & Food Chemistry* 52: 4401-4405.
- Moreira PI, Siedlak SL, Aliev G, Zhu X, Cash AD, Smith MA, Perry G (2005) Oxidative stress mechanisms and potential therapeutics in Alzheimer disease. *Journal of Neural Transmission* 112: 921-31.
- Moreira PI, Smith MA, Zhu X, Santos MS, Oliveira CR, Perry G (2004) Therapeutic potential of oxidant mechanisms in Alzheimer's disease. *Expert Review of neurotherapeutics* 4:995-1004.
- Mori E, Tabuchi M, Yoshida T, Yamadori A (1988) Intracarotid urokinase with

- thromboembolic occlusion of the middle cerebral artery. *Stroke* 19:802-812.
- Mori E, Yoneda Y, Tabuchi M, Yoshida T, Ohkawa S, Ohsumi Y, Kitano K, Tsutsumi A, Yamadori A (1992) Intravenous recombinant tissue plasminogen activator in acute carotid artery territory stroke. *Neurology* 42:976-982.
- Mosmann T (1983) Rapid colorimetric assay for growth and survival: application to proliferation and cytotoxicity assay. *Journal of Immunological Method* 65:55-63.
- Muir KW, Lees KR (1995) Clinical experience with excitatory amino acid antagonist drugs. *Stroke* 26: 503-513.
- Murphy TH, Miyamoto M, Sastre A, Schnaar RL, Coyle JT (1989) Glutamate toxicity in a neuronal cell line involves inhibition of cystine transport leading to oxidative stress. *Neuron* 2: 1547-1558.
- Naito T, Ireya Y, Okada M, Mistubishi H, Maruno M (1996) Two phthalides from *Ligusticum chuanxiong*. *Phytochemistry* 41: 233-236.
- Naito T, Katsuhara T, Niitsu K, Ikeya Y, Okada M and Mitsuhashi LH (1991) Phthalide Dimers from *Ligusticum chuanxiong* Hort. *Heterocycles* 32:2433-2442.
- Naito T, Katsuhara T, Niitsu K, Ikeya Y, Okada M, Mitsuhashi H (1992) Two phthalides from *Ligusticum chuanxiong*. *Phytochemistry* 31: 639-642.
- Naito T, Kubota K, Shimoda Y, Sato T, Ikeya Y, Okada M, Maruno M (1995) Effects of constituents of a Chinese crude drug, *Ligustici chuanxiong* rhizoma, on vasoconstriction and blood viscosity. *Natural Medicines* 49: 288-292.
- Nakagawa T, Zhu H, Morishima N, Li E, Xu J, Yankner BA, Yuan J (2000) Caspase-12 mediates endoplasmic-reticulum-specific apoptosis and cytotoxicity

- by amyloid-beta. *Nature* 403: 98-103.
- Nakane PK, Pierce GB, Jr. (1967) Enzyme-labeled antibodies for the light and electron microscopic localization of tissue antigens. *The Journal of cell biology.* 33:307-318.
- Nakase H, Kempinski OS, Heimann A, Takeshima T, Tintera J (1997) Microcirculation after cerebral venous occlusions as assessed by laser Doppler scanning. *Journal of Neurosurgery* 87: 307-314.
- Nakayama R, Yano T, Ushijima K, Abe E, Terasaki H (2002) Effects of dantrolene on extracellular glutamate concentration and neuronal death in the rat hippocampal CA1 region subjected to transient ischemia. *Anesthesiology* 96:705-710.
- Namura S, Nagata I, Takami S, Masayasu H, Kikuchi H (2001) Ebselen reduces cytochrome c release from mitochondria and subsequent DNA fragmentation after transient focal cerebral ischemia in mice. *Stroke* 32: 1906-1911.
- Namura S, Zhu J, Fink K, Endres M, Srinivasan A, Tomaselli KJ, Yuan J, and Moskowitz MA (1998) Activation and cleavage of caspase-3 in apoptosis induced by experimental cerebral ischemia. *The Journal of Neuroscience* 18:3659-3668.
- Naves YR (1943) Volatile plant materials. XXIV. Composition of the essential oil and resinoid of lovage root. *Helvetica Chimica Acta* 26:1281-1295.
- Nicholson DW, Thornberry NA (1997) Caspases: killer proteases. *Trends in Biochemical Sciences* 22: 299-306.
- Nicotera P, Leist M, Fava E, Berliocchi L, Volbracht C (2000) Energy requirement for caspase activation and neuronal cell death. *Brain Pathology* 10: 276-282.

- Nicotera P, Leist M, Ferrando-May E (1998) Intracellular ATP, a switch in the decision between apoptosis and necrosis. *Toxicology Letters* 102/103:139-142.
- Nogawa S, Forster C, Zhang F, Nagayama M, Ross ME, Iadecola C (1998) Interaction between inducible nitric oxide synthetas and cyclooxygenase-2 after cerebral ischemia. *Proceedings of the National Academy of Sciences of the United States of America* 95: 10966-10971.
- Nogawa S, Zhang F, Ross ME, Iadecola C (1997) Cyclooxygenase-2 gene expression in neurons contributes to ischemic brain damage. *The Journal of Neuroscience* 17: 2746-2755.
- Noor R, Wang CX, Shuaib A (2003) Effects of hyperthermia on infarct volume in focal embolic model of cerebral ischemia in rats. *Neuroscience Letters* 349: 130-132.
- Northington FJ, Ferriero DM, Flock DL, Martin LJ (2001) Delayed neurodegeneration in neonatal rat thalamus after hypoxia–ischemia is apoptosis. *The Journal of Neuroscience* 21: 1931-1938.
- Noshita N, Sugawara T, Fujimura M, Morita-Fujimura Y, and Chan PH (2001) Manganese superoxide dismutase affects cytochrome c release and caspase-9 activation after transient focal cerebral ischemia in mice. *Journal of Cerebral Blood Flow and Metabolism* 21:557-567.
- Ogden JE, Moore PK (1995) Inhibition of nitric oxide synthase-potential for a novel class of therapeutic agent? *Trends in Biotechnology* 13: 70-78.
- Ohkawa H, Ohishi N, Yagi K (1979) Assay for lipid peroxides in animal tissues by

- thiobarbituric acid reaction. *Analytical Biochemistry* 95:351-358.
- O'Neill LA and Kaltschmidt C (1997) NF-kappa B: a crucial transcription factor for glial and neuronal cell function. *Trends in Neurosciences* 20: 252-258.
- Onténiente B, Couriaud C, Braudeau J, Benchoua A, Guegan C (2003) The mechanisms of cell death in focal cerebral ischemia highlight neuroprotective perspectives by anti-caspase therapy. *Biochemical Pharmacology* 66: 1643-1649.
- Ozaki Y, Sekita S, Harada M (1989) Centrally acting muscle relaxant effect of phthalides (ligustilide, cnidilide and senkyunolide) obtained from *Cnidium officinale* Makino. *Yakugaku Zasshi. Journal of the Pharmaceutical Society of Japan* 109:402-406.
- Ozawa S, Kamiya H, Tsuzuki K (1998) Glutamate receptors in the mammalian central nervous system. *Progress in Neurobiology* 54: 581-618.
- Pabello NG, Tracy SJ, Keller RW Jr (2004) Protective effects of brief intra- and delayed postischemic hypothermia in a transient focal ischemia model in the neonatal rat. *Brain Research* 995:29-38.
- Pade V, Stavchansky S. (1998) Link between drug absorption solubility and permeability measurements in Caco-2 cells. *Journal of Pharmaceutical Sciences* 87:1604-1607.
- Padosch SA, Popp E, Vogel P, Böttiger BW (2003) Altered protein expression levels of Fas/CD95 and Fas ligand in differentially vulnerable brain areas in rats after global cerebral ischemia. *Neuroscience Letters* 338:247-251.
- Papadopoulos SM, Chandler WF, Salamat MS, Topol EJ, Sackellares JC (1987)

- Recombinant human tissue-type plasminogen activator therapy in acute thromboembolic stroke. *Journal of Neurosurgery* 67: 394-398.
- Park CK, Nehls DG, Teasdale GM and McCulloch J (1989) Effect of the NMDA antagonist MK-801 on local cerebral blood flow in focal cerebral ischaemia in the rat. *Journal of Cerebral Blood Flow Metabolism* 9: 617-622.
- Pathansali R, Bath PM (1998) IST and CAST: some answers but more questions. *Journal of Human Hypertension* 12:73-74.
- Peters GR, Hwang LJ, Musch B, Brosse DM, Orgogozo JM (1996) Safety and efficacy of 6mg/kg/day tirilazad mesylate in patients with acute ischemic stroke (TESS Study). *Stroke* 27: 195-196.
- Pinto M, Robine-Leon S, Appay MD, Kedinger M, Triadou N, Dussaulx E, Lacroix B, Simon-Assmann P, Haffen K, Fogh J, Zweibaum A. (1983) Enterocyte-like differentiation and polarization of the human colon carcinoma cell line Caco-2 in culture. *Biology of the Cell* 47: 323-330.
- Planas AM, Soriano MA, Berruezo M, Justicia C, Estrada A, Pitarch S, Ferrer I (1996) Induction of Stat3, a signal transducer and transcription factor, in reactive microglia following transient focal cerebral ischaemia. *European Journal of Neuroscience*. 8: 2612-2618.
- Prakasa Babu P, Yoshida Y, Su M, Segura M, Kawamura S, Yasui N (2000) Immunohistochemical expression of Bcl-2, Bax and cytochrome c following focal cerebral ischemia and effect of hypothermia in rat. *Neuroscience Letters* 291:196-200.

- Prass K, Dirnagl U (1998) Glutamate antagonists in therapy of stroke. *Restorative Neurology and Neuroscience* 13: 3-10.
- Pulsinelli WA and Brierley JB (1979) A new model of bilateral hemispheric ischemia in the unanesthetized rat. *Stroke* 10:267-272.
- Qureshi AI, Ali Z, Suri MF, Kim SH, Shatla AA, Ringer AJ, Lopes DK, Guterman LR, Hopkins LN (2001) Intra-arterial third-generation recombinant tissue plasminogen activator (reteplase) for acute ischemic stroke. *Neurosurgery* 49:41-48.
- Qureshi AI, Siddiqui AM, Suri MF, Kim SH, Ali Z, Yahia AM, Lopes DK, Boulos AS, Ringer AJ, Saad M, Guterman LR, Hopkins LN (2002) Aggressive mechanical clot disruption and low-dose intra-arterial third-generation thrombolytic agent for ischemic stroke: a prospective study. *Neurosurgery* 51:1319-1327.
- Radi R, Rodriguez M, Castro L, Telleri R (1994) Inhibition of mitochondrial electron transport by peroxynitrite. *Archives of Biochemistry and Biophysics* 308: 89-95.
- Raff M (1998) Cell suicide for beginners. *Nature* 396:119-122.
- Ranaldi G, Consalvo R, Sambuy Y, Scarino ML (2003) Permeability characteristic of parental and clonal human intestinal Caco-2 cell lines differentiated in serum-supplemented and serum-free media. *Toxicology in Vitro* 17:761-767.
- Ratan RR, Murphy TH, Baraban JM (1994) Oxidative stress induces apoptosis in embryonic cortical neurons. *Journal of Neurochemistry* 62:376-379.
- Reiter RJ (1995) Oxidative processes and antioxidative defense mechanisms in the aging brain. *The Federation of American Societies for Experimental Biology Journal* 9: 526-533.
- Reith J, Jorgensen HS, Pedersen PM, Nakayama H, Raaschou HO, Jeppesen LL,

- Olsen TS (1996) Body temperature in acute stroke: relation to stroke severity, infarct size, mortality, and outcome. *Lancet* 347: 422-425.
- Ringdahl U, Sjöbring U (2000) Analysis of plasminogen-binding M proteins of streptococcus pyogenes. *METHODS* 21:143-150.
- Ringelstein EB, Biniek R, Weiller C, Ammeling B, Nolte PN, Thron A (1992) Type and extent of hemispheric brain infarctions and clinical outcome in early and delayed middle cerebral artery recanalization. *Neurology* 42: 289-298.
- Robinson MJ, Macrae IM, Todd M, Reid JL, McCulloch J (1990) Reduction of local cerebral blood flow to pathological levels by endothelin-1 applied to the middle cerebral artery in the rat. *Neuroscience Letters* 118: 269-272.
- Roth KA (2001) Caspases, apoptosis, and Alzheimer disease: causation, correlation, and confusion. *Journal of Neuropathology and Experimental Neurology* 60: 829-38.
- Rothwell NJ and Hopkins SJ (1995) Cytokines and the nervous system II: Actions and mechanisms of action. *Trends in Neurosciences* 18: 130-136.
- Rubas W, Jezyk N, Grass GM (1993) Comparison of the permeability characteristic of a human colonic epithelial (Caco-2) cell line to colon of rabbit, monkey, and dog intestine and human drug absorption. *Pharmaceutical Research* 10:113-118.
- Ruscher K, Isaev N, Trendelenburg G, Weih M, Iurato L, Meisel A, Dirnagl U (1998) Induction of hypoxia inducible factor 1 by oxygen glucose deprivation is attenuated by hypoxic preconditioning in rat cultured neurons. *Neuroscience Letters* 254: 117-120.
- Saito I, Segawa H, Shiokawa Y, Taniguchi M, Tsutsumi, K (1987) Middle cerebral

- artery occlusion: correlation of computed tomography and angiography with clinical outcome. *Stroke* 18: 863-868.
- Salzman EW (1992) Low-molecular-weight heparin and other new antithrombotic drugs. *The New England Journal of Medicine* 326:1017-1019.
- Samdani AF, Dawson TM, Daweson VL (1997) Nitric oxide synthase in models of focal ischemia. *Stroke* 28: 1283-1288.
- Sandercock P (1999) Is there still a role for intravenous heparin in acute stroke? No. *Archives of Neurology* 56:1160-1161.
- Sapirstein A and Bonventre JV (2000) Phospholipase A2 in ischemic and toxic brain injury. *Neurochemical Research* 25:745-753.
- Sasaki O, Takeuchi S, Koike T, Koizumi T, Tanaka R (1995) Fibrinolytic therapy for acute embolic stroke: intravenous, intracarotid, and intra-arterial local approaches. *Neurosurgery* 36:246-253.
- Schmid-Elsaesser R, Zausinger S, Hungerhuber E, Baethmann A, Reulen HJ (1998) Monotherapy with dextromethorphan or tirilazad-but not a combination of both-improves outcome after transient focal cerebral ischemia in rats. *Experimental Brain Research. Experimentelle Hirnforschung. Experimentation Cerebrale* 122:121-127.
- Schmidt CF, Read BE, Chen KK (1924) Experiments with Chinese drug. *Chinese Medicine Journal* 38: 362-375.
- Schwab S, Georgiadis D, Berrouschot J, Schellinger PD, Graffagnino C, Mayer SA (2001) Feasibility and safety of moderate hypothermia after massive hemispheric

- infarction. *Stroke* 32: 2033-2035.
- Schwab S, Schwarz S, Spranger M, Keller E, Bertram M, Hacke W (1998) Moderate hypothermia in the treatment of patients with severe middle cerebral artery infarction. *Stroke* 29:2461-2466.
- Schwarz K, Bertelsen G, Nissen LR, Gardner PT, Heinonen MI, Hopia A, Huynh-Ba T, Lambelet P, McPhail D, Skibsted LH, & Tijburg L (2001) Investigation of plant extracts for the protection of processed foods against lipid oxidation. Comparison of antioxidant assays based on radical scavenging. Lipid oxidation and analysis of the principal antioxidant compounds. *European Food Research and Technology* 212:319-328.
- Seigel GM, Campbell LM (2004) High-throughput microtiter assay for Hoechst 33342 dye uptake. *Cytotechnology* 45:155-160.
- Sherman DG, Atkinson RP, Chippendale T, Levin KA, Ng K, Futrell N, Hsu CY, Levy DE (2000) Intravenous ancrod for treatment of acute ischemic stroke: the STAT study: a randomized controlled trial. *Journal of the American Medical Association* 283:2395-2403.
- Shi LF, Zheng XM, Cai Z, Wu, BS (1995) Comparison of influence of essential oil from *Ligusticum chuanxiong* Hort. on microcirculation in rabbit conjunctiva bulbar before and after decomposition of ligustilide. *Chinese Journal of Pharmacology and Toxicology* 9: 157-158.
- Shigeno T, Teasdale GM, McCulloch J, Graham DI (1985) Recirculation model following MCA occlusion in rats. Cerebral blood flow, cerebrovascular

- permeability, and brain edema. *Journal of Neurosurgery* 63: 272-277.
- Shimohama S (2000) Apoptosis in Alzheimer's disease-an update. *Apoptosis* 5: 9-16.
- Simonian NA, Coyle JT (1996) Oxidative stress in neurodegenerative diseases. *Annual Review of Pharmacology and Toxicology* 36: 83-106.
- Smalling RW, Bode C, Kalbfleisch J, Sen S, Limbourg P, Forycki F, Habib G, Feldman R, Hohnloser S, Seals A (1995) More rapid, complete, and stable coronary thrombolysis with bolus administration of reteplase compared with alteplase infusion in acute myocardial infarction. *RAPID Investigator. Circulation* 91:2725-2732.
- Smith ML, Bendek G, Dahlgren N, Rosen I, Wieloch T, Siesjo BK (1984) Models for studying long-term recovery following forebrain ischemia in the rat. 2. A 2-vessel occlusion model. *Acta Neurologica Scandinavica* 69:385-401.
- Soehle M, Heimann A, Kempfski O (1998) Postischemic application of lipid peroxidation inhibitor U-101033E reduced neuronal damage after global cerebral ischemia in rats. *Stroke* 29: 1240-1247.
- Sterz F, Safar P, Tisherman S, Radovsky A, Kuboyama K, Oku K (1991) Mild hypothermic cardiopulmonary resuscitation improves outcome after prolonged cardiac arrest in dogs. *Critical Care Medicine* 19:379-389.
- Stuehr DJ, Griffith OW (1992) Mammalian nitric oxide synthases. *Advances in Enzymology and Related Areas of Molecular Biology* 65:287-346.
- Su DM, Yu SS, Qin HL (2005) New dimeric phthalide derivative from *Angelica sinensis*. *Acta Pharmaceutica Sinica* 40:141-144.

- Sur P, Sribnick EA, Wingrave JM, Nowak MW, Ray SK, Banik NL (2003) Estrogen attenuates oxidative stress-induced apoptosis in C6 glial cells. *Brain Research* 971:178-188.
- Sydserrff SG, Borelli AR, Green AR, Cross AJ (2002) Effect of NXY-059 on infarct volume after transient or permanent middle cerebral artery occlusion in the rat; studies on dose, plasma concentration and therapeutic time window. *British Journal of Pharmacology* 135: 103-112.
- Sydserrff SG, Cross AJ, Green AR (1995a) The neuroprotective effect of chlormethiazole on ischaemic neuronal damage following permanent middle cerebral artery ischaemia in the rat. *Neurodegeneration* 4: 323-328.
- Sydserrff SG, Cross AJ, West KJ, Green AR (1995b) The effect of chlormethiazole on neuronal damage in a model of transient focal ischaemia. *British Journal of Pharmacology* 114: 1631-1635.
- Tanaka K, Fujita N, Higashi Y, Ogawa N (2002) Effects of immunophilin ligands on hydrogen peroxide-induced apoptosis in C6 glioma cells. *Synapse* 43: 219-222.
- Tao JY, Ruan YP, Mei QB, Liu S, Tian QL, Chen YZ, Zhang HD, Duan ZX (1984) Studies of antiasthmatic action of ligustilide of DANG-GUI, *Angelica sinensis* (Oliv.) Diels. *Acta Pharmaceutica Sinica* 19: 561-565.
- Tewodros W, Karlsson I, Kronvall G (1996) Allelic variation of the streptokinase gene in  $\beta$ -hemolytic streptococci group C and G isolates of human origin. *FEMS Immunology and Medical Microbiology* 13:29-34.
- The International Stroke Trial (IST) (1997) a randomised trial of aspirin, subcutaneous

heparin, both, or neither among 19435 patients with acute ischaemic stroke. Lancet 349:1569-1581.

The Multicenter Acute Stroke Trial-Europe Study Group (The MAST-ESG) (1996) Thrombolytic therapy with streptokinase in acute ischemic stroke. The New England Journal of Medicine 335:145-150. The National Institute of Neurological Disorders and Stroke rt-PA Stroke Study Group (The NINDS) (1995) Tissue plasminogen activator for acute ischemic stroke. The New England Journal of Medicine 333:1581-1587.

The Multicenter Acute Stroke Trial—Italy Group (The MAST-IG) (1995) Randomised controlled trial of streptokinase, aspirin, and combination of both in treatment of acute ischaemic stroke. Lancet 346:1509-1514.

The NINDS t-PA Stroke Study Group (1997) Intracerebral hemorrhage after intravenous t-PA therapy for ischemic stroke. Stroke 28:2109-2118.

The Publications Committee for the Trial of ORG 10172 in Acute Stroke Treatment (TOAST) Investigators (1998) Low molecular weight heparinoid, ORG 10172 (danaparoid), and outcome after acute ischemic stroke: a randomized controlled trial. Journal of the American Medical Association 279:1265-1272.

The State Pharmacopoeia Commission of People's Republic of China, Pharmacopoeia of the People's Republic of China, vol. 1, Chemical Industry Press, Beijing, 2000, p. 101.

Thornhill J, Corbett D (2001) Therapeutic implications of hypothermic and hyperthermic temperature conditions in stroke patients. Canadian Journal of

- Physiology and Pharmacology 79:254-261.
- Traynelis SF, Lipton SA (2001) Is tissue plasminogen activator a threat to neurons?  
Nature Medicine 7: 17-18.
- Traystman RJ (2003) Animal models of focal and global cerebral ischemia. ILAR  
Journal 44: 85-95.
- Traystman RJ, Kirsch JR, Koehler RC (1991) Oxygen radical mechanisms of brain  
injury following ischemia and reperfusion. Journal of Applied Physiology  
71:1185-1195.
- Trump BF, Berezesky IK, Sato T, Laiho KU, Phelps PC, DeClaris N (1984) Cell  
calcium, cell injury and cell death. Environmental Health Perspectives 57:  
281-287.
- Turski L, Huth A, Sheardown M, McDonald F, Neuhaus R, Schneider HH, Dirnagl U,  
Wiegand F, Jacobsen P, Ottow E (1998) ZK200775: a phosphonate  
quinoxalinedione AMPA antagonist for neuroprotection in stroke and trauma.  
Proceedings of the National Academy of Sciences of the United States of America  
95: 10960-10965.
- Uchino H, Minamikawa-Tachino R, Kristian T, Perkins G, Narazaki M, Siesjo BK,  
Shibasaki F (2002) Differential neuroprotection by cyclosporin A and FK506  
following ischemia corresponds with differing abilities to inhibit calcineurin and  
the mitochondrial permeability transition. Neurobiology of Disease 10: 219-233.
- Velier JJ, Ellison JA, Kikly KK, Spera PA, Barone FC, and Feuerstein GZ (1999)  
Caspase-8 and caspase-3 are expressed by different populations of cortical

- neurons undergoing delayed cell death after focal stroke in the rat. *The Journal of Neuroscience* 19:5932-5941.
- Von Coelln R, Kugler S, Bahr M, Weller M, Dichgans J, Schulz JB (2001) Rescue from death but not from functional impairment: caspase inhibition protects dopaminergic cells against 6-hydroxydopamine-induced apoptosis but not against the loss of their terminals. *Journal of Neurochemistry* 77: 263-273.
- Wahlgren NG, Ranasinha KW, Rosolacci T, Franke CL, van Erven PM, Ashwood T, Claesson L (1999) Clomethiazole acute stroke study (CLASS): results of a randomized, controlled trial of clomethiazole versus placebo in 1360 acute stroke patients. *Stroke* 30: 21-28.
- Wang CX, Yang Y, Yang T, Shuaib A (2001) A focal embolic model of cerebral ischemia in rats: introduction and evaluation. *Brain Research, Brain Research Protocols* 7: 115-120.
- Wang HY and Huang HY (2003) The production of a new drug-butylphthalide in Shi Jia Zhuang Pharmaceutical Company. *Chinese Journal of Medicinal Guide* 5: 448.
- Wang PS, Gao XL, Fukuyama Y, Sugawara M (1985) Studies on the constituents of Chinese traditional medicine-five lactone compounds. *Chinese Traditional and Herbal Drugs*. 16:137-138.
- Wang PS, Gao XL, Wang YX, Fukuyama Y, Miura I, Sugawara M (1984) Phthalides from the rhizome of *Ligusticum wallichii*. *Phytochemistry* 23: 2033-2038.
- Wang Y, Lim LL, Levi C, Heller RF, Fisher J (2000) Influence of admission body temperature on stroke mortality. *Stroke* 31: 404-409.

- Wardlaw JM, Warlow CP, Counsell C (1997) Systematic review of evidence on thrombolytic therapy for acute ischaemic stroke. *Lancet* 350: 607 - 614.
- Warlow CP (1998) Epidemiology of stroke. *Lancet* 352: SIII1-SIII4.
- Watanabe Y, Littleton-Kearney MT, Traystman RJ, Hurn PD (2001) Estrogen restores postischemic pial microvascular dilation. *American Journal of Physiology Heart and Circulatory Physiology* 281:155-160.
- Watson BD, Dietrich WD, Busto R, Wachtel MS, Ginsberg MD (1985) Induction of reproducible brain infarction by photochemically initiated thrombosis. *Annals of Neurology* 17: 497-504.
- Weber CH, Vincenz C (2001) The death domain superfamily: a tale of two interfaces? *Trends in Biochemical Sciences* 26: 475-481.
- Whittemore ER, Loo DT, Watt JA, Cotman CW (1995) A detailed analysis of hydrogen peroxide-induced cell death in primary neuronal culture. *Neuroscience* 67: 921-932.
- Wolpert SM, Bruckmann H, Greenlee R, Wechsler L, Pessin MS, Del Zoppo GJ (1993) Neuroradiologic evaluation of patients with acute stroke treated with recombinant tissue plasminogen activator. *American Journal of Neuroradiology* 14: 3-13.
- Wyllie AH, Kerr JF, Currie AR (1980) Cell death: The significance of apoptosis. *International Review of Cytology* 68: 251-306.
- Wyllie AH, Morris RG, Smith AL, Dunlop D (1984) Chromatin cleavage in apoptosis: association with condensed chromatin morphology and dependence on macromolecular synthesis. *Journal of Pathology* 142: 67-77.

- Xie FX, Tao JY (1985) Central nervous inhibition of ligustilide from the rhizome of *Angelica sinensis* (Oliv.) Diels. Shan Xi New Medicine 14:59-62.
- Xu HL and Feng YP (1999) Effects of 3-n-butylphthalide on pial arterioles in focal cerebral ischemia rats. Acta Pharmaceutica Sinica 34:172-175.
- Yamagishi T, Kaneshima H (1977) Constituents of *Cnidium officinale* Makino. Structure of senkyunolide and gas chromatography-mass spectrometry of the related phthalides. Journal of the Pharmaceutical Society of Japan 97: 237-243.
- Yamaguchi T, Hayakawa T, Kiuchi H, and the Japanese Thrombolysis in Stroke Group (1993) Intravenous tissue plasminogen activator ameliorates the outcome of hyperacute embolic stroke. Cerebrovascular Diseases 3:269-272.
- Yamaguchi T, Sano K, Takakura K, Saito I, Shinohara Y, Asano T, Yasuhara H (1998) Ebselen in acute ischemic stroke: a placebo-controlled, double-blind clinical trial. Ebselen Study Group. Stroke 29: 12-17.
- Yamasaki Y, Matsuo Y, Matsuura N, Onodera H, Itoyama Y, Kogure K, (1995) Transient increase of cytokine-induced neutrophil chemoattractant, a member of the interleukin-8 family, in ischemic brain areas after focal ischemia in rats. Stroke 26: 318-322.
- Yamori Y, Horie R, Handa H, Sato M, Fukase M (1976) Pathogenetic similarity of strokes in stroke-prone spontaneously hypertensive rats and humans. Stroke 7:46-53.
- Yano T, Nakayama R, Ushijima K (2000) Intracerebroventricular propofol is neuroprotective against transient global ischemia in rats: extracellular glutamate

- level is not a major determinant. *Brain Research* 883:69-76.
- Yee S (1997) In vitro permeability across Caco-2 cell (colonic) can predict in vivo (small intestinal) absorption in man-fact or myth. *Pharmaceutical Research* 14: 763-766.
- Yu SR and You SQ (1984) The anticonvulsive action of 3-n-butylphthalide and 3-n-butyl-4,5-dihydrophthalide. *Acta Pharmaceutica Sinica* 19: 566 - 570.
- Yu SR, Gao NN, Li LL (1988) Facilitated performance of learning and memory in rats by 3-n-butylphthalide. *Acta Pharmacologica Sinica* 9: 385-388.
- Zakeri ZF, Quaglino D, Latham T, Lockshi RA (1993) Delayed internucleosomal DNA fragmentation in programmed cell death. *The Federation of American Societies for Experimental Biology Journal* 7: 470-478.
- Zeumer H, Freitag HJ, Zanella F, Thie A, Arning C (1993) Local intra-arterial fibrinolytic therapy in patients with stroke: urokinase versus recombinant tissue plasminogen activator (r-TPA). *Neuroradiology* 35:159-162.
- Zhang LY and Feng YP (1996) Effect of dl-3-N-butylphthalide on life span and neurological deficit in SHPsp rats. *Acta Pharmaceutica Sinica* 31:18-23.
- Zhang R, Chopp M, Zhang Z, Jiang N, Powers C (1998) The expression of P- and E-selectins in three models of middle cerebral artery occlusion. *Brain Research* 785: 207-214.
- Zhang RL, Chopp M, Li Y, Zaloga C, Jiang N, Jones ML, Miyasaka M, Ward PA (1994) Anti-ICAM-1 antibody reduces ischemic cell damage after transient middle cerebral artery occlusion in the rat. *Neurology* 44: 1747-1751.

- Zhang Z, Chopp M, Goussev A, Powers C (1998) Cerebral vessels express interleukin 1beta after focal cerebral ischemia. *Brain Research* 784: 210-217.
- Zhao Q, Memezawa H, Smith ML, Siesjo BK (1994) Hyperthermia complicates middle cerebral artery occlusion induced by an intraluminal filament. *Brain Research* 649: 253-259.
- Zhao W, Richardson JS, Mombourquette MJ, Weil JA, Ijaz S, Shuaib A (1996) Neuroprotective effects of hypothermia and U-78517F in cerebral ischemia are due to reducing oxygen-based free radicals: an electron paramagnetic resonance study with gerbils. *Journal of Neuroscience Research* 45:282-288.
- Zhao X, Ross ME, Iadecola C (2003) L-Arginine increases ischemic injury in wild-type mice but not in iNOS-deficient mice. *Brain Research* 966:308-311.
- Zhou CX, Li XH (2001) Studies on the stability of ligustilide with solvent effect. *Acta Pharmaceutica Sinica* 36: 793-795.
- Ziv I, Melamed E, Nardi N, Luria D, Achiron A, Offen D, Barzilai A (1994) Dopamine induces apoptosis-like cell death in cultured chick sympathetic neurons--a possible novel pathogenetic mechanism in Parkinson's disease. *Neuroscience Letters* 170:136-40.